

Automated Optimal Glycaemic Control using a Physiology-Based Pharmacokinetic/Pharmacodynamic Model

Von der Fakultät für Maschinenwesen der Rheinisch-Westfälischen
Technischen Hochschule Aachen zur Erlangung des akademischen Grades
eines Doktors der Ingenieurwissenschaften genehmigte Dissertation

vorgelegt von

Stephan Schaller

Berichter:	Univ.-Prof. Dr.rer.nat. Andreas Schuppert Univ.-Prof. Alexander Mitsos, Ph.D.
Tag der mündlichen Prüfung:	09.12.2014

„Diese Dissertation ist auf den Internetseiten der
Universitätsbibliothek online verfügbar.“

Abstract

After decades of research, Automated Glucose Control (AGC) is still out of reach for everyday control of blood glucose. The inter- and intra-individual variability of glucose dynamics largely arising from variability in insulin absorption, distribution, and action, and related physiological lag-times remain a core problem in the development of suitable control algorithms. Over the years, model predictive control (MPC) has established itself as the gold standard in AGC systems in research. Models of glucose metabolism are a core element of MPC control schemes. The standard two- or three-compartmental models, i.e. the “Minimal-Model” [1], represent little biological detail, hampering the integration of multi-scale data, thus confining capabilities of model extrapolation.

To overcome remaining challenges, a new approach to MPC AGC is developed here. The MPC uses, for the first time, an individualizable generic whole-body physiology-based pharmacokinetic/pharmacodynamic (PBPK/PD) model of the glucose-insulin-glucagon regulatory system. The model reflects detailed physiological properties of healthy populations and type 1 diabetes individuals expressed in the respective parameterizations. The model features a detailed representation of absorption models for oral glucose, subcutaneous insulin and glucagon, and an insulin receptor model relating pharmacokinetic properties to pharmacodynamic effects. Model development and validation is based on literature data. The quality of predictions is high and captures relevant observed inter- and intra-individual variability, thus improving model long-term predictions. This significantly strengthens the rationale for the use of MPC. To increase robustness vs. uncertainties (closed-loop stability), model kernels were updated with growing patient data and the MPC was integrated in a control cascade with a proportional, integrative, derivative (PID) based offset-control. Both, model and control algorithm, were validated and evaluated within an *in-silico* environment before testing the control approach within two 30-h clinical trials. The trials were each conducted in ten subjects with type 1 diabetes without endogenous insulin secretion. Blood glucose was controlled by subcutaneous delivery of insulin based on plasma glucose (PG, in trial #1) and continuous blood glucose monitors (CGMs, subcutaneous sampling, trial #2) measurements in 15 min intervals. Meal information, but no priming bolus (pre-meal insulin), was given to the controller at start of each meal.

For the first clinical trial, the overall mean ($n=10$) PG was 156 mg/dL, with 74% time of PG values in the target range of 70–180 mg/dL. With 2 incidents during 240 h of closed-loop control, hypoglycemia ($PG < 60$ mg/dL) was rare. During nighttime control, prior to model adaptation (adaptation was slow if successful at all), mean PG was elevated (149 mg/dL, with 38% time in target 70–140 mg/dL). For the second clinical trial, control performance improved significantly due to an improved workflow and faster (earlier) model adaptation with an overall mean ($n=10$) PG of 127 mg/dL, with 76% time of PG values in the target range of 70–180 mg/dL. With 9 incidents during 240 h of closed-loop control, hypoglycemia ($PG < 60$ mg/dL) was slightly increased. Nighttime control improved the most with a mean PG exactly on target (110 mg/dL, with 78% time in target 70–140 mg/dL). Retrospective analysis of insulin and glucagon measurements collected during the trial, revealed significant glucagon surges, which were observed postprandial and coincided with severe morning insulin resistance for some patients. Whereas a consistent interpretation of the observed behavior is outstanding, the modeling framework allowed a structural mode-of-action

evaluation to shed new light on the role of glucagon and nutrition (i.e. coffee) in the “dawn-effect” in Diabetes.

This work shows that large-scale in-silico models of the glucose metabolism can provide a framework to improve diabetes research, the development of automatic control strategies for diabetes and ultimately every day diabetes management. The algorithm for the integrated closed-loop control system was benchmarked both, within in-silico clinical trials as well as within clinical feasibility studies. Once the relevance of (postprandial) glucagon in T1DM has been analyzed, fully understood and captured by PBPK/PD modeling, future trials testing the improved system seem very promising.

Zusammenfassung

Auch nach jahrzehntelanger Forschung steht die automatisierte Blutzuckerregelung (AGC) noch nicht für den täglichen Gebrauch zur Verfügung. Die inter- und intraindividuelle Variabilität der Blutzuckerverläufe, die sich weitgehend aus Variabilität in der Insulin- Absorption, Verteilung, und Wirkung, und der damit verbundenen physiologischen Verzögerungszeiten zusammensetzt, bleibt ein Kernproblem bei der Entwicklung von geeigneten Regelalgorithmen. Im Laufe der Jahre hat sich die Modellprädiktive Regelung (MPC) als Goldstandard bei AGC-Systemen in der Forschung etabliert. Modelle des Glukosestoffwechsels sind hierbei ein Kernelement der MPC Systeme. Einfache kompartmentelle (Regressions-) Modelle beinhalten nur wenig physiologisches (strukturelles) Detail, was die Integration von Multi-Skalen Daten einschränkt und die Gültigkeit von Extrapolationen einschränkt.

Um diese verbleibenden Herausforderungen zu überwinden, wird hier ein neuer robuster MPC AGC Regelungsansatz entwickelt. Dieser MPC-Ansatz verwendet, zum ersten Mal, eine individualisierbares generisches Physiologie-basiertes Ganzkörper- pharmakokinetisches/pharmakodynamisches (PBPK/PD) Modell des Glukose-Insulin-Glukagon Stoffwechselsystems. Das Modell spiegelt detaillierte physiologische Eigenschaften gesunder Individuen, sowie Individuen mit Typ-1-Diabetes in den jeweiligen Parametrisierungen wieder. Das Modell verfügt über eine detaillierte Darstellung der Absorption oraler Glukose, und von subkutanem Insulin und Glukagon. Es beinhaltet außerdem ein Insulin-Rezeptor-Modell zur Abbildung der pharmakodynamischen Wirkung auf das pharmakokinetische Verhalten von Insulin. Modellentwicklung und Validierung basiert auf Literaturdaten. Das Modell liefert qualitativ hochwertige Vorhersagen und bildet auch beobachtete relevante inter- und intraindividuelle Variabilität ab womit auch langfristige Modellvorhersagen gestützt werden. Dies stärkt deutlich die Argumentation für den Einsatz von einer MPC Strategie. Um die Robustheit gegen Unsicherheiten (Closed-Loop-Stabilität) zu erhöhen, wird der Modellkern mit Hilfe der kontinuierlich gemessenen Patientendaten aktualisiert und zusätzlich in einer Regelkaskade mit einem PID-Regler zur Offset-Regelung integriert. Modell und Regelalgorithmus wurden *in-silico* validiert um dann in zwei 30 stündigen klinischen Machbarkeitsstudien getestet. Die Studien wurden an jeweils zehn Patienten mit Typ-1-Diabetes ohne endogene Insulinsekretion durchgeführt. Der Blutzucker wurde durch subkutane Verabreichung von Insulin, basierend auf Messungen der Plasmaglukose (PG, in Studie 1) und mit Hilfe von kontinuierlichen Blutzuckermessgeräten (CGMs, subkutane Messung, Studie 2) in Intervallen von 15 min geregelt. Zu den Mahlzeiten wurde die Information über Mahlzeitzusammensetzung an den Regler übergeben. Es wurde jedoch kein vorab Insulin-Bolus zu den Mahlzeiten verabreicht.

Der mittlere Blutzuckerwert während der ersten Studie ($n = 10$) war 156 mg / dl, wobei 74% der PG -Werte im Zielbereich von 70 bis 180 mg/dL lagen. Insgesamt gab es nur zwei Vorfälle von Hypoglykämie (PG <60 mg/dL) innerhalb 240 h. Über die Nacht war, ohne Modellanpassung (da zu langsam oder nicht möglich), ein leicht erhöhter mittlerer PG festzustellen (149 mg/dL, mit 38% Zeit im Zielbereich 70-140 mg/dL). Die Regelgüte konnte in der zweiten Studie ($n = 10$) aufgrund eines verbesserten Ablaufplans und einer schnelleren (frühzeitigen) Modelladaptation signifikant verbessert werden. Der mittlere Blutzuckerwert war 127 mg / dl, wobei 76% der PG -Werte im Zielbereich von 70 bis 180 mg/dL lagen. Insgesamt gab es mit 9 Vorfällen einen leichten Anstieg von Hypoglykämie (PG <60 mg/dL) innerhalb

240 h. Die größte Verbesserung der Regelgüte konnte über die Nacht erzielt werden und es konnte ein mittlerer PG erreicht werden, der exakt dem Zielwert entspricht (110 ml/dL, mit 78% Zeit im Zielbereich 70-140 mg/dL). Retrospektive Analyse der Insulin- und Glukagon-Messungen aus der Studie zeigten einen erheblichen Anstieg von Glukagon während der Mahlzeiten, der bei einigen Patienten mit schwerer morgendlicher Insulinresistenz einherging. Obwohl eine konsistente Interpretation des beobachteten Verhaltens aussteht, erlaubt der Modellierungsansatz eine Strukturelle Analyse der Wirkungsweise und bringt damit neue Erkenntnisse zur Rolle von Glukagon und Nahrungsbestandteilen (z.B. Kaffee/Koffein) im "Morgengrauen-Effekt" in Diabetes Mellitus.

Diese Arbeit zeigt, dass physiologische Modelle des Glukosestoffwechsels die Diabetes-Forschung, die Entwicklung von automatisierten Blutzuckerregelungssystemen und letztlich den täglichen Umgang mit Diabetes verbessern können. Der modellbasierte Regler wurde sowohl *in-silico*, als auch in klinischen Machbarkeitsstudien erfolgreich getestet. Das Gesamtverständnis zum Glukosestoffwechsel und speziell zur Bedeutung von Glukagon in T1DM kann durch die PBPK/PD-Modellierung signifikant verbessert werden, womit zukünftige Studien mit dem hier vorgestellten Systems sehr vielversprechend sind.

Acknowledgements

It really is a pleasure to thank all those people (and institutions) who gave me all their support throughout my doctoral studies. Firstly, I'd like to thank my supervisor Professor Andreas Schuppert, without whom this work, as a joint research project of RWTH Aachen University and Bayer Technology Services (BTS) GmbH, would not have been possible. In this regard I would also like to thank my former "boss" and Head of Computational Systems Biology @ BTS, Dr. Jörg Lippert. You both have proven a bottomless pool of new ideas and always helped in setting the path forward especially throughout the first years of my candidature. Andreas, your knowledge of the field of industrial mathematics, both, in an academic and industrial context, and holistic view of this work have helped make it what it is today. Likewise I'm very grateful of your experienced input and scrutiny, Jörg, for taking me on-board in the first place and not holding back on painful yet healthy criticism, especially of my writing and presentation skills, which sufficiently challenged me to ensure the quality of my work was accepted into the realm of scientific publications and presentations. I would also like to thank my supervisor Professor Alexander Mitsos for a thorough review of my work, coming up and with 12 pages of valued correction suggestions.

I'd like to thank my current boss and Head of Systems Pharmacology CV @ BTS, Dr. Thomas Eissing, who took over about halfway through my doctoral studies. Thomas, I would like to thank you in particular for supporting me in situations that were somewhat delicate at times (details shall not be mentioned here-in) sobering (yet to some humorous) on reflection. I also would like to thank you for the strong support for and belief in my research, which now allows me to continue my work on the topic within projects in industry (also thanks to Dr. Ingo Gaida).

I would like to thank all my colleagues at BTS and the AICES Graduate School, Thomas Gaub, Juri Solodenko, Michael Sevestre and Dr. Katrin Coboeken as software developers, who I was able to persuade into implementing my (hopefully valued) feature requests for the modelling platform and Dr. Christoph Niederal, Dr. Lars K  pfer, Dr. Stefan Willmann and Dr. Kirstin Thelen for valued discussions on biological, physiological and pharmacological questions and of course Dr. Sebastian Schneckener and again Thomas Gaub for great off-topic discussions during rock-climbing in- and outdoors and a later acquisition, Dr. Kai Tappe, for great loughs during far off-topic conversations. I'd also like to thank Martin Hobe for his support in polishing the work to a presentable and marketable form and the opportunities for overseas presentations (Wha?) and valuable work-life counsel. Not to forget the managing director of AICES, Nicole Faber, for her support in tedious administrative issues (not to go into detail, really appreciated) and assistants Nadine (AICES) and Sonja and Efi (BTS) for their support and not to forget patience with my travel reimbursements.

I'd also like to thank my interns and master students (and not only the ones working on diabetes related topics), Markus Krauss, Annett Steinert, Ralf T  ngler, Maria Wetzels, Diane Lefaudeux, Luisa Schulze Langenhorst, Helene Kaffka, Frederico Wedahn, Julio Lahoz Beneytez and Pavel Balazski, the work of which helped me to gain a wider perception of the topic and beyond.

The whole of Bayer for the Leadership I was given, the Integrity of all actions and decisions I was confronted with, the Flexibility I was granted in doing my work and the Efficiency in terms of how things were done (Honestly!).

Special thanks go to the team and the students at the Medical University of Graz, Dr. Lukas Schaupp and Professor Tomas R. Pieber, for their outstanding support in preparing and conducting the clinical trials and as valued men in arms in diabetes research. In this regard I'd also like to thank my colleague Michael Block for the support in quality and risk management during preparations for the clinical trial and Juri Solodenko (also for introducing me to the world of Salsa) and especially Jan F. Schlender, who accompanied me to Graz, for their great support during the clinical trial (and almost protest-free handling of my control algorithm).

Following my urbanization into the lively city of Cologne I have found friends and cronies (on and off work) who made my time here unforgettable with outstanding urban adventures and memorable moments (yes, honestly?!). Thank you Markus, Jan, Stephan (Steller), Max, Axel, Sascha, Alisha, and Dr. Kristin Dickschen (who actually made it through first, no hard feelings) and all others I have not mentioned but should be mentioned here. And of course my long term friends and school buddies Thomas Schumacher, Martin Matuschek, Daniel CS Münch, Andreas Iby, Jürgen Schneider and Philipp Schaller, now also partners in crime in our (back-up plan) brewery "7 Schwaben", trying our own off-grid biocatalyzation of "drugs", but also Philipp Cordier, Constantin Schuss, Christoph Hager and of course my best mate Martin "Weizi" Kälble for memories that will be with us for the rest of our lives (Great times in Munich!).

Last but definitely not least! My own family for all the support I was given by accepting the fact that I did not have time to visit on the weekends. My dad (himself an engineer) for relentless questions about the inner workings of glucose homeostasis and possible connections to own ailments and the repeated and of course for (not?) pressuring me into this in the first place (which I was repeatedly reassured of by him telling me I could always come and help him as a lumberjack). My mum for helping me test the glucose measurement devices, and of course for being my mum. Thanks also to my bro Felix (with SiL Kerstin, kids Leander and little Neomi for always thinking differently and to my sis Manu (with BiL Matt and kids Leah and Emma) for being my voice of reason and of course my bro David (with SiL Rosie and little sweet Reuben) for giving me the ease and inspiration required to formulate these acknowledgements and for treading this path before me and leaving me a very generous (time-) window to follow...and "slightly" improve on.

And last but certainly not least, my fiancée Linda, love of my life, who bore with me during the last stressful months before my doctoral defence with great support and patience. Thank you! Thank you for believing in me and saying "Yes!" to marrying me on the 11th of the 11th! I look forward to our live together, numerous sessions of "Lindi Hop" and adventures to come!

And thanks to everyone else who has shared memories with me during this time and before and who I have not mentioned here. Thank you all! For being part of my life and making this possible, it was WORTH IT! (Honestly!)

best, Stephan

Table of Contents

PART I. INTRODUCTION & OUTLINE	15
I.1 BACKGROUND & MOTIVATION	16
I.2 OUTLINE.....	21
PART II. PHYSIOLOGY-BASED PHARMACOKINETIC / PHARMACODYNAMIC MODEL	23
II.1 STATE OF THE ART IN GLUCOSE INSULIN MODELS.....	24
II.1.1 <i>The “Minimal Model”</i>	24
II.1.2 <i>Compartmental PK/PD Models of the GIM</i>	25
II.2 MATERIALS AND METHODS.....	29
II.2.1 <i>Physiology-based PK/PD Modelling</i>	29
II.2.2 <i>Datasets and Model Individualization</i>	48
II.3 RESULTS.....	57
II.3.1 <i>Dynamics of the Glucose Metabolism Model</i>	57
II.3.2 <i>Post-hoc Evaluation of T1DM Model Predictions</i>	58
PART III. AUTOMATED GLUCOSE CONTROL	63
III.1 STATE OF THE ART IN BLOOD GLUCOSE CONTROL.....	64
III.1.1 <i>Algorithms</i>	64
III.1.2 <i>Integrated “Artificial Pancreas” Systems</i>	67
III.2 MATERIALS AND METHODS.....	69
III.2.1 <i>The Integrated System</i>	69
III.2.2 <i>Virtual Patient Generation & Trial Design</i>	73
III.2.3 <i>The Control Algorithm</i>	73
III.3 RESULTS.....	79
III.3.1 <i>In-silico Evaluation (First Trial, Blood Glucose)</i>	79
III.3.2 <i>In-silico Evaluation (Second Trial, CGM)</i>	84
PART IV. RESULTS FROM A CLINICAL TRIAL	89
IV.1 CLINICAL TRIALS: MATERIALS AND METHODS	90
IV.1.1 <i>Trials</i>	90
IV.1.2 <i>Outcome Measures</i>	92
IV.1.3 <i>Laboratory Analyses</i>	92
IV.1.4 <i>Control Algorithm</i>	92
IV.2 CONTROL PERFORMANCE	95
IV.2.1 <i>Glycaemic Control</i>	95
IV.2.2 <i>Insulin PK/PD</i>	97
IV.2.3 <i>Endogenous Glucagon PK/PD</i>	98
IV.2.4 <i>Adherence to Dose Recommendations</i>	100
IV.2.5 <i>Hypoglycaemia</i>	101
IV.2.6 <i>Summary</i>	102
PART V. DISCUSSION & APPENDIX.....	103
V.1 MODEL	104
V.2 CONTROLLER.....	107
V.3 CLINICAL TRIAL	109
V.4 CONCLUSION.....	111
V.5 APPENDIX.....	113
V.5.1 <i>PBPK/PD Model</i>	113
V.5.2 <i>Control Algorithm</i>	123
V.5.3 <i>Clinical Trials</i>	129
V.6 REFERENCES.....	151
V.7 LEBENS LAUF (CV)	163

List of Abbreviations

ADICOL	Advanced Insulin Infusion using a Control Loop
ADME	Absorption, distribution, metabolism and excretion
AP	Artificial pancreas
BTS	Bayer technology Services
CGM	Continuous Glucose Monitor
CHO	Carbohydrates
CO ₂	Carbon dioxide
CSII	Continuous subcutaneous insulin infusion
CVD	Cardiovascular disease
DAG	Diacyl glycerol
DM	Diabetes Mellitus
EDTA	Ethylenediaminetetraacetic acid, an anticoagulant for blood samples
FcRn receptor	Fragment crystallisable Region receptor
FDA	Federal Drug Administration
FFA	Free fatty acid
FMPD	Fading-memory proportional derivative
GC	Glucocorticoids
GIM	Glucose-Insulin metabolism
GI-tract	Gastrointestinal tract
GLP-1	Glucagon-like peptide 1
GLUT	Glucose transporter
GPCR	G-protein coupled receptor
HPA	hypothalamic-pituitary-adrenal axis
HSL	hormone-sensitive lipase
i.v.	Intravenous
ICING-model	Intensive Control Insulin-Nutrition-Glucose-model
ICU	Intensive care unit
IgG	Immune Gamma Globulin
IL-1/6	Interleukin-1/6
IR	Insulin receptor
IRS-1	Insulin receptor substrate-1
IVGTT	Intravenous glucose tolerance test
IVITT	Intravenous insulin tolerance test
LPL	Lipoprotein lipase

MARE	Mean absolute relative error
MPC	Model predictive control
MUG	Medical University of Graz
ODE	Ordinary differential equation
OGTT	Oral glucose tolerance test
PB	Physiology-based
PBPK/PD	Physiology-based pharmacokinetics / pharmacodynamics
PD	Pharmacodynamics
PDE	Partial differential equation
PID	Proportional integral derivative (controller)
PK	Pharmacokinetics
PKC	Protein kinase C
PTP1B	Protein tyrosine phosphatase 1B
RCT	randomized control trial
s.c.	Subcutaneous
SGLT	Sodium-dependent glucose transporter 1
T1DM	Type 1 diabetes mellitus
T2DM	Type 2 diabetes mellitus
TAG	Triacylglycerol
TNF-alpha	Tumour necrosis factor alpha
VLDL	Very low density lipoprotein

List of Original Papers

This thesis is based on the following papers [2-4]:

- I. Schaller S, Willmann S, Schaupp L, Pieber TR, Schuppert A, Lippert J, Eissing T: **A generic integrated physiologically-based whole-body model of the glucose-insulin-glucagon regulatory system.** *CPT: PSP* 2013.
- II. Schaller S, Willmann S, Schaupp L, Pieber TR, Schuppert A, Lippert J, Eissing T: **Robust MPC of blood glucose using generic whole-body physiology-based PK/PD model kernels.** *Submitted to IEEE Transactions in Biomedical Engineering*, 2014.
- III. Schaller S, Eissing T, Schaupp L, Schlender J, Solodenko J, Willmann S, Lippert J, , Schuppert A, Pieber TR: **Blood glucose control in T1DM subjects- prospects for generic whole-body physiology-based PK/PD model kernels: Clinical Trial and Post-Hoc Study.** *In internal revision* 2014.

Part I.

Introduction & Outline

I.1 Background & Motivation

Diabetes Mellitus is a metabolic disorder characterized by hyperglycaemia (high blood sugar) resulting from defects in the production of, or in the body's response to, insulin. Diabetes affects a continuously growing population of already over 382 million patients worldwide. The associated morbidity and mortality of diabetes represents a major healthcare burden. Diabetes (Type1 and 2) is affecting approx. 6 % of the adult population and approx. 15 % of the population over 65. In 2013, the disease caused 5.1 million deaths and accounted for global healthcare expenditures of USD 548 billion [5].

Blood glucose levels in healthy humans lie within a narrow range of approximately 70-110 mg/dl at fasting conditions. In diabetes mellitus type 1 the Insulin secreting beta-cells in the pancreas are destroyed by a selective auto-immune reaction, whereas in diabetes type 2 the body's autonomous regulation of blood glucose, managed by complex interactions of neuronal, hormonal and metabolic signalling networks is defective and glucose levels spiral out of control. In both cases the balance of insulin and glucose can only be controlled by constant vigilant manual insulin therapy by the afflicted individual. Maintaining blood glucose levels within a normal range is crucial to reduce long-term complications in patients with diabetes mellitus [6, 7]. Automation of this task would relieve patients of the burden of manual control and has been shown to lower risk of hypoglycaemia [8] increasing quality of life. It also offers good prospects in clinical and economic terms [9], important factors which drive the research of automated, integrated glucose control systems aiming for an artificial, technical substitution of the defective natural regulatory system in diabetes patients. Combined with a subcutaneous (s.c.) continuous glucose monitor (CGM) and an insulin infusion pump (IIP), such an integrated system is often referred to as an "Artificial Pancreas" (AP).

To improve both, preventive measures and economic disease management options, more research is required to understand all relevant aspects of the glucose insulin metabolism (GIM). These can range from disease prevention to management by identification of novel targets for type 1- and type 2 diabetes mellitus (T1 and T2DM) pharmacotherapies and automation of blood glucose control, i.e. the development of artificial pancreas systems [10-13].

AP systems have been in research & development for over 50 years but are still out of reach for everyday control of blood glucose. Improvements in glucose sensing and insulin analogs and their delivery devices have advanced the conditions for developing a feasible solution for a fully integrated AP system [14, 15]. The superiority of automatic glucose control by s.c. glucose measurements and s.c. insulin infusions (s.c.-s.c. route) over manual control has already been demonstrated [16].

Although various control strategies have been designed for the AP [12, 17-21], safety concerns remain, which makes bringing these systems to market maturity cumbersome. Remaining concerns are partly owed to technical and system inherent hurdles such as: (a) accuracy of (s.c.) CGM devices, and (b) physiologic lag times of s.c. glucose (measurements) during rapid changes in blood glucose, (c) onset of insulin action after s.c. administration, and (d) lingering/tailing insulin action after s.c. injection [13, 14, 22]. Various control strategies, from proportional-integral-derivative

(PID) control [17-19], to complex fuzzy-logic methods, imitating the decision-making of an expert, i.e. the physician [20, 21] have been designed for the AP.

Nevertheless, physiologic lag times remain a core problem in reactive feedback-control solutions [12]. Lag-times are best handled with feed-forward control solutions, the most widely used approach being model predictive control (MPC) [23-26]. A key component for such model predictive control approaches are mathematical models of the relevant processes. Understanding the complex system of interacting hormonal and metabolic signalling networks on the molecular level regulating whole-body blood glucose homeostasis, however, still remains challenging. Model based research is a standard approach for gaining a deeper understanding of diabetes for over half a century now and has since become the state-of-the-art approach. Mathematical models of the GIM are developed mainly for two reasons: as a tool for fundamental research to analyze the underlying properties of the GIM in healthy individuals and individuals with diabetes or as a model kernel for automatic blood glucose control in T1DM.

Structures of early mathematical models of the GIM [1, 27] are, as in classical (empirical/descriptive) PK/PD modelling, an abstracted and lumped reflection of the underlying physiological properties and mechanisms involved in hormonal glycaemic control. Over the years, the availability of highly informative but complex physiological data over multiple scales has steadily increased, allowing for detailed mechanistic modelling approaches through holistic data integration. Whereas empirical modelling is a data-driven, abstract description of input/output relations, mechanistic modelling is a direct mechanism-based mathematical representation of the underlying physics and chemistry of a certain process using knowledge of the interaction/interdependency of process variables.

The identification of drug targets and the development of pharmaceutical intervention strategies as well as modern model-based glucose control algorithms can benefit from model kernels with increased accuracy and predictive power [12, 13, 28] achieved through detailed mechanistic and structural representations of physiology. In recent years, semi-mechanistic modelling approaches with an increased level of detail have gained in popularity. The UVa/Padova simulator [29, 30], and the Cambridge Model [31] for closed-loop glucose control, do contain physiological aspects and represent the current state-of-the-art in glucose modelling used for model-based glucose control. However, to date, no system for automatic glucose control has been brought to market [15]. Current state-of-the-art models contain semi-mechanistic aspects and lumped designs as used in classical PK/PD modelling, but are not physiology-based, i.e. do not explicitly reflect physiology in their structure by using blood flows for mass flows or organ volumes for model compartmentalization. A state-of-the-art model developed more than 25 years ago by Sorensen [32] already included such details for the distribution, metabolization and excretion dynamics of glucose, insulin, and even glucagon but is no longer used in current research..

Thus, currently used models only partly accommodate the increased availability of data with augmented model structures or by only analyzing subsystems leaving the following issues: 1) An abstracted, lumped model design (semi-mechanistic/physiological) masks the mechanistic and structural relation to processes and compartments of the organism, making the integration of multi-scale data and related translation steps required for fundamental research difficult. Integration of multi-scale data can strengthen the extrapolative properties of the

simulation models, a critical aspect in automatic glucose control. 2) Isolated analysis of subsystems neglects the effect of interacting subsystems. 3) Model simplification (abstraction and lumping) obliterates the structural relation between important physiology and its mathematical representation, hindering the identification and direct quantification of detailed (metabolic) processes to distinguish physiologic differences in healthy and diabetic populations. Most importantly for individualized glucose control, this simplification also 4) masks the lag-times of distribution processes and 5) does not allow the integration of a generic framework for model individualization based on patient physiology.

To address these challenges, a new approach to AGC is taken, which, for the first time, combines a detailed generic whole-body PBPK/PD model [2], with a robust MPC algorithm for automatic glucose control. The integrated approach presented here will address above raised issues with a generic, widely applicable physiological model of the glucose-insulin-glucagon regulatory system providing 1) the necessary structural detail for the integration of multi-scale data, and 2) detailed mathematical descriptions of physiologic processes and properties. 3) It combines subcellular systems in one single model, 4) including detailed mechanistic description of distribution and action processes (thereby addressing system inherent time-delays, i.e. lag-times) and 5) it provides a generic framework for a-priori model-individualization. The generic mechanistic approach of PBPK models is therefore well suited to mechanistically link PK and PD at an organ and molecular level. Based on an accurate prediction (PBPK/PD) model of the individual's core dynamics of blood glucose levels [2], adapted over time using continuously gathered patient data, the MPC computes an optimal feed-forward control input. To increase closed-loop stability and robustness against disturbances and model uncertainties a PID-based feedback controller is used for compensation of prediction errors (offset).

After having evaluated the reliability of the developed PBPK/PD models of the GIM [2], and the integrated model predictive control approach [3] *in-silico*, two mono-centric, open, non-controlled feasibility studies in subjects with type 1 diabetes were conducted.

Whereas most control approaches [12, 13, 33-35], even semi-physiological MPC approaches using the UVa/Padova simulator [29, 30] or the Cambridge Model [31], only use insulin for closed loop glucose control, a new approach is bi-hormonal control, using glucagon in addition and as a counter-regulating measure to insulin to avert episodes of hypoglycaemia [26, 36, 37]. Although El-Khatib et al. have evaluated the efficacy of exogenous glucagon in treating hypoglycaemia [38], the relevance and influence of endogenous glucagon in the control of blood glucose in T1DM is diversely discussed [39]. Even though no exogenous glucagon was used for control, blood glucagon levels were measured.

Retrospective analysis of insulin and glucagon measurements collected during the trial, revealed significant glucagon surges, which were observed postprandial and coincided with severe insulin resistance for some patients. It has been reported that postprandial glucagon surges may occur in individuals with T1DM [40], however, no strong evidence for postprandial glucagon was found in previous studies [2, 26, 36]. A structural mode-of-action evaluation was conducted to analyze the role of glucagon in the "dawn-effect" [41, 42] in T1DM and to evaluate the relevance of glucagon for glycaemic control (in T1DM).

Here, the results of model development and validation, *in-silico* evaluation of the developed model-based control concept and last but not least the clinical evaluation of the integrated control approach within in two 24h feasibility studies for automatic glucose control is reported. The studies have been designed as a feasibility study to evaluate for the first time the in-vivo performance of the algorithm, first using accurate i.v. blood glucose measurements and in the second study using commercially available continuous glucose monitors (CGM), in a sedated scenario including four meal challenges.

I.2 Outline

This work describes the development of a new control approach, combining a detailed generic whole-body physiology-based pharmacokinetic/pharmacodynamic (PBPK/PD) model [2], with a robust MPC algorithm for automatic glucose control which was subsequently tested within clinical trials. The work is composed of three major parts with Part I providing details of the developed model, describing modelling methodologies and tools as well as a detailed description of the relevant model equations and the methods used for model individualization, 2) Part III describing the control concept and the developed algorithm in detail and lastly 3) Part IV, documenting the detailed results of two 24h feasibility clinical trials/studies for the validation of the integrated control system. As listed above, these three main outcomes have been published, are, or will be submitted in peer-reviewed journal articles [2-4].

After providing background information in Part I, Part II starts with a brief overview on state-of-the-art in glucose modelling in Section II.1. Section II.2 gives an introduction into modelling tools and then describes the model development and the used material. Model development is described in detail in Section II.2.1. A description of modelling tools, data used for model development as well as background information on the physiology and pathophysiology of the glucose metabolism is provided in Section II.2.2 (and Appendix V.5.2.1.2). Results of the model prediction performance are presented in Section II.3.

Part III describes in detail the integrated control concept. State-of-the-art in control algorithms used for glucose control and the most prominent representatives of glucose control systems are presented in Section III.1. Background information, challenges in glucose control and system integration as well as a detailed description of the implemented algorithm, and the methods used to improve control performance are described in Section III.2. Results of the *in-silico* validation and retrospective analysis of the control algorithm are then presented in Section III.3.

Part IV describes the clinical evaluation of the integrated Automatic Glycaemic Control (AGC) system within two 24h feasibility studies conducted at the Medical University of Graz. Section IV.1 gives an overview on the setup of the clinical trials. The results of the clinical trial are then presented in Section IV.2. The whole approach of combining a detailed generic whole-body PBPK/PD model, with a robust MPC algorithm for automatic glucose control is then discussed in Part V.

Part II.

Physiology-Based Pharmacokinetic / Pharmacodynamic Model

II.1 State of the Art in Glucose Insulin Models

The first simple mathematical models of the glucose-insulin metabolism (GIM) appeared around 1960 [27]. More advanced models appeared in the following years [43]. In 1979, Bergman and Cobelli et al. [1] published the “original” 3 compartmental Minimal Model of the GIM that can be considered a milestone and which is still subject to examination and criticism in these days [44, 45].

Since then, countless models were published trying to capture the dynamics of the GIM using different approaches. Attempts were made to:

- combine the advantages of existing models [46],
- stabilize model dynamics and improve physiological acceptance [47],
- derive detailed (glucose absorption) dynamics and equip the models for simulation studies [48-50],
- include transient physiological phenomena like changes in ultradian/circadian glucose metabolism and insulin action, as well as oscillations in secretion [50-53],
- derive/better characterize specific mechanistic properties (e.g. hepatic glucose dynamics) through specific experimental designs [54],
- model external influences like exercise [55] or
- use novel modelling techniques like population driven stochastic/Bayesian approaches [56-58] or data driven non-parametric (Volterra-type) models [59].

A review of model types (ODE, PDE, etc.) is given in [60] including parameter estimation techniques. A detailed review of PK/PD models with different modelling aspects in diabetes mellitus (e.g. effect of catecholamines, fatty acids, steroids and drugs) is given in [61]. Further models of the GIM are reviewed in [62] including exercise, closed-loop control strategies and global disease models. Up to date reviews of current simulation models used for blood glucose control in T1DM was published by Roman Hovorka [63] for in-silico evaluation and by Frank J Doyle [64] for in-vivo (i.e. clinical) application.

II.1.1 The “Minimal Model”

The first model of the glucose metabolism that had a remarkable influence on the scientific society was the “Minimal Model” developed by Bergman and Cobelli in 1979 [1]. Its main purpose was to assess the insulin sensitivity S_I and glucose effectiveness S_G in a human individual [65, 66].

The model was developed to describe the dynamics of the GIM during an intravenous glucose tolerance test (IVGTT) with simple equations (linear and second order mass action kinetics) and a minimal number of states and parameters. Over the years, a number of groups have adapted the “original” Minimal Model, adjusted, and even extended it according to their needs [44, 50, 67]. The model was used for meal tests [68, 69] and even in industrial applications [63] and extended to describe the dynamics of the oral glucose tolerance test (OGTT). A short review of the adaptations and extensions (including beta-cell function, insulin secretion and its dynamics on a molecular level) of the minimal model is given in [70].

II.1.2 Compartmental PK/PD Models of the GIM

Many of the compartmental models of the GIM evolved from the “Minimal Model”. In many cases existing models are augmented but new models are still developed and tailored towards the specific interest of each research group. Due to the vast impact of Diabetes on society, a number of research groups elevated the topic of the GIM to one of their main research areas [71-73].

II.1.2.1 The “ICING” Model (Canterbury Model)

A number of groups elaborated on the “original” functions of the Minimal Model to create their own version of a parsimonious model. For the “ICING” (Intensive Control Insulin-Nutrition-Glucose) model developed at the University of Canterbury by Chase et al., the Minimal Model was adapted by using nonlinear saturation dynamics (Michaelis Menten) for plasma insulin clearance and insulin-dependent glucose uptake. Hepatic glucose production as well as glucose uptake by the central nervous system was accounted for [74-77].

Chase et al. concentrated their research on blood glucose control in intensive care wards (ICU) developing simple but effective protocols for glucose management [74]. They are further working on the prediction of sepsis using model-based estimates of insulin sensitivity derived from blood glucose measurements [78, 79].

II.1.2.2 The UVa/Padova Simulator

This simulator was jointly developed by the University of Virginia, United States, and the University of Padova, Italy. The latest model version originally developed by Dalla Man et al. [29] *has been accepted by the Federal Drug Administration (FDA) to replace animal testing of glucose controllers* [30, 63].

The simulation model is made up of several parsimonious sub-models. There are two main subsystems in the model: the glucose subsystem, and the insulin subsystem, which are both described by a two-compartment model. The main novelty of this simulation model is a more detailed representation of glucose transit through the gastrointestinal tract. The main weakness, however, is that the diurnal variations, i.e. intra individual variability, of certain model parameters have not been modelled [63]. The model is published as a “mean” model [29] and in contrast to [31] no information on the inter-individual distribution of the model parameters (variability), which would be required for robust testing of glucose controllers, is given.

An overview of the up to date model equations (now including influences of physical exercise) can be found in the appendix of [80].

II.1.2.3 The Cambridge Model

Hovorka et al., one of the leading groups in diabetes modelling and control also work with compartmental models [81] of the GIM and use model based approaches to gain greater detail of the GIM (e.g.: glucose flux distributions during OGTT [82]; interstitial- and plasma glucose dynamics [83]).

The model consists basically of 3 sub-models. One for glucose dynamics (two compartmental), a second for insulin dynamics (4 compartmental with one for plasma insulin and 3 for interstitial insulin effects) and a third for oral glucose absorption (two compartments; a more detailed gut absorption model is used by Dalla Man [29]).

The current model (2008) is used for tight glycaemic control in critical care [31] as well as for continuous blood glucose control trials for (juvenile and adult) patients with T1DM mellitus (T1DM) [16, 84, 85].

In the early 2000s, Hovorka participated in the project “Advanced Insulin Infusion using a Control Loop” (ADICOL) [86]. His first, often cited approach of a nonlinear MPC approach with T1DM patients can be found in [24]. In [87], the ability of the MPC algorithm to regulate fasting blood glucose concentration in T1DM patients using the s.c.–s.c. route is tested. This method is compared with 2 own algorithms in [88]. The dataset generated within “ADICOL” was never published but has now been provided by the Medical University of Graz (MUG) for the use within this work.

Later, Hovorka started to focus his work on tight glycaemic control in ICU patients using time variant sampling [89] to estimate changes in insulin sensitivity. He compared the performance of tight glycaemic control with standard care [90]. In his present work, he still uses the same model in combination with an adaptive algorithm for the closed-loop system that is based on model-predictive control (MPC algorithm from [22]) [84].

II.1.2.4 Physiology-based Modelling

As mentioned, parsimonious models like the “Minimal Model” originating from classical PK/PD modelling did not represent human physiology in detail and semi-mechanistic modelling approaches with an increased level of detail have gained in popularity in recent years [62]. The above mentioned UVa/Padova simulator [29, 30] and the Cambridge Model [31] but also the AIDA simulator [91-95], a model initially developed for educational purposes, which can also be accessed and used via an online platform [96], contain physiological aspects. Although they can be considered as semi-mechanistic, they are not physiology-based, e.g. do not explicitly consider blood flows or organ volumes.

The latest physiology-based state-of-the-art model was developed more than 25 years ago by Sorensen [32]. This model already explicitly included details on blood flows and organ volumes and deduced processes for the distribution, metabolism and excretion dynamics of glucose, insulin, and even glucagon, the latter of which is neglected in most other models. The model is adapted to the dynamics of a mean T1DM individual and concepts for an optimal controller for glucose administration in T1DM patients under consideration of glucose measurement limitations are also provided. The mean diabetic patient was characterized by nineteen differential equations, with eleven describing glucose dynamics, seven for insulin dynamics, and a single compartment for glucagon. Drawbacks of Sorensen’s approach are missing detail on the organ level, and a missing framework for model individualization, making model individualization and adjustments to inter-individual variability (IIV) cumbersome, if not impossible. This may be the reason why on the one hand this model was used only for *in-silico* studies in closed loop control [23, 97-100], meal absorption [91] and exercise metabolism [101], but has never been used as a kernel for automated closed loop control in a clinical trial for individual patients, and why on the other hand current state-of-the-art models rely on a more parsimonious but easy to individualize model structure.

Since then (the work by Sorensen), no physiology-based model of the glucose-, insulin-metabolism has been published. The development of a new integrated physiology-based whole-body PK/PD model of the glucose-insulin-glucagon

regulatory system consisting of three coupled PBPK models for glucose, insulin, and glucagon, built on an easy to individualize modelling framework, will be presented here.

II.2 Materials and Methods

II.2.1 Physiology-based PK/PD Modelling

In the pharmaceutical field, an iterative process is established in which generic PBPK models are informed by experimental data, ranging from biochemical molecule properties over protein expression data to concentration time profiles. This multi-scale integration of experimental data is used to “learn” systems behaviour of the physiological question at hand and subsequently the informed model is used to predict outside of the experimental data space. Using this step-wise procedure, all experimental data can be effectively integrated into the PBPK model as it becomes available over time, as is the case in clinical development.

The coupled PBPK/PD model of glucose metabolism was developed using Computational Systems Biology Software Suite® 5.1.3 (PK-Sim® 5.1.3 and MoBi® 3.1.3), commercial software packages for PBPK and molecular biology modeling [102-104]. The detailed model is described in II.2.1.1. Model identifications and model parameterization have been conducted using the MoBi® Toolbox for MATLAB® 2.2 (PK-Sim®, MoBi®, and the MoBi® Toolbox for MATLAB® have been developed by Bayer Technology Services GmbH, Germany, available free of charge for academic use @ www.systems-biology.com; MATLAB® is a product of The MathWorks Inc., USA). A general description of the software platform including a detailed example of how to build coupled PBPK models and simulate virtual populations has been published [103, 105]. Model development is described in detail in Section II.2.1.1.

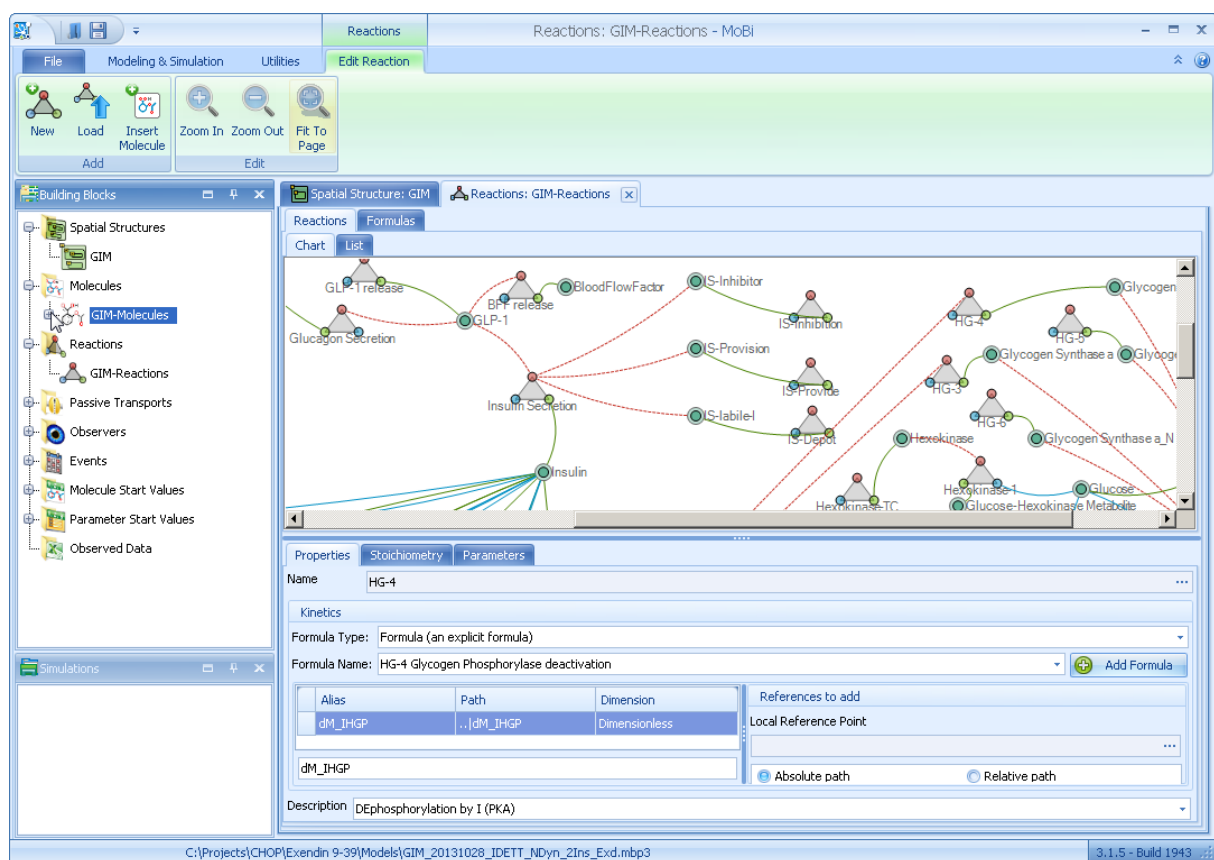


Figure 1: Graphical user interface of MoBi®

PK-Sim® provides a framework to efficiently implement all important absorption, distribution, metabolism and excretion (ADME) processes with a number of different basic model structures available for choice. PK-Sim® can be used generically because the model structure is independent from the substance to be examined, i.e. without modifying the underlying model structure, compounds can be defined and compound parameters can be modified [104]. PK-Sim® enables the simulation of drug distribution kinetics (PK) resulting from single and multiple applications of one drug at-a-time through all relevant routes of administration. Multiple single-compound PK-Sim® models can be linked in MoBi® for the development of coupled PBPK/PD models and can also be edited in MoBi® adding customized mechanistic sub-models, i.e. pharmacodynamic interactions (see Section II.2.1.1.3).

MoBi® is a tool for mechanistic and dynamic modelling of biological processes. It is fully compatible with PK-Sim®. Models that were created in PK-Sim® can be exported to MoBi® to be modified, extended, and/or coupled. By connecting PK-Sim® models in MoBi®, complex PBPK/PD models of models with interacting compounds such as glucose, insulin and glucagon in the glucose-insulin-glucagon regulatory system can be developed [103]. In this work, all models created with PK-Sim® were exported to MoBi® for coupling via the known PD interactions, as described in Section II.2.1.1.

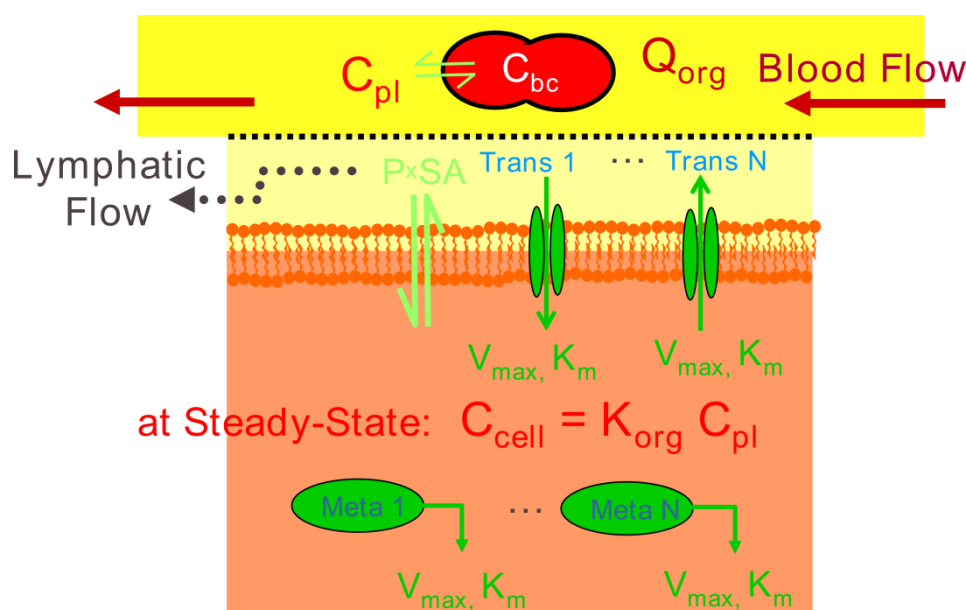


Figure 2: General mechanistic principles of an organ representation in PK-Sim® with four sub-compartments (intracellular, interstitial, plasma and blood-cells) and the corresponding flow rates and transports. C: concentrations, Q: flow rates, $P \times SA$: permeability surface area products, K: partition coefficient, V_{max} , K_m : Michaelis-Menten constants (Willmann et al, 2003 [102]).

The MoBi® GUI allows implementation of detailed mechanistic processes like reaction networks (compound metabolism or protein-protein interaction like signal transduction networks) or transport processes (diffusion or clearance processes). Furthermore, optimizations and sensitivity analysis can be performed by the integration of Matlab® via the MoBi® Toolbox for Matlab®.

Once a model structure is chosen based on substance properties, many parameters such as sub-compartment volumes or flow rates are calculated based on physiological knowledge contained in the software database. The compound properties then define the distribution behaviour within this whole-body framework

(Figure 2), mainly in terms of permeation and partitioning into the different sub-compartments. A detailed description of the distribution equations can be found in [103].

Starting with a general model overview, the following section describes in detail the development of the PBPK/PD model of the glucose-insulin metabolism.

II.2.1.1 Modelling the Glucose Insulin Metabolism

The strategy for the development of a computational kernel for individualised mechanistic models was to start with healthy subjects and then move towards modelling of subjects with diabetes. Although individuals with T2DM, in severe cases, do also use insulin replacement therapy, this work focuses on automated glucose control in T1DM. This was done mainly for two reasons: First, there is a lot more data available on subjects with T1DM than for T2DM and healthy individuals, and second, the glucose metabolism of subjects with T2DM is far more challenging to model due to co-morbidities and the multifaceted background from which the disease evolved.

The dynamics of glucose, insulin and glucagon are interdependent [106]. The models of each compound can thus not be developed separately [103] by first fitting the compound pharmacokinetics (PK) and then being coupled by the pharmacodynamic (PD) interactions. The models have to be developed together as an integrated PK/PD model of all three compounds.

II.2.1.1.1 Model Overview

The basis for the model is the combination of formalisms for drug distribution with the spatial structure of the physiology-based compartmentalization. The modeling platform [104] offers two formalisms for drug distribution: a 4-compartment model with reduced complexity [102] used for the calculation of small molecules, and a two-pore formalism model (describing endothelial diffusion using a porous-membrane model based on [107]) developed for large proteins (therapeutic proteins/biologics). As, insulin and glucagon are proteins 20 and 30 times the size of glucose, the two-pore formalism model was chosen as the common calculation method for all three compounds.

The rates of PK-Sim[®] default distribution processes as well as all additionally implemented transport and metabolism processes and PD interactions of the GIM model are implemented dependent on organ sizes to allow individualization, generally using allometric scaling considerations.

This is done by incorporation of a priori knowledge into the model that is relevant for predicting the pharmacokinetics of a drug in adults with varying anthropometric properties. Required knowledge on anthropometric properties includes the anatomical and physiological changes associated with age, weight, height, gender and race (e.g. age dependence or whole-body weight dependence of organ sizes, blood flows, etc.) as well as an understanding of how the activity of active processes (e.g. clearance processes, transporters), which affect drug pharmacokinetics, scale with relation to these properties. Once this adult PBPK model has been established, it can be used to extrapolate to individuals, be it adults, children or elderly outside the selected cohort [85].

The workflow for the model development was to use publicly available glucose-metabolism models as a basis and inspiration for the physiology-based PK/PD model (see Table 1). Due to the very detailed compartmental structure of the PBPK models

that are developed with PK-Sim® a strong physiological focus is paramount. After reviewing the literature, the physiological model developed by Sorensen [32] was used as an initial basis. The implemented pharmacodynamic interactions of the PBPK/PD model developed here are based on the Sorensen model equations. These pharmacodynamic interactions were extended and refined based on current biomedical knowledge and new experimental data. Data from literature, from a clinical partner (the Medical University of Graz (MUG)), and data collected during the clinical trials conducted within the framework of this thesis was used for model development. The latter also led to a redesign of pharmacodynamic effects of glucagon (Section II.2.1.1.3.1.2). Also, the model developed here provides a more detailed compartmental model structure with a powerful database and framework for model individualization which comes with PK-Sim®.

The concept of translating whole-body GIM physiology into a PBPK model structure is depicted in Figure 3A/B and, on a more detailed (mechanistic) organ and molecular level, in Figure 3C. The model components and sub-models, characterized by number of parameters (#P) and system states (#S) as well as their developmental history are listed in Table 1.

The glucose PK model features a detailed compartmental oral absorption model [108] reflecting gastrointestinal (GI) physiology such as anatomical dimensions and mucosal blood flow with explicit representations of facilitating and sodium-dependent glucose transporters 2 and 1 (GLUT2 and SGLT1). To reflect known glucose distribution physiology the model features tissue specific facilitating transporters (Figure 3C, h, GLUT-2,-3,-4) in liver, brain and periphery. The PBPK model for insulin was extended by an adapted version of a published subcutaneous (s.c.) absorption model [109, 110] to account for s.c. administrations. As literature data [111] and model simulations suggest that insulin distribution, i.e. extravasation, is an insulin-receptor (IR) mediated process [112], receptor-mediated transcytosis of insulin was implemented as PD dependent PK (Figure 3C, g). Similar as for insulin, the PBPK description of glucagon, a generally omitted [1, 31, 113] or lumped [32, 46] component in state-of-the-art models, was also extended by a s.c. absorption model.

The PBPK models are interlinked via detailed molecular PD mechanisms (Figure 3A/C, Table 1 lower half). As in Sorensen [32], the mathematical representation of the PD interactions is based on sigmoidal transfer-functions. The model features two additional key PD components. A model representing the incretin mediated effects following oral absorption of carbohydrates and an insulin receptor model within the insulin sensitive tissues, fat, muscle, and liver. The insulin receptor is the key mediator of insulin action but also clearance. It thereby couples PK with PD and reflects in a natural physiological way the observation that insulin action in insulin sensitive tissues correlates better with degradation than with delivery [117, 118]. Standard compartmental GIMs do not explicitly represent this dependency.

Model development was based on datasets from standard tolerance tests (glucose and insulin) [32] and a published clinical-trial dataset by El-Khatib et al. [36]. The respective simulation results are presented in Section II.3. First, the performance of mean models for healthy volunteers and T1DM patients are described. In a second part, evaluation results for individualized models based on the clinical-trial data are presented. Here, data from the first visit was used for parameter identification, and data from the second visit was used for model evaluation. Details on the model development are documented in Section II.2.1.1.

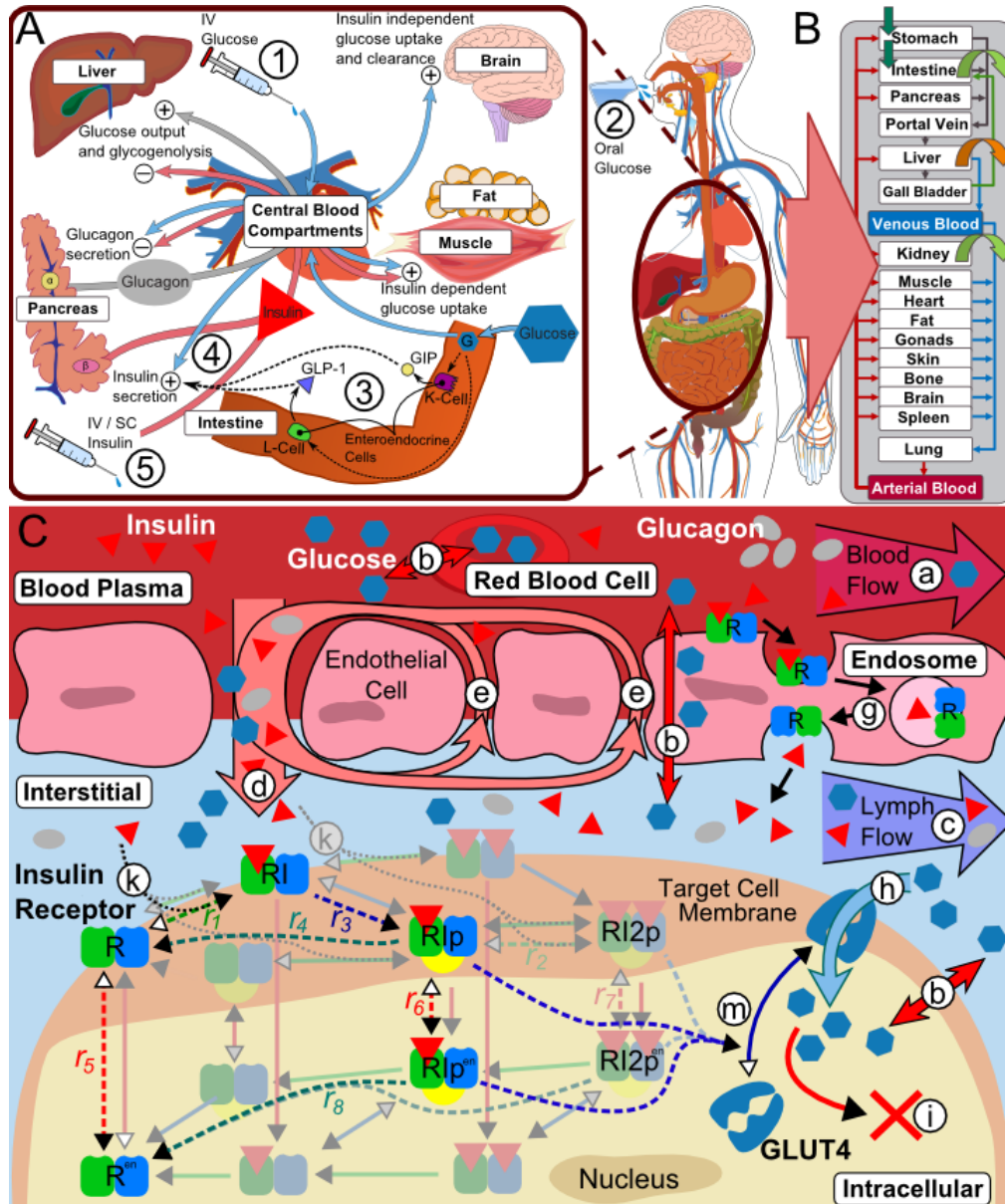


Figure 3: GIM structure overview. B) Organ-level structure of whole-body model: Each physiological organ translates to a compartment with several sub-compartments interconnected with convection and diffusion flows (see C). A) Overview on PD interactions: Glucose has self-regulating effects consisting of suppression of endogenous glucose production, insulin-independent glucose uptake, renal glucose clearance, and stimulation of pancreatic insulin secretion (4), as well as, during episodes of low glucose concentrations, the stimulation of pancreatic glucagon secretion. Insulin, as a glucoregulatory hormone, maintains glucose homeostasis by insulin-dependent glucose uptake in muscle and adipose tissue and suppression of endogenous (hepatic) glucose production as well as activation of hepatic glucose uptake. Glucagon, released at low glucose levels, counter-regulates low blood glucose levels, i.e. hypoglycemia, through stimulation of hepatic glucose production. Interactions of glucose, insulin, and glucagon vary depending on the type of glucose challenge and pathological conditions. In contrast to intravenous (i.v.) glucose (1), oral glucose (2) additionally triggers the incretin effect (3), which effects insulin secretion (4) via the secretion of gastric hormones (e.g. GLP-1) prior to glucose appearance in the blood. In T1DM insulin secretion (4) is no longer functional, necessitating the infusion of exogenous insulin (5) via the i.v. or subcutaneous (s.c.) route. C) Sub-organ-level and molecular details (a-m): Organs are divided into five sub-compartments (blood plasma and cells, endothelial endosomes, interstitial, and intracellular). All compartments are interconnected via passive convection and diffusion flows (a-e) and facilitative transports (h). Distribution of compounds is ultimately dependent on e.g. concentration gradients, flow rates, permeability, partition coefficients, transporter properties, and target protein binding properties [102]. Both insulin distribution and its glucoregulatory PD effects are influenced or mediated at the molecular level. Bound to insulin receptors

(IR) insulin is eliminated from the plasma (g) by trans-endothelial transport, and in the interstitial space (k) triggering molecular signaling in target tissues inherently coupling its PK and PD (k, m). Two receptor models from literature (Quon et al. [114], dashed lines; Koschorreck et al. [115], solid shaded lines) were evaluated. Adapted to the same organism and tissues (human fat, muscle, and liver), both models show similar responses to insulin stimulation [116]. Thus, the less complex model by Quon et al. was implemented in the PBPK model, curated and adapted to human physiology (un-shaded receptor-states, see Section II.2.1.1.3.3). At the molecular level, downstream signaling of the insulin receptor model in fat and muscle triggers translocation of insulin sensitive glucose transporter GLUT4, increasing peripheral glucose uptake (m, h).

Table 1: Overview of model components/sub-models giving a short description of used model components and the associated number of parameters (#P) and system states (#S). Models are described in detail in Section II.2.1.1 and referenced publications. Modified parameters are documented in Appendix V.5.1.2.

Model	#P	#S	Description	Source ^a
PK				
Base model				
PBPK models	~2000	~1000	Coupled protein (2-pore formalism) PBPK models for glucose, insulin and glucagon	None, developed within this work; for software see Eissing et al. [103]
Subcellular models				
Insulin Receptor	18	6x15	Published receptor model, neglecting the twice bound insulin receptor state; used for trans-endothelial transport of insulin in 15 organs.	Quon/Sedaghat et al. [114, 119]
Add. absorption models				
Oral Glucose Absorption	10	[-]	GI-Tract model integrated in the PBPK modelling platform (PK-Sim®) extended by facilitating glucose transporters in the small intestine.	Extension of Thelen et al. [108]
Insulin Absorption	6	3	Single shell representation (mainly used for fast-acting insulin) of a published model.	Tarín et al. [109, 110]
Glucagon Absorption	2	2	Parsimonious absorption model with unspecific binding and degradation reactions.	None, developed within this work
PD				
Base model				
PD interactions	34	2	PD interaction transfer functions, adapted and refitted.	Sorensen et al. [32]
Incretin Effect	10	2	Empirical model to describe the effect of oral glucose absorption on insulin secretion.	None, developed within this work
Subcellular models				
Insulin Receptor	22	6x3	Published receptor model, neglecting the twice bound insulin receptor state; used for target tissue effect of insulin in 3 organs (muscle, fat, and liver).	Quon/Sedaghat et al. [114, 119]
Insulin Secretion	12	3	Published insulin secretion model, implemented from literature.	Sorensen et al. [32]
Glucagon secretion	4	-	Published insulin secretion model, implemented from literature.	Sorensen et al. [32]

II.2.1.1.2 Pharmacokinetics

In this section, the pharmacokinetics, i.e. in simple terms the processes exerted on the drug by the body, the ADME of glucose, insulin and glucagon are described together with their mathematical representation in the model. The

pharmacodynamics, in simple terms the effects of glucose, insulin, and glucagon on the body, is documented in Section II.2.1.1.3.

II.2.1.1.2.1 PK of Glucose

Distribution of glucose, as shown in the schematic in Figure 3C, is mediated by the PK transport processes blood flow (a) and diffusion (b) and to a minor extent by two-pore transport (e) and lymph flow (c).

Facilitative processes for glucose uptake were implemented in the model to reflect known glucose distribution physiology via tissue specific facilitating transporters (Figure 3C, f); Sodium-dependent glucose co-Transporter-1 (SGLT-1) in the intestinal mucosa, Glucose Transporter 2 (GLUT-2) in the liver and intestinal mucosa, Glucose Transporter 3 (GLUT-3) in the brain, and insulin sensitive Glucose Transporter 4 (GLUT-4) was implemented in the insulin sensitive tissues fat and skeletal muscle.

Further, glucose is metabolized in all tissues in the intracellular compartment as well as in red blood cells and, at high plasma concentrations, excreted by the kidneys. The renal glucose excretion function was adapted from Sorensen [32].

II.2.1.1.2.1.1 Oral Glucose Absorption

The default PBPK model features a detailed generic oral absorption model structure [108, 120] reflecting detailed GI physiology such as anatomical dimensions, mucosal blood flow, local pH profiles, fluid secretion and resorption as well as entero-hepatic circulation [121]. The generic structure allows for (multiple) applications of multiple drugs to transit at any time, which is important for repeated food intake in combination with (anti-diabetic) drugs. Basolateral facilitating and apical active sodium-dependent glucose transporters GLUT2 and SGLT1 are added for glucose transit from lumen to the mucosal interstitial space [122-125].

The extent of the postprandial appearance of glucose in the blood is defined by the amount of carbohydrates (CHO) per meal [126]. The GI model accounts for food effects on gastric emptying time and intestinal transit times in the small and large intestine dependent on the caloric content, meal volume and the fraction solid of a meal [104].

Once absorbed, glucose is transported to the interstitial space of the mucosa by GLUT2 on the basolateral membrane of the enterocytes. Transport processes were modeled using Michaelis-Menten kinetics for SGLT1 and Convenience kinetics [127] for the bi-directional GLUT2:

$$SGLT1 = C_{SGLT1} k_{cat} f_{cell} V^{org} \frac{G_{lum}}{(K_m^{lum} + G_{lum})}$$

$$GLUT2 = C_{GLUT2} k_{cat} f_{cell} V^{org} \frac{k_{cat}^{cell} G_{cell}^{mus} - k_{cat}^{int} G_{int}^{mus}}{(1 + G_{cell}^{mus}/K_m^{cell}) + (1 + G_{int}^{mus}/K_m^{int}) - 1}$$

with transporter concentrations C_{SGLT1} and C_{GLUT2} , catalyzation constants k_{cat} for luminal SGLT1 uptake of glucose, k_{cat}^{cell} for GLUT2 transport of glucose from mucosa cellular to interstitial space, k_{cat}^{int} for reverse GLUT2 transport of glucose from mucosa

interstitial to cellular space, f_{cell} the volume fraction of mucosa cellular space, V^{org} the total volume of mucosal tissue, K_m^{lum} concentration for half maximal SGLT1 uptake rate of glucose from intestinal lumen, K_m^{cell} concentration for half maximal GLUT2 transport rate of glucose from cellular to interstitial space, K_m^{int} concentration for half maximal GLUT2 transport rate of glucose from interstitial to cellular space, G_{lum} luminal glucose concentration, G_{cell}^{mus} cellular mucosal glucose concentration, and G_{int}^{mus} interstitial mucosal glucose concentration.

K_m values were taken from literature [128] and set to 17 mmol/l (~300 mg/dl) and 0,2 mmol/l (~11,11 mg/dl) for GLUT2 and SGLT1, respectively. Values for absolute local expression levels $E_0^{Segment}$ in the respective segment of the small intestine and a global catalytic rate constant k_{cat} (giving $v_{max} = k_{cat} E_0^{Segment}$ [129]) of the SGLT-1 transporters distributed over the small intestine (duodenum, jejunum, ileum and caecum) have been fitted using the glucose appearance rate from the OGTT in [32]. The values identified (for a 70 kg male) are depicted in Table 4.

Accordingly, absolute local expression levels $E_0^{Segment}$ in the respective segment of the small intestine of the corresponding GLUT2 transporters were set to the same value. The estimated glucose appearance rate profile can be partially validated as the total amount absorbed from a OGTT corresponds to values that have been reported in literature (approx. 97-100% of total glucose administered) [32]. Also, the model predictions of glucose absorption from meals in the tested datasets were satisfactory.

Oral ingestion of glucose triggers a pharmacodynamic effect on insulin secretion and intestinal blood flow. This effect is called the incretin-effect and is described in II.2.1.1.3.5.

II.2.1.1.2.1.2 Organ Glucose Metabolization

Basal metabolization rates (Figure 3C, i) of glucose in brain tissue, peripheral tissue (fat and muscle), the liver, and red blood cells (RBC) were taken from [32], while the RBC metabolization of glucose was distributed over all RBC compartments. The metabolization rate of the periphery was divided between fat and muscle tissue and gut tissue metabolization was redistributed over all remaining passive tissues in the PBPK model. The first step in glucose metabolization (respectively glycolysis) is mediated by hexokinase:

$$C_{HK} V_{cell} v_{max} \frac{G_{cell}}{(K_m + G_{cell})}$$

With cellular concentrations of hexokinase C_{HK} , organ cellular volume V_{cell} , maximal rate of metabolization v_{max} , cellular glucose concentrations G_{cell} , and concentration value of half maximal rate K_m .

We neglected an explicit distinction of resting energy expenditure by both, age as well as sex, as effects are below 5% over 30 years and non-existent below 30 years, respectively [130]. The resulting cellular concentrations of hexokinase in each organ are listed in Table 4, Appendix V.5.1.2.

II.2.1.1.2.1.3 Glucose Transporters

The number of known glucose transporters (GLUT) which have been identified over the past years has increased considerably [131]. Besides facilitating glucose transporter GLUT2 and sodium-dependent glucose transporter SGLT1 in the small

intestine, GLUT2 in hepatic tissue, GLUT3 in the Brain and GLUT4 in insulin sensitive peripheral tissue are also included.

Rate of GLUT4-dependent glucose uptake is defined as saturating irreversible MM kinetics with a K_m -Value of 8 mmol/l ((144 mg/dl), approx. two fold above steady state of physiological glucose concentrations [128]). The v_{max} -value of GLUT4 is determined by the amount of GLUT4 translocated to the cell surface through the stimulation of insulin. This process is described in Section II.2.1.1.3.4.

The basal glucose uptake from the periphery, r_{BPGU} , i.e. fat tissue and skeletal muscle, amounts to approximately 35 mg/min for a mean adult male individual [32]. As adipose and muscular tissues are modelled separately, this basal rate is divided between those two tissues. Fat is reported to account for approx. 20% and muscle for approx. 80% of peripheral glucose uptake [132]. This is reflected by the relative distribution of amounts of GLUT4 available for translocation in the respective tissue.

GLUT2 in the liver is modelled as in the small intestine (see Section II.2.1.1.2.1.1). GLUT3 in the Brain was also implemented as a reversible Michaelis-Menten kinetics to overcome the blood-brain barrier and defined as:

$$GLUT3 = C_{GLUT3} k_{cat} f_{pls} V^{Org} \frac{k_{cat}^{cell} G_{pls}^{brn} - k_{cat}^{int} G_{cell}^{brn}}{(1 + G_{pls}^{mus} / K_m^{pls}) + (1 + G_{cell}^{mus} / K_m^{cell}) - 1}$$

with transporter concentration C_{GLUT3} , catalyzation constants k_{cat} , f_{pls} the volume fraction of brain vascular space, V^{Org} the total volume of brain tissue, K_m^{cell} concentration for half maximal GLUT3 transport rate of glucose from cellular to vascular space, K_m^{pls} concentration for half maximal GLUT2 transport rate of glucose from vascular to cellular space, G_{cell}^{brn} cellular cerebral glucose concentration, and G_{pls}^{brn} vascular cerebral glucose concentration.

II.2.1.1.2.2 PK of Insulin

Key features of the insulin PK model are the role of the insulin receptor in distribution and uptake/excretion of insulin and the absorption of subcutaneously (s.c.) administered insulin. Further, as a large molecule, passive diffusion of insulin is significantly reduced, thus increasing the relevance/impact of lymph flow, as well as endothelial convection and diffusion flows through endothelial pores [107], based on the hydrodynamic radius and the molecular weight of the compound.

Especially in insulin sensitive tissues like muscle, fat, and the liver, diffusion across the endothelial barrier is enhanced via receptor-mediated transcytosis [112]. In these tissues, uptake, metabolization, and excretion (or degradation) of insulin is also mediated by the insulin receptor (Figure 3C, k). Insulin receptor mediated clearance, besides glomerular filtration, is also involved in renal clearance, but not specifically accounted for within the PBPK/PD model. Renal insulin clearance, was modeled as a non-saturating plasma clearance process expressed in Fractions of the standard glomerular filtration rate.

Degradation and transport of insulin can be impaired by circulating levels of anti-insulin antibodies [133]. Effects of antibodies were modeled using the standard PBPK description of protein binding to compounds assuming quasi-stationary dynamics [104].

II.2.1.1.2.2.1 Subcutaneous Absorption

Injected insulin in the s.c. depot can transfer to hexameric and microprecipitated states, thus complicating the absorption process. As insulin is typically administered s.c. in clinical practice, the PBPK model for insulin was extended by a loose single compartment adaptation of a published s.c. absorption model [109, 110], here used only for the absorption of rapid acting insulin. Hexamerization is substituted for unspecific binding, as tendency of rapid-acting insulin to form hexamers is minimized [134]. The absorption model was implemented in a small fat-depot, with physiological properties identical to fat tissue as represented in PK-Sim®, which was added to the compartmental structure.

We added s.c. degradation, as it is reported that s.c. insulin has a bioavailability of below 100%. Degradation of s.c. insulin is not accounted for in the model of Tarín et al. [110]. However, insulin Lispro, which is used in this study, has a reported bioavailability of only 55-77% [135]. Although, other models of s.c. insulin absorption already account for s.c. degradation [136], the model used here showed the best results (data not shown). Transport of insulin monomer/dimer from the depot to plasma and through lymph was calculated by standard PK-Sim® distribution rates.

$$\begin{aligned}\frac{dI_{int}}{dt} &= u_{inj} - r_{bind} - r_{abs} - r_{degr} \\ \frac{dI_{int}^{bound}}{dt} &= r_{trans} \\ r_{bind} &= P_I(Q_{fact}Q_I I_{int} - I_{int}^{bound}) \\ r_{degr} &= k_{degr} I_{int} \\ r_{abs} &= \text{PK-Sim}^{\circledR} \text{ processes}\end{aligned}$$

with interstitial insulin concentration, I_{int} , bound interstitial insulin concentration, I_{int}^{bound} , rate of s.c. insulin infusion, u_{inj} , rate of s.c. unspecific insulin binding, r_{bind} , with binding affinities, Q , and rate constant, P_I , rate of insulin absorption from the s.c. depot, r_{abs} , which is described by the standard passive PK distribution processes from PK-Sim®, rate of s.c. insulin degradation, r_{degr} , with degradation constant, k_{degr} . The model concept of Tarín et al. [110] was designed for bolus injections and is unsuitable for the continuous mass flow of continuous insulin infusions as volumes for injection depots were calculated from the amount and concentration of the injected insulin, and thus only suitable for single injections. Switching to mass balances and dynamically changing volumes for continuous infusion on the other hand proved computationally exhaustive. Thus, for now, only a single static shell was retained. Effects of individual properties of s.c. tissue on hexamerization were fitted individually via the parameter Q_{fact} . The extent of s.c. degradation k_{degr} was also fitted individually. The default parameters [110] were scaled to the base unit [$\mu\text{mol/l}$].

II.2.1.1.2.2.2 Trans-endothelial Insulin Transport

The exchange across capillary walls in each organ is modeled using the 2 pore model formalism. The exchange across capillary walls is described by the two pore theory, assuming convection and diffusion through two types of pores [107, 137]. Compound-dependent parameters (permeability and osmotic reflection coefficients) are estimated from the hydrodynamic radius or the molecular weight of the compound. From the interstitial space the drug is transported back to circulation by lymphatic flow.

Model simulations show that the passive diffusion processes (2-pore transport and trans-membrane diffusion) across the vascular endothelium is too slow to account for observed peripheral plasma/interstitial concentration gradients [111], suggesting additional transport mechanisms. Additional unidirectional apical to basolateral trans-endothelial transport, mediated by insulin receptors (transcytosis), was implemented to take place in endothelial cells (via endosomes) of each organ [112, 138, 139]. Even for liver endothelium, extensive receptor-based transcytosis was observed suggesting the presence of a tissue-blood barrier in the liver [140]. Once ligands are bound to the insulin receptor in the endosome they are transported one-way from plasma to the interstitial space of the organs (Figure 3C, g). Receptor-based transcytosis of insulin uses the same receptor model as for target tissues but within the endosomal compartment. Endosomal degradation of insulin was neglected assuming a recycled fraction of 100%. Insulin is released into the interstitial space in parallel to reaction r_8 (Figure 3C) also with the rate of r_8 .

As insulin stimulates trans-endothelial transport, an insulin stimulated increase in endosomal insulin receptor transcription is assumed. A slow change in the rate of receptor transcription is assumed and thus the total amount of endosomal insulin receptor is scaled with the value for insulin sensitivity:

$$IR_0^{End} = \widehat{IR}_0^{End} S_I$$

With the default basal endosomal insulin receptor concentration \widehat{IR}_0^{End} and insulin sensitivity S_I . Further, endocytosis of insulin receptor to the apical membrane is stimulated by receptor phosphorylation:

$$k_{-5} = \hat{k}_{-5} S_I \frac{IRp_{total}^{End}}{IRp_0^{End}} = \hat{k}_{-5} \frac{IRp_{total}^{End}}{\widehat{IR}_0^{End}}$$

With the default endocytosis rate constant \hat{k}_{-5} [119], insulin sensitivity, S_I , and basal (IRp_0^{End}) and total (IRp_{total}^{End} , sum of edocytosed and membrane standing) phosphorylated insulin receptor.

II.2.1.1.2.3 PK of Glucagon

ADME properties for glucagon are less well understood as for glucose and insulin and glucagon kinetics are generally omitted in state-of-the-art models [1, 31, 113] or implemented using parsimonious models [32, 46]. Here a full PBPK description of the glucagon model is used. The model was only extended by processes for s.c. absorption and hepatic uptake, excretion, and metabolism and Dipeptidyl Peptidase-4 (DPP-4) associated plasma degradation.

Based on new insights gained from the clinical feasibility study conducted within the framework of this thesis (see Section IV.2.3, Figure 31), the original glucagon secretion function from [32] is extended by an incretin effect mediated component (Section II.2.1.1.3.5).

II.2.1.1.2.3.1 Subcutaneous Absorption

As for insulin, a reduced one-shell adaptation of the model by [110] was implemented into the PBPK/PD model structure for the s.c. absorption of glucagon. Parameter values were recalculated for the model base unit $\mu\text{mol/l}$.

The model consists of two states and two reactions. Molecular glucagon ready for absorption can react to an unspecific-bound glucagon state but is also subject to s.c. degradation to account for the low bioavailability, as glucagon reaches the systemic

circulation with a minor time-delay and a bioavailability of 35%-39% [141]. The model was identified using the glucagon data from the study by El-Khatib. The model is defined as follows:

$$\frac{dN_{int}}{dt} = u_{inj} - r_{bind} - r_{abs} - r_{degr}$$

$$\frac{dN_{int}^{bound}}{dt} = r_{trans}$$

$$r_{bind} = P_N(Q_N N_{int} - N_{int}^{bound})$$

with interstitial unbound and bound glucagon, N_{int} , and, N_{int}^{bound} , injected glucagon, u_{inj} , rate of absorption from the interstitial compartment, r_{abs} , which corresponds to the standard passive transports from a PBPK/PD model, the rate of unspecified binding r_{bind} , with binding affinity, Q_N , and rate constant, P_N , and s.c. clearance, r_{degr} . The default parameters [110] were scaled to the base unit [$\mu\text{mol/l}$].

II.2.1.1.2.3.2 Glucagon Clearance/Degradation

The mechanisms regulating degradation and clearance of glucagon from the plasma remain incompletely understood. The enzyme Neutralendopeptidase 24.11 in pigs [142, 143] and DPP-4 in vitro [144, 145] have been shown to degrade Glucagon. The kidney also remains as a major determinant for glucagon elimination [146]. Enzymatic plasma degradation (i.e. by DPP-4) has been implemented as:

$$CL_{int}/V_{pls}^{tot} \cdot f_{org}^{vas} (1 - HCT) V_{org} C_{pls} fu$$

with vascular organ glucagon concentration, C_{pls} , Hematocrit, HCT , total organism plasma volume, V_{pls}^{tot} , f_{org}^{vas} , the volume fraction of the respective organ vascular space, V_{org} , the total organ volume the fraction unbound, fu , of glucagon.

As insulin, glucagon is most likely cleared by the liver through receptor-mediated endocytosis. Due to the limited knowledge about glucagon receptor, a G-protein coupled receptor (GPCR), a simple representation of receptor dynamics in liver tissue was chosen. Glucagon is extracted from hepatic interstitial space when it binds to its receptor and cleared in the hepatic endosome upon receptor internalization. The receptor dynamics are defined:

$$\frac{dGPCR_{int}}{dt} = r_{rec} - r_{end} = - \frac{dGPCR_{end}^{bound}}{dt}$$

$$\frac{dN_{int}}{dt} = r_{end} + r_{PKSim}$$

$$r_{end} = k_1 N_{int} GPCR_{int} - k_2 GPCR_{end}^{bound}$$

$$r_{rec} = k_3 GPCR_{end}^{bound}$$

with rate constants k_{1-3} , free membrane receptor $GPCR_{int}$, bound and endocytosed receptor $GPCR_{end}^{bound}$, endocytosis rate r_{end} and receptor recycling rate r_{rec} .

II.2.1.1.3 Pharmacodynamics

The pharmacodynamic (PD) processes of the GIM model describe the direct and indirect interaction of glucose, insulin and glucagon. Pharmacodynamics can be either modelled as empirical/descriptive effect models, i.e. black boxes or as (molecular) mechanistic models. A number of interactions are described by the

threshold functions adapted from Sorensen et al. [32]. However, the insulin modulated functions are now modulated by concentration of activated (phosphorylated) insulin receptor. For this, an insulin receptor model adapted from Quon et al. [114] is included. For peripheral translocation of GLUT4, a simplification of the post-receptor signaling cascade model developed by Sedaghat et al. [119] is used. Further, model descriptions for the incretin-effect describing the PD effect of orally ingested glucose on insulin secretion and intestinal blood flow is added.

In many cases, enzymatic pharmacodynamic effects (i.e. mediated by a signalling cascade) are often described with empirical functions (or transfer-functions) that directly relate the applied input to the observed effect. Enzymatic interactions are often described by Michaelis-Menten or Hill equations [147]. For example, Figure 4 describes the relative change in hepatic glucose production as a function of hepatic interstitial glucagon concentrations. As described above, the generic modulating functions M used for the description of PD effects of glucose, insulin and glucagon were inspired by the threshold functions in [32] and are defined as:

$$M = V_0 + \Delta V_{max} \frac{(C_{rel} \cdot S)^{n \cdot S_R}}{(K_m)^n + (C_{rel} \cdot S)^{n \cdot S_R}}$$

with effector responsiveness S_R , effector sensitivity S , the relative effector (e.g. relative concentration of phosphorylated insulin receptors: IR_p/IR_p^0 , or interstitial glucagon or glucose) concentration C_{rel} , the reaction rate at zero concentration V_0 , the maximal change in the rate of reaction ΔV_{max} , the relative concentration of half maximal change in rate of reaction K_m and the cooperativity exponent n . The effect of changes in S_R , S and C_{rel} , are shown exemplary for glucagon-dependent hepatic glucose production in Figure 4.

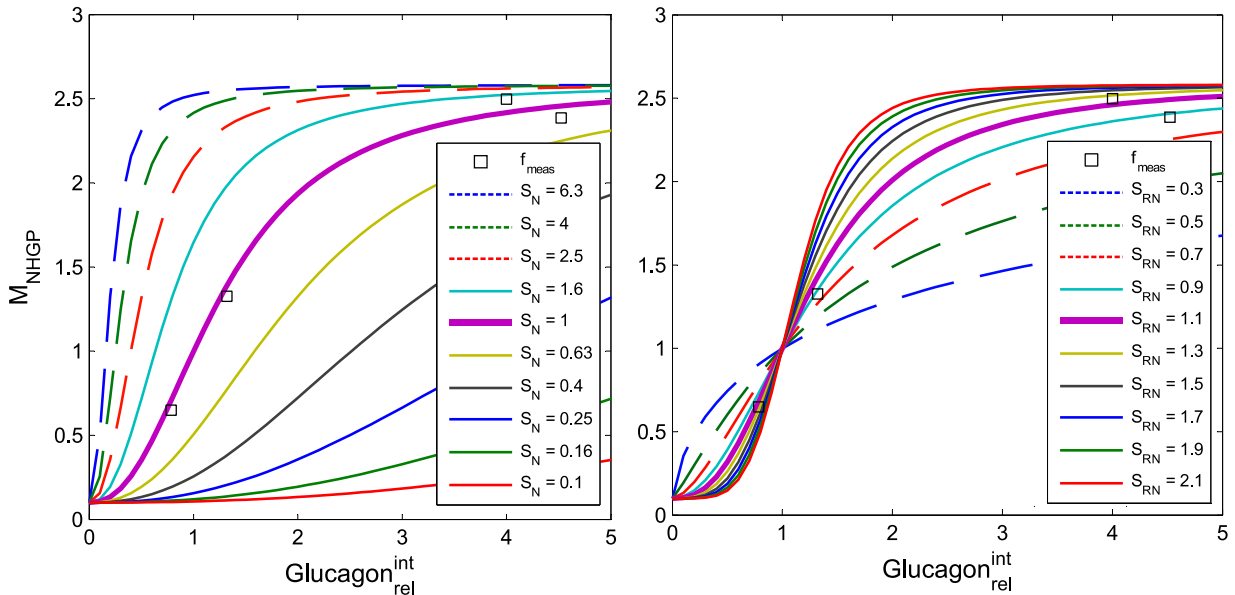


Figure 4: Exemplary illustration of how changes in the sensitivity (S , left plot, sensitivities ranging from 0.1 (flat) to 6 (steep), or right to left) and responsiveness (S_R , right plot, responsiveness ranging from 0.1 to 6, from flat to steep at (1/1)) of a PD function changes its properties. The thick line represents the PD function at $S=1$ (left plot) and $S_R=1$ (right plot) which is the same for both plots. Shown is the effect of glucagon on liver glucose production as modelled by the generalized Hill-function and corresponding data shown as squares (M_{NHGP} from Section II.2.1.1.3.1.2)

The reason why generalized Hill-functions were used instead of hyperbolic tangent functions for the description of the threshold function is the intuitive parameterization for changes in sensitivity and responsiveness. Here, only changes in the threshold functions in comparison to the functions used by Sorensen [32] will be described.

Functions for peripheral glucose uptake were replaced by the GLUT4 transporter subsystem (Sections II.2.1.1.2.1.3 and II.2.1.1.3.4). Earlier publications showed that glucose effectiveness of the original Sorensen model and other glucose models seemed to be excessive in studies with type 1 diabetes [45, 148] (no studies for healthy individuals available). Thus, glucose effectiveness was reduced to dampen the fast decrease from high glucose levels at basal insulin. Consequently the effect of insulin on glucose production was increased for low insulin levels and glucose uptake was increased for high insulin levels (Figure 5, Section II.2.1.1.3.1.1, and Table 4, Appendix V.5.1.2). Insulin PD functions are now dependent on concentrations of phosphorylated insulin receptor. Taking the time-delay of the insulin receptor subsystem into account, the time constant for the insulin PD functions was reduced from 25 min to 5 min. Changes are described in detail in the following section.

II.2.1.1.3.1 Liver Glucose Homeostasis

The liver is an organ that can both, store glucose and release glucose back into the blood stream. Glucose is mainly stored in the liver as glycogen and the liver is also capable of generating new glucose from proteins and pyruvate (gluconeogenesis). The liver is therefore responsible for maintaining a steady glucose balance, i.e. homeostasis, in the blood. The equations to describe (saturating) insulin, glucagon, and glucose-dependent glucose production and storage in the liver were implemented in the PBPK model and are described in the following. Again, for many of the following equations, the model by Sorensen [32] served as a template from which the final equations were derived.

II.2.1.1.3.1.1 The Effect of Insulin

Insulin exerts its effect in liver glucose homeostasis via two partly distinct pathways: the stimulation of hepatic glucose uptake (HGU) and the inhibition of hepatic glucose production (HGP). In the Sorensen model, the effects of insulin on HGU and HGP were implemented as modulating functions M_{IHGU} and M_{IHGP} using the hyperbolic tangent function. With the implementation of the insulin receptor model (described in Section II.2.1.1.3.3) the effector of both, M_{IHGU} and M_{IHGP} , were changed to the sum phosphorylated insulin receptor IR_p . The function of insulin-dependent glucose production (M_{IHGP}), here described once as an example for all modulating functions is thus defined:

$$M_{IHGP} = 3 - 2.95 \frac{\left(\frac{IR_p}{IR_p^0}\right)^{3 \cdot S_{RI}^{liv}}}{(0.78 \cdot S_I^{liv})^{3 \cdot S_{RI}^{liv}} + \left(\frac{IR_p}{IR_p^0}\right)^{3 \cdot S_{RI}^{liv}}}$$

with sum of phosphorylated insulin receptor IR_p , sum of basal phosphorylated insulin receptor IR_p^0 , liver insulin responsiveness S_{RI} , and liver insulin sensitivity S_I . As explained above, the insulin effect on glucose production was increased because at low insulin levels it was observed that glucose production was higher than previously assumed by Sorensen. The function of dM_{IHGP} is shown in Figure 5 (left).

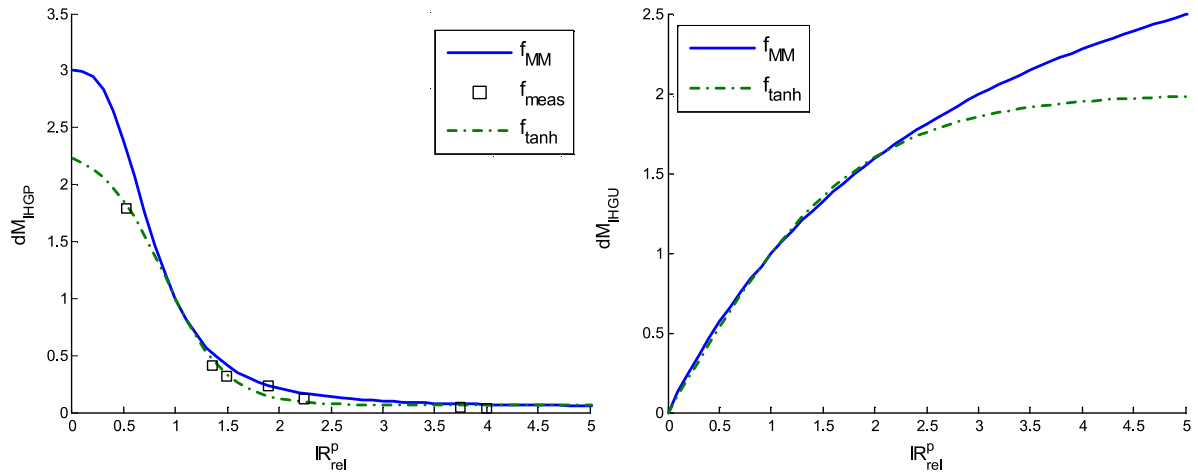


Figure 5: Corrected PD-function of dM_{IHGP} (left) and dM_{IHGU} (right). The green line represents the original hyperbolic tangent threshold function used by Sorensen. The blue line represents the refitted generalized Michaelis-Menten/Hill-equation used here. Measurement data as extracted from [32] is plotted as black squares.

Insulin-dependent glucose uptake is also adjusted. As the glucose effectiveness of the original Sorensen model is excessive [148], glucose effectiveness is reduced to dampen the fast decrease of glucose at basal insulin; consequently the insulin effect had to be increased (see Results, Figure 11, Section II.3.1). The resulting function of dM_{IHGU} is shown Figure 5 (right).

It is to be noted that in state-of-the-art models of glucose metabolism [149], basal hepatic glucose production for subjects with type 1 diabetes is adjusted (i.e. increased) to emulate the reduced hepatic exposure to insulin (see Section II.2.2.2.2). Given the physiologic structural detail of the model developed here, a different approach is taken. In healthy subjects, insulin is endogenous, meaning that the liver is exposed to high levels of insulin which is released from the pancreas in close proximity to the liver, and this proximity is actually reflected in the compartmental structure and connectivity of the model. In subjects with T1DM, where insulin is exogenous and the pancreas does not release insulin, the liver is exposed to a lower level of insulin and insulin control over hepatic glucose homeostasis is reduced. This natural distribution of insulin is thus accounted for in the physiology-based PK/PD model due to its detailed description of the human physiology and distributive fluid flows.

On the other hand, with exogenous insulin, the periphery is now exposed to a higher level of insulin compared to the healthy subject. Insulin may thus still exert almost its full inhibitory effects on hepatic glucose production by indirect means by reducing gluconeogenic precursor load or insulinization of the brain, thus activating a central nervous system signal to the liver [150]. However, this route of insulin action is difficult to quantify and has never been modelled before and is not included here.

II.2.1.1.3.1.2 The Effect of Glucagon

Glucagon kinetics may be deteriorated in subjects with T1DM [151]. As this may be the case only for some subjects, the effects of glucagon on glucose homeostasis are especially hard to be identified when using mainly clinical data from subjects with T1DM as it was done here. Due to the yet limited knowledge on the PK/PD of glucagon, initial implementations were based on the simple model from [32].

Based on the data gathered from the clinical feasibility study conducted within the framework of this thesis (see Section IV.2.3, Figure 31), the possibilities of glucagon not only affecting hepatic glucose production, M_{NHGP} , but also uptake, M_{NHGU} , was evaluated to assess if postprandial surges of glucagon, caused by the incretin effect (Section II.2.1.1.3.5) may explain temporary periods of insulin resistance in the early morning. However, no consistent explanation was found. Elucidating the role of glucagon in glucose homeostasis is thus an on-going effort. The parameterizations for M_{NHGP} and M_{NHGU} are listed in Table 4.

II.2.1.1.3.1.3 The Effect of Glucose

In simulation experiments (see Results, Figure 11, Section II.3.1) it was observed that the counter-regulation of glucose at the low and high end of glucose levels is generally too strong. Even at basal insulin (infusion of a basal rate in Subjects with T1DM assured a constant low basal insulin concentration) the decrease in glucose levels was immense. The values of the generalized Hill-function for M_{GHGP} and M_{GHGU} were thus reduced at the upper and lower end of glucose concentration scale, respectively, as can be seen in Figure 6. Parameterizations are listed in Table 4, Appendix V.5.1.2.

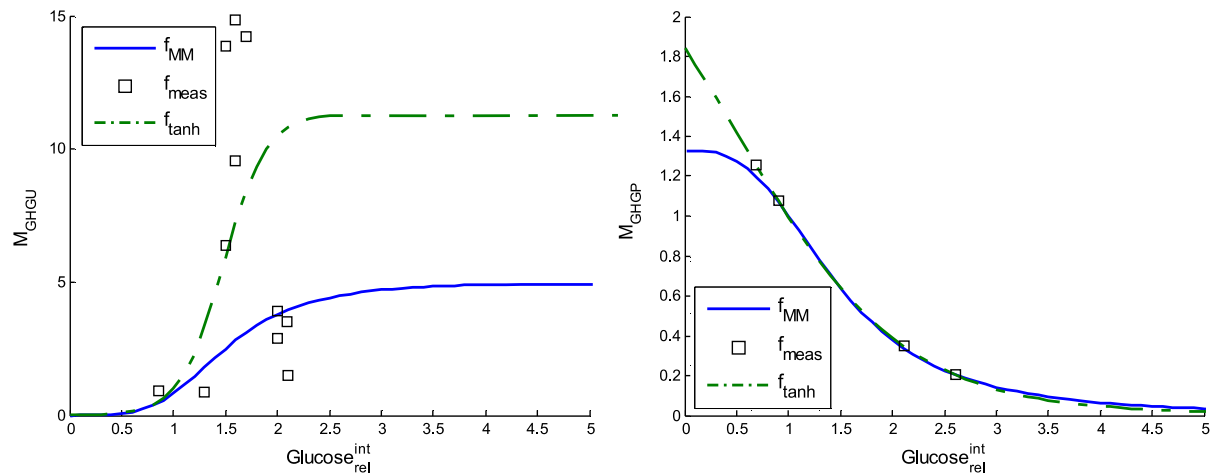


Figure 6: Corrected PD-function of M_{GHGU} (left) and M_{GHGP} (right). The green line represents the original hyperbolic tangent threshold function used by Sorensen. The blue line represents the refitted generalized Michaelis-Menten/Hill-equation used here. Measurement data as extracted from [32] is plotted as black squares.

II.2.1.1.3.2 Insulin Production and Secretion

The pancreatic islets are innervated by the autonomic nervous system and some of the pathways have been traced. Islet cells are excitable and their membrane potentials may oscillate. Glucose is transported into beta-cells through low affinity GLUT1 and GLUT2 (mainly GLUT1) plasma membrane transporters. However, this means of glucose supplementation are inefficient at basal blood glucose concentrations (5 mM) such that the cells are starved for glucose. Any increase in plasma glucose consequently increases glucose availability within the cells.

Glucose phosphorylation in beta-cells uses low-affinity glucokinase. The enzyme is not saturated with its substrate. The phosphorylation rate varies with intracellular glucose concentration, so in beta-cells the glycolytic rate ultimately depends on the glucose concentration in arterial blood. This means that intra-islet ATP concentrations rise directly with arterial blood glucose levels causing Potassium

efflux channels to close which leads to a drop in potassium levels and depolarization and activation of voltage-dependent calcium channels. This leads to calcium spikes and action potentials triggering exocytosis and insulin release from stored secretory granules.

A pancreatic insulin secretion sub-model from Landahl and Grodsky [152], re-parameterized to the human metabolism in [32], was implemented in the PBPK model. A schematic of the model can be seen in Figure 7. The insulin secretion model was extended by incorporating the influence of incretins after oral glucose absorption as described in Section II.2.1.1.3.5.

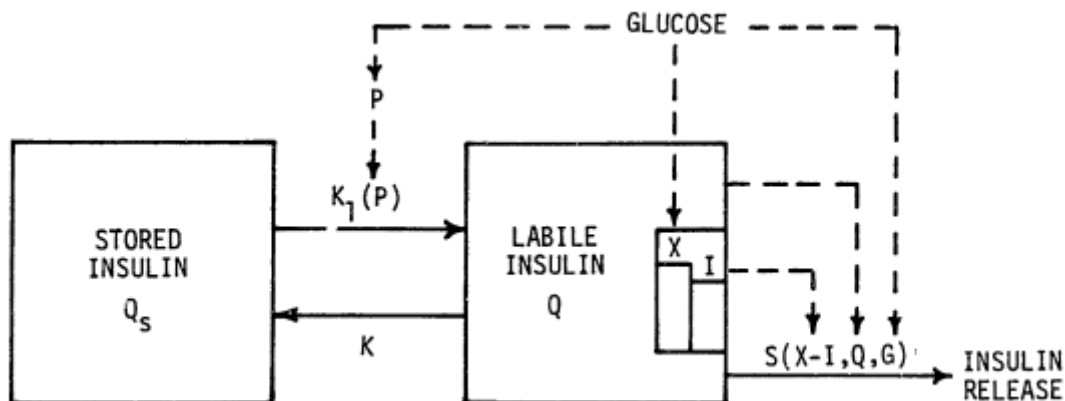


Figure 7: Schematic of the insulin secretion model developed by Landahl and Grodsky [78] taken from [32].

A small labile insulin compartment was assumed in exchange with a large storage compartment, with a glucose-stimulated provisional factor P regulating the rate of labile compartment filling. The rate of insulin secretion S is dependent on the quantity of labile insulin Q and the difference between a glucose enhanced excitation moiety X and its inhibitor I . The model was basically adapted in its original form for humans. Only the effect of incretins after oral carbohydrate absorption in non T1DM patients and a volume specific scaling factor to account for individual volumes of the pancreas was introduced.

Secretion is directly stimulated by the incretin GLP and probably via the vagus nerves by GIP. GLP stimulation of insulin release was integrated in the enhanced excitation moiety X and is described in section II.2.1.1.3.5.

For C-Peptide negative individuals with T1DM the insulin secretion model was deactivated. For individuals with T1DM and remaining basal secretion activity (C-Peptide positive) the insulin secretion model can be fixed at basal secretion rate.

II.2.1.1.3.3 Insulin Receptor Model

The importance of the insulin receptor for insulin PK and PD and the observation that insulin action in liver and adipocytes correlates better with degradation than with delivery [117, 118] made it necessary to evaluate the benefits of the implementation of a receptor model.

Two models of rat insulin receptor dynamics from literature [114, 115] were evaluated as the receptor model for the PBPK model. The model by Koschorreck et al. [115] was parameterized for hepatocytes and showed a 10 fold higher rate of receptor internalization. Once the model by Quon et al. was aligned to this rate, the dynamic

properties of the two models were too similar to discern their benefits for the PBPK model (data not shown). In the end, an adapted and curated version of the model by Quon et al. [114] was chosen due to the parsimonious structure. As only minor elements of the original literature model were adapted, only these changes are documented here. A detailed description of the original model can be found in [119].

The original receptor model was developed on the basis of insulin receptor dynamics in rat adipocyte including feedback mechanisms from receptor downstream signaling and receptor degradation and transcription. Both feedback mechanisms and receptor degradation and transcription were omitted in the present model development, as both properties were not validated properly in the original model. When tested, receptor degradation did not affect receptor dynamics in the time horizon it was validated in. Feedback mechanisms were also not included in the receptor model from [115].

When transferring a receptor model developed and verified for adipocyte cells in rats to human fat, muscular and hepatic tissue it has to be considered if:

- Kinetic parameters have to be adjusted when switching the model organism?
- Kinetic parameters and receptor concentrations vary in between tissue types?

Molecular structure of insulin receptors in the respective organism could differ, affecting its dynamic properties. No data could be found from which these properties could be inferred, thus two scaling parameters for receptor internalization (*IntFac*, multiplied with the original rate constants k_{4i} , k_{-4}) and receptor recycling rates (*RecFac*, multiplied with the original rate constants k_{4i} , k_6 , k_{-4}) are included.

For receptor concentrations in the different tissue types, literature values are available for hepatic and adipose tissue [115, 119]. Koschorreck et al. assumes the same concentrations for muscular and adipose tissue. However, in hepatic, fat and muscle tissue, insulin is cleared via receptor binding and internalization processes. The contribution of peripheral (muscle and fat) tissue to insulin clearance is relatively low but not negligible when compared to liver clearance rates (5-15% in comparison to 40-50% [118]).

From quantitative data on the receptor concentrations in muscle tissue of bovine heifers [153] the insulin receptor concentration in 16 month old heifers was calculated to amount to approximately 50 fmol/mg protein, which corresponds to a receptor concentration in muscle tissue of 10 nM, assuming a muscle protein content of 20% and tissue density of 1kg/l. For receptor internalization, a similar value as in adipocytes was assumed. Taking into account the approx. 10 fold difference in tissue volume (25 l of muscle volume compared to 2-3 l of liver volume) an approximate difference of factor 3 between muscle tissue and the liver was calculated, which corresponds well with clearance values found in literature [118] (15% periphery to approx. 50% liver).

These concentration values served as initial guesses and final receptor concentrations were fitted (Table 5) based on their contribution to insulin clearance (see above) and taking into account tissue specific insulin concentration gradients [111]. These two adaptations regarding initial concentrations and internalization rates were made when the receptor model was implemented in the PBPK / PD model of the glucose metabolism for humans. Downstream signaling and the translocation of GLUT4 transporters are described in the following section.

II.2.1.1.3.4 Peripheral Glucose Uptake

As mentioned in Section II.2.1.1.2.1.3, cellular peripheral glucose uptake is mainly managed by insulin sensitive glucose transporter GLUT4 [128, 132, 154, 155]. The specific glucose-dependent rate of GLUT4 mediated glucose uptake was modelled using irreversible MM-Kinetics. The V_{max} -Value of GLUT4 is determined by the amount of GLUT4 translocated to the cell surface through the stimulation of insulin. The processes involved in GLUT4 translocation is described in the following.

The translocation of GLUT4 to the cell surface is stimulated by a downstream signalling cascade of the insulin receptor model (which is described in Section II.2.1.1.3.3), as described and modelled for example in [119]. Describing the full post-receptor signal transduction cascade is not required here and is thus replaced by a simple single function. The rate of translocation is now directly stimulated via the sum of phosphorylated insulin receptors. The equations for the post-receptor signalling cascade are then defined:

$$\frac{dGLUT4_{cyt}}{dt} = -\frac{dGLUT4_{mem}}{dt} = r_{trans}$$

with cytosolic $GLUT4_{cyt}$ and translocated $GLUT4_{mem}$ and the translocation rate r_{trans} defined:

$$r_{trans} = k_{trans} \left(\left(k_1 + k_2 S_I \left(\frac{IR_p^{tot}}{IR_p^0} \right)^2 \right) GLUT4_{cyt} - GLUT4_{mem} \right)$$

with constants k_{trans} , k_1 and k_2 , insulin sensitivity S_I , and the total sum of phosphorylated receptors IR_p^{tot} . Total peripheral (here exemplary for muscle tissue) glucose uptake is defined as a generalized Hill-equation for the GLUT4 transporter:

$$PGU_{mus} = V_{max} \frac{\left(\frac{G_{int}^{mus}}{G_{0int}^{mus}} \right)^{S_{GR}}}{(2 \cdot S_G)^{S_{GR}} + \left(\frac{G_{int}^{mus}}{G_{0int}^{mus}} \right)^{S_{GR}}}$$

with actual and basal interstitial glucose concentrations G_{int}^{mus} and G_{0int}^{mus} , glucose responsiveness and sensitivity S_{GR} and S_G and rate of maximal GLUT4 dependent peripheral glucose uptake V_{max} , which is defined:

$$V_{max} = GLUT4_{PSF} (r_{BPGU}^{mus} k_{GLUT4} GLUT4_{mem}^{(2S_{RI})})$$

with the organ volume-specific scaling factor $GLUT4_{PSF}$, basal muscular rate of glucose uptake r_{BPGU}^{mus} (corresponding to 80% of total basal peripheral glucose uptake as described in Section II.2.1.1.2.1.3: $r_{BPGU}^{mus} = 0.8 \cdot r_{BPGU}$), insulin responsiveness S_{IR} , and concentration of translocated $GLUT4_{mem}$.

II.2.1.1.3.5 The Incretin Effect

Here, the influence of oral glucose on the secretory profile of gastric hormones (incretins) and their effect on the GIM, more specifically on insulin secretion, is described in detail.

Glucagon-like peptide 1 (GLP) is not modelled as an actual drug concentration with an individual PBPK model but rather as a state describing the overall incretin effect. It

is augmented in relation to the total (sum of all intestinal SGLT-1 transport rates) SGLT-1 glucose uptake rate using saturating dynamics and decreases according to a first order rate law, representing a simple clearance process:

$$\frac{dGLP}{dt} = -k_1(GLP - GLP_0) + k_2 * \frac{r_{GA}^2}{K_m^{r_{GA}^2} + r_{GA}^2}$$

The effect of GLP on insulin secretion, as mentioned in Section II.2.1.1.3.2, was implemented, like glucose, as an additional increase in excitation moiety X of the insulin secretion model from Section II.2.1.1.3.1:

$$X = \frac{G^{3,27}}{G_0^{3,27} + 5,93G^{3,02}} + \frac{K_{GLP}GLP^3}{K_m^{GLP^3} + GLP^3}$$

This function was developed using data published in [32] of a 100 g OGTT. In [32] the necessary insulin secretion profile was estimated (omitting the pancreatic insulin secretion model) from the measured insulin concentrations in the peripheral venous blood. In a second step, the needed glucose appearance rate in the portal vein from gut glucose absorption was estimated from the measured glucose concentrations in the peripheral venous blood. The parameters k_1, k_2, K_m and K_{GLP}, K_m^{GLP} were fitted based on the estimated glucose absorption rate and by forcing the actual insulin secretion rate to the estimated necessary insulin secretion profile from [32] (see Figure 11 D).

It has been reported in literature that mixed meals may cause glucagon surges in individuals with T1DM [39, 156]. This may be caused by meal composition and especially the protein content of these meals. (In T1DM, influence of glucose levels on glucagon secretion subside over time probably due to a deficiency in amylin-mediated intra-islet signalling necessary for glucose sensing [157]).

Whereas this was not observed in early datasets used for model development (El-Khatib dataset [36], Section II.2.2.1), significant postprandial glucagon surges were observed in the data gathered from the clinical feasibility study conducted within the framework of this thesis (see Section IV.2.3, Figure 31). The original version of the model as it was used in the control trial did not account for this behaviour. To better describe the observed glucagon dynamics, incretin-dependent prandial glucagon secretion was modelled dependent on oral meal (glucose) absorption.

In addition to the multiplicative modulation function for insulin and glucose-dependent glucagon secretion (M_{IPNR} and M_{GPNR}), a modulation function for GLP-1 was included (multiplicative), which only increased glucagon secretion for GLP-1 concentrations above basal level:

$$M_{GLPNR} = 1 + k_{GLPNR}GLP$$

with scaling constant, k_{GLPNR} . However, as discussed in Section V.1, no consistent explanation could be found. Elucidating the role of glucagon in glucose homeostasis is an on-going effort. The parameterizations for incretin mediated glucagon secretion are listed in Table 4.

II.2.2 Datasets and Model Individualization

For the development and individualization of the generic whole-body physiology-based pharmacokinetic/pharmacodynamic model kernel of the glucose-insulin-

glucagon metabolism, an extensive amount of data as well as a good understanding of inter- and intra-individual diversity in physiological properties is required.

In the following sections a brief overview is given on the two main datasets used as well as a review is given on the physiology and pathophysiology relevant for distinguishing healthy and diabetic populations and model individualization.

II.2.2.1 Clinical Trials Datasets

The two main datasets of full day clinical trials in a controlled clinical environment have been used for model development and validation and also for development and *in-silico* as well as retrospective validation of the AGC system. Results obtained with the respective datasets are documented in Sections II.3 and III.3.

In 2010 a detailed dataset of a clinical bi-hormonal closed-loop glucose control trial was published by El-Khatib et al. [36]. This dataset contains 30 hours of measurement data of glucose insulin and glucagon per visit and patient from 8 subjects with two clinical visits each (glucose measured every 5 min for closed loop control and once per hour for control measurements. Insulin and glucagon measured every 15-30 min retrospectively). Subjects were required to be 18 years of age or older and diagnosed with T1DM at least 5 years before enrolment. They had to have a HbA1c of <8.5%, have body mass index between 20 and 31 kg/m², and be treated with an insulin pump with a total daily insulin dose of <1 U/kg. Potential subjects were excluded if their C-peptide after a mixed-meal challenge was >0.03 nM. Other exclusion criteria are detailed in the supplementary material Note 4 of [36]. An exemplary extract from the dataset from the supplementary material is shown in Figure 8.

The study was a bi-hormonal control trial with both insulin and glucagon used for glucose control. Both hormones were administered via the subcutaneous route and glucose interventions were administered (15 g) intravenously. All measurements of glucose, insulin, and glucagon were taken from venous blood samples. Thus, blood glucose was controlled via the i.v.-s.c. route and not via the more challenging s.c.-s.c. route. Also, for the second visit, the internal PK-model of insulin was re-parameterized based on the measurements from the first visit.

Subjects received meals for dinner, breakfast and lunch with a fixed nutritional composition from carbohydrates, fat and proteins. The full details can be found in [36] and the supplementary material thereof.

The second dataset from MUG was collected from 12 patients during a 2-phase randomized crossover trial with patients with T1DM in 2004 (unpublished) and kindly provided for the purpose of this research. The trial was conducted for the comparison of conventional insulin pump therapy, i.e. continuous subcutaneous insulin infusion (CSII), and an insulin dosing algorithm, i.e. model predictive control algorithm (MPC), for the control of blood glucose in the everyday life of patients. The dataset was generated within the project “Advanced Insulin Infusion using a Control Loop” (ADICOL) [86] using the MPC from Hovorka et al. [24]. Relevant information of the trial is summarized below, as extracted from an unpublished internal report of MUG.

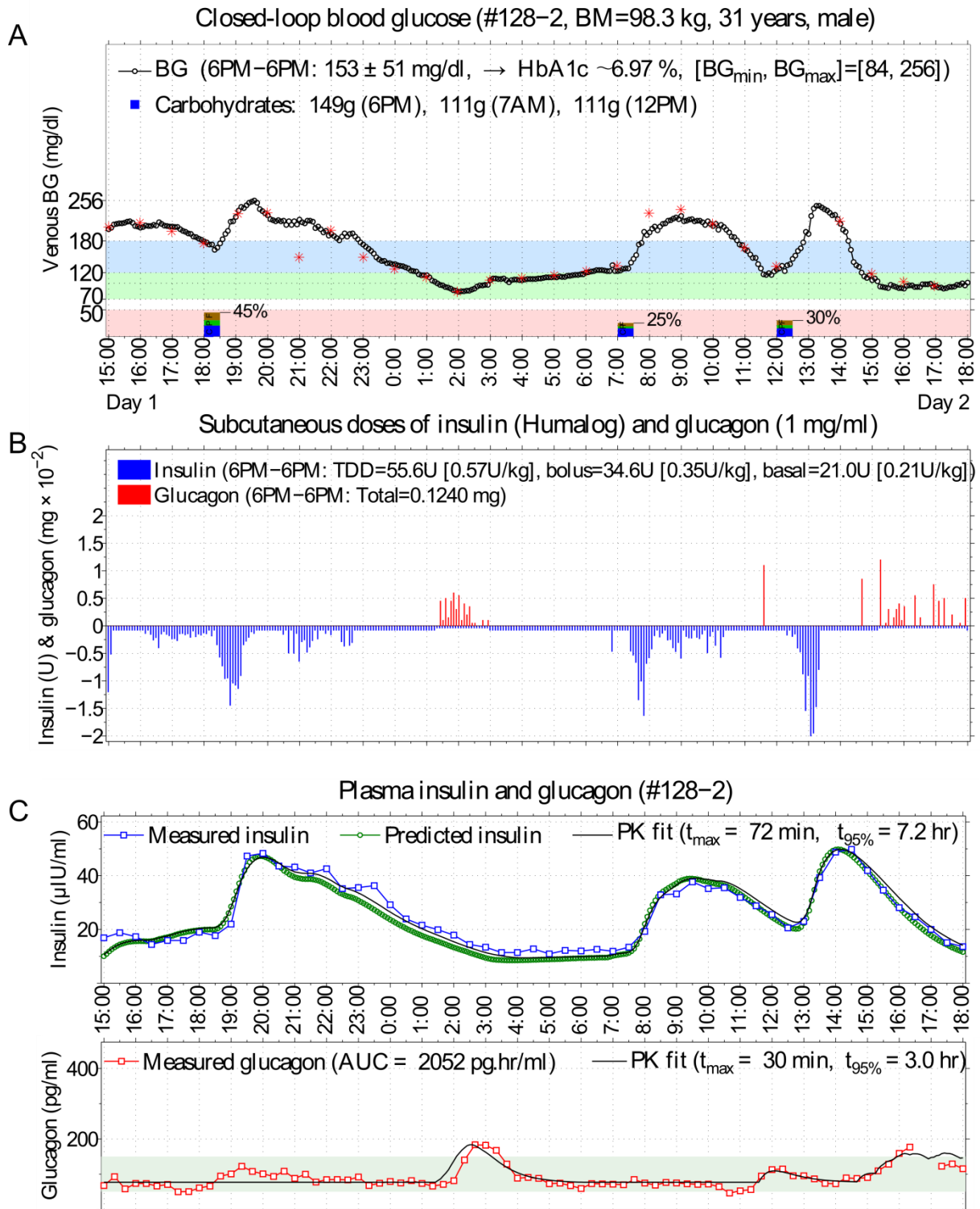


Figure 8: Exemplary dataset from El-Khatib et al. of the second closed-loop experiment with Subject #128 with slow insulin PK parameter settings (based on measurements of the first closed-loop experiment). No carbohydrate intervention was required during this control run. Shown are the i.v. measurements of blood glucose and administered meals (A), the administered amounts of insulin and glucagon (B), and the retrospective measurements of plasma insulin and glucagon as well as their fitted simulated PK-profiles (C). From [36] (Supplementary Material Figure S21) Reprinted with permission from AAAS.

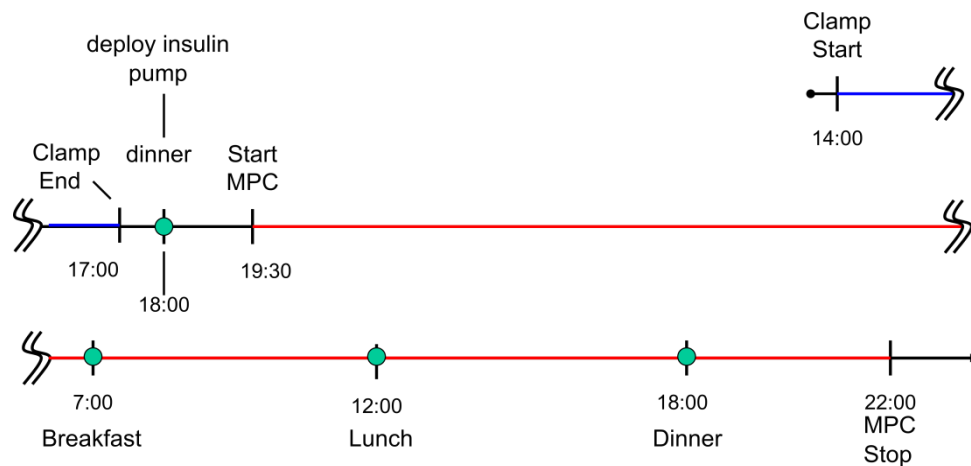


Figure 9: Protocol of the 2-Phase RCT at MUG. Marked are the three phases: 1) Clamp phase in blue (3 hours) 2) supervised phase with 1 meal in black (2.5 hours) and 3) actual phase of blood glucose control with 3 meals marked in red.

The trial started with a 3 hours glucose clamp phase, during which the blood glucose of the patients was brought to a target level of 100-140 mg/dl. During the second phase, the observation phase, patients were closely supervised for 2.5 hours and received 1 meal (dinner). This was followed by the 3rd and last phase during which blood glucose was controlled for 26.5 hours by either the CSII or MPC algorithm. During this last phase, patients received 3 meals, breakfast, lunch, and dinner. The trial protocol is depicted in Figure 9. Throughout the trial, patients received oral glucose intervention of 12 g in the form of orange juice (100 ml) if they went hypoglycaemic by either reaching blood glucose levels below 60 mg/dl or if the patient felt the need.

ADICOL04 Graz Subject 2 MPC

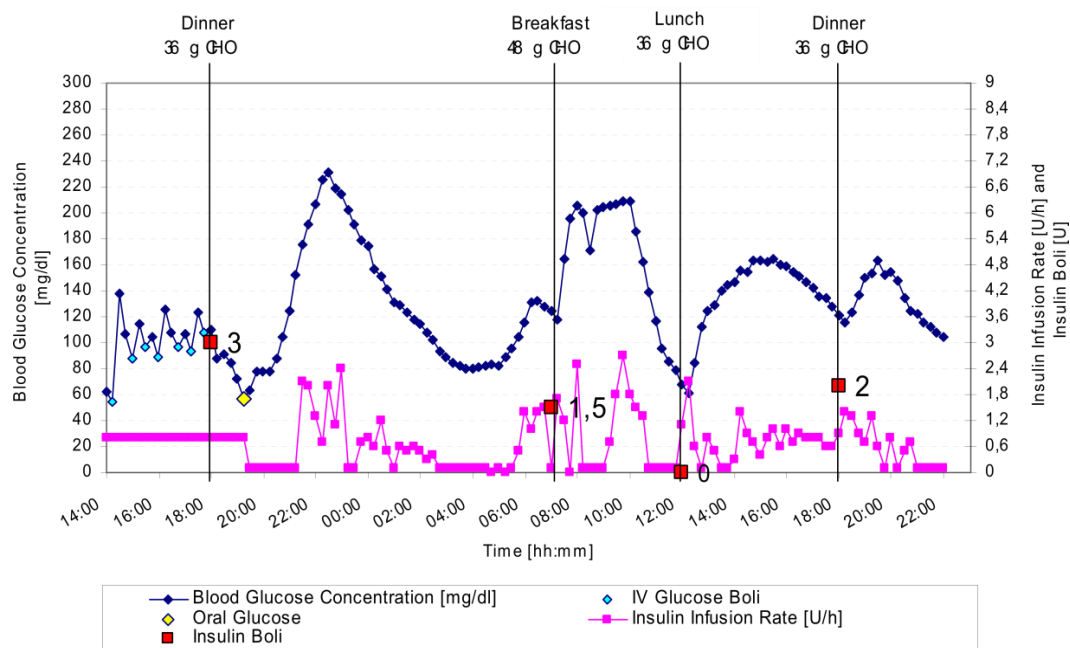


Figure 10: Exemplary dataset of the 2-phase RCT at MUG. Depicted is the dataset from Subject 2 undergoing glucose control by the MPC algorithm. Blood glucose measurements (mg/dl) are depicted in blue, while insulin infusion rates (U/h) are depicted in pink.

Glucose measurements were taken intravenously, although for the trial a simulated s.c.-s.c. route was mimicked by delaying glucose measurements by 30 min. Insulin was administered subcutaneously. Every 15 min blood glucose measurements were taken and the insulin infusion rate was adjusted according to the respective algorithm. An exemplary Datasheet is shown in Figure 10.

The dataset provided by MUG was used not only for model development and validation, but also for *in-silico* controller evaluation as described in Part III.

II.2.2.2 Individual Properties

One possible route to the development of an AP for the individual diabetes patient is through control algorithms using mathematical modelling and computer simulation. A number of simulation models have been proposed in the last 4 decades and used to assess the performance of control algorithms and insulin infusion routes, some of which have been presented in Section II.1. However, many of these models are only able to simulate mean population dynamics but do not account for inter-individual variability. Mean models are not sufficient for realistic *in-silico* evaluation of control scenarios [14] and short-term risk analysis. For this purpose, model kernels that allow the simulation of inter-individual variability in physiological properties such as key metabolic parameters and drug distribution parameters are required. The knowledge on inter-individual variability is indeed crucial to the design of robust controllers, providing valuable information about their safety and limitations.

In the following sections a brief overview is given on the implications of inter-individual (patho-) physiological changes, extremes of which occur during diabetes, obesity, sickness and stress, on the individualization of a glucoregulatory model. These implications are to some extent similar to the influences of differences in individual physiology on the glucoregulatory system. For an in-depth review on physiological changes associated with insulin resistance, please refer to Appendix V.5.1.1.

II.2.2.2.1 Insulin Resistance

The term “Insulin Resistance” describes a reduction of “Insulin Sensitivity” and is usually used to refer to the defective regulation of carbohydrate metabolism by insulin. Insulin sensitivity is characterized as the “gearing” ratio for insulin-dependent glucose uptake in muscle, adipose and hepatic tissue. Insulin resistance has been quantified by numerous methods [158], usually by measuring the amount of glucose infused to maintain euglycaemia at a fixed insulin concentration (glucose clamp). The main consequences of insulin resistance include [159]:

- Impaired insulin-dependent down-regulation of hepatic glucose release.
- Impaired insulin-mediated increase in peripheral (muscular, adipose) glucose uptake.

A reduction in insulin sensitivity, called a state of insulin resistance, therefore impairs the body’s ability to control its blood glucose levels and reduce hyperglycaemia. The causes for the reduction in insulin sensitivity are many-sided, making insulin sensitivity a multi-parametric property.

In general, the interaction of signalling proteins, including insulin itself, with the insulin signalling pathway are thought to cause these changes in insulin sensitivity. Known mechanisms to reduce insulin sensitivity are reduction in receptor transcription and

receptor translocation or effects on downstream signalling like serine phosphorylation of insulin receptor substrate-1 (IRS-1) or activation of protein kinase C (PKC). Several of these crosstalk signalling pathways are known [158].

Within the GIM model, changes in insulin sensitivity (and similar for glucose and glucagon sensitivity) are expressed within the global fitting parameter $S_{(I)}$. This parameter is part of most pharmacodynamic functions (see Section II.2.1.1.3) mediating the effect of insulin (and glucose and glucagon) on target tissue glucose metabolism.

II.2.2.2.2 T1DM

T1DM is characterized by the destruction of insulin secreting pancreatic beta-cells during a selective auto-immune reaction [106]. Whereas this happens in most cases at a very young age, T1DM can also be developed as late as at the age of 40. Due to the loss of endogenous insulin, blood glucose levels, left untreated, can climb to 5 to 10 times normal. Fat metabolism in liver and kidney is increased to substitute for the loss of energy provided by glucose metabolism, producing ketone bodies as by-products. These keto acids are moderately strong acids and can be toxic at high levels.

A key difference between subjects with type 1 diabetes and healthy subjects is, from a modelling perspective, the distinctive route by which insulin is provided to the body. Whereas insulin in healthy subjects is released by the pancreas into the portal vein, subjects with Diabetes receive exogenous insulin via subcutaneous (or IV) injections. This means that in healthy subjects the liver is saturated in insulin, compared to subjects with T1DM, where insulin basically only part wise stimulates the full glucose-lowering capabilities of the liver.

The important question for model development is how this could affect the physiology and hence the parameterization of the model. Semi-physiological models like the UVa/Padova Simulator [29] assume an increase in basal glucose concentration of in average 50 mg/dl compared to healthy subjects and also steady-state insulin concentration (due to an external insulin pump) is assumed to be on average (four times) higher than in healthy subjects. To achieve this, they changed parameters for basal endogenous glucose production (+ 35%) and steady-state insulin clearance (- 33%) as well as parameters relating to insulin action on both glucose production and utilization (- 33%) as compared to subjects in health [160].

However, it is known that stimulation with insulin reduces receptor expression but increases receptor recycling rates [161-163]. The detailed description of the human physiology and distributive fluid flows within the PBPK/PD model result in the naturally expected change in insulin concentration levels at the target tissue following a shift from endogenous to exogenous insulin supply. Fits for the PBPK/PD model show that the reduced hepatic insulin levels in T1DM result in an increased receptor expression, but reduced recycling rate, in-line with the experimental observations, delivering a physiological explanation for the changes during disease progression (Results Section II.3.2, parameter sets for healthy vs. T1DM are listed in Table 5).

II.2.2.2.3 Absorption

As described in Sections II.2.1.1.2.2.1 and II.2.1.1.2.3.1 insulin, and also glucagon for bi-hormonal control, are typically administered s.c. in clinical practice. Injected insulin in the s.c. depot can transfer to hexameric and microprecipitated states or

undergo unspecified binding, as does glucagon, thus complicating the absorption process. Further, bioavailability of both, insulin and glucagon, are far below 100% [135, 141]. Depending on the individuals tissue composition and the injection site for insulin and glucagon, absorption is subjected to a high degree of inter- and –intra-individual variability with respect to binding properties and local degradation [164, 165]. As intra-individual variability is mostly due to a change in injection site, this is not of relevance here, as patients use insulin pumps, for which the location of injection is not altered during a trial.

Effects of individual properties of s.c. tissue on unspecific s.c. binding were fitted individually via the parameter Q_{fact} . The extent of s.c. degradation k_{degr} was also fitted individually.

II.2.2.3 Model Identification

In an identifiable (PK/PD) model, all parameters are uniquely determinable if the required measurement data is available. In an analytical sense, this is called structural identifiability, if the data is not subjected to limitations such as noise or sample size. This means that the uncertainty in the data determines the uncertainty in the model parameter estimates. In a practical sense, i.e. practical identifiability, parameter uncertainty is quantified considering the data set and deemed practically identifiable, if the remaining uncertainty is acceptable [166]. For classical PB/PK models analysis of remaining uncertainty is done using local measures, such as the Fisher Information Matrix, the Covariance Matrix, and the posterior distribution.

PBPK models, especially a coupled PBPK/PD model as developed here, are much larger (in terms of the number of systems states and parameters) than the average PKPD model. If data informativity stays the same, i.e. the same data is used, overfitting and non-identifiability may become an issue. Thus, PBPK/PD modelling takes a different, i.e. a structural, approach. As shown in Section II.2.1, most of the model parameters are defined by a-priori data gained from data-bases on physiology and compound properties or from existing sub-models, which have been integrated (see Table 1). Furthermore, the detailed PBPK/PD model structure allows the integration of additional data on different scales than standard PK/PD models, e.g. measurements for glucose concentrations in specific compartments or insulin receptor concentrations in the different target tissues (Section II.2.1.1.3.3).

There is no straightforward, rigorous, methodology for parameterization of coupled PBPK/PD models with complex or nonlinear dynamics. Assumptions are built on bounding conditions derived from combining literature data on different scales. This could be e.g. the amount of insulin receptors, which, through their abundance, determine tissue insulin clearance, in combination with measurement for insulin concentration gradients across an organ/tissue, which is again dependent on the rate of tissue insulin clearance. The inter-dependency then confirms or strengthens the validity of the assumption.

In general, fitting of a PBPK/PD model such as the GIM model, has to take into account a number of considerations:

- Patient Populations
 - How do healthy individuals and individuals with diabetes compare
 - Are there possible parameter subsets that differ in populations?

- What can we learn from animal studies and parameter values obtained from them?
- Individual Patients
 - What subset of parameters is required for model individualization?
 - Are glucose measurements obtained during a clinical trial sufficient for model individualization?
- Variability in Datasets/Experiments
 - What dynamics are captured in the data
 - Are observed model deviations due to structural model deficits or suboptimal model fits?
 - How precise is the data
 - Are observed model deviations due to measurement errors or suboptimal model fits?
 - How do disturbances/Measurement errors influence identifiability?

A large number of the remaining parameters have been either directly taken or estimated for their population mean from literature data (see model development process as described in Section II.2.1). Based on their inter-individual variability the parameters were divided into three sets: 1) a global set displaying the lowest variability and assumed equal for all subjects, 2) a set of parameters distinguishing healthy volunteers and T1DM patients, and 3) a set of parameters for patient individualization (Table 4, Table 5, and Table 6, Appendix V.5.1.2). All model parameters are time-invariant.

Global and group parameters were defined as population mean values. The parameters from the individual parameter-set were identified for each individual during the glucose control trials. Grouping of the three different parameter-sets evolved from experience as the model development advanced, based on the general knowledge (values found in literature) or knowledge on variability, either in between individuals or the two patient groups. Informed parameters were kept in the global group, if no strong evidence for inter-individual variability was found. The patient group sets are mostly representing insulin receptor related parameters which had to be adjusted for each group to accommodate the different routes of insulin entry to the circulation. The size of the individual dataset was set by trial-and-error by checking identifiability (convergence of optimization runs within a reasonable time frame feasible for online blood glucose control in a clinical setting, see IV.1) and weighing the parameter by its physiological relevance in inter-individual variability.

The defined range of distribution of parameter values for the individual parameter-set used for model-individualization in the clinical trials was guided by experience, i.e. by the range of parameter values which were obtained from model fits from existing datasets, and literature data. Individuals were identified by optimizing the individual parameter set (Table 6, Appendix V.5.1.2) using the *fmincon* routine from the MATLAB® identification toolbox.

II.3 Results

II.3.1 Dynamics of the Glucose Metabolism Model

The parameterization of a mean model for healthy subjects and subjects with T1DM was initialized with boundary conditions and parameter values over multiple scales extracted from literature. Values included tissue clearance fractions [118], tissue concentration gradients [111], protein properties (i.e. Km-values) [128], and expression levels [115]. The PK model basis and the PD functions were then continuously refined using experimental data. Based on their IIV the parameters were divided into three sets: 1) a global set displaying the lowest variability and assumed equal for all subjects, 2) a set of parameters distinguishing healthy volunteers and T1DM patients, and 3) a set of parameters for patient individualization (See Table 4 to Table 6). All model parameters are time-invariant.

For parameterization of the mean models, datasets from intravenous (i.v.) glucose (healthy and T1DM) and insulin tolerance tests (IVGTT, IVITT), oral glucose tolerance tests (OGTT) as well as continuous i.v. insulin infusion (CIVII) as displayed in Figure 11 were used.

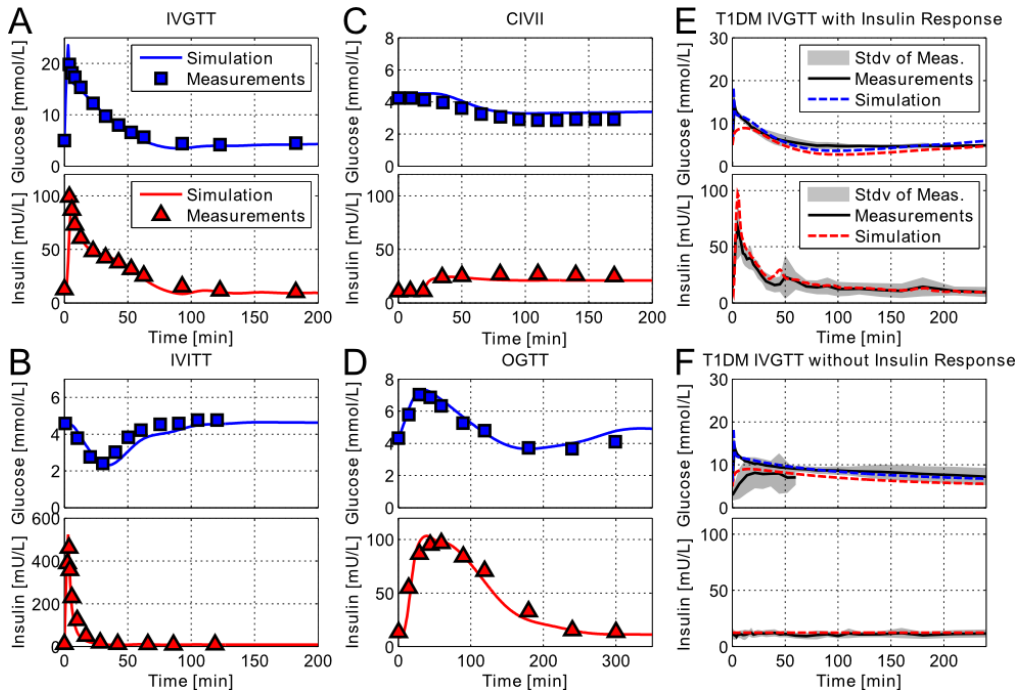


Figure 11: Model development steps including fits to different tolerance test data sets in healthy individuals (A-D) [32] and individuals with T1DM (E+F) [45]. A) IVGTT: 3 min intravenous (i.v.) glucose infusion of 0.5 g/kg glucose in 110 normal adult males. The datasets were used to identify the systemic distribution behavior of glucose and for validation of the adapted insulin secretion model. B) IVITT: 15 subjects received a 3 min infusion of 0.04 U/kg i.v. insulin, used to identify the systemic distribution behavior of insulin and the PD effect of insulin, especially the response times to and recovery times from insulin. C) CIVII: At $t=20$ min an infusion of 0.25 mU/min/kg was started in six normal subjects. This test evaluates the shift in steady state behavior during a forced prolonged hypoglycemic state. D) Oral glucose tolerance test (OGTT): Data was obtained from 145 normal adult males who received a 100g oral glucose challenge. This dataset was used for the identification of the oral glucose absorption and the incretin effect model. E+F) IVGTT of 250 mg/kg glucose in six T1DM subjects; once with an imitated physiological insulin response using the biostator algorithm (E) and once

without insulin response (F). The dataset triggered the reevaluation of glucose effectiveness and was necessary for the identification of the vascular and cellular insulin receptor parameterization in T1DM (Table S2).

The identified mean models for healthy subjects and subjects with T1DM agree well with the experimental datasets with only a minor delay in the recovery of glucose levels after an IVITT.

The study by Regittnig et al. [45] using a hot and cold IVGTT for T1DM patients with artificial and without insulin response was designed for the estimation of glucose effectiveness using a minimal model. The purpose of the study was to point out that the minimal model was not suitable for the reliable estimation of glucose effectiveness. It is postulated that this may be due to a missing remote compartment for glucose, or even a missing distinction between peripheral and hepatic remote glucose compartments.

The model by Sorensen et al. [32] in its original parameterization was also not able to reproduce the kinetics of the IVGTT with basal insulin [148]. When the original PD functions of the Sorensen model into the PBPK/PD model were implemented, the same results were obtained. Thus, the pharmacodynamic functions were refitted in such a way (see Section II.2.1.1.3.1) that they could reproduce both, the IVGTT for T1DM with biostator response and at basal insulin (Figure 11E/F).

The key result here is the distinguishing parameterization for healthy subjects and subjects with T1DM. Dynamics in healthy individuals, especially with respect to insulin action, are faster as compared to subjects with T1DM. This is reflected in the difference in receptor recycling and internalization rates but also insulin receptor expression levels (Table 5). For T1DM, model fits showed a 50% increase in liver receptor concentrations with minor changes in concentrations in muscle and adipose tissue. Also, receptor recycling- and internalization rates were reduced by 20% - 30% in T1DM.

II.3.2 Post-hoc Evaluation of T1DM Model Predictions

We parameterized and validated the PBPK/PD model for T1DM in a post-hoc *in-silico* study using the published dataset by El-Khatib [36]. The cohort investigated in this study covers a broad range of individual PK/PD properties for validation of the model. Although the individuals in the study were sedated, the dataset is challenging, as the time between the two visits spanned up to several months. For each subject, the dataset obtained in the first visit was used for model individualization (fit). This individualized model was then used to predict the outcome (i.e. dataset) of the second visit of the same subject. Differences between the two visits in their experimental setup (i.e. time-course and amount of injection rates) were considered. Without a treatment plan for each subject in between visits, estimates on long-term intra-individual changes in patients cannot be obtained and were neglected in the following.

We present model results for a single representative patient (Subject 117, Figure 12), as well as the summarized results for the whole cohort (Figure 13). The fitted individualized PBPK/PD model of the single subject accurately captures the measurement data of all three compounds, glucose, insulin, and glucagon (Figure 12A). For the initial conditions of each patient, the steady state with half of the total daily insulin dose (see Table 7, Appendix V.5.1.2) given s.c. over 24 h were simulated.

Starting with the resulting model fits, the residual error over time of the fitted trajectories throughout the cohort (visit 1, Figure 13A) is comparable to Subject 117 (11% absolute normalized fit error, cohort: 12%). In Figure 13C, the quality of model fits for glucose is displayed as a summarized visual predictive check (VPC). For the VPC plot, the Clarkes Error Grid, although it is commonly used to evaluate glucose sensors rather than models, was used to give an idea of for model accuracy for dosing decisions in clinical practice. The VPC shows that the average absolute value of the fit error is evenly distributed around the line of identity indicating no systematic bias and a suitable description along the whole concentration range.

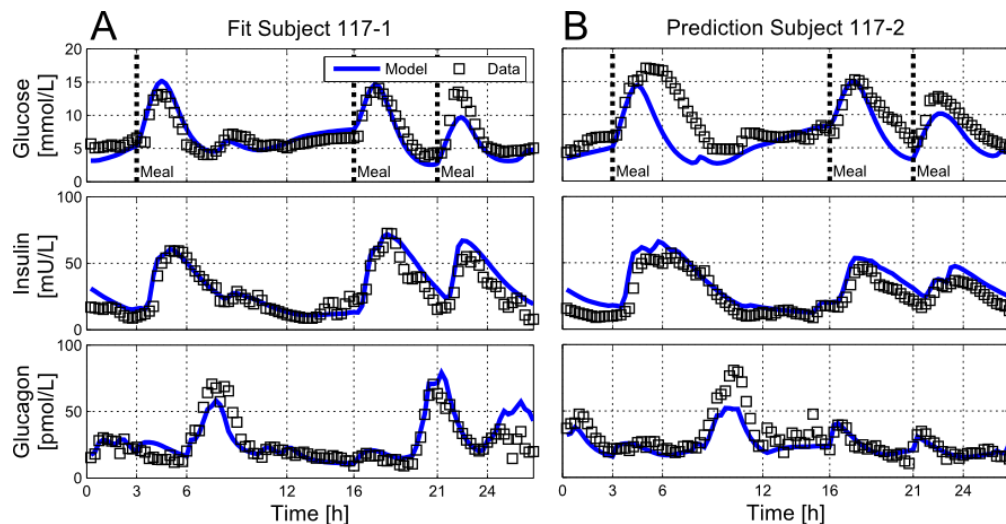


Figure 12: Simulated fitted (A) and predicted (B) trajectories of Subject 117 from the first (A) and second (B) visit, respectively. Simulated trajectories are displayed as blue lines; data for comparison is displayed as black squares. Displayed are peripheral venous blood plasma concentrations of glucose (top), insulin (center), and glucagon (bottom).

The residual error of the model fits, although small, shows minor systematic characteristics. In some cases, subjects, including Subject 117, received large infusions of glucagon (Figure 12A, bottom, $t = 6-8$ h; 3B, bottom, $t = 8-10$ h) following postprandial hypoglycemia (Figure 12A, top, $t = 6-7$ h; 3B, top, $t = 8-9$ h). Measured glucose then quickly rise to normo-glycemic levels (Figure 12A, top, $t = 8$ h; 3B, top, $t = 10$ h). The corresponding simulated effect of glucagon in this situation is too small indicating that the modeled effect of glucagon in this situation is too low. A second point is that postprandial rise of measured glucose levels is slightly delayed and absorption is in some cases prolonged when compared to simulations. Outside these observations, however, the dynamics of glucose levels (Figure 13A, top) show no systematic error suggesting no further structural shortcomings of the glucose PBPK/PD model.

For insulin (Figure 13A, center) the residual error of fits show a minor overshoot (Figure 13A, center, i.e. $t = 4$ h) at times of steep increases in insulin infusion rate (following a meal). During these occasions, simulated insulin levels rise too quickly. The insulin error peaks in Figure 13A/B (center, $t = \text{approx. } 4, 17, \text{ and } 22$ h) suggest that this behavior seems systematic for the whole cohort and likely associated with the s.c. absorption model. Overall, the fitted trajectories of insulin are very accurate.

For glucagon only one systematic error, the overestimation of glucagon levels after the last meal was observed. Establishing a physiological interpretation for this observation remains challenging. Also, this behavior was not observed during model

predictions. Otherwise, the residual mean error of glucagon fits and predictions is non-systematic (Figure 13A/B, both bottom plots) but with a larger absolute error during high infusion rates likely reflecting inter-occasional variability (IOV) of s.c. absorption. Overall, the residual error shows a noise-like behavior with faster changes in measured than in simulated concentration values and thus may be attributable to measurement noise, but otherwise shows no large deviations for both Subject 117 and the whole cohort.

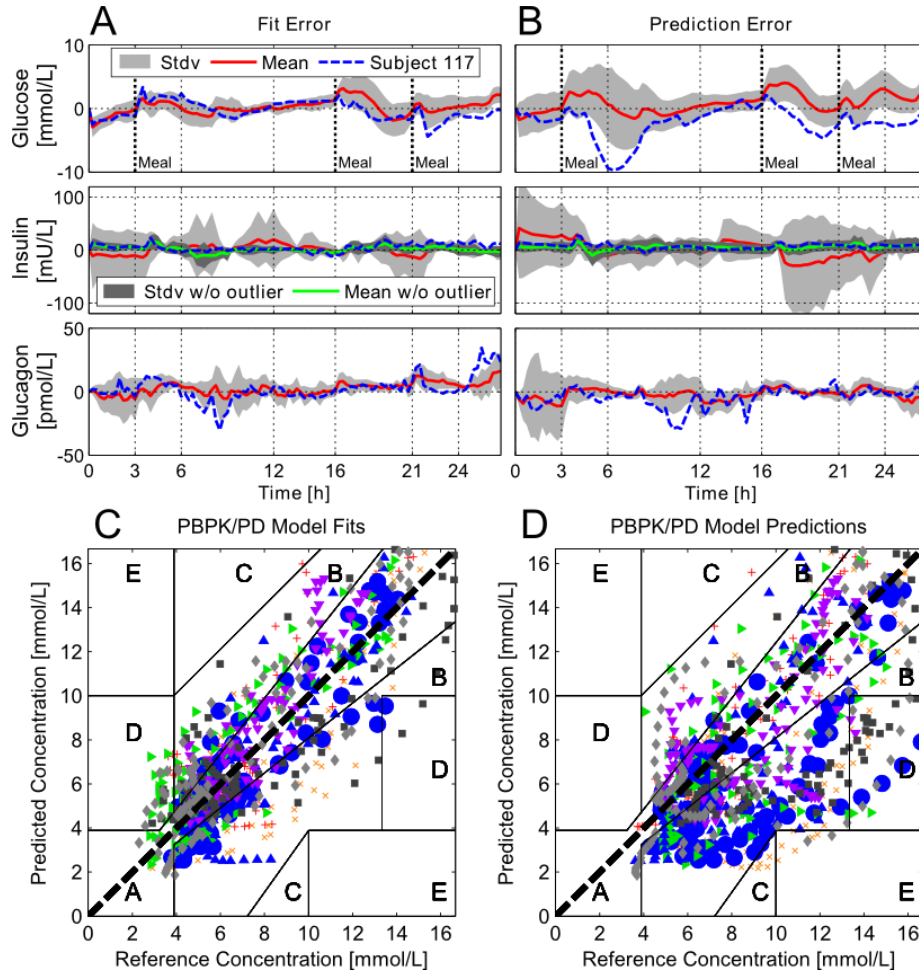


Figure 13: Mean error residuals of simulated fitted (A+C) and predicted (B+D) trajectories of peripheral venous blood plasma concentrations of glucose (top), insulin (center), and glucagon (bottom) from all 8 Subjects from the first (A) and second (B) visit, respectively, displayed in comparison to the exemplary residual error from Subject 117. Visualized as time-concentration-error curves (A+B, for glucose (top), insulin (center), and glucagon (bottom) concentrations) and in a Clarke's Error Grid Analysis styled visual predictive check (C+D, only glucose concentrations). Displayed are for the 8 subjects the mean error residuals (red solid lines, A+B), standard deviation of mean error residuals (light grey shaded area, A+B), all individual residual errors of glucose (C+D) as well as the single residual error from Subject 117 (blue dashed line, A+B, and large blue dots, C+D). For insulin concentration curves (A+B, center), the dark shaded area represents the mean error residuals without the outlier Subject 122.

For a single subject (Subject 122) the total plasma insulin was approx. 20 times higher than for all other individuals and the Subject can be considered as an outlier in that respect. Although quality of fit for Subject 122 with respect to the relative error is comparable to the other subjects, the resulting absolute error distorts the average results (compare light and dark shadings Figure 13A/B, center).

During model predictions, all parameters, including meal parameters, were left at their fit values. The second half of the glucose prediction (i.e. second visit) of Subject 117 corresponds well with the measurement data (Figure 12B, top), whereas the first half is characterized by a large error during absorption of the first meal (average error: Individual 117: 25% absolute normalized prediction error, cohort: 29%). In average, the variations in meal absorption become apparent for the prediction of the second visit (Figure 13B, top). Although the patients received the exactly same meals with respect to carbohydrate, fat and protein content, the qualitative shape of the measured glucose curves during a meal were strikingly different, reflecting IOV of glucose absorption from meals. In the Clarkes Error Grid, in contrast to the model fits, the predictions show a larger absolute error in the hyperglycemic range than in the normo-glycemic range. This indicates that the predictions during meal absorption are less reliable as compared to predictions in the fasted state.

Prediction of glucagon and insulin profiles are equally good as the model fit, indicating a reduced long-term IOV of PK properties but also underlining the very good long term predictive power of the model when taking into consideration that the two visits were months apart.

Part III.

Automated Glucose Control

III.1 State of the Art in Blood Glucose Control

In diabetes the body's autonomous regulation of blood glucose managed by complex interactions of neuronal, hormonal, and metabolic signalling networks is defective and at present can only be controlled by constant vigilant manual insulin therapy by the affected individual. The concept of blood glucose control in diabetes is the compensation of these malfunctions in the body's own glucoregulatory system. The challenge is to design algorithms that can make the right decision, at the right time, with minimal human (user) input (fully autonomous). The elements needed to create such an algorithm are based on a structured modular approach. The modular architecture includes three main components [14]:

- A module responsible for basal-rate and pre-meal control that is adjusted every 24 hours (run-to-run control for improvements on a long time-scale)
- A module to address real-time corrections of insulin delivered as needed (actual glycaemic control at medium time-scale)
- A safety module that monitors the risk for hypoglycaemia continuously and adjusts insulin delivery accordingly (e.g. insulin pump shut-off) to increase the robustness of the control algorithm.

Such a modular approach allows for incremental testing and potential for increased acceptance by regulatory authorities, offering some flexibility to the developer as each control module can be used separately or within an integrated control system. The following sections cover a short introduction on control algorithms used in glycaemic control as well as describe a number of control systems which have been used in practice.

III.1.1 Algorithms

Automatic blood glucose control has been the subject of intensive research for over 3 decades and is becoming more important as the knowledge about diabetes and the computational power and capabilities of small electronic devices increases.

Effective automatic control of blood glucose levels can reduce the burden of manual therapy and may improve risk profiles of most people with type 1 diabetes thereby improving quality of life and offers good prospects in clinical and economic terms [9]. Research groups, partly in cooperation with industry and non-profit organizations are putting a lot of effort in the development of the artificial pancreas. Even though the first positive reports have been published, remaining hurdles have to be overcome before automated blood glucose control becomes possible [14, 15].

One of the main issues of current model-based approaches is the empirical modelling approach. A drawback of existing compartmental models in literature with respect to model-based control is the parsimonious model structure as discussed in Section II.1.2.4, which may result in limitations in the predictive quality of the model, thus, requiring robust controllers.

A number of reviews have been published on control systems used for blood glucose control [12, 15, 22, 31, 167-169] as well as on suitable models for model based control [63], and control strategies for intensive care units [75, 170].

Control concepts that received the most attention in glucose control over the last years are briefly reviewed in the following.

III.1.1.1 Model-Free Control

In principle, there is actually no such thing as model-free control, as every control algorithm reflects in some way the dynamic properties of the process it is designed to control. The control laws, e.g. output feedback controllers like PID controllers, are tuned from the response to perturbation experiment from the process (Ziegler & Nichols [171]) or using loop shaping/tuning based on input-output transfer functions (i.e. simple models) of the process [172, 173]. Even lookup tables are based on heuristics which have been inferred from experience and with extensive amounts of data from experiments with the respective process.

However, once designed, these control algorithms and protocols are no longer dependent on a model representation of the controlled process for online control performance, which is why they are referred to as model-free controllers.

III.1.1.1.1 Lookup Tables

The main advantages of lookup-tables are savings in terms of processing time, which can be significant, and their simple implementation. A runtime computation is basically replaced with a simpler associative array indexing operation. Retrieving a value from memory is often faster than undergoing a computation or input/output operation. In most cases, the tables are pre-calculated and stored on a database or simple memory.

Prominent representatives of lookup-tables in glucose control are the Rabbit2 trial for patients with T2DM [174], the SPRINT protocol used in intensive care [175] and the REACTION algorithm [176] developed by MUG.

III.1.1.1.2 PID Control

The **proportional-integral-derivative** (PID) controller is widely used in industrial processes. This controller calculates the feedback control input from the present state (proportional), the history (integral) and the change (derivative) of the output error [172].

An argument for the use of PID control is that a glucose control system should emulate the normal physiology of the pancreatic beta-cell [17], which responds to a glucose challenge in a way similar to the characteristics of a PID system. However, it has to be considered that the glycaemic control of the beta-cell is not subjected to severe time-delays as compared to glucose control through the s.c.-s.c. route. To enhance robustness and performance properties of PID control in glucose control various adaptations of the control law have been published.

Steil et al. have been instrumental in conceptualizing and testing PID algorithms for closed loop control and tested PID control on different glucose models [177]. Marchetti et al. evaluated a number of adaptations like feed forward control (pre-meal insulin boluses) and switching strategies like, on/off time points, gain scheduling and time-varying set-points (reducing the set-point prior to a meal) [178]. Meal information was assumed for most of these strategies. A promising PID-like controller is the PD controller with fading memory [18], emulating, unlike integral control, the less than infinity memory of a physiological pancreas.

A version of a PID like controller with fading memory was also implemented within the framework of this work. The details of the controller development are documented in Section III.2.3.

III.1.1.1.3 Fuzzy (Logic) Control

In the control theory field, the fuzzy logic has emerged as a powerful tool to incorporate expert knowledge about the systems into the controllers design [179]. Fuzzy Logic Control is based on the model representation by fuzzy logic modelling using fuzzy sets or membership functions [180]. Unlike bang-bang control (or on-off control) that has only two values, namely true or false, membership functions are defined as graded truths for a number of criteria.

Fuzzy logic has the advantage that the solution to the problem can be cast in terms that human operators can understand, so that their experience can be used in the design of the controller. This makes it easier to mechanize tasks that are already successfully performed by humans and allows the integration of expert knowledge into the controller, e.g. the experience of diabetologists in glycaemic control [20, 21, 181]. Other examples of fuzzy control in glucose management are [99, 182].

Another noteworthy approach using fuzzy logic is the combination of fuzzy modelling with neural networks, the so-called neuro-fuzzy method [183], where neuronal models are used to adapt the membership functions of the fuzzy system.

III.1.1.2 Model-based Control

In model-based control, the control method uses a model representation of the controlled process for the calculation of the control input.

III.1.1.2.1 H-infinity Control

Linear H-infinity control is a robust control method. The goal of this control methodology is to lower-bound the worst-case closed-loop performance of the process under study. The feedback controller design is thus based on an optimization problem to minimize the H-infinity norm, which is the maximal amplitude or singular value of the frequency response of the system transfer function, of the closed loop system considering structured and unstructured uncertainties [184, 185].

Robust H-infinity control has been applied in *in-silico* glycaemic control using large scale physiologic models [98, 100] as well as simpler minimal-model type glycaemic models [186]. H-infinity based glucose control has, however, never been evaluated in a clinical setting.

III.1.1.2.2 Model Predictive Control (MPC)

MPC is one of the most successful and most popular advanced control methods. It is based on the repeated solution of a finite-horizon optimal control problem subject to a performance specification, constraints on states and inputs, and a system model [187, 188]. The success of the MPC is mostly attributed to its optimization based approach. In many control problems it is desired to be optimal with respect to some performance specification as profit or yield. However, it is often hard or even impossible to find analytically a closed form solution to such a problem. Therefore, in MPC, the given optimal control problem is solved repeatedly online based on the current measurement of the system states. Additionally, MPC is one of the few control methods able to explicitly consider state and input constraints [188]. Constraints occur in a vast number of practical applications, such as the use of actuators, as in this case an insulin pump, which are naturally limited, or the necessity to operate within safety bounds as in this case the blood glucose concentration range.

MPC is probably also the most popular control method used for glycaemic control since around the year 2000, following the easy availability of computational power necessary for MPC. In earlier studies, MPC was applied for 1 day crossover trials, for example, in “Advanced Insulin Infusion using a Control Loop” (ADICOL) [86] (with algorithm [24]). However, as daytime control proved challenging due to the unpredictability of meal absorption, research switched to trials under increasingly controlled conditions, for example, the control of a single meal [87], but in most cases overnight studies in children [84, 189] and adults [16, 33]. A current review in overnight and day and night trials with duration of more than 8 h can be found in [13]. Another field of application is tight glycaemic control of the critically ill in intensive care units [74, 75, 77, 78, 88-90, 186].

III.1.2 Integrated “Artificial Pancreas” Systems

The “Artificial Pancreas” is a concept that describes an integrated system coupling s.c. continuous blood glucose monitoring (CGM) systems with insulin infusion pumps (IIP) that are worn externally by the patient and automatically inject an insulin dose calculated from a blood glucose measurement value [12, 167, 168].

AP systems are investigated for more than 50 years but are still not in use for everyday control of blood glucose, partly owed to technical and system inherent hurdles such as: (a) accuracy of s.c. CGM devices, (b) physiologic lag times of s.c. glucose (measurements) during rapid changes in blood glucose, (c) onset of insulin action after s.c. insulin administration, and (d) lingering/tailing insulin action after s.c. injection [13, 14, 22].

Recent improvements in the accuracy of s.c. CGM devices, IIPs and safety systems have advanced the conditions for developing a feasible solution for a fully integrated AP system [14, 15]. The superiority of automatic glucose control by s.c. glucose measurements and s.c. insulin infusions (s.c.-s.c. route) over manual control has already been demonstrated [16].

In the following, a brief overview is given on the state of the art of control algorithms used in integrated (artificial pancreas) systems that have been tested clinically.

III.1.2.1 The UVa/Padova Simulator combined with the iAP

In September 2006, the JDRF initiated the (international) Artificial Pancreas Project (iAP or APP) and funded a consortium of centres to carry out closed-loop control research [33]. The work of some of the main groups involved is centred around a glucose model, the UVa/Padova Simulator, originally developed by Dalla Man et al. [29], which has been accepted by the Federal Drug Administration (FDA) to replace animal testing of glucose controllers [30, 63].

In the past, the model of the UVa/Padova Simulator was used in combination with various control concepts for blood glucose control. In most cases, the model was used in combination with model-predictive control algorithms (MPC) [25, 30, 149, 160, 190]. Along this line of development it is now further developed and evaluated within the EU funded research project AP@Home [191, 192].

III.1.2.2 The Cambridge Model and MPC

Hovorka et al. from Cambridge, one of the leading groups in diabetes modelling and control also works with compartmental models [81] of the GIM and uses model based

approaches to gain greater detail of the GIM (e.g.: glucose flux distributions during OGTT [82]; interstitial- and plasma glucose dynamics [83]).

In the early 2000s, Hovorka et al. have been working on the project “Advanced Insulin Infusion using a Control Loop” (ADICOL) [86] using their first, often cited approach of a nonlinear MPC approach with T1DM patients [24]. The MPC algorithm was applied to regulate fasting blood glucose concentration in Type 1 diabetic patients using the s.c.–s.c. route [87] and repeatedly re-evaluated [88] and adapted [16, 84, 89], also for tight glycaemic control in ICU patients [90]. The current model (2008) is also used within a MPC framework for tight glycaemic control in critical care [31] as well as for continuous blood glucose control trials for (juvenile and adult) patients with T1DM [16, 84]. The algorithm is currently also further developed and evaluated within the EU funded research project AP@Home [191, 193].

III.1.2.3 Controllers using Physiology-based Models

Even though the first models did not accurately represent physiological properties in their structure, the criteria of physiology-based models with parameters that have physiological meaning became more important [62].

However, to date, the only real physiology based model of the GIM is the Sorensen model [32]. The model was used as a basis for closed loop control research [23, 97-99] and in one case augmented by a generalized meal model developed by Lehmann and Deutsch [91] to be used again as a reduced linear model by Parker and Doyle for proof of concept of H-infinity control in Diabetes [100].

To date, the model has never been used for closed loop control in a clinical trial. Thus, the physiology-based pharmacokinetic / pharmacodynamics (PBPK/PD) model developed here was the first of its kind to be clinically tested as a model kernel for model based automatic glucose control.

III.2 Materials and Methods

We have developed a new approach to AGC, which, for the first time, combines a detailed a-priori individualizable generic whole-body physiology-based pharmacokinetic/pharmacodynamic (PBPK/PD) model [2], with a robust MPC algorithm for automatic glucose control in a post-hoc *in-silico* study. Based on this accurate prediction (PBPK/PD) model of the individuals core dynamics of blood glucose levels, adapted over time using continuously gathered patient data, the MPC computes an optimal feed-forward control input. To increase closed-loop stability and robustness against disturbances and model uncertainties a PID-based feedback controller is used for compensation of prediction errors (off-set).

The following sections show that the PBPK/PD modeling approach can make significant contributions to the automatic glucose control community both, for controller evaluation, but also as a component within the presented MPC framework.

For the evaluation of the control algorithm, an *in-silico* clinical trial was simulated based on the dataset provided by the clinical partner MUG (details in Section II.2.2.1). In the following section, the clinical dataset and the implementation and evaluation of the implemented algorithms is presented.

III.2.1 The Integrated System

III.2.1.1 Integration of Automatic Glucose Control in a Clinical Setting

The developed glucose control framework allows both, *in-silico* evaluation of controller concepts and control of blood glucose of type 1 diabetes patients in a clinical setting. A block diagram of the presented MPC strategy for an integrated system within a clinical environment is shown in Figure 14.

The interaction of the components of the integrated system is based on the modular approach described in [14]. Here, interacting layers work on different timescales, where the outer layer with the larger timescale adjusts the parameters of the inner, fast layer. For the system described here, the outer layer is represented by the model adaptation, i.e. individualization routine, using glucose measurement data for the adjustment of the model kernel of the control algorithm (middle layer), which calculates insulin delivery based on latest CGM data, and meal information. The middle layer is further restricted by the innermost layer, the robustness layer. The robustness layer is comprised of the offset-controller with algorithms for pump shutoff and insulin-on-board constraints and adjusts or rejects the insulin doses calculated by the MPC and also adjusts the blood glucose target value for the MPC.

Once the integrated system is in place, various increasingly complex configurations of an AP system become possible. The modular approach is necessary for the control system to adapt to or handle the process variability at the different time-scales. Whereas the offline optimization adjusts the model to the core dynamics of the controlled individual on a long term, the MPC adjusts Insulin doses based on known boundary conditions (e.g. meal input and past insulin infusions) whereas the innermost layer reacts to disturbances/uncertainties not captured by the model.

III.2.1.2 Control Concept

Model-based glucose control algorithms require a model kernel which is tuned to the system it is supposed to control in order to work properly. In blood glucose control, a paradigm for personalized medicine, the model is tuned for each patient using the experimental data gathered over time [18].

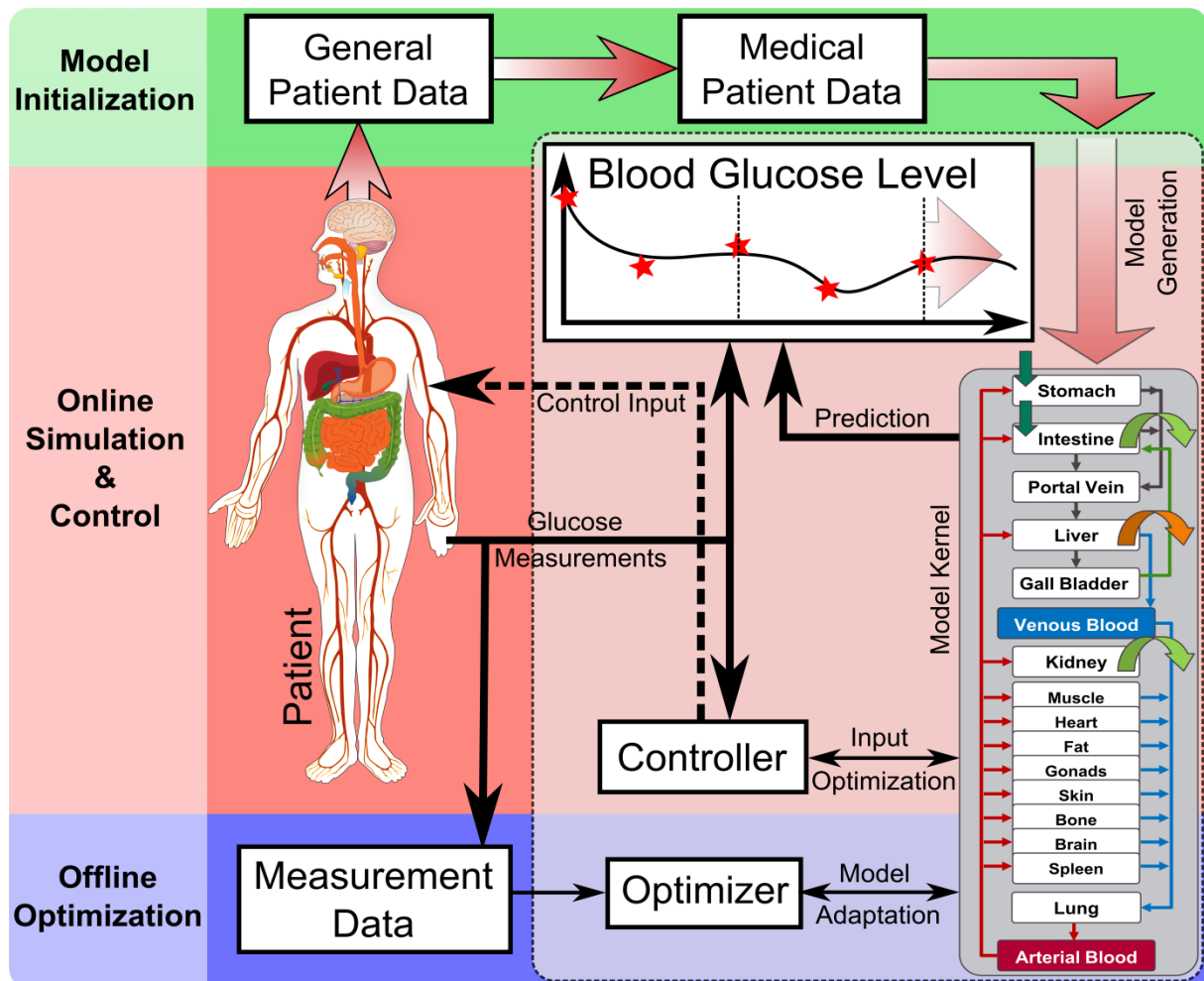


Figure 14: Schematic of the work- and information flow of an integrated system within a clinical environment during continuous closed-loop glucose control. The PBPK/PD model kernel is initialized with patient data (physiological parameters, e.g. weight, height, gender). Blood glucose measurements are taken frequently, stored and the most recent measurements are delivered to the controller. The process works on two time-frames: the online calculation of the optimal insulin dose ("control input" for closed-loop glucose control) based on recent glucose measurements on a short timeframe, and the offline "model adaptation" based on the full measurement data history on an extended time-frame.

The robust MPC algorithm was developed and validated on *in-silico* trials designed with the same protocol as the clinical trial described above. To simulate accuracy of blood glucose measurements, measurement noise was added to the individual virtual (simulated) measurements (Section III.3).

The algorithm first initializes a mean model of the GIM which is then scaled by the physiologic properties (age, weight, height, gender and race) of the enrolled patient. With the first blood glucose measurement at 2:00 p.m. model individualization is started. To increase the efficiency, and thereby the success of the individualization,

virtual populations are generated a priori based on the known physiologic properties of the patient in combination with individual parameter set value distributions which have been pre-calculated based on known model parameterizations [2]. The resulting virtual population is screened for the best fit to data collected during the clamp phase (observation phase) from 14:00 until 19:30 on the first day. The best fit parameter set is used to initiate MPC at 19:30, calculating an optimal insulin dose $u_{MPC}(t)$ based on model predictions (Figure 15).

As even a detailed PBPK/PD model does not fully account for all dynamics that may cause a change observed in blood glucose levels, the offset-controller (innermost layer) filters the residual error of the model predictions made by the MPC (Figure 15).

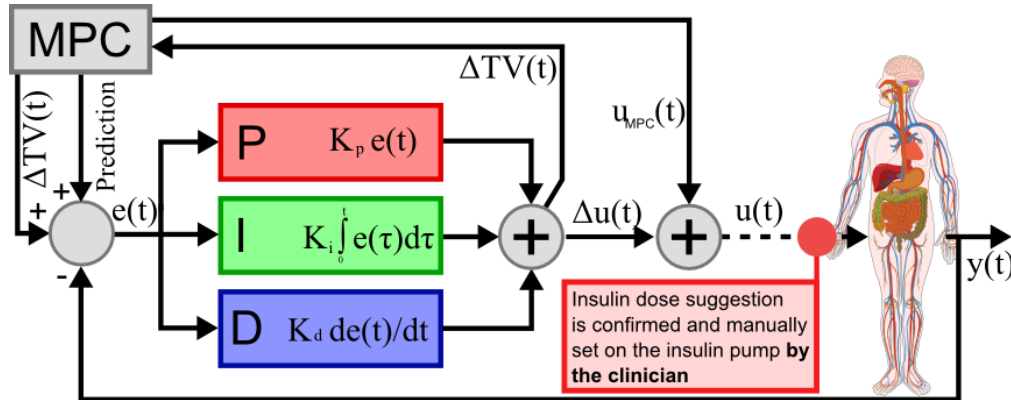


Figure 15: Principal concept of robust MPC with proportional integral derivative offset-control. Based on the tracking error $e(t)$, the weighted actual absolute error (P), the weighted sum of all past errors (I), and the weighted change in error compared to the error at the last sampling point (D) are summarized for the calculation of a target value shift for the MPC controller ΔTV and the control correction $\Delta u(t)$. Manual setting of the dose is only required in clinical trials for safety reasons, but not for the general control concept.

Based on the full measurement data history collected during the trial, the model kernel used by the MPC is continuously improved by optimizing the individual dataset (Table 6, Appendix V.5.1.2). A “Growing Horizon Estimation” was chosen, using all glucose measurement data collected since start of the trial (Figure 16).

The algorithm runs on a Laptop PC. The algorithm has been implemented in MATLAB® and is controlled via a graphical user interface (MATLAB® GUIDE). For model adaptation and the input optimization, the functions *fmincon* and *fminbnd* were used, respectively, from the MATLAB® optimization toolbox.

III.2.1.3 Challenges in Glucose Control

Once a glucose control system is in place, e.g. at a clinical site, the AP system is faced with the challenge of controlling blood glucose in various conditions and within individual subjects. Here, variations in the response of individual patients to insulin as well as unpredictable events like stress, physical activity and in some cases the onset of sickness but more importantly the variations in absorption characteristics of a meal come into play. In the following a brief overview on the challenges in blood glucose control is given.

For a review on disturbances and inter and –intra-individual variability on an in-depth physiological level, see Appendix V.5.2.1.

III.2.1.3.1 Disturbances

Despite important developments in sensor and pump technology, the AP must cope with the delays and inaccuracies in both glucose sensing and insulin delivery described in the previous sections. This is particularly difficult when a system disturbance, e.g., a meal, occurs and triggers a rapid glucose rise that is substantially faster than the time needed for insulin absorption and action [14] or physical activity reduces (consumes) the blood glucose levels in addition to the injected insulin [194, 195].

Even if the carbohydrate (CHO) content of a meal is known beforehand, it is not assured that the controlled subject will show the same glucose response for meals with the same CHO content as the absorption of a meal also depends on the specific type of CHO [126] as well as on the amount of fat and protein contained in the meal. Meal composition may have an effect on gastric emptying time as well as on the speed CHOs are processed for absorption. As both these properties can be explicitly taken into account by the PBPK/PD model kernel, the effect of nutrition-based variability of glucose absorption is currently investigated. Thus, meals by themselves are not treated as disturbances but with variation in meal-to-meal absorption properties contribute to inter-occasion (intra-individual) variability.

Another major influence on whole-body glucose metabolism is the cellular energy expenditure during physical activity (exercise). Physical (muscular) activity increases the whole-body energy expenditure and thereby muscular glucose consumption and hepatic glucose output. Model-based control algorithms may need to get informed by the user regarding oncoming exercise episodes. However, here, physical activity is treated as a disturbance and its effect is not explicitly included in the model and related changes in blood glucose levels have to be compensated by the robustness (FMPD feedback-controller) component of the control algorithm.

Other disturbances, all yet unaccounted for, include patient conditions and treatments as they occur in intensive care. Medication, inflammatory stress and other changes in patient conditions may have severe influences on the patient's response to insulin, i.e. insulin sensitivity. However, control of blood glucose in critically ill is outside the scope of this work, but has been done before by others (algorithms listed in Sections II.1.2.1 and III.1.2.2). Here, the focus is on disturbances as they occur in otherwise healthy subjects with T1DM.

III.2.1.3.2 Inter- and Intra-Individual Variability

Additional difficulties that the control algorithm must face arise from coping with inter- and intra-patient variability.

Although a number of simulation models have been proposed in the last four decades (Section III.1.2), many of these models are “average”, meaning that they are only able to simulate average population dynamics but not the inter-individual variability. However, realistic *in-silico* experimentation within control scenarios requires computational mechanistic model kernels [14] that allow the simulation of inter-individual variability of physiological properties as key metabolic parameters and drug distribution parameters in the type 1 diabetic population.

As mentioned in Section II.2.2.2, the knowledge on inter-individual variability provides valuable information on safety and limitations of the chosen control concept. Thus, successful control concepts should focus on the inter-patient variability of the integral term “insulin sensitivity”. Insulin sensitivity is expressed as a single parameter or as a

number of model parameters at the interface of insulin action that have to be estimated from patient specific measurement data. Its reliable estimation for sensitivity-value-based blood glucose control is the basis of the control concept that has been developed here.

Model based controllers allow for relatively straightforward individualization using the patient-specific parameters of the individualized model core. However, identification of accurate individual models still proves challenging. Here, inter individual variability on a physiological level (e.g. organ volumes, blood flows) are covered by the PBPK framework the model is built on (Section II.2.1). The inter-individual variability in pharmacodynamics (drug action/interaction properties) is defined through a small set of parameters (individual patient dataset Table 6, Appendix V.5.1.2) which is initially identified from glucose clamp data at start of the trial (Section III.2.1.2).

Intra-individual (or intra-occasion) variability is partly system-inherent. This is expressed by changes in the dose/effect relation of insulin e.g. within the insulin receptor model upon insulin treatment. Unexplained (by the model) intra-individual variability, i.e. possible diurnal variations in insulin action (see Appendix V.5.2.1.2) is handled by the adaptive control scheme, i.e. the dynamic target value shift and dose correction of the FMPD controller (Section III.2.3.1).

III.2.2 Virtual Patient Generation & Trial Design

The model used for generation of the *in-silico* subjects of the simulation environment has been previously described in detail (Part II, [2]). Individualized virtual patient models were generated from datasets of a 2-phase randomized crossover trial (2PRCT from MUG, Section II.2.2.1) collected from 12 patients with T1DM.

The *in-silico* trials for the evaluation of the integrated algorithms followed the same protocol as the 2PRCT. The trial data and protocol, as it is also used here, is described in detail in Section II.2.2.1. Subjects were admitted to the clinical research center at the Medical University of Graz (MUG) and received basal insulin from insulin pumps corresponding to their own basal insulin infusion rate until initiation of closed-loop control. Meal information was transferred to the controller at the time of meal onset, so no insulin infusions prior to the meal were injected for better meal rejection. Parameterization of the algorithm is documented in Table 8 in Appendix V.5.2.4.

III.2.3 The Control Algorithm

Many algorithms, as listed in Section III.1, have been developed for AGC to date. MPC became the approach of choice in current research, for a number of reasons: it is a predictive approach, allowing the handling of system inherent time-delays (subcutaneous glucose monitoring and subcutaneous insulin infusion); It is model-based, allowing a straightforward personalization using patient-specific parameterization [196], and it is optimization-based, allowing the integration of performance specifications, e.g. through constraints on states (i.e. penalization of hypoglycaemia) and inputs (constraining insulin infusions).

The common approach to AGC using MPC, additionally to patient-specific parameterization of the model by adaptation of a number of (time-invariant) model parameters to individual experimental data, is adjustment of a single input-output sensitive parameter for each sampling time to handle/explain process variability as time advances (intra-individual or inter-occasion variability), resulting in a discrete-

time dependent profile for this parameter. Commonly, a parameter representing insulin sensitivity in the model is chosen for this time-dependent adaptation [24, 197]. Feed-forward calculation of the control input is then based on the identified sensitivity from the past.

Here, a different approach to handle process variability is chosen. As adaptation/optimization of a single parameter (i.e. insulin sensitivity) within the PBPK/PD model is too time-consuming and would exceed the time in-between sampling times, instead the target value for the MPC is adapted to mitigate transient changes in process variability. The necessary shift in target value is calculated from the model deviation from measurement data using Fading Memory Proportional Derivative control (FMPD).

III.2.3.1 MPC Algorithm for Glucose Control

MPC is a form of control in which the current control action is obtained by solving, at each sampling instant, a finite horizon open-loop optimal control problem $P(x, k)$. A schematic of the general concept is shown in Figure 16. The optimization of the cost function $V(x, k, u)$ at time $k = t_k$, subject to any imposed control, state and terminal constraints, yields an optimal control sequence u of N piecewise constant calculated control inputs and the first control in this sequence at time $k = t_k$ is applied to the controlled system [187, 188]. In this way, a closed-loop control strategy is obtained solving an open-loop optimization problem. The general control problem is defined:

$$P(x, k) = \min_u V(x, k, u).$$

with the discretized point in time t_k , and the general cost function

$$V(x, k, u) = \sum_{i=k}^{k+N} l(x_i, u_i) + F(x_{k+N})$$

With stage cost l , the optimized input sequence $u = \{u_k, u_{k+1}, \dots, u_{k+N-1}\}$, system state x_i , and terminal cost $F(x_{k+N})$. At time k the optimal control problem $P(x, k)$ of minimizing $V(x, k, u)$ subject to any imposed control, state and terminal constraints is solved, yielding the optimizing control sequence

$$u^0 = \{u_k^0, u_{k+1}^0, \dots, u_{k+N-1}^0\}$$

and the resulting cost value function

$$V^0(x, k, u^0).$$

However, this is a multidimensional optimal control problem using a sequence of piecewise constant inputs $u = \{u_k, u_{k+1}, \dots, u_{k+N-1}\}$ and may become computationally demanding. A common approach to save computational time and to increase the convergence of the optimization problem is to restrict optimization on the first input of a sequence. The cost function is defined:

$$V(x, k, u) = \sum_{i=k}^{k+N} l(x_i) + u_k$$

yielding the control feedback law:

$$u^0 = u_k^0.$$

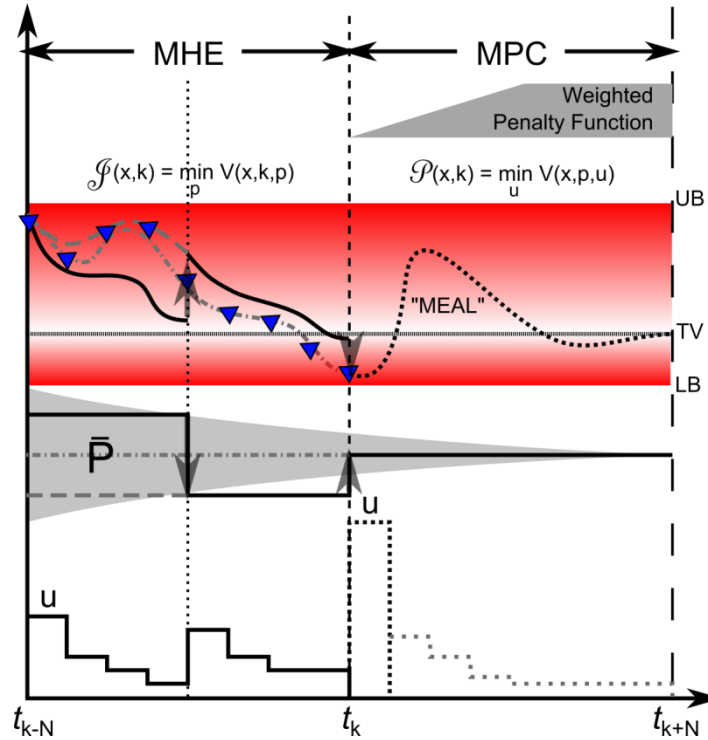


Figure 16: Schematic of the MPC control concept. Solving the optimization problem P at time t_k over the prediction horizon N (here, $N=8$) results in the feedback control law u_k . The collected data before time t_k resulting from past control is used to improve the internal model of the MPC by optimizing the model fit of past data by solving the optimization problem J with respect to the model parameters p using for example a moving horizon estimator (MHE). A growing horizon estimator with $N = k$ is used. The MPC is subsequently updated with the new model parameters to improve feedback control. Whereas P is solved at every sampling point, J is in general solved only once every few sampling points (here at every fourth sampling point).

III.2.3.1 Offset-Control/Error Compensation (PID)

The development of a PID controller is based on basic concepts of feedback control [172, 173]. A PID controller is based on three characteristics of the output tracking error $e(t)$. The weighted current absolute error (proportional component, P), the weighted sum of all past errors (integral component, I), and the weighted change in error compared to the error at the last sampling point (derivative component, D). These three components are summarized for the calculation of the control input. A schematic of an integrated closed loop setup using PID control is depicted in Figure 15.

The offset-controller is to compensate for the residual error of the model predictions made by the MPC (Figure 15). Thus, here, the tracking error, $e(t)$, is calculated from the deviation of the simulated blood glucose predictions, $x(t)$, and the blood glucose measurements, $y(t)$. From these, the offset-controller calculates two corrections in a feedback loop based on the prediction error, $e(t)$: a set-point correction ΔTV (i.e. target value shift) of the MPC and a control input correction, $\Delta u(t)$, for the insulin pump which is used to correct the insulin infusion recommendations $u_{MPC}(t)$.

The tracking error is thus calculated:

$$e(t) = x(t) - y(t).$$

The concept of what is considered the composition of such an error is depicted in Figure 17.

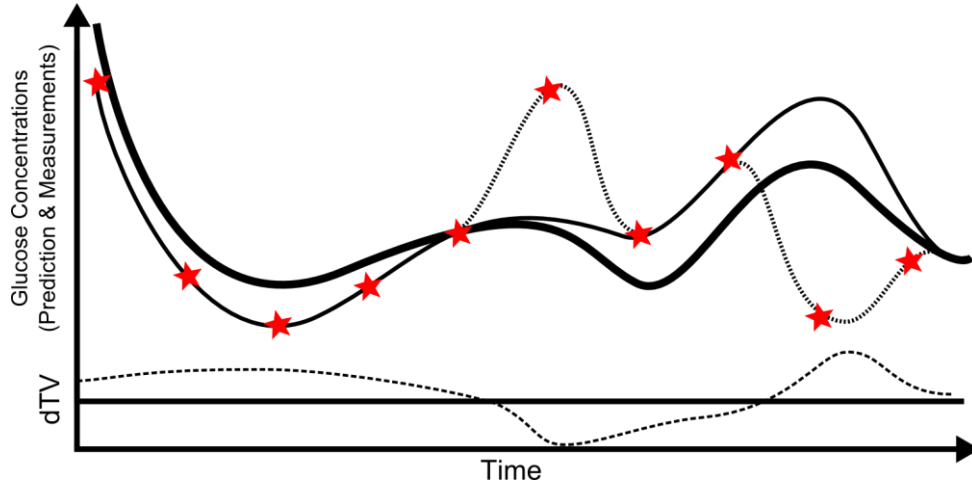


Figure 17: Schematic showing an exemplary composition of the model prediction error $e(t)$ which is the deviation of the simulated glucose prediction (solid line) from the blood glucose measurements (red stars): The difference to the slim solid line represents the error resulting from a below-optimal model fit (with the slim solid line being a possible simulation prediction given an optimal model fit). The dotted line represents disturbance-dependent dynamics. The dashed line at the lower end of the plot represents the dynamic target value shift ΔTV calculated from the prediction error.

To increase robustness of offset control against sensor noise and model uncertainties on a small time-scale, here, the fading memory principle from FMPD [18] is adapted. The reason for a dynamic target value correction, ΔTV , is that in spite of model errors, most of the insulin input will still be calculated by the MPC and not by the feedback controller. As the MPC is a feed-forward controller, shifting input amounts to the FMPD feedback component, being a reactive controller, would reduce overall response times.

ΔTV is calculated from the relative prediction error $e(t) = x(t) - y(t)$, such that the dynamic target value $DTV = TV + \Delta TV$ and $\Delta TV(t = 0) = 0$. With fading memory, this gives:

$$\Delta TV = K_p \int_0^t e^{-W_p(t-\tau)} e(\tau) d\tau + K_i \int_0^t e(\tau) d\tau \approx K_p \sum_{j=0}^k e^{-W_p(k-j)} e_j + K_i \sum_{j=0}^k e_j$$

with the controller gains K and the forgetting factor W_p , for the proportional component, which determines how fast past values fade from memory. Here an exponentially decaying fading function is chosen.

A drawback of dynamic target value shifting is the nonlinear behaviour of some components of the GIM model, which could “distort” the required insulin dose due to model inherent nonlinearities, but an improved fit (i.e. individualization) of the model kernel also reduces the required shift, diminishing the influences of nonlinearities. The reason for only taking the proportional and integral component is that ΔTV should only compensate for the overall drift in the model predictive error, as short term deviations and disturbances are corrected by the input correction and especially the derivative component thereof.

The second component of the offset controller is the input correction of the MPC dose calculations. Here, the error calculation also takes into account the target value shift for the MPC controller, only correcting remaining deviations, which gives a prediction error of $\hat{e}(t) = \Delta TV - e(t)$, taking into consideration the dynamic shift ΔTV of the MPC such that the input correction $\Delta u(t)$ becomes zero once the target value is shifted by the value of the prediction error ($e(t) = \Delta TV$). A generalized formulation of FMPD control for the calculation of the input correction $\Delta u(t)$ is:

$$\Delta u_k = K_p \sum_{j=0}^k \hat{e}^{-W_p(k-j)} \hat{e}_j + K_i \sum_{j=0}^k \hat{e}_j + K_d \sum_{j=0}^k \hat{e}^{-W_d(k-j)} (\hat{e}_j - \hat{e}_{j-1})$$

with the controller gains K and the forgetting factors W_p and W_d , which determine how fast past values fade from memory. Again, an exponentially decaying fading function is chosen.

The input correction was tuned to react quicker to changes in $e(t)$. The tuning of the forgetting factors W_p and W_d within a real control setting is always a trade-off between the susceptibility to sensor error/noise and increase in controller time delay or “sluggishness”. As the D component represents the fast first response characteristic of a beta-cell a larger factor and thus a faster decay of the memory was chosen. Also, to accommodate for the effects of model nonlinearity, in both cases, an integral component is included to obtain zero set-point (dynamic target value) error.

Both, MPC (penalty function) and offset-control are subject to additional safety constraints and parameterizations which are described in detail in Appendix V.5.2.

Although the control algorithm is robust in case of significant prediction errors, as will be shown, the model kernel is continuously updated as more measurements become available over time. For this a standard optimization routine was chosen (*fmincon*, MATLAB®) optimizing the individual parameter set [2].

III.3 Results

The *in-silico* trials for the evaluation of the integrated algorithms followed the same protocol as the 2PRCT described in Section II.2.2.1. *In-silico* evaluation of the control algorithm was conducted to assess control performance and safety/risk before each of the two clinical trials. The *in-silico* evaluation was tailored to the specific workflow setting of the respective clinical trial. For each *in-silico* evaluation, the mentioned 2PRCT trial dataset is used in two different scenarios.

The first scenario is for online controller evaluation within an *in-silico* re-simulation of the clinical trial. The controller was evaluated in three test cases vs. model uncertainty, disturbances, and noise. For the first trial, low measurement noise (Gaussian) is used to emulate the error in i.v. blood glucose measurements. For the second trial, a noise generator is used to emulate the measurement error observed in continuous blood glucose measurement devices (CGMs) [198] as commercial CGMs are used to obtain the blood glucose values for glucose control. The test cases have been conducted all at once for each of the 12 *in-silico* patients. To evaluate controller performance in a critical-case scenario, kernel adaptation is omitted, thus using sub-optimal model-fits for uncertainty evaluation.

The second scenario is retrospective verification. In preparation for the first trial, the actual measurement data obtained during the 2PRCT trial is used for offline controller evaluation. For the second trial, an actual sensor noise signal obtained within the first clinical trial (in parallel to glucose control in the first trial, a sensor development group tested a newly developed CGM device on the same patients) is used to assess controller performance in the presence of high sensor noise.

III.3.1 *In-silico* Evaluation (First Trial, Blood Glucose)

In-silico evaluation is used for verification and validation for closed-loop control algorithms and is a prerequisite for in-vivo tests of artificial pancreas systems within clinical trials [30]. It provides valuable information about controller performance (safety and limitations) and may help guiding the optimal design of clinical studies.

We have tested the developed control system against the 12 *in-silico* individuals parameterized based on clinical trial data. Controller performance is evaluated versus 1) model uncertainties, with a sub-optimal fit of the internal MPC model kernel; 2) disturbances, testing the robustness properties of the offset-controller in case of unannounced intake of carbohydrates; and 3) sensor error, with simulated sensor noise with a mean standard deviation of 5% (expected measurement error within the planned clinical trial is 2% for i.v. glucose measurements).

For the MPC algorithm a prediction horizon of $N = 240$ min (6 h) was chosen. A piecewise constant insulin infusion over the first 15 min was calculated solving the nonlinear constrained optimization problem described in Appendix V.5.2.2.1. Meal information was transferred to the controller only at the time of meal onset, so no insulin infusions prior to the meal were administered for better meal rejection.

III.3.1.1 Model Uncertainties

The glucose control algorithm relies on an internal model description of the controlled subject. Wrong parameterizations could lead to miscalculations of insulin doses by the MPC component. Figure 18 shows an exemplary *in-silico* trial run for Subject 08.

Especially during the early phase, directly after the clamp phase, without adaptation of the model kernel, model uncertainties are more likely and both, the target value shift and the offset-control adapt only slowly to prediction errors. The controller thus starts with an increased target value (150 mg/dl) at start of control ($t = 330$ min), which is continuously lowered to the desired target level (110 mg/dl).

We have conducted the *in-silico* evaluation based on the initial model parameterization during clamp phase, but without additional kernel adaptation, thus using inaccurate model-fits for uncertainty evaluation. Also, parameters affecting meal absorption (caloric content, fraction solid, and meal volume) which have the highest inter-occasion variability within the model [2], were varied for each meal within a uniform distribution of max. relative change of 30%.

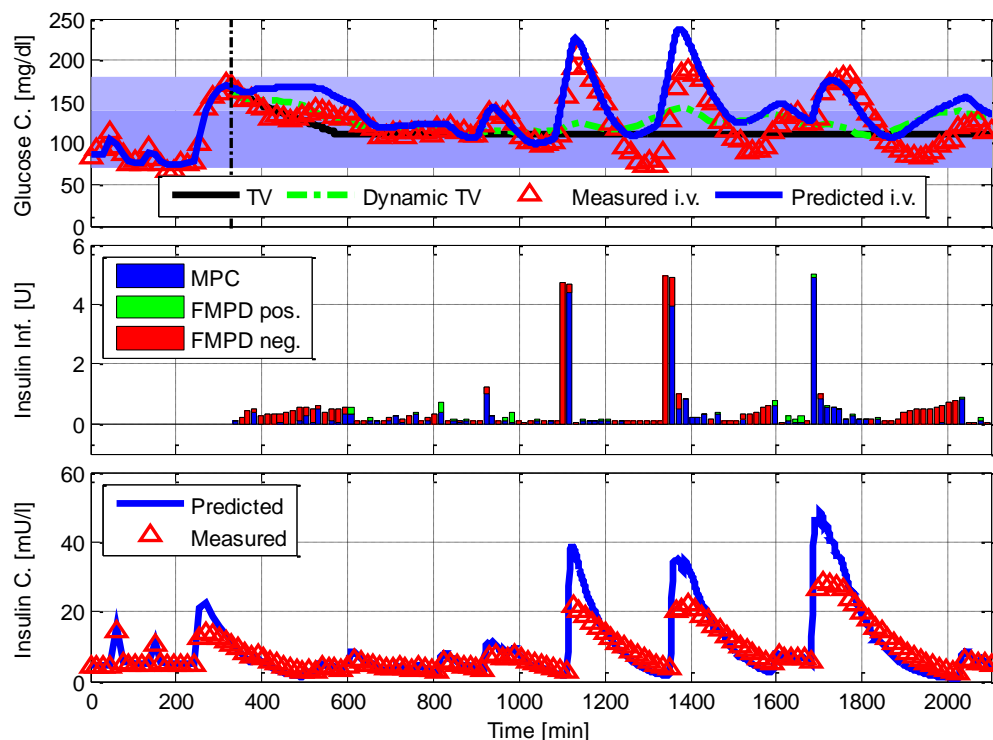


Figure 18: Evaluation of an *in-silico* control run for Subject 08 to assess effects of model uncertainty. Red triangles represent measurements from the *in-silico* individual. Blue curves represent model predictions. The chosen blood glucose concentration target value for control is 110 mg/dl. Only carbohydrates (meals and i.v. / oral glucose) are administered based on the original protocol of the clinical trial. Information on carbohydrate intake is passed to the controller upon start of intake, except for extra orange juice (12g) on day 2 (4:00 p.m., $t=1560$ min). The optimal insulin dose is calculated by the controller and applied to the process (centre plot). Blue bars represent doses calculated by the MPC and red parts subtracted and green parts added by the offset controller.

For the exemplary virtual patient displayed in Figure 18, the predicted half-life time for insulin has been underestimated causing a faster decay of predicted insulin values and consequently a faster rise of predicted glucose levels than measured levels ($t = 400$ min). This prediction causes the MPC to supplement the falling predicted insulin levels with additional insulin. However, measured insulin is still sufficient and measured glucose is already below target, causing the offset controller to correct (restrict) the dose calculated by the MPC. Once glucose rises above target level again, dose reduction by the offset controller abates. This reactive control

behaviour slightly restricts the feed-forward capabilities of the MPC and causes the glucose trajectories to slightly oscillate. Especially for high doses, i.e. prandial insulin, underestimated half-life time of insulin action is critical, e.g. for breakfast at time $t = 1000$ to 1200 min. However, overall the glucose trajectories stay well in target, also after a glucose disturbance at $t = 1560$ min (elaborated in next section).

III.3.1.2 Disturbance Rejection

Despite important developments in sensor and pump technology, the controller must cope with both, inaccuracies in glucose sensing and delays in insulin action. This is particularly problematic when a system disturbance, e.g., an unannounced meal, occurs and triggers a rapid glucose rise that is substantially faster than the time needed for insulin absorption and action [14]. Other disturbances include changes in metabolism, i.e. during exercise, stress or medical treatment.

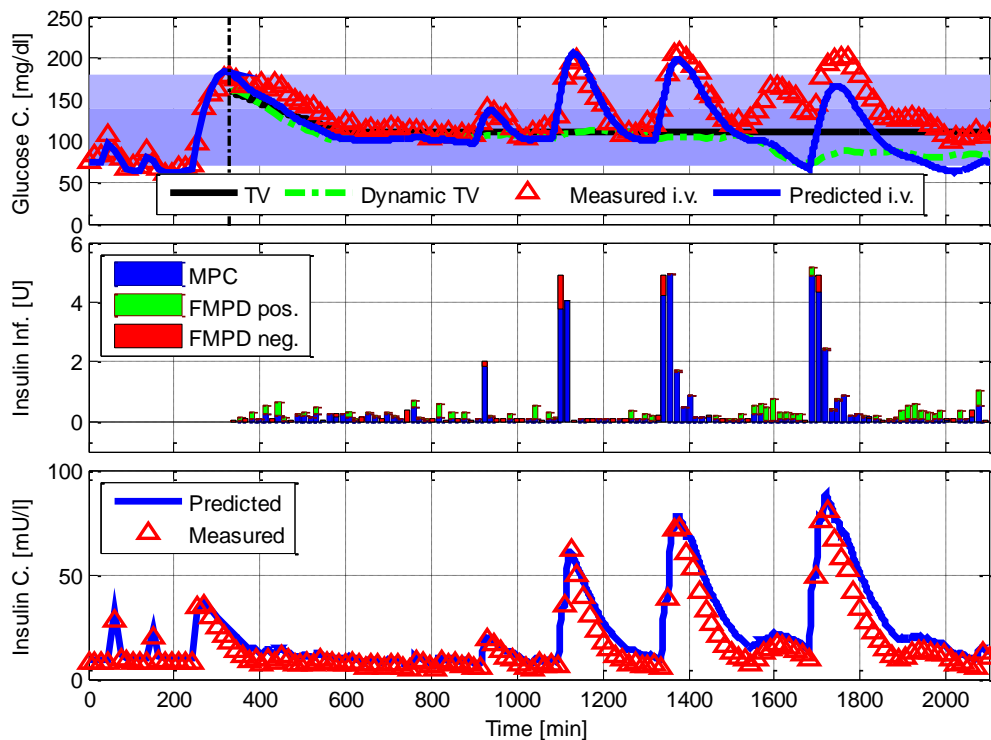


Figure 19: Evaluation of an *in-silico* control run for Subject 06 to assess effects of disturbances. Red triangles represent measurements from the *in-silico* individual. Blue curves represent model predictions. The chosen blood glucose concentration target value for control is 110 mg/dl. Only carbohydrates (meals and i.v. / oral glucose) are administered based on the original protocol of the clinical trial. Information on carbohydrate intake is passed to the controller upon start of intake, except for extra orange juice (12g) on day 2 (4:00 p.m., $t = 1560$ min). The optimal insulin dose is calculated by the controller and applied to the process (centre plot). Blue bars represent doses calculated by the MPC and red parts subtracted and green parts added by the offset.

Here, to evaluate disturbance rejection, a disturbance corresponding to an intake of 1 glass of orange juice (12 g glucose) was triggered at 4:00 p.m. on the second day ($t = 1560$ min). As shown exemplary for Subject 06 in Figure 4, the resulting divergence of model predictions and measurements triggers a quick reaction by the offset-control and a slow and steady shift of the dynamic target value. In spite of under-prediction of insulin half-life time, the disturbance is handled well and does not result in a controller overreaction with a risk for hypoglycaemia.

III.3.1.3 Measurement Error/Noise and overall Performance

We are evaluating the control algorithm for glucose measurements with a mean absolute relative error (MARE) of 5%. Although the algorithm is first (required by the Ethics Commission for Clinical Trials at the Medical University of Graz, where the trials were conducted, for safety reasons for a first-in-man study of the controller) evaluated in a clinical setting in an i.v.-s.c. route with an expected MARE of i.v. measurements below 2%, a higher simulated MARE was chosen for conservative evaluation. As the results show, the chosen level of noise had no significant adverse effect on glucose control.

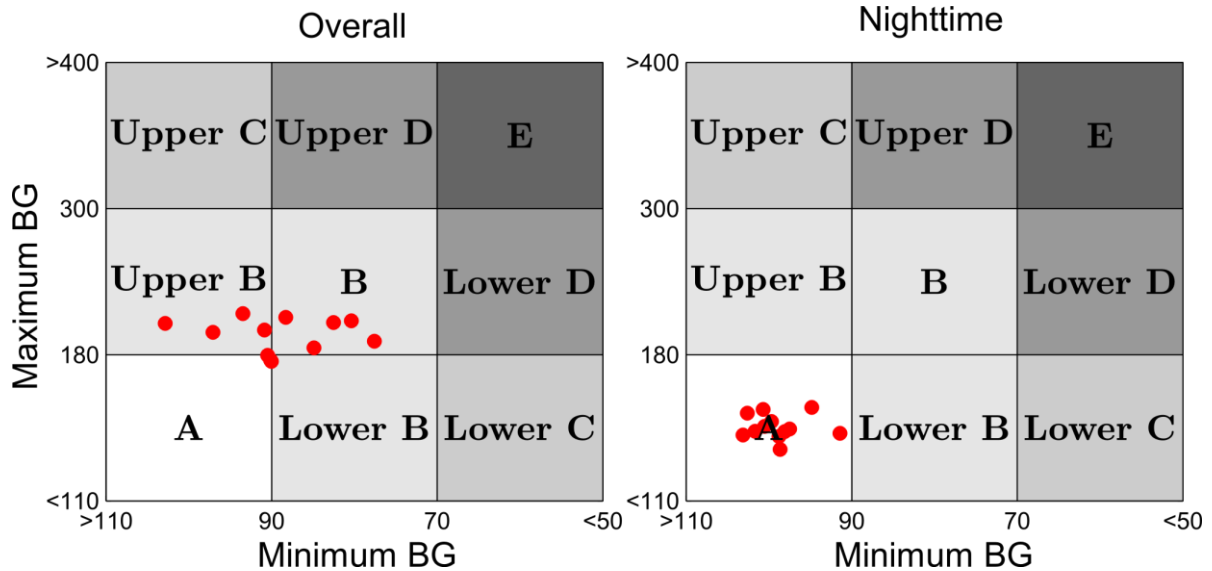


Figure 20: CVGA (95%tile) of *in-silico* controller evaluation for the whole virtual cohort. Left: Control variability over the whole duration of the trial (7:30 p.m., Day 1 to 10 p.m., Day 2). Right: Control variability of overnight control (10:00 p.m., Day 1 to 8 a.m., Day 2).

To assess overall performance of the control system throughout the cohort, a control variability grid analysis [199] (CVGA, Figure 20A/B) is conducted. The CVGA shows that the glucose trajectories are well within normoglycaemic range, without episodes of hypoglycemia (see also Table 2).

Also, night-time control (Figure 20, right) was almost completely within target range with a mean blood glucose level only slightly above target value (TV: 110 mg/dl).

Table 2: Dataset (Results) statistics of *in-silico* control trial. Target range was defined as 70 to 180 mg/dl 3h postprandial and 70 to 140 mg/dl on all other times. “OVERALL” defines the whole duration of the trial (7:30 p.m., Day 1 to 10 p.m., Day 2); “DAYTIME” refers to the time after breakfast until the end of trial (8:00 a.m., Day 2 to 10 p.m., Day 2); “OVERNIGHT” defines nighttime period during the trial (10:00 p.m., Day 1 to 8 a.m., Day 2).

	OVERALL	DAYTIME	OVERNIGHT
t in Target [%]	84 (72 to 92)	79 (67 to 90)	94 (83 to 100)
t below 52 mg/dl [%]	0 (0 to 0)	0 (0 to 0)	0 (0 to 0)
t below 70 mg/dl [%]	0 (0 to 0)	0 (0 to 0)	0 (0 to 0)
t above 180 mg/dl [%]	26 (19 to 41)	34 (26 to 46)	6 (0 to 17)
Mean Glucose [mg/dl]	128	132	117
Glucose stdv [mg/dl]	28	32	11
Glucose Amp [mg/dl]	115 (95 to 134)	115 (95 to 134)	43 (32 to 65)

III.3.1.4 Retrospective Controller Verification

Retrospective controller verification returns, at each sampling point, the theoretically calculated control input by the *in-silico* AGC system given the (control) input history of the actual clinical trial before that sampling point. The verification of the control algorithm is conducted on the glucose measurement data from the original 2PRCT clinical trial. The control trajectories and the given doses of the original trial and the *in-silico* AGC system can thus not be compared in whole, but only point-wise. This allows a judgment on the reasonability and verity of the theoretically calculated dose within a realistic clinical trial setting. However, the effect of the calculated control input by the *in-silico* AGC system, as well as its overall stability and performance cannot be validated as the analysis is retrospective.

As initial conditions (IC) are subjected to high uncertainty, if no information on prior inputs is available, the workflow as described above, using initial model screening, is not applicable. Here, the scenario if the controller has already been provided with a reasonable model fit is evaluated.

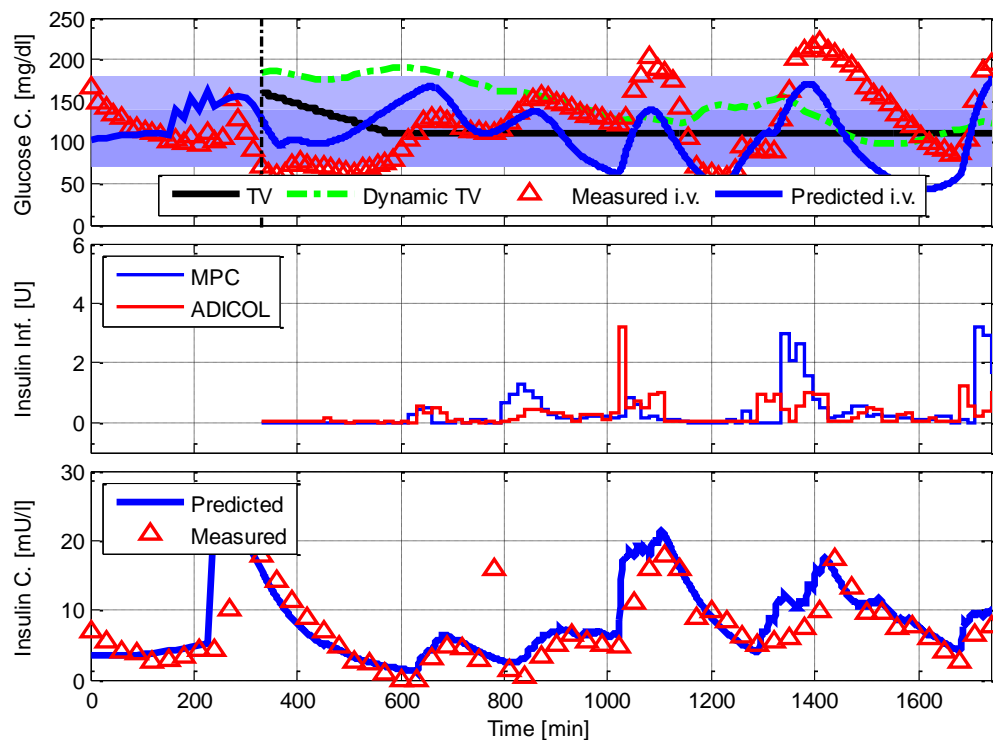


Figure 21: Retrospective evaluation of the MPC glucose control algorithm. Red triangles represent measurements from **Subject 03** of the original trial dataset. Blue curves represent model simulations. Quality of model predictions here is average (compare to profiles in Appendix V.5.3.2.2). The chosen blood glucose target value for control is 110 mg/dl. Blood glucose is predicted based on the original input history of the clinical trial. In parallel, hypothetical insulin dosing suggestions are calculated at each time-step by the controller, but are not applied to the process, and therefore repeatedly high doses are recommended. This allows a qualitative comparison of the controller output within real clinical trial conditions (prediction error in glucose levels).

Figure 21 shows an exemplary run of retrospective controller evaluation for Subject 03. Overall, the glucose (top) and the corresponding insulin infusion rate (middle) trajectories show that the algorithm increases insulin dosing correspondingly by reasonable amounts as glucose levels rise (e.g. at times $t = 600$ min, $t = 1100$ min, $t = 1350$ min and $t = 1700$ min). Also, there is no insulin dosing at low glucose levels and insulin infusion is correctly reduced at times of low glucose levels.

III.3.2 *In-silico* Evaluation (Second Trial, CGM)

As a step forward and to comply with current state-of-the-art, it was planned for the 2nd trial to use CGM devices (s.c. measurements) to drive the control algorithm. The MATLAB based tool (including a Graphical User Interface) for glucose control in subjects with type 1 Diabetes Mellitus T1DM was extended and adapted for control by subcutaneous glucose measurements from CGM (Dexcom G4 Platinum) devices. The integrated system has been thoroughly evaluated *in-silico* by conducting an extensive robustness analysis vs. measurement errors and time-delays associated with s.c. measuring methods to define acceptance criteria for the required sensor system. The results of this analysis are presented here.

III.3.2.1 Model Uncertainties

To evaluate the effect of sensor error on AGC performance, a robustness analysis within an *in-silico* clinical trial (trial protocol as described in Section II.2.2.1) of automatic glucose control (on the same virtual patient cohort as described above) is conducted. For each patient, 15 tested artificial error/time-delay sets were evaluated resulting in a total of 180 trial runs. Tested error/time-delay sets were assembled assuming sensor errors ranging from 3 to 17 % MARE and subjected to a time delay of 0 to 30 min (Figure 22). Additionally, the sensor output error of a newly developed sensor (Fraunhofer ICT-**IMM**) was evaluated retrospectively using the sensor output data collected during the first clinical trial (REACTbyALGO, n=8) in month 35 with time-delays of 0, 15 and 30 min, resulting in additional 36 *in-silico* individuals simulated.

Following the trial protocol ensures an evaluation under realistic conditions. Under realistic conditions, the initial model identification may result in a non-ideal model fit, thus the effect of sensor error is evaluated in the presence of model errors (see Figure 25).

III.3.2.2 *In-silico*-Sensor Noise

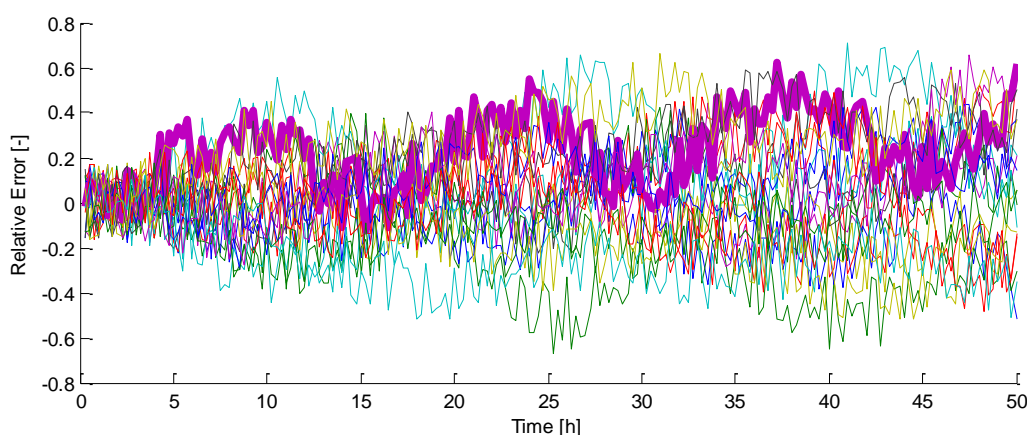


Figure 22: 300 random in-silico sensor noise signal profiles generated with the method described by Fachinetti et al. [198].

To generate the artificial error signal, the method described by Fachinetti et al. [198] is used. The s.c. measurement (*SCGM*) signal is calculated:

$$SCGM(t) = (1 + s(t))IG(t) + v(t).$$

with $v(t)$, a Gaussian noise signal (zero mean, max. rel. error 35%), $IG(t)$, the actual interstitial (s.c.) glucose levels and $s(t)$, the error drift factor generated from integration of a Gaussian noise signal:

$$s(t + 1) = 3s(t) - 3s(t - 1) + s(t - 2) + w(t).$$

With $w(t)$ as the Gaussian noise (zero mean and max 1% random drift per time step of 15 min) resulting in a maximal relative drift of $\max(s) = 80\%$ within a 24 h time interval. Exemplary relative time-error profiles are displayed in Figure 22.

The artificial s.c. glucose measurement ($SCGM(t)$) is thus generated by superimposing the raw glucose trajectories from the subcutaneous compartment (interstitial skin) from the simulated individual with a single artificial sensor noise signal profile from Figure 22.

III.3.2.3 Retrospective Evaluation of IMM Sensor Noise

To evaluate the impact of the actual sensor error generated by the IMM sensor, the error signal from the measurement output collected with the IMM sensor during the first clinical trial (REACTbyALGO at MUG in M35) is used. To extract the relative error, the difference between collected i.v. measurements and the IMM output divided by the i.v. values was calculated:

$$RelErr = (IV - IMM)/IV$$

The calculated relative error was then multiplied with the simulated in-silico predictions of subcutaneous glucose from the respective virtual patient (exemplary result displayed in Figure 23; Aggregated results of controller performance based on the IMM sensor error signal are displayed in Figure 26). The retrospectively calibrated IMM sensor output has a MARD of 14%.

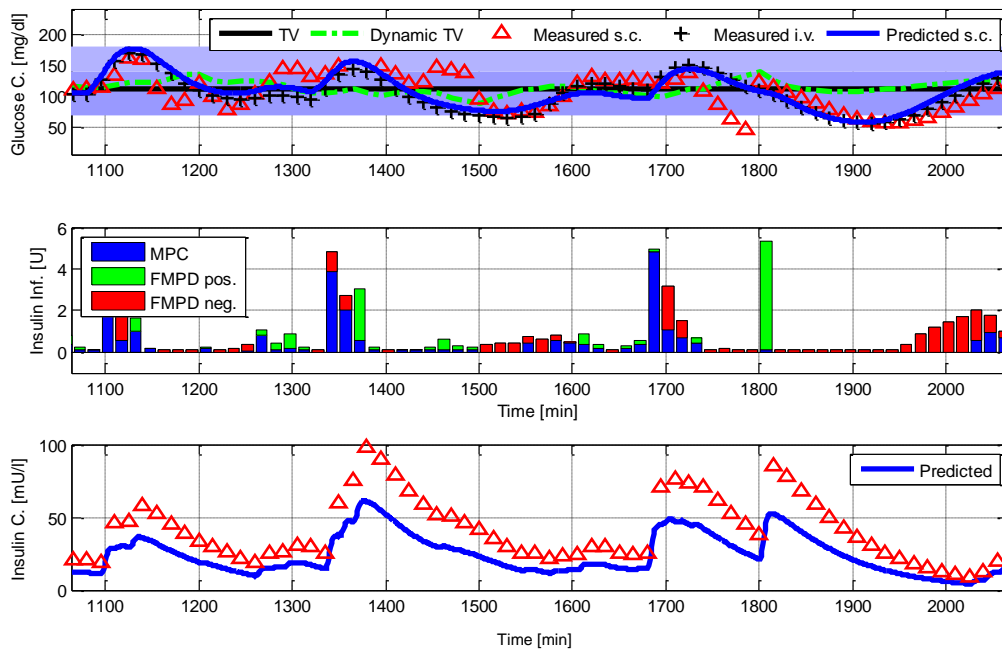


Figure 23: Exemplary take-out from an in-silico trial using the error signal from the measurement output collected with the IMM sensor during the first clinical trial (REACTbyALGO1). Sensor signal was collected from

individual No. 10 with a simulated time-delay of 30 min. Top plot displays glucose trajectories from: s.c. measurements by simulated IMM sensor (red triangle), i.v. reference measurements (black crosses) and the predicted glucose level by the algorithm (blue line). The black line represents the base target value the glucose levels and the dynamic target value which represents the actual target, the controller is aiming for due to differences in measured and predicted glucose values. Middle plot: infused insulin (every 15 min), infused dose is blue amount increased by green or reduced by red amount (increase and reduction corresponds to FMPD based input correction). Lower plot: measured (red triangles) and predicted (blue lines) insulin levels.

III.3.2.4 Measurement Error/Noise and overall Performance

To visualize the results of the robustness analysis, a control-variability grid analysis chart (Figure 24) and a traffic-light plot (Figure 26) were generated. The control-variability grid analysis shows that increasing error leads to a higher prevalence of hypoglycaemic events whereas an increase in time-delay especially increases the glucose levels at the higher end with a higher prevalence for hyperglycaemia. An exemplary trial run is displayed in Figure 25.

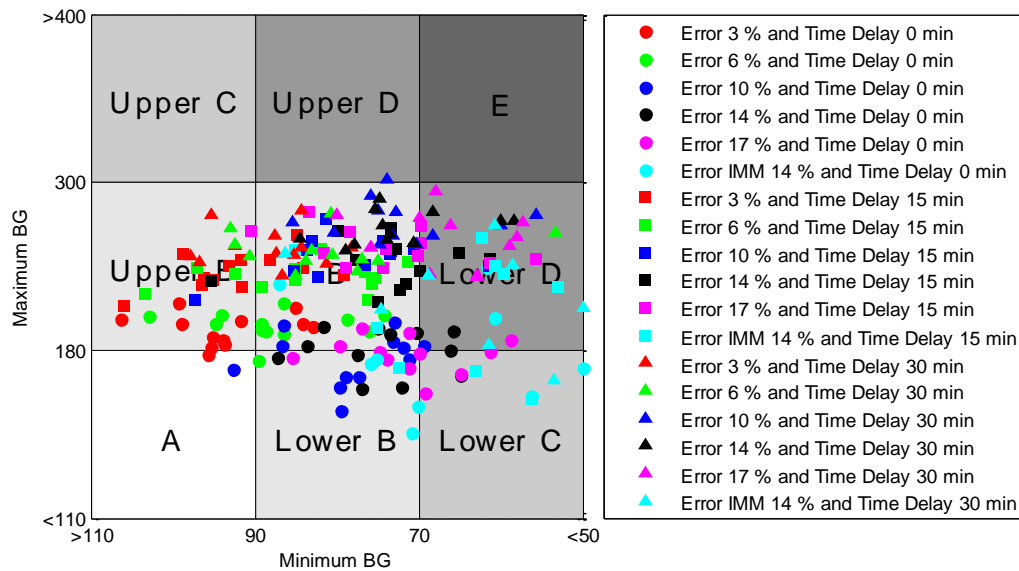


Figure 24: Control-variability grid analysis of the simulated 216 individuals (15x12 with artificial sensor noise plus 3x8 with IMM sensor). Error sets are separated as: circles for zero time-delay, squares for 15 min time-delay and triangles for 30 min time-delay. Colours code the different relative errors of 3 (red), 6 (green), 10 (blue), 14 (black), 17 (magenta), and IMM with 14% (turquoise). Control variability deteriorates for increasing time-delay and increasing relative error.

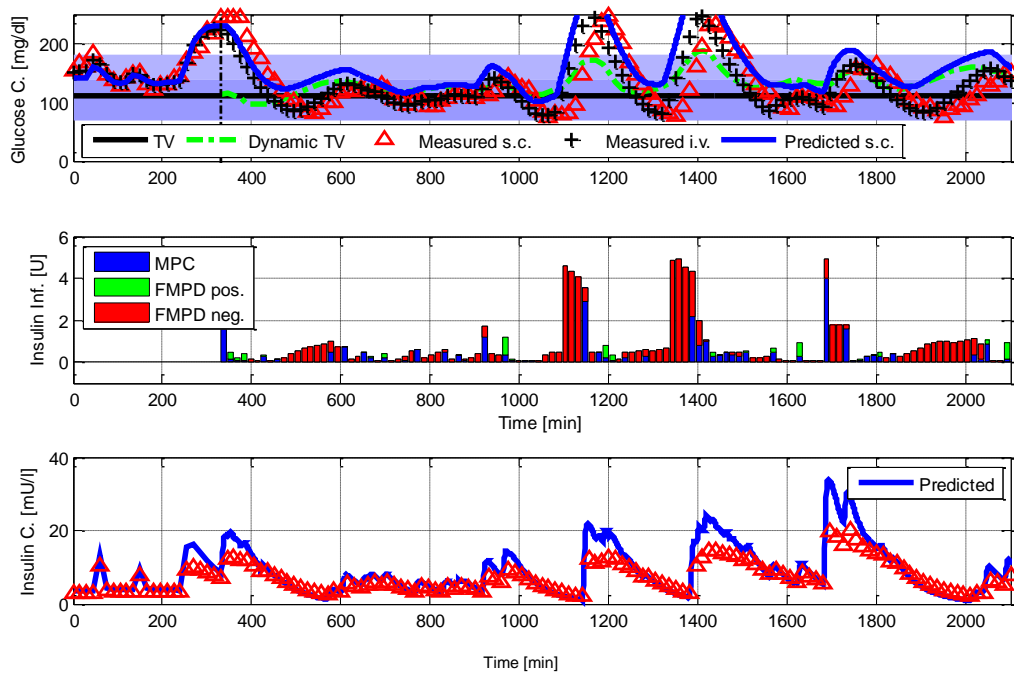


Figure 25: Exemplary summary plot of in-silico evaluation of AGC robustness properties vs. sensor errors. Simulated sensor error was 6% MARD with a time-delay of 30 min. Displayed are: Top plot: in-silico s.c. glucose measurements subjected to simulated error (red triangles), in-silico i.v. reference glucose measurements (black crosses) and predicted s.c. measurements (blue line). The black line represents the base target value the glucose levels and the dynamic target value which represents the actual target, the controller is aiming for due to differences in measured and predicted glucose values. Middle plot: infused insulin (every 15 min), infused dose is blue amount increased by green or reduced by red amount (increase and reduction corresponds to FMPD based input correction). Lower plot: measured (red triangles) and predicted (blue lines) insulin levels.

To define criteria for acceptable measurement errors, metrics for control performance are evaluated. Ranges for time-in-target (glucose levels between 70 and 180 mg/dl up to 3h postprandial and between 70 and 140 mg/dl during other times), time below 70 mg/dl (mild hypoglycaemia), time below 50 mg/dl (hypoglycaemia) and time above 140 mg/dl (hyperglycaemic episodes) were defined.

For each criterion, an acceptable total amount of measurements in the defined range is defined. The colours green, orange and red highlight, if control performance (acceptable total amount of measurements in the defined range) is good (acceptable), critical (acceptable in controlled conditions) or bad (unacceptable). For each criterion, the colours have been specified together with experts from MUG, indicating the acceptance level of time in the respective range:

- Time in target: green: above 80 %, red: below 60 %;
- Time above 140 mg/dl: green below 30 %, red above 50 %;
- Time below 70 mg/dl: green below 1 % (exact, not rounded), red above 3 %;
- Time below 50 mg/dl: green for 0 %, red above 1 % (both exact, not rounded);

Everything in-between the values for red and green is still acceptable in controlled conditions and marked in colour orange. The summarized results are plotted in Figure 26.

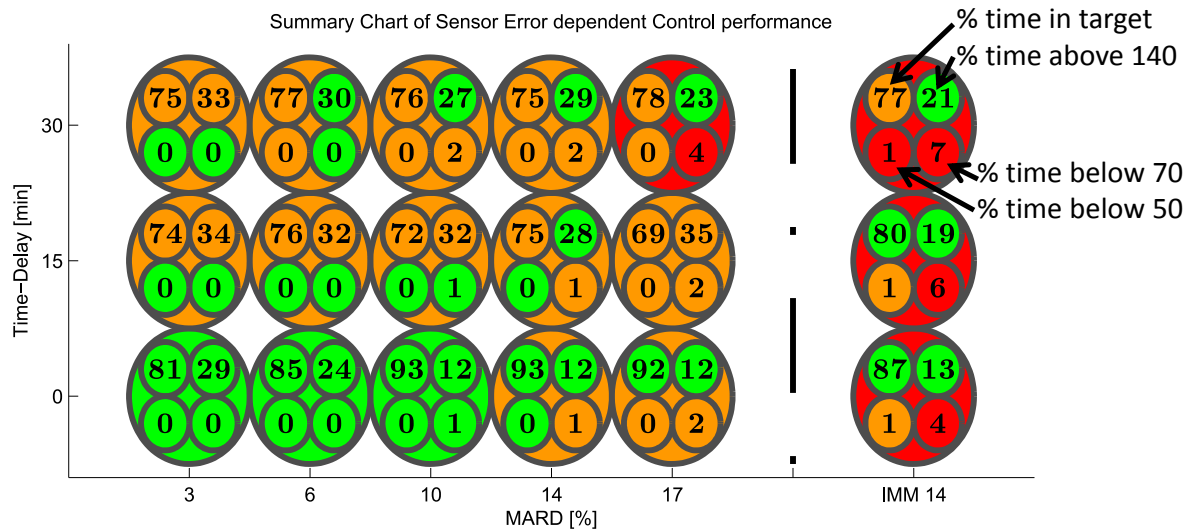


Figure 26: Summary chart of sensor error-dependent control performance. Each large circle represents a trial using a virtual cohort ($n=12$) to evaluate the effect of error (expressed as MARD in %) and time-delay (up to 30 min) in s.c. measurements. The left part represents in-silico trials with artificially generated sensor noise (Breton 2008, Facchinetti 2007 & 2010) and the right part represents in-silico trials with the sensor noise observed during REACTbyALGO by the IMM sensor. The chart shows (in % of total time) the time in target, time above 140 mg/dl, time below 70 mg/dl (mild hypoglycaemia) and the time below 50 mg/dl (hypoglycaemia). The colours green, orange and red highlight, if control performance is good, critical or bad. For each criteria, colours have been specified as follows: time in target: green above 80 %, red below 60 %; time above 140 mg/dl: green below 30 %, red above 50 %; time below 70 mg/dl: green below 1 % (absolute, not rounded), red above 3 %; time below 50 mg/dl: green for 0 %, red above 1 % (both absolute, not rounded); Everything in-between the values for red and green is still acceptable in controlled conditions and marked in colour orange.

The analysis (Figure 26) shows that sensor noise up to 14 % MARD without time-delay (i.e. the commercial sensor “Dexcom G4 Platinum” with just above 10% [200], which was also used later in the clinical trial #2) is acceptable for closed-loop control and that the sensor error by the IMM sensor is not suitable for driving an AGC algorithm.

In principle, the controller could still handle a time delay of 15 min. However, this would result in a significant reduction of time in target-range. These results now allow an overall assessment of the controller performance, also required for risk evaluation for the in-vivo clinical trial (Part IV). The in-silico evaluation shows, that the controller is able to control blood glucose in an acceptable range even in the presence of model uncertainties, disturbances and significant measurement errors.

Part IV.

Results from a Clinical Trial

IV.1 Clinical Trials: Materials and Methods

After having evaluated the reliability of the developed PBPK/PD models of the GIM [2], and the integrated model predictive control approach [3], two mono-centric, open, non-controlled feasibility studies in subjects with type 1 diabetes were conducted in successive steps.

The glucose control algorithm (GCA) developed here has never before been used on patients in a clinical trial. The first (iteration) prototypes have been evaluated *in-silico* (Section III.3.1) before tests were conducted in a first clinical feasibility (REACTbyALGO) study in Graz in Jan/Feb 2013 using, for safety reasons, accurate glucose measurements from blood.

In the second iteration, the AGC has been tailored towards blood-glucose control using subcutaneous continuous glucose monitoring (CGMs) data for the calculation of insulin dosing, which corresponds to the state of the art in (other) AGC systems currently in development [64, 192]. Performance of the control system using CGM data has first been evaluated *in-silico* to assess the required sensor accuracy for safe control in a clinical trial. The final system was then evaluated within the second clinical trial for AGC in Jan 2014.

In both trials, each of the 10 subjects participated in a 6h clamp and 24h-manual-closed-loop blood glucose control experiment (total 30h). The trials were performed in a controlled setting at the Clinical Research Centre (CRC) at Medical University of Graz. The patients were recruited from the diabetes outpatient clinic of the centre. The results of the 24h feasibility studies for automatic glucose control are presented in the following sections.

IV.1.1 Trials

IV.1.1.1 REACTbyALGO (Trial #1)

We conducted two mono-centric, open, non-controlled feasibility studies in subjects with type 1 diabetes, the first in February 2013, the second in January 2014. The study protocol was approved by the local ethics committee and performed in accordance with the Declaration of Helsinki and the principles of Good Clinical Practice. The study included a total of 10 subjects and was performed in a controlled setting at the Clinical Research Centre (CRC) at Medical University of Graz. The patients were recruited from the diabetes outpatient clinic of the centre.

IV.1.1.1.1 Subjects

Signed informed consent was obtained before any trial-related activities. (Trial-related activities are any procedure that would not have been performed during standard medical care). Subjects were 40.7 ± 12.5 (25-59) years of age and had type 1 diabetes (as defined by WHO) for at least 24 months with C-peptide levels below detection threshold. Subject's HbA1c was required to be below 10%, and the Body Mass Index (BMI) was 27 ± 3 (24-32) kg/m², with body weights of 87.5 ± 10.5 (67-101) kg and body heights of 179 ± 6.5 (169-191) cm. All subjects have been treated with continuous subcutaneous insulin infusion (CSII) for at least 3 months prior to start of the study. Further exclusion and withdrawal criteria, analysis methods as well as intervention and stopping rules are listed in Appendix V.5.3.1.

IV.1.1.1.2 Trial Protocol

The trial protocol was adapted from the protocol of the 2PRCT described in Section II.2.2.1, Figure 9. Subjects were admitted to the clinical research centre at 1:30 p.m. in the afternoon of the study day and underwent the study day examination (concomitant illness, vital signs, adverse events) and preparation (insertion of cannulas for blood sampling). Patients arrived in fasted state (last meal and above basal insulin dose at 10:00 a.m.) and switched basal insulin delivery from their own pump to a constant basal insulin infusion rate from the study pump. Throughout the study blood glucose measurements were taken every 15 min. During clamp phase (2:00 p.m. until 5:00 p.m.), patients received additional i.v. insulin Actrapid (NovoNordisk) or i.v. glucose if required to stabilize patients at a glucose level in the range of 100 mg/dl (5.55 mmol/l) < BG < 120 mg/dl (6.67 mmol/l) at 5:00 p.m. After 5 p.m., the clamp protocol (i.v. insulin and glucose administration) was discontinued. Basal insulin (IIP) was continued. From 2:00 p.m. on blood samples for insulin and glucagon measurements are taken every 30 min postprandial and once every hour during the night.

At 6:00 p.m. the patients received standardized first dinner. The prandial insulin need is covered by a dose of short acting insulin delivered with the installed insulin pump. The basal insulin infusion rate from 1:30 p.m. until 7:30 p.m. and the insulin dose before the first standard dinner was derived from the individual insulin need and determined by the investigator. Patients received four standardized meals: Dinner (60 g CHO, 18:00 p.m. day 1), breakfast (48 g CHO, 8:00 p.m. day 2), lunch (60 g CHO, 12:00 p.m. day 2), and again dinner (60 g CHO, 18:00 p.m. day 2). From 7:30 p.m. until end of the study day all insulin doses, including the prandial insulin doses (breakfast, lunch, second dinner), have been determined by the MPC algorithm administered via the insulin infusion pump. At 7:30 p.m. the next day all patients followed their normal treatment regimen and came back 3 days later for a follow up visit.

IV.1.1.2 REACTbyALGO2 (Trial #2)

IV.1.1.2.1 Adapted Trial Protocol

The trial protocol was further adapted from the protocol of the first trial described above. In the first trial, initial model identification was based on the clamp data during the first 6h of the trial. At this time, insulin was infused i.v., and blood glucose levels were stabilized. The resulting smooth dynamics (containing only a reduced amount of information on dynamic model behaviour) and missing information on absorption behaviour of s.c. glucose did not suffice for good model identification. Thus, for the second trial, subjects were screened one day prior to start of the clinical trial, where they also were equipped with a CGM device. They were then admitted on the following day to the clinical research centre at the Medical University of Graz (MUG) for the clinical trial and received basal insulin from insulin pumps until initiation of closed-loop control. After start of control, the protocol and all criteria are as in the protocol for the first trial.

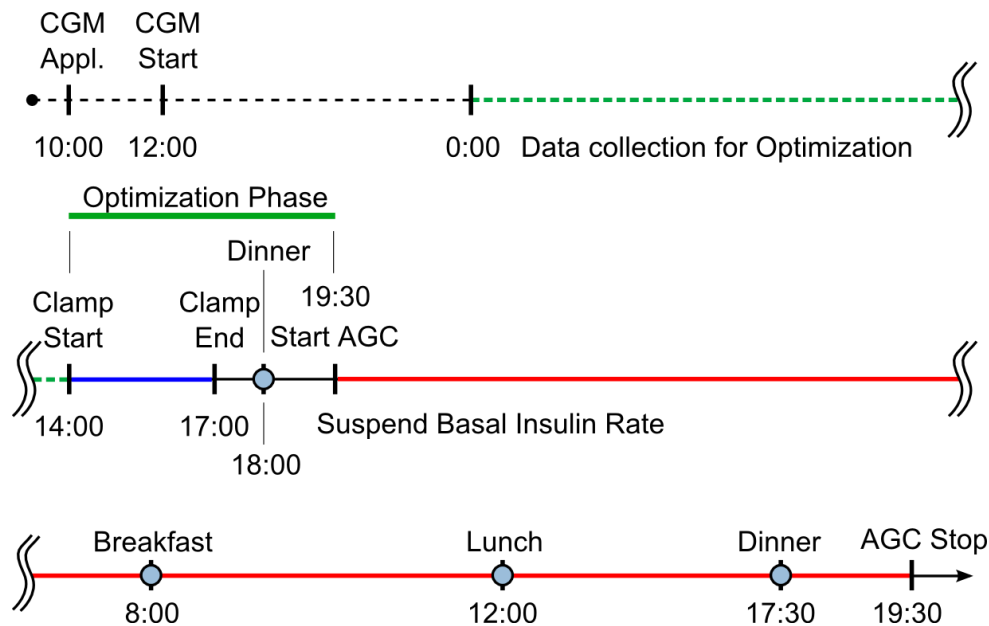


Figure 27: Trial Protocol overview from the second clinical trial (REACTbyALGO2). The first line is the day prior to the trial, when the CGM device was applied to the patient at 10:00. Day 1 (starting at 14:00) and day 2 of the trial are represented by the middle and lower line, respectively. Data collected by the CGM from 0:00 to 14:00 at the day of the trial was used for model optimization (i.e. individualization).

IV.1.2 Outcome Measures

The specified parameters for the assessment of the effectiveness of the control system were: mean BG; Time/Percent of BG values in Target (70 - 180 mg/dl 3h postprandial and 70 - 140 mg/dl on all other times), time/percent below 70 mg/dl, and above 180 mg/dl, as well as number of hypoglycaemic events < 60 mg/dl treated with carbohydrates. Outcomes were calculated for the total of 24h of control, and separately for night-time (10:00 p.m. - 8:00 a.m.) and day-time (8:00 a.m. – 7:30 p.m.).

Two experiments from trial#1 were affected by technical failures (Subject 1 and Subject 2) in the model core (Subject 2) and associated with control algorithm parameterization (Subject 1). The results of Subject 1 were still included in the analysis as the algorithm, once corrected (there was a sign error in calculating ΔTV), quickly recovered autonomously after the second failure (Subject 1) but could not be brought back online after the first failure (Subject 2).

Outcome statistics were calculated using MATLAB®.

IV.1.3 Laboratory Analyses

Blood for insulin and glucagon measurements was drawn into tubes containing EDTA and put immediately on ice. Plasma was isolated by centrifugation at 4°C and frozen within 30 min from the time of sampling. Insulin and glucagon were measured by immunoassay.

IV.1.4 Control Algorithm

The robust MPC algorithm is described in Section III.2.3 [3]. The algorithm runs on a PC where, once every 15 min, the blood glucose data (trial#1) and CGM data (trial#2) is entered manually. After processing the data, the algorithm suggests an

insulin infusion rate. This insulin infusion rate is checked for plausibility by the staff and entered manually into the insulin pump. The insulin pump is filled with short-acting insulin (Lispro) whose PK/PD parameters are part of the kernel/algorithm. Clinical parameters and patients' clinical history data including age, sex, race, height, weight, BMI, and history of diabetes are collected prospectively.

IV.2 Control Performance

The GCA has not been used on patients within a feasibility study before. Thus, within the first study glucose control was performed with intravenous glucose measurements for reasons of safety. For the second study, after adaptation of the control algorithm to cope with s.c. measurements, CGM data was used to drive the algorithm. Each of the 10 subjects in the two trials participated in a 6h clamp and 24h-manual-closed-loop blood glucose control experiment (total 30h). The aggregated results of the study are shown in Figure 28 and Table 3.

IV.2.1 Glycaemic Control

To demonstrate clinical performance of the AGC system, the control performance of the two trials are compared to competitor systems (for which data was available). The times in target range achieved by the different Algorithms is listed in Table 3. A visual representation of the key performance indicators is shown in Figure 28.

Table 3: Summary statistics of results of all 30-h closed-loop experiments of REACTbyALGO (RbA1 and RbA2) in comparison to trial results from studies by El-Khatib-1 et al. (with two visits for each patient, EK-11 and EK-12) [36] and the ADICOL trial (comparison of an open-loop CSII standard-of-care protocol and the Cambridge algorithm, results unpublished, Dataset presented in Section II.2.2.1). Results are separated into overall, day-time-, and night-time-control. The left 3 columns correspond to the first visit/protocol/algorithm version and the right 3 columns correspond to the second visit/protocol/algorithm version of the respective clinical trial.

	EK-11	CSII	RbA1	EK-12	Cambridge	RbA2
OVERALL						
t in Target1	70 (54 to 82)	81 (56 to 97)	74 (51 to 93)	61 (50 to 70)	83 (58 to 98)	76 (60 to 93)
t in Target2	64 (50 to 81)	71 (43 to 97)	50 (32 to 80)	52 (40 to 58)	68 (42 to 92)	66 (52 to 89)
t below 50 mg/dl	3 (0 to 11)	3 (0 to 20)	0 (0 to 3)	0 (0 to 0)	0 (0 to 2)	3 (0 to 6)
t below 70 mg/dl	7 (0 to 19)	11 (0 to 44)	1 (0 to 7)	2 (0 to 8)	3 (0 to 13)	9 (0 to 17)
t above 170 mg/dl	36 (24 to 42)	26 (1 to 65)	61 (19 to 82)	51 (44 to 64)	41 (25 to 65)	32 (18 to 59)
Mean Glucose	137	117	156	161	138	128
Mean Glucose stdv	60	36	38	60	38	47
Mean Glucose Amp	215 (152 to 299)	148 (80 to 232)	157 (93 to 223)	202 (170 to 230)	154 (105 to 227)	194 (158 to 247)
OVERNIGHT						
t in Target1	91 (70 to 100)	81 (22 to 100)	79 (12 to 100)	95 (85 to 100)	95 (78 to 100)	90 (78 to 100)
t in Target2	88 (67 to 100)	71 (3 to 100)	38 (0 to 83)	81 (70 to 97)	75 (35 to 100)	78 (56 to 90)
t below 50 mg/dl	5 (0 to 18)	2 (0 to 8)	1 (0 to 7)	0 (0 to 0)	0 (0 to 3)	1 (0 to 7)
t below 70 mg/dl	9 (0 to 27)	13 (0 to 49)	2 (0 to 17)	0 (0 to 0)	2 (0 to 16)	9 (0 to 22)
t above 170 mg/dl	3 (0 to 6)	17 (0 to 100)	61 (0 to 100)	19 (3 to 30)	23 (0 to 65)	14 (0 to 34)
Mean Glucose	100	110	149	119	124	109
Mean Glucose stdv	18	17	21	24	21	27
Mean Glucose Amp	69 (37 to 107)	61 (25 to 168)	74 (49 to 133)	89 (49 to 113)	74 (39 to 151)	113 (61 to 184)
DAYTIME						
t in Target1	63 (50 to 77)	79 (37 to 100)	69 (50 to 93)	53 (23 to 61)	79 (38 to 98)	67 (54 to 85)
t in Target2	57 (45 to 70)	71 (37 to 100)	63 (43 to 93)	44 (11 to 57)	68 (28 to 87)	62 (48 to 85)
t below 50 mg/dl	2 (0 to 7)	4 (0 to 32)	0 (0 to 0)	0 (0 to 0)	0 (0 to 3)	4 (0 to 11)
t below 70 mg/dl	5 (0 to 9)	11 (0 to 63)	0 (0 to 0)	0 (0 to 0)	2 (0 to 8)	9 (0 to 17)
t above 170 mg/dl	51 (39 to 59)	32 (2 to 85)	62 (37 to 89)	65 (55 to 91)	53 (33 to 93)	43 (17 to 74)
Mean Glucose	150	123	163	175	149	140
Mean Glucose stdv	60	33	41	52	37	53
Mean Glucose Amp	189 (113 to 238)	132 (80 to 186)	142 (93 to 198)	160 (109 to 186)	135 (98 to 227)	189 (147 to 236)

As can be seen in Figure 28, the developed algorithm can compete with existing algorithms, especially in its second version in RbA2. When comparing the different trials, it has to be noted: the El-Khatib, the Cambridge, and the RbA1 trial use i.v. glucose measurements with an accuracy of approximately 2% MARE, although the Cambridge algorithm emulates the time-delay of s.c. measurements by delaying the sensor signal by 15 min. The RbA2 trial uses real s.c. measurements by CGM devices (Dexcom G4 Platinum) with an MARE of 10%. The values show that

improved time-in-target is overall bought with a higher risk for hypoglycaemia. When looking only at daytime control, in both trials the controller can compete very well with other algorithms. It shows similar values for time in target and only slightly higher than average values for time in low glucose ranges (< 70 mg/dl), although still less so than the open-loop CSII standard-of-care protocol. However, the figure shows that night-time control of the system in RbA1 (trial #1) was below average (see also Figure 29). In RbA2 (trial #2), also night-time control was very good in terms of time in target.

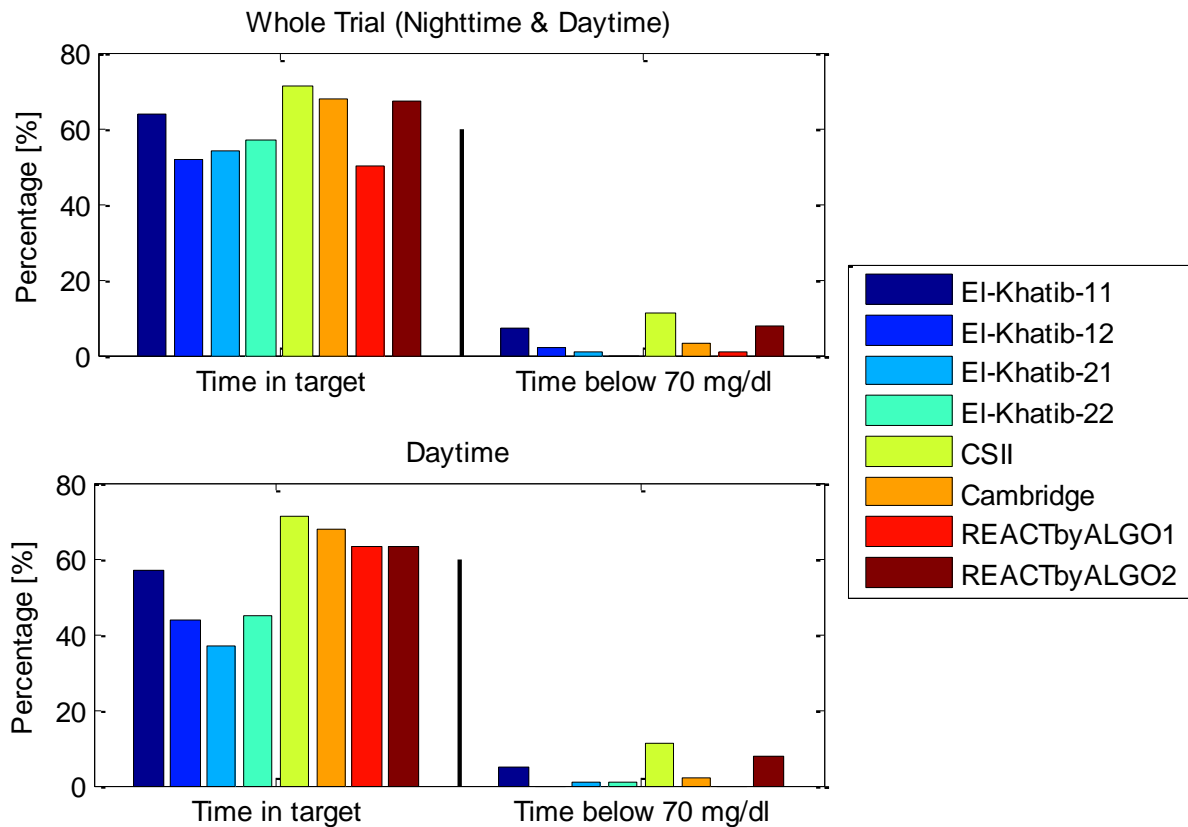


Figure 28: Graphical representation of the key performance indicators of published control trials (El-Khatib-1 [36]; El-Khatib-2 [26] and unpublished Data (CSII: standard clinical (non-automated) basal-bolus therapy; Cambridge: Hovorka et al. [24]) and the REACTION control trials (REACTbyALGO1/2: the two control-trials using the control algorithm developed here). Time in Target (left) is defined as Time of measured blood glucose levels within: $70 \text{ mg/dl} < BG < 140 \text{ mg/dl}$ (in fasted state) and $70 \text{ mg/dl} < BG < 180 \text{ mg/dl}$ (for 3h postprandial). Time below 70 mg/dl (right) is defined as Time of measured blood glucose levels $BG < 70 \text{ mg/dl}$. Displayed are percentages of measured glucose values in the respective range for overall control performance (top axis) and daytime control (bottom axis).

Even though in trial #1, the controller overall does not achieve the best scores for “Time in Target Range”, the glucose trajectories within trial #1 show the least individuals with episodes below 70 mg/dl. In general, basal insulin provision was too restrictive (especially during the night). Insulin action was overestimated and dose correction did not adapt accordingly. This was the case due to a conservative parameterization of the correction module (the FMPD controller) and due to issues in initial model identification. Initial model identification was based on the clamp data during the first 6h of the trial. At this time, insulin was infused i.v., and blood glucose levels were stabilized. The resulting smooth dynamics (containing only a reduced

amount of information on dynamic model behaviour) and missing information on absorption behaviour of s.c. glucose did not suffice for good model identification.

In trial #2, control performance was significantly improved. Due to the change in workflow (i.e. trial protocol), initial model identification was significantly improved resulting in good glucose control right from the start and a strong improvement of night-time control. Although time in target for day-time control was very good, there were a number of incidents of hypoglycaemia after lunch/before dinner on day 2, possibly caused by overdosing of insulin during meals due to an compensation of the model deviation during meals (predictions often too low) as well as during the decrease in insulin sensitivity in the morning followed by an increase in sensitivity in the afternoon (“dawn-effect”, see following Section IV.2.3) by the FMPD controller.

Another reason for the suboptimal control during the night, but low amount of hypos in trial #1 compared to trial #2 were the higher rejection rates for dose recommendations (see Section IV.2.4).

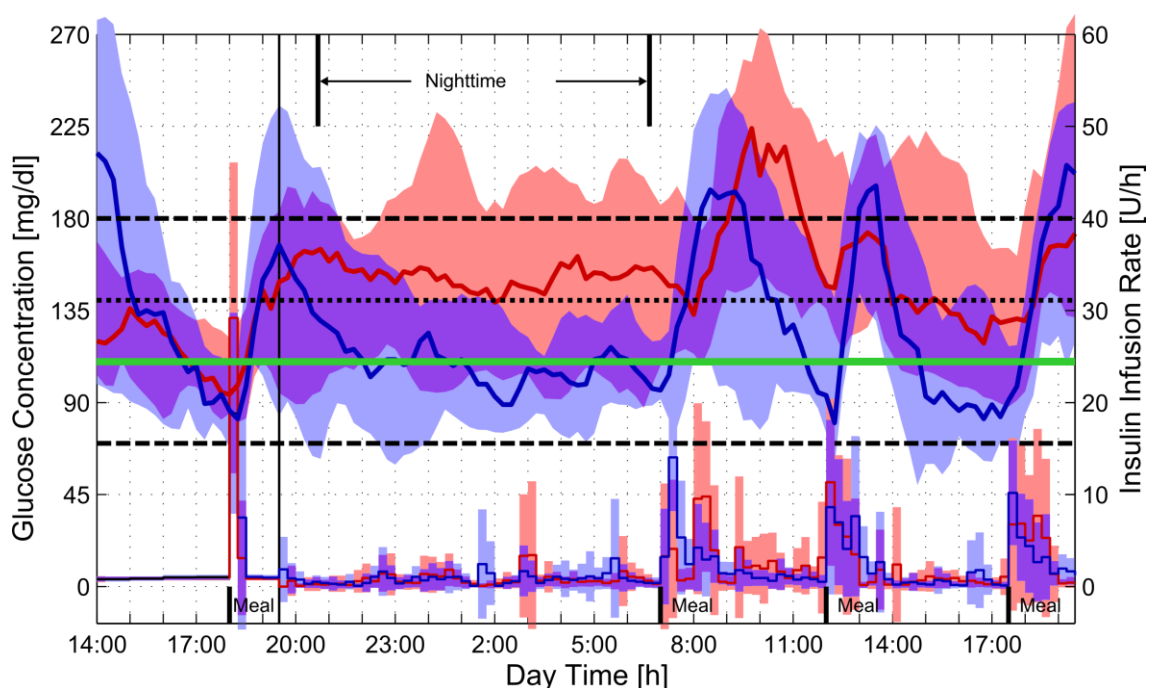


Figure 29: Mean (\pm SD) of venous peripheral glucose levels and insulin doses for REACTbyALGO1 ($n=10$, red trajectories and shaded areas) as well as REACTbyALGO2 ($n=10$, blue trajectories and shaded areas). The mean (SD) of venous plasma glucose (PG) levels with 15-min sampling is shown from all ($N=10$) 30-h experiments in ten subjects for each trial, respectively. **REACTbyALGO1:** During control ($t > 330$ min) the maximum in mean PG was 225 mg/dL at 10:00 A.M. after the first breakfast, and the mean nadir was 105 mg/dL at 4:45 P.M. before dinner on day 2. The overall mean of all 30-h PG results ($N = 119$ measurements per experiment) was 156 mg/dL. The overall mean PG during night-time (10 P.M.–8 A.M.) was 149 mg/dL ($N=66$ measurements per experiment). **REACTbyALGO2:** During control ($t > 330$ min) the maximum in mean PG was 205 mg/dL at 7:15 P.M. after the second lunch, and the mean nadir was 85 mg/dL at 12:00 P.M. before lunch on day 2. The overall mean of all 30-h PG results ($N = 119$ measurements per experiment) was 127 mg/dL. The overall mean PG during night-time (10 P.M.–8 A.M.) was 110 mg/dL ($N = 66$ measurements per experiment). The four meals are indicated by the black bar at the bottom of the plot. The mean of subcutaneous insulin infusion rates administered by the controller are plotted at lower end of plot (right axis).

IV.2.2 Insulin PK/PD

We have collected blood samples of insulin to evaluate if the insulin PK properties could be identified from glucose measurements. Dynamic properties of insulin were

estimated from glucose response dynamics during the clamp phase and then refined during the trial by model adaptation. Parameters for insulin sensitivity (S_I), renal clearance (GFR_{fac}^I), subcutaneous degradation (k_{SCD}^I), and subcutaneous unspecified binding (Q_{fac}) were identified. No a-priori assumptions on insulin PK parameters were used as compared to other algorithms [36].

In the first trial, for four out of ten subjects (Subjects 01, 03, 04 and 05), insulin PK properties were correctly identified from glucose clamp data before start of control (For all individual plots, see Appendix V.5.3.2). For all others, insulin half-life was overestimated, except for Subject 09, where it was underestimated. For Subjects 08-10, the qualitative prediction of insulin PK was significantly improved through model adaptation during control.

In the second trial, insulin PK was correctly estimated in 7 out of 10 subjects. For the remaining 3 (Subjects 7-9), the qualitative fit, with respect to $t_{1/2}$, was still good. This means that insulin PK can be identified from subcutaneous glucose measurements in most cases and at least qualitatively (quantitative mismatch compensated for by insulin sensitivity S_I) in all cases.

IV.2.3 Endogenous Glucagon PK/PD

We have collected blood samples of glucagon to gain insight in possible dysregulation of glucagon plasma levels and to evaluate the influence of glucagon in glucose control in T1DM within a post-hoc evaluation.

The model used during the trial only assumed plasma glucose regulated endogenous secretion of glucagon resulting in basal glucagon levels throughout, with small variations during high and low glucose.

The retrieved glucagon measurements revealed, however, that for many patients, significant postprandial surges of glucagon levels were observed (Figure 30, and Appendix V.5.3.2 for all individual profiles). In some patients, Subjects 3 and 4 for trial #1 (early morning until midday on the second day, see Figure 30 for Subject 03 and also Figure 31 for Subject 03 and Subject 04 from trial #1) and Subjects 1, 2, 5-9 for trial #2, glucose values remained significantly above predicted levels. This could be associated to the observed glucagon surges for all subjects except Subjects 5, 6 and 9 from trial #2, for which glucagon levels did not significantly increase.

It has been reported in literature that mixed meals may cause glucagon surges in individuals with T1DM [39, 156]. This may be caused by meal composition and especially the protein content of these meals. In T1DM, influence of glucose levels on glucagon secretion subside over time probably due to a deficiency in amylin-mediated intra-islet signalling necessary for glucose sensing [157]. Thus, the glucose absorbed from a meal does no longer suppress glucagon secretion.

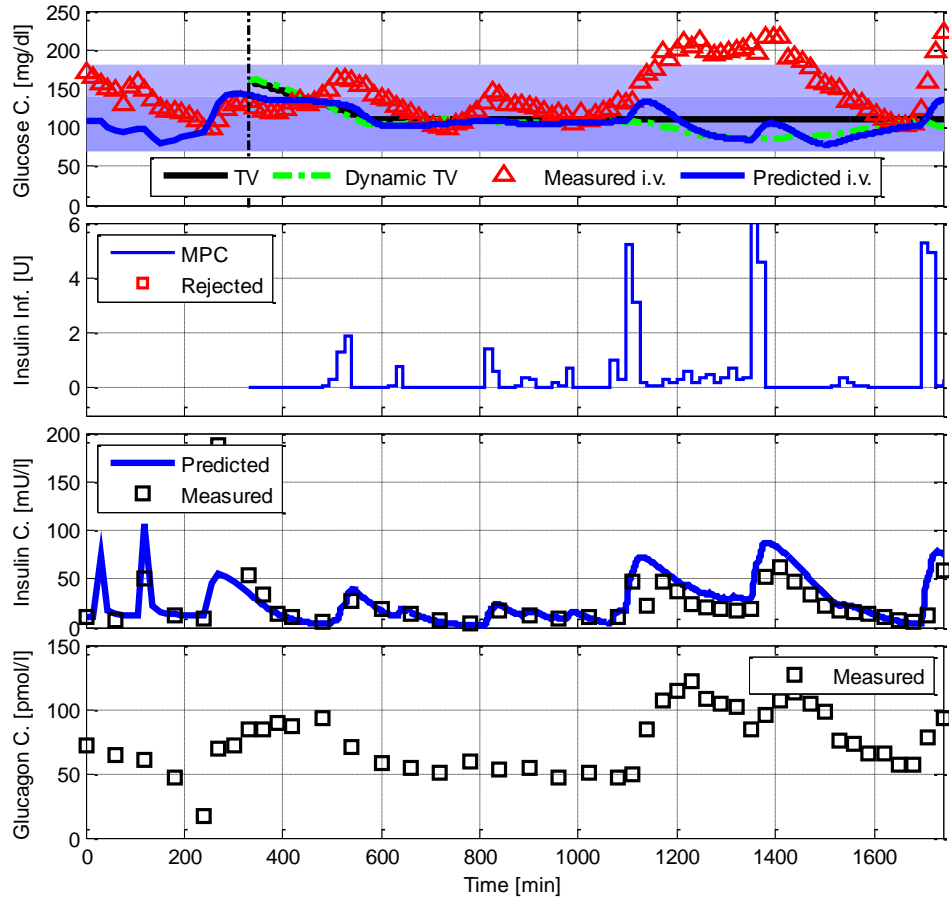


Figure 30: Glucose control experiment in Subject 03. During morning hours and early afternoon (8:00 a.m. ($t = 1100$ min) until 2:00 p.m. ($t = 1100$ min)) a systematic error of glucose predictions (underprediction) can be observed. At the same time, a distinct elevation of glucagon (postprandial glucagon surge) has been observed.

The original version of the model as it was used in the control trial was adapted to account for an alternative mode of action for glucagon on liver glucose homeostasis to better describe the observed glucagon dynamics (Figure 31). Incretin-dependent prandial glucagon secretion is modelled dependent on oral meal (glucose) absorption (Section II.2.1.1.3.5). In addition, a function for glucagon-dependent suppression of hepatic glucose uptake (M_{NHGU} , Section II.2.1.1.3.1.2) is included which was not accounted for before but as previously hypothesized [2] could be necessary to strengthen the effect of glucagon. Two refitted simulations on Subjects 03 and 04 (From trial#1, Figure 31) are compared, once without and once with the new glucagon mechanistic to illustrate the evaluation and effect of the tested mode of action.

Although the postprandial glucagon surges are now better captured, the deviations in the morning of the second day ($t = 1150$ to $t = 1400$) remain. In return, glucose levels after dinner on day one are now overestimated, as are the underlying glucagon levels.

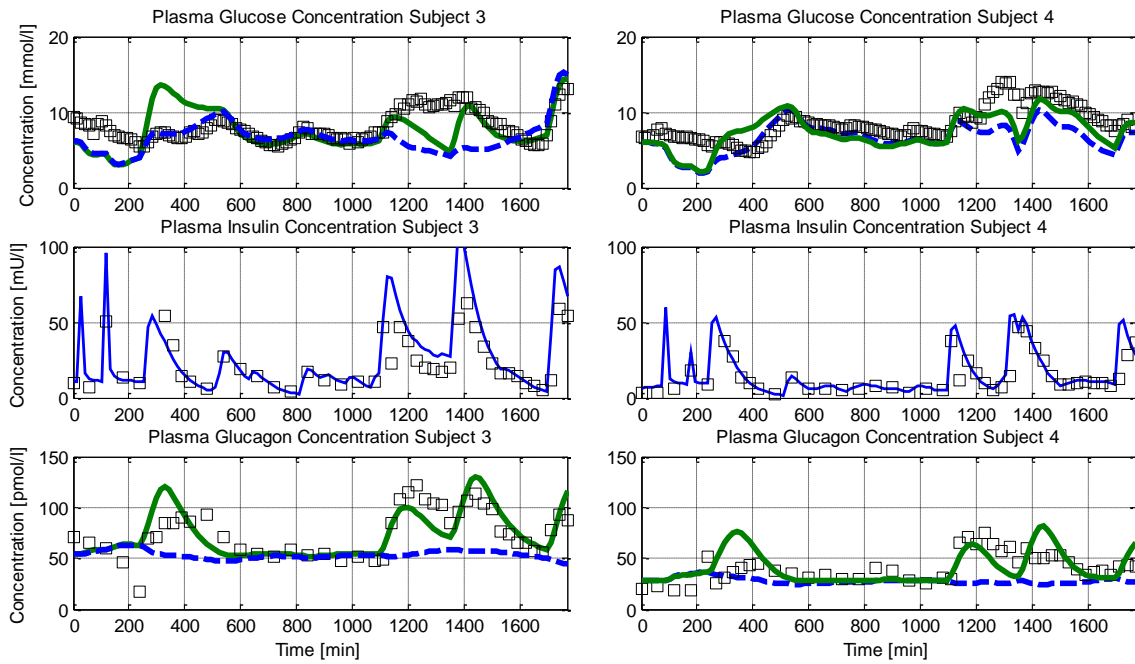


Figure 31: Post-hoc simulation: dynamics of Subject 03 and Subject 04 with the new mechanistics for prandial glucagon secretion and glucagon-dependent suppression of glucose uptake (M_{NHGU}).

In the second trial, deviations of model predictions in the morning (possibly “dawn-effect”) were even more prominent, but accompanied by smaller glucagon surges. But as this effect was not associated with glucagon surges in Subjects 5, 6 and 9, and the adapted model, as shown in in Figure 31, could also not fully connect this effect to glucagon, a different explanation was sought. Thorough retrospective analysis of trial documentation of the second trial revealed that these deviations were always accompanied by consumption of coffee with breakfast. And caffeine has been associated with acute insulin resistance [201]. However, morning coffee consumption was not documented consistently throughout the trial (only Subjects 1, 6, 8 & 9), limiting the impact of this observation.

IV.2.4 Adherence to Dose Recommendations

Adherence to dose recommendations by the medical staff during the trial was an issue. For the trial, medical doctors were present to confirm the dose recommendations given by the algorithm. Although the trial protocol provided rigorous rules for the adherence to dose recommendations within a given value range for blood glucose measurements, final decision on the given dose could still be decided on by the physician. In many cases dose recommendations were rejected although individuals were not outside (below 110 mg/dl) the specified range for glucose measurements, but rather within a range for which the recommended dose could have been feasible. An example is Subject 05 (Figure 32). Even though glucose values remain above 140 mg/dl after dinner on the first day (time > 400 min), dose recommendations were not accepted. After a further increase to 180 mg/dl (time = 800 min), a single dose recommendation was accepted but subsequent suggestions were again rejected even though glucose levels did not fall below 140 mg/dl.

This circumstance significantly reduces the impact of the aggregated statistics on the feasibility study (RbA1 in Table 3 and Figure 28). Rejection of dose recommendations in general leads to increased glucose levels and avoids low blood glucose levels. This means, that statistics of RbA1 are biased towards a higher glucose level and a lower risk for hypoglycaemia. This has to be taken into account when interpreting the results.

In the second trial, physicians were instructed to be more rigorous in adherence to the protocol. Thus, almost all, except for 3 time-periods in Subjects 1, 4 and 10, dose recommendations were adhered to. This allows interpretation of the trial results with respect to performance of the control algorithm.

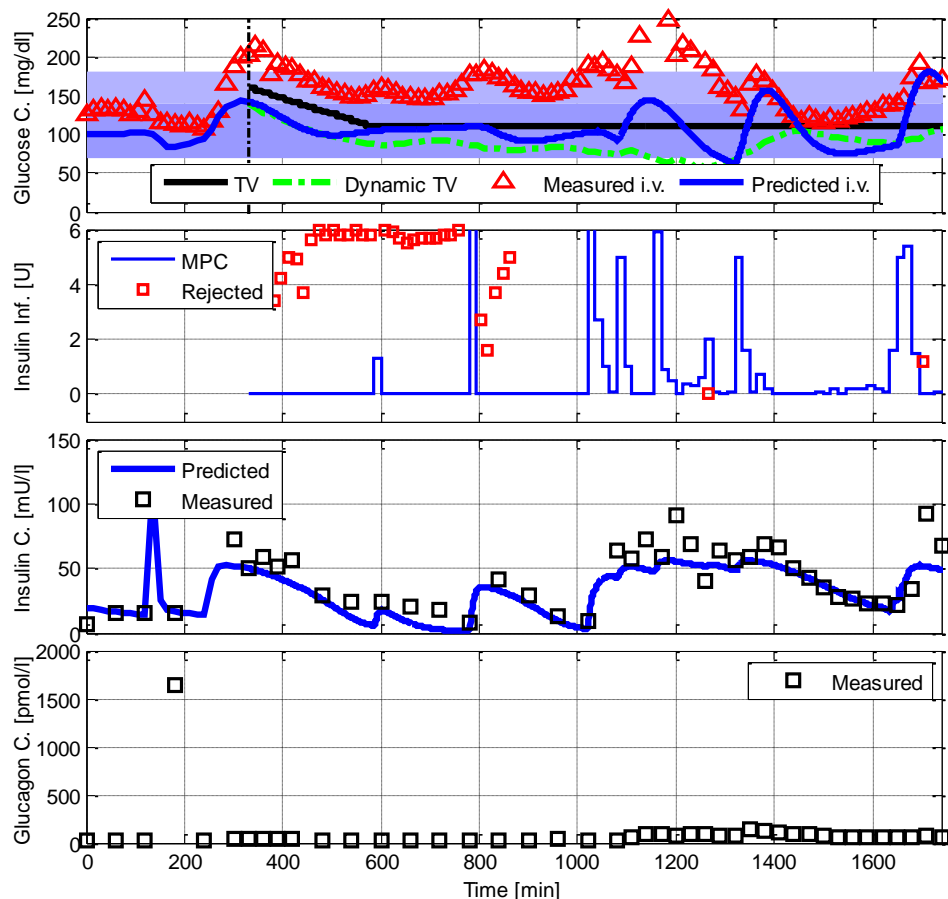


Figure 32: Glucose control experiment in Subject 05. MPC dose recommendations were rejected from the start of control (7:30 p.m., $t = 330$ min) until 7:00 a.m. ($t = 1020$ min). Following that, dose recommendations were accepted and control results were good. Two more dose rejection at 11:00 a.m. ($t = 1260$ min, recommendation of 0 units was raised to 2 units of insulin, unnecessarily as glucose levels were already falling steeply) and 6:15 p.m. ($t = 1695$ min, 1.2 U recommended, 0 U applied, medical staff was taking no risks for overdose as this was shortly before end of trial).

IV.2.5 Hypoglycaemia

In the first trial, there were two incidents of hypoglycaemia (Glucose < 60 mg/dl, Subject 01 and Subject 02), and both were caused by technical issues.

In the second trial, there were 9 hypoglycaemia incidents caused by the algorithm, most of which occurred before dinner in between 3-5 p.m. (Subjects 2, 4-7 and 10). All of them were related to unpredicted mid-day increase in insulin sensitivity. For

some (Subjects 2, 4, and 10) hypoglycaemia incidents occurred at the end of the first day (between 10 p.m. and midnight) due to sub-optimal model fits. A reason for the low number of hypoglycaemic incidents in the first trial is the fact that physicians more often rejected dose recommendations. In the second trial, almost all, except for 3 time-periods in Subjects 1, 4 and 10, dose recommendations were adhered to.

IV.2.6 Summary

When comparing the different trials and considering the fact that the RbA2 trial uses real s.c. measurements by CGM devices (Dexcom G4 Platinum) with an MARE of 10%, ultimately the controller can compete with current state-of-the-art algorithms and is superior to standard-of-care open-loop control.

The fact that insulin PK was correctly estimated in 7 out of 10 subjects and 10 out of 10 qualitatively shows, that the established workflow for the PBPK/PD model individualization is a feasible approach. In addition, the PBPK/PD approach also helps to reveal yet unexplained phenomena within the system and allows systematic post-hoc analysis thereof (mode-of-action analysis of “dawn-effect”).

An issue was adherence to dose recommendations, limiting the impact of the aggregated statistics on the first feasibility study (RbA1) and the outcomes are biased towards a higher glucose level and a lower risk for hypoglycaemia. This has to be taken into account when interpreting the results. This could be avoided for the second trial.

Overall, it can be said, that a tighter control of blood glucose levels (improved time-in-target) is bought with a higher risk for hypoglycaemia, even more so, if glucose measurements become less accurate and this fact poses the greatest hurdle (safety of control) for commercialization of ACG devices.

Part V.

Discussion & Appendix

V.1 Model

Within the second part of this thesis (Part II, Section II.2.1.1), the development of a physiology-based PK/PD model for glucose, insulin, and glucagon is described. Application to clinical data in Section II.3.2 showed that the model is able to predict the time-courses of these three substances with one consistent time-invariant parameter set with an overall good accuracy. While this clearly demonstrates the power of the PBPK/PD modeling approach, a full quantification of the quality of fit and predictions of the model presented here in comparison to state-of-the-art model implementations of the GIM is difficult as no validations of individual model predictions of full-day trials are published, but only pure predictions without data [113] or only fitted trajectories [202]. In summary, the here chosen modeling approach distinguishes itself from state-of-the-art models by its generic concept separating compound and organism properties, the detailed whole-body physiological compartmental structure, the a-priori individualization framework, and the integration of detailed cellular mechanistic processes. Although the resulting models are computationally demanding, they were solved on standard laptop computers within a minute and the steady increase in computational power makes this a minor drawback.

Given the individualization framework and the detailed model structure, the developed model captures IIV and IOV. With respect to the numbers of parameters, the lion's share of IIV is captured by a-priori parameterization of the individual physiology which is mapped by the modeling platform based on the individual's anthropology. With over six hundred unique parameters in the whole model, only 38 for the global mean and 26 distinctive parameters for healthy and T1DM mean population models were fitted. Ultimately only 10 parameters were used for model individualization. As the results clearly show, each of the patients was fitted successfully.

Although the development of a global generic integrated GIM model with parameters representing explicit physiological detail, e.g. transporter expression and parameterization, is new, a key result is the distinguishing parameterization for healthy and T1DM individuals (Section II.2.2.2.2). Current state-of-the-art models of glucose metabolism merely change basal hepatic glucose production to distinguish these groups [32, 149]. However, considering subjects with T1DM, where insulin secretion and the incretin effect are lacking, a key difference to healthy subjects is, from a modeling perspective, the distinctive route by which insulin is provided to the body. In healthy subjects large amounts of endogenous insulin first pass the liver before being distributed to other tissues, whereas in subjects with T1DM, where insulin is exogenous, the liver is exposed only downstream to a lower level of insulin and insulin may exert only a fraction of its regulatory (e.g. glucose lowering) effect on the liver.

It is known that stimulation with insulin reduces receptor expression but increases receptor recycling rates [161-163]. The detailed description of the human physiology and distributive fluid flows within the PBPK/PD model result in the naturally expected change in insulin concentration levels at the target tissue following a shift from endogenous to exogenous insulin supply. Model fits show that the reduced hepatic insulin levels in T1DM result in an increased receptor expression but reduced recycling rate, in-line with the experimental observations.

To predict concentration levels or even to fit data over a longer time-scale, the model also needs to capture IOV, i.e. dynamics on a separate time scale than plasma glucose or insulin levels, e.g. insulin receptor dynamics or vascular endosomal transit of insulin. In current state-of-the-art models IOV is captured by time-variant parameter-sets [24, 113]. However, to improve the predictive power of the model, a mechanistic, preferably also physiologic description of IOV is paramount. The here integrated insulin receptor model is a first step in this direction, as it directly couples insulin clearance with insulin action as a dynamic system with long-term changes in surface receptor levels dependent on long-term cellular insulin load due to the slow receptor recycling rates. However, long-term changes in post-receptor signaling may also be a yet unresolved issue. The rationale for the distinguishing parameter set for T1DM and healthy individuals is a self-regulating feedback-loop of insulin receptor transcription and recycling rates [203]. As insulin levels were predicted with high accuracy, the lion's share of the residual error of glucose predictions in Figure 4B probably arises at the post-receptor level. And, indeed, the observed average drift, caused by a major deviation of fasting glucose levels in only one single subject out of eight, can be compensated by a change in the single parameter insulin sensitivity (data not shown).

In general, model components, which self-adapt would be beneficial. Adaptation on a long time-scale could be e.g. insulin signal transduction or transcription and degradation dynamics of insulin receptors adjusting to average cellular insulin load [53]. Adaptation on a short time-scale could be e.g. an exercise model with metabolic and regulatory networks [204, 205], to exogenous influences. Here, however, the subjects were sedated, experiencing only little change in physical activity and variation in metabolic rate.

One of the largest sources of IOV is probably the absorption of carbohydrates of a meal as outlined in Section II.3. The most likely explanation for the changes observed in meal absorption is the high variability in the characteristic properties of meal absorption, depending on nutrient content. Different types of carbohydrates, with varying glycemic indices define how quickly glucose is available for absorption [126], i.e. in the "dissolved" state. The effects of amount and types of fat and proteins, meal texture as well as fiber content influence stomach emptying rates as well as intestine transit rates [206] and additional regulation of hepatic glucose control [207, 208]. Due to a lack of information, only total carbohydrates, caloric content, meal texture (fraction solid) and total meal volume is considered. Detailed a-priori food characterization, with respect to covariates influencing gastric emptying (i.e. through the incretin effect itself), intestinal transit and absorption, integrated within a reliable mechanistic model describing effects of nutrition [206, 209, 210] could likely improve predictions of meal absorption.

Another source of IOV (mainly glucagon) but also IIV is subcutaneous absorption. The reduced-order adaptation for continuous infusion of the s.c. absorption model also reduces the effect on the time delay of insulin appearance by local distribution at the injection site. However, implementation of the full model, adapted to continuous infusions seemed excessive as the time delay is only minor and shows high variability. Possibly, variability could be reduced if a better understanding of insulin distribution and degradation at the s.c. injection site is obtained [211]. For s.c. glucagon absorption this could be due to changing s.c. properties over time or changing injection sites with different s.c. diffusion/absorption properties and/or additional subcutaneous degradation [212].

Not only insulin absorption, but also action and/or secretion in healthy subjects are reported to be subjected to a circadian rhythm leading to additional variation [213]. However, the results within this post-hoc study including only individuals with T1DM do not further support this observation (Figure 13). A plausible explanation could be that these circadian properties are a property of insulin secretion or are otherwise disturbed in T1DM [214]. Another unresolved issue is the effect on hepatic glucose production of high hepatic glucagon levels in the presence of increased insulin levels (Figure 12 A, top, Section II.3.2). This strongly indicates that insulin inhibition of glucagon action is too strong or too prolonged. This indicates a necessity for stronger dynamic decoupling either at the interstitial or intracellular level. Solutions for dynamic decoupling of insulin and glucagon could be decoupling of plasma and interstitial dynamics in general or the inclusion of an intracellular cAMP pool affected by both hormones [215, 216], instead of the direct multiplicative inhibition as adapted from Sorensen.

Lastly, for the outlier Subject 122, a consistent explanation has to be validated with respect to the abnormally high insulin levels. Possible reasons could be differences in insulin receptor levels or insulin antibodies, both strongly impacting the distribution and clearance. During model development, both hypotheses were tested, latter being carried forward as it both resulted in better predictions and was supported in discussions with El-Khatib (data not shown; personal communication). A fraction unbound of 1% was necessary for Subject 122 to achieve the observed 20-fold increase in total plasma insulin levels. Plausibility of the low fraction unbound for insulin in Subject 122 remains to be confirmed and requires trials where antibody levels are measured.

V.2 Controller

Within the third part of this thesis, the development of a novel approach to individualized automated glucose control is presented. The control approach uses, for the first time, a detailed generic whole-body physiology-based pharmacokinetic/pharmacodynamic (PBPK/PD) model [2] within a robust MPC algorithm. The control approach was evaluated within a post-hoc *in-silico* study. The algorithm was tested vs. model uncertainty using sub-optimal model fits, and scenarios were subjected to glucose sensor noise and unannounced carbohydrate disturbances. As input, the algorithm only requires the individual's physiologic properties (height, weight, gender and age) and the amount of consumed carbohydrates. The approach combines a predictive system (MPC) with a reactive system (FMPD), which significantly increases the controller's robustness vs. uncertainty. All control insulin inputs are calculated and no additional pre-meal insulin bolus is required. Overall, the controller shows good control performance.

Comparison of AGC algorithms generally problematic as ultimately it is only possible within a clinical field trial on a large number of individuals. In some cases, others have conducted similar *in-silico* studies [23, 25, 30, 31, 149, 160, 217]. The main drawback of such studies is that the *in-silico* patient on which the controller is tested is always derived from the same model that the controller works with. These evaluations thus only reflect the controller performance in conditions of wrong model parameterizations, disturbances and measurement errors relative to a "perfect model fit" which could never be achieved. This is why a comparison of algorithms from different research groups has never been done before *in-silico*.

The main difference between state-of-the-art MPC AGC algorithms [24, 74, 149] and the MPC developed here is, besides the different core models used, the handling of transient process variability, i.e. the dose-effect ratio of infused insulin. Whereas all approaches are self-adapting over time through an optimization of the internal model, state-of-the-art MPC AGC algorithms in addition use piecewise (per sampling interval) fitting of the model parameter "insulin sensitivity" for point-wise exact model fits [12]. Here, the model adaptation is not designed to accommodate for short term changes through a parameter change in insulin sensitivity. This is thought to be partly captured by the internal model [2]. Self-adaptation of the model over time is solely for improving prediction of the individual's core-dynamics. Remaining uncertainties and disturbances on a shorter time-scale are handled by the dynamic target value shift and dose correction components of the offset-controller.

Although performance of the controller was good, it will require further development for future versions. Model uncertainties in insulin dynamics/predictions reflecting wrong half-life time of insulin do result in inversely oscillating measured patient plasma glucose and insulin infusion rates. This is due to the resulting slight shift in time scales between the dynamic behaviour of the patient's insulin dynamics and the insulin dynamics of the internal model and attenuated by model adaptation and may be critical for high, e.g. prandial, insulin doses. Overall, the MPC AGC algorithm can handle control using a CGM device for glucose measurements with sensor noise up to 14 % MARD with up to 15 minutes of time-delay, although a time-delay would result in a significant reduction of time in target-range. The *in-silico* evaluation further indicates, that the controller is able to control blood glucose in an acceptable range in the presence of model uncertainties and disturbances, in addition to measurement errors.

V.3 Clinical Trial

Part four of this thesis the new control approach is evaluated within two clinical feasibility studies. In the first study, as prior information, the controller only requires the individual's physiologic properties (height, weight, gender and age) and the basal rate of the insulin infusion pump prior to trial start. In the second trial, CGM data, collected 24h prior to start of the trial was required for initial model identification, i.e. model individualization. The approach, as presented in Part III, combines a predictive system (MPC) with a reactive system (FMPD), increasing the controller's robustness vs. uncertainty. The controller directly calculates all insulin inputs and does not require (partial) meal-priming boluses of insulin. In the first trial, the controller shows acceptable control performance. Although the latest state-of-the-art systems are developed for s.c. glucose measurements this controller has in a first step been evaluated in a clinical setting with plasma glucose measurements for safety reasons. In the second trial, after thorough in-silico testing, the controller was applied in a control setting using s.c. glucose measurements and achieved very good control performance.

Although the controller has achieved satisfactory results in trial #1, workflow adjustments were required for the second trial. As the controller needs an initial estimate of the individualized model [3] at start of control, clamp data was used for initial model individualization. This step was required as online model adaptation within the algorithm is computationally demanding and does not deliver the required estimates in time by start of control. But data collected during the clamp phase has a high degree of uncertainty due to an unknown initial state. It was assumed that subjects arrived in a well-controlled steady state as they arrived at the clinic in a fasted state, with only the basal rate of their insulin pumps running. However, many subjects arrived in an uncontrolled state with extreme hypo/hyperglycaemia, possibly caused by distress from travelling or from anticipation of the enrolment process (preparation of catheters for clamps and sensor micro-dialysis access catheters), introducing a significant amount of disturbance/uncertainty. Partly, patients then either omitted or reduced basal insulin to correct glucose levels at time of enrolment and required either oral or i.v. glucose or insulin interventions. Also, the use of different insulin during clamp (Aspart, in contrast to the s.c. pump insulin Lispro) could have influenced model identification as insulin properties (PK and PD) of insulin Lispro and insulin Aspart were assumed as being identical, which may not be the case. In addition, conditions for model identification were suboptimal as i.v. clamping does not deliver information on absorption properties of subcutaneous insulin and the s.c. insulin infusion rate was kept constant except for the meal bolus right before start of control. Further, patients arrived in fasted state, omitting lunch. The fasted state itself may be a condition not well described by the model with processes of cellular glucose metabolism (glycogen storage and glucose production) affecting glucose homeostasis. All these criteria make initial model optimization challenging and resulted in below optimal performance of the controller.

Thus, for the second trial, an extension of the observation phase with additional time-data on the effect of s.c. insulin was decided to handle these uncertainties. This new workflow approach was successful, as the controller performance improved significantly. Although this algorithm now requires an initial model fit from a priori glucose measurements, the adapted workflow shows that this approach, by a-priori data collection or a 24h run-in phase for the algorithm, is feasible. Taking into

account that long-term core dynamics [2] are stable, and the model can subsequently be adapted for long-term shifts (change in life-style etc.) as long as intra-day variability is structurally captured (glucagon dynamics) or informed (e.g. better meal characterization).

An unresolved issue in this regard is the observed deviations in model predictions on the morning of the second day ("dawn-effect"), possibly associated with meal/nutrition-dependent postprandial glucagon secretion. In most control studies, the dynamics and influence of glucagon is omitted completely [24, 149]. And in glucose control studies which explicitly use exogenous glucagon for glycaemic control, these postprandial surges are not discussed as they are not observed in the studied T1DM individuals [2, 26, 36]. And in trial #1 the associated model deviations are only observed in the morning, and only in the presence of glucagon surges, but this was not the case for Subjects 05, 06 and 09 from trial #2, where these deviations occurred even though no significant glucagon surges were observed. The observed peak postprandial excursion of endogenous glucagon are comparable to peak concentration levels reached in bi-hormonal control of T1DM [36] for effective treatment of hypoglycaemia [38, 218]. However, if at all, only in Subjects 03, 04, and 06 (trial #1) and Subjects 01, 02, 07 and 09 (trial #2), the rising glucagon may have caused these deviations, but had not effect on glucose levels in Subject 09 (trial #1) or Subject 10 (trial #2). The fact that a morning rise in glucose has been observed without a simultaneous rise in glucagon and, on the other hand, a rise in glucagon did not cause a simultaneous rise in glucose, indicates other processes involved.

In T2DM, it is a well-established rule to calculate a relatively higher dose for breakfast than for later meals [219] to counteract this "dawn-effect". But also in T2DM [220, 221] (and the elderly [222]) this does not seem to be associated with increased glucagon levels. Also, in healthy, young individuals, the "dawn-effect", is absent, and even an inverse behavior, with increased morning glucose tolerance [213, 219], is observed, possibly by circadian insulin receptor modulation [222]. In trials #1 and #2 conducted here (in T1DM), the effect seems only meal associated and unlike in T2DM [221] does not occur before onset of Breakfast. This effect could thus be a combinatory effect which occurs due to diurnal variations in regulatory hormones such as cortisol, which are known to effect glucose homeostasis and are elevated in the morning [223] and a defective regulation of postprandial intra-islet signalling, e.g. suppression of glucagon secretion by amylin [157] or glucose [40, 151, 224, 225] as well as nutrition.

As analyzed here, it is now questionable, if the rise in glucagon or change in metabolism is the main cause for the observed model deviations, as, on the one hand this effect is not observed in all patients, and not during the evening meals and on the other hand does not occur before start of a meal. Rather, nutritional effects, e.g. coffee [201] as the data from trial #2 indicates, are likely to be the cause for these episodes of insulin resistance.

In the second trial, a slight increase in the number of hypoglycaemic events was observed, especially after lunch. Data indicates that the midday increase in insulin sensitivity following the morning episode of reduced insulin sensitivity accompanied by uncertainty in meal absorption leading to a slight insulin overdose are most likely the cause for this. Nevertheless, the model developed here does not use time-variant parameters but rather builds on a mechanistic description of the systemic properties underlying these variations over time. In this regard, in combination with additional

experimental studies, the “dawn-effect” in T1DM will have to be further analyzed for a better understanding of the relevant processes and effectors underlying this effect.

V.4 Conclusion

Within this thesis a blood glucose control system has been described and evaluated that combines a highly predictive whole-body physiology-based pharmacokinetic/pharmacodynamic (PBPK/PD) model [2] within a model predictive control framework and a reactive dose-correction module reacting to unpredictable individual patient behaviour.

As personalized control of blood glucose requires an understanding of the mechanistic properties within an individual subject with T1DM and PBPK/PD models deliver the ideal framework for such ambitious integration of knowledge and information. With all the remaining issues considered, the GIM model presented here shows reliable predictive capabilities, also on a long time frame, once it has been parameterized for the respective individual as shown in Section II.3. The model was developed in such a way that its purpose of use is versatile. The generic modeling concept provides a rigorous framework for individualization (even across organisms), data integration, and model extension for (given the good model predictivity) e.g. mode-of-action analysis. It could thus also be used for 1) fundamental research to uncover physiological properties and the relevance of cellular processes in whole-body physiology, as well as 2) fundamental research on diabetes related drug targets and corresponding pharmaceutical intervention strategies. Last but not least, the model can be used, as it is here, for the 2) prediction and automatic control of blood glucose in T1DM.

And although the automatic control system has been developed for use in a controlled clinical environment and evaluated w.r.t. model uncertainty and carbohydrate disturbances, it would be of interest how the system would cope with sickness, medication, and stress i.e. in an intensive-care setting, or physical exercise. Although, *in-silico* evaluation and results from the feasibility study indicate that the controller can handle significant disturbances. The question for the future here is, how predictive should such a system be if it does not account for all external or internal disturbances to the patient.

Whereas the PBPK/PD model-based MPC approach is a feasible approach to AGC, the modeling framework can also help to better understand the inner working in the body’s control of glucose homeostasis. Whereas existing models are built for - and continuously adapted to - an operating point, the model developed here captures glucose core dynamics in a time-invariant and global manner. Nevertheless, a better understanding of individual counter-regulatory mechanisms in extreme situations, e.g. the effect of prolonged hyperglycaemia (glucose toxicity [226]) in Subject 10 (trial #1), or hypoinsulinaemia after insulin under-dosing in Subjects 04, 06, 08, and 10 (trial #1), is required to increase efficiency (robustness and tightness) of glycaemic control.

This work demonstrated, that the predictive control approach using PBPK/PD models is well suited for automated glucose control, especially to handle the long dead-time in effect of subcutaneous insulin. The trade-off for highly predictive systems is the computational power they require within a model predictive control setting and the reduced flexibility in case of short-term changes in patient behaviour. Nevertheless, the control approach showed comparable performance to competing approaches

with overall promising results and significant improvement after workflow adaptation and improved online model identification.

This work brings a new approach to the AGC (or AP) community by introducing PBPK/PD models as computational kernels for the MPC algorithm. Ultimately, performance of the different systems, be it in terms of predictivity or control performance, which have been developed to date (Section III.1), will only be possible in a head-to-head comparison within the same clinical setting. The PBPK/PD approach has been developed with a perspective towards the increase in data availability on multiple scales and to gain a better understanding of the physiologic processes involved in the regulation of whole-body glucose homeostasis, as e.g. the role of glucagon during the “dawn-effect”. Until this system can be brought to market it will require additional validation in a wider variation of real-life scenarios and stronger system integration, i.e. miniaturization. Similarly as for an in-silico analysis of predictivity of different model types, comparison of AGC algorithm performances from different trials is problematic and statistically questionable due to the low number of participants, and is only feasible within the same clinical field trial on a large number of individuals. Common practice is a general statistical analysis as done in Section IV.2.1 giving a rough estimate of controller performance [192, 193]. However it has to be noticed, that boundary conditions during clinical trials may have a strong influence on outcome measures, amongst others: the selected individuals (strong inter-individual variability, requiring a large number of subjects to achieve statistical relevant outcome measures) and trial protocol (especially initial conditions, nutrition and allowed physical activity). This should be considered when comparing different algorithms. Another difficulty for offline-AGC comparison are the additional support or add-on systems like post-sensor signal processing [227] which are not fully disseminated in the public domain.

Even within AP@Home [191], a EU research funded project currently in progress, where two different MPC AGC algorithms [190, 228] are further developed and evaluated, no head to head comparison was conducted within a single field trial. Judging from published trial summaries, a time-in-target value (70-180 mg/dl, corresponding to “target1” in Table 3, of 60 % and time in and hypoglycaemia (< 70 mg/dl) < 5 % is currently the benchmark in AGC; Values which were almost also reached within RbA2 (trial #2) here.

To this state, using predictions of the core dynamics of an individual’s blood glucose levels within the proposed control approach has proven feasible proving that once an individual’s physiologic properties have been captured with the right model parameterization, safe and good control of blood glucose levels is possible.

V.5 Appendix

V.5.1 PBPK/PD Model

V.5.1.1 Medical Conditions for Model Individualization

V.5.1.1.1 T1DM

T1DM is characterized by the destruction of insulin secreting pancreatic beta-cells during a selective auto-immune reaction [106]. Whereas this happens in most cases at a very young age, T1DM can also be developed as late as at the age of 40. Due to the loss of endogenous insulin, blood glucose levels, left untreated, can climb to 5 to 10 times normal. Fat metabolism in liver and kidney is increased to substitute for the loss of energy provided by glucose metabolism, producing ketone bodies as by-products when fatty acids are broken down for energy. The resulting increase in glucose and ketone bodies provides an immense solute load to the kidneys. Additionally the keto acids that are produced are moderately strong acids and their increased production causes severe metabolic acidosis. Another problem is the imbalance in the regulation of the remaining glucoregulatory hormones. A major dysregulation is postprandial hyperglycaemia caused by glucagon surges. This could be caused by the missing amylin mediated suppression of glucagon secretion from endocrine inter-islet insulin signalling [151, 225]. The relevance of glucagon in T1DM has been further evaluated in this thesis and is presented in Section IV.2.3, and discussed in Section V.3.

A Key difference between subjects with type 1 diabetes and healthy subjects is, from a modelling perspective, the distinctive route by which insulin is provided to the body. Whereas insulin in healthy subjects is released by the pancreas into the portal vein (also the superior mesenteric vein ((SMV) is a blood vessel that drains blood from the small intestine (jejunum and ileum)) and the splenic vein. At its termination behind the neck of the pancreas, the SMV combines with the splenic vein to form the hepatic portal vein [106], subjects with Diabetes (also) receive exogenous insulin via subcutaneous (or IV) injections.

This means that in healthy subjects the liver is saturated in insulin, compared to the T1DM type, where insulin basically only part wise stimulates the full glucose-lowering capabilities of the liver. However, insulin may still exert its full inhibitory effects on hepatic glucose production through indirect means by reducing gluconeogenic precursor load or insulinization of the brain thus activating a central nervous system signal to the liver [150].

The important question for model development is how this could affect the physiology and hence the parameterization of the model. Semi-physiological models like the UVa/Padova Simulator [29] assume an increase in basal glucose concentration of in average 50 mg/dl compared to subjects in health and also steady-state insulin concentration (due to an external insulin pump) is assumed to be on average (four times) higher than in subjects in health. To achieve this, they changed parameters for basal endogenous glucose production (+ 35%) and steady-state insulin clearance (- 33%) as well as parameters relating to insulin action on both glucose production and utilization (- 33%) as compared to subjects in health [160].

However, it is known that stimulation with insulin reduces receptor expression but increases receptor recycling rates [161-163]. The detailed description of the human physiology and distributive fluid flows within the PBPK/PD model result in the naturally expected change in insulin concentration levels at the target tissue following a shift from endogenous to exogenous insulin supply. Fits for the PBPK/PD model show that the reduced hepatic insulin levels in T1DM result in an increased receptor expression, but reduced recycling rate, in-line with the experimental observations, delivering a physiological explanation for the changes during disease progression (Results Section II.3.2).

Subjects with T1DM are the population group for which the physiology-based model and the automatic glucose control system is developed and if left untreated, subjects with T1DM can experience severe acidosis and dehydration that can ultimately lead to death from diabetic ketoacidosis [106].

V.5.1.1.2 Tissue Resistance to Insulin Action

In all subjects with T2DM, some subjects with T1DM, and also the critically ill, the metabolic system is compromised in its ability to maintain homeostatic control of glucose levels. This is due to a reduced sensitivity to insulin. Insulin sensitivity is of major importance at intensive care units, where the effects of inflammation and its treatment, e.g. with anti-inflammatory steroids like cortisone, can cause severe dynamic changes in insulin sensitivity [158, 229-234]. Hyperglycaemia is prevalent in critical care [75, 235-238]. Tight control of blood glucose has been shown to improve clinical outcomes [237, 238]. More importantly, van den Berghe et al [235-238], and Chase et al [75] have shown that tight glucose control can reduce mortality in the intensive care unit (ICU) by 18-45%. Glucocorticoids are used in critical care to treat a variety of inflammatory and allergic disorders, but may inadvertently cause hyperglycaemia through reduced insulin sensitivity.

It would go beyond the scope of this work to quantify all of the crosstalk mechanisms that are thought to be interacting with insulin action (i.e. the insulin signalling pathway). Therefore this work focuses on the most relevant and best studied pathways that are known to be interacting with insulin signalling. In the following sections, a short review of the effects of nutrition, (inflammatory) stress and medication (steroids) on insulin signalling is given, including the potential role of the involved cross signalling mechanisms in hepatic, adipose, and muscular tissues.

V.5.1.1.2.1 Inflammation and Cellular Stress

In septic patients, inflammation and related cellular stress responses are causes for increased insulin resistance. Inflammation causes macrophages to release cytokines, which cause a rise in anti-inflammatory steroids, catecholamines and glucagon via activation of the hypothalamic-pituitary-adrenal (HPA) axis [239].

Cytokines are important mediators of septic shock, having a pivotal role in regulating the host response to sepsis. Important cytokines are tumour necrosis factor (TNF- α) and interleukins (IL-1 and IL-6). Cytokines are released in response to injury, infection and also by adipocytes to control their fat content. Studies have demonstrated that TNF- α causes insulin resistance and that this is associated with increased levels of fatty acids and impaired insulin signalling in skeletal muscle, hepatic and fat tissues [158, 233, 240-244].

The mechanisms by which TNF-alpha modulates the insulin signalling pathway involve the activation of the phosphatase PTP1B [234], reduction of insulin stimulated tyrosine phosphorylation and site-specific serine/threonine phosphorylation of IRS-1 [158]. This causes inhibition of IRS protein binding to the insulin receptor, thus preventing propagation of the insulin signal. TNF-alpha also reduces the availability of IRS-1 and GLUT4 in the adipocyte by reducing gene transcription [158, 240].

TNF-alpha may also promote insulin resistance through its effects on fat metabolism by increasing levels of FFAs in the blood plasma [158, 240]. Also, the TNF-alpha mediated rise in catecholamines and glucagon may cause a rise in glucose production [241].

When the body experiences inflammatory stress, e.g. during sepsis, catecholamine levels are increased. Catecholamines are sympathomimetic “fight-or-flight” hormones that are released by the adrenal glands in response to stress. The metabolic effects of catecholamines are mediated through adrenergic receptors, so called G-protein coupled receptors (GPCR) that mediate different cell responses. Catecholamines cause, among other things, endogenous glucose production, inhibition of insulin secretion, inhibition of insulin-dependent glucose uptake and lipolysis [158].

Free fatty acid (FFA) concentrations in blood plasma play a significant part in the regulation of the glucose metabolism. Increased quantities of free fatty acids are released from adipocytes under conditions of starvation, diabetes, obesity and inflammation as described above. FFAs can be utilized interchangeably with glucose for energy in most tissues [158, 239, 245]. The FFAs are released from the adipocyte into the blood plasma to be extracted as metabolic fuel by the muscle or the liver [239]. In the liver, FFAs are split into ketone bodies as an alternative metabolic fuel for the nervous system and the heart. They are oxidized, or used to form TAGs to be released back into the blood.

Fat is the preferred fuel for oxidation in patients with sepsis. The high resting energy expenditure in sepsis is accompanied by increased FFA and glycerol turnover, although fat mobilization is far greater than fat oxidation, causing raised levels of plasma FFA concentrations. These changes in the metabolism during sepsis are mediated by cytokines and hormones, amongst others steroids and catecholamines and glucagon [239, 246]. A schematic of the effects of Inflammation and cellular stress is shown in Figure 33.

The mechanism through which FFAs bring about insulin resistance is by elevating intracellular long-chain acetyl CoA, producing diacyl glycerol (DAG), which activates the serine/threonine kinase protein kinase C (PKC) isoform θ [158]. PKC- θ can interfere with the intracellular signalling pathway of insulin via serine/threonine phosphorylation of IRs and IRS proteins. FFAs may also impair GLUT4 translocation directly [231]. Because lipolysis in adipocytes is repressed by insulin, insulin resistance from any cause can lead to FFA elevation, which, in turn, induces additional insulin resistance as part of a vicious cycle [229].

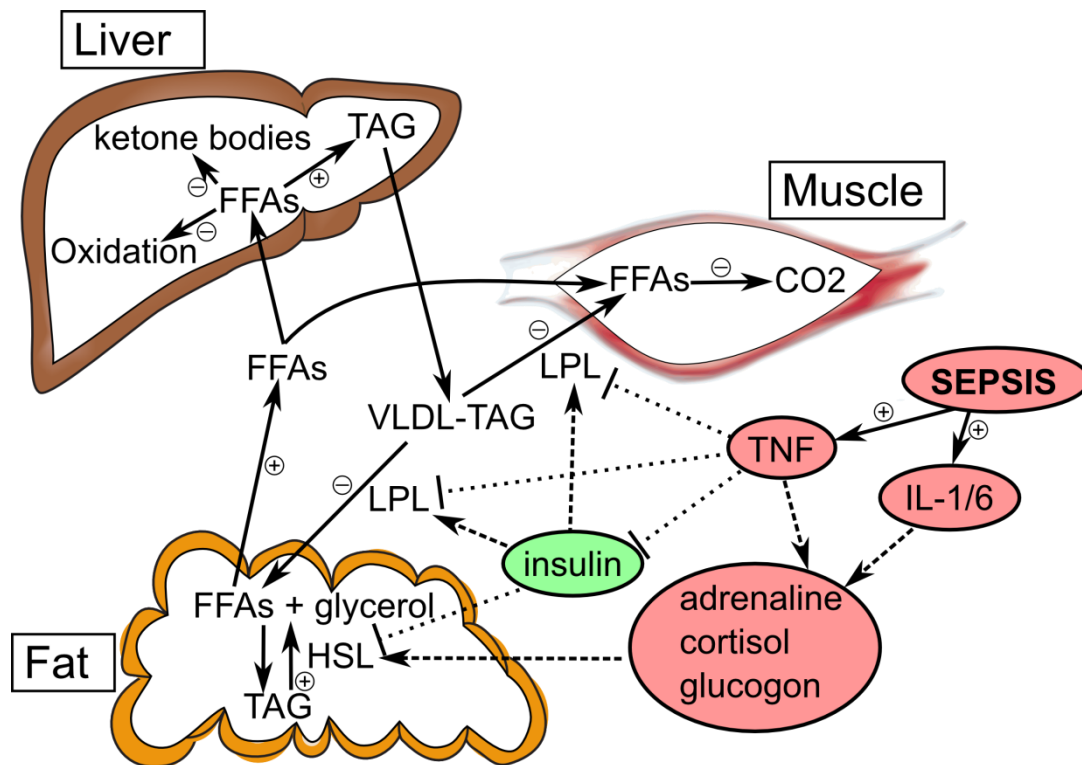


Figure 33: Effect of inflammation (sepsis) on lipid metabolism. Primary effects are expressed with dashed arrows for up-regulation and dotted stops for down-regulation; secondary effects are expressed with “+” and “-”. TAG, triacylglycerol; VLDL, very low density lipoprotein; LPL, lipoprotein lipase; TNF, tumour necrosis factor; IL, interleukin; CO₂, carbon dioxide; FFAs, Free fatty acids; HSL, hormone-sensitive lipase.

V.5.1.1.2.2 Anti-inflammatory Steroids

The steroids that can be found in the human body are basically divided into the three groups: sex steroids, anabolic steroids and corticosteroids. Mainly glucocorticoids, a type of corticosteroids are significant in relation to sepsis and metabolic defects like insulin resistance. Glucocorticoids are a class of steroid hormones that are produced in the adrenal cortex. They are involved in a wide range of physiologic systems such as stress response, immune response and regulation of inflammation, carbohydrate metabolism and protein catabolism [159].

Glucocorticoids are so named because it was recognized that one of their actions is on carbohydrate metabolism [159]. The term “glucocorticoid” represents both secreted hormones and anti-inflammatory and immunosuppressive agents. As a family of therapeutic drugs, glucocorticoids are used in a broad spectrum of anti-inflammatory and immunosuppressive therapies [247]. Cortisol (or hydrocortisone) is the most important human glucocorticoid. It is essential for life, and regulates or supports a variety of important cardiovascular, metabolic, immunologic, and homeostatic functions. Glucocorticoid receptors are found in the cells of almost all vertebrate tissues.

The extend of GCs effects on insulin-dependent glucose uptake needs further examination as there have been contradictory reports on GCs influence on almost all insulin signalling aspects as shown above. However, endogenous cortisol is a very good predictor of stress induced insulin resistance during inflammatory reactions [235].

V.5.1.1.2.3 Nutrition

The effect of nutrition on blood glucose levels is still one of the greatest challenges in glucose modelling and control [14]. Especially the variation in glucose absorption observed in between meals but also in between individuals cannot be predicted reliably. It is known that the composition of a meal can be associated with the absorption characteristics of oral glucose. For example the effects of glycaemic index and glycaemic load on glucose absorption was reported in [126]. Other studies show that the fat content of a meal has a significant influence on gastric emptying and that a high fat diet is associated with delayed gastric emptying [248, 249]. However in most cases, the exact composition of a meal is unknown or in the worst case even the fact that a meal is absorbed is unknown, which makes predictions of characteristics of oral glucose absorption challenging.

Effects of meal composition are incorporated within the Model, taking into consideration (besides CHO content) the volume, solid fraction and caloric load of the meal. Structure and processes of the new GI-tract are documented in Section II.2.1.1.2.1.1.

V.5.1.1.3 Effects of Insulin Antibodies

In [32] an extensive review on the effects of insulin antibodies is given. However, at that time (1980s) swine insulin was a common analogue used for insulin replacement. With swine insulin, subjects were more prone to develop anti-insulin antibodies than they are nowadays using modern recombinant analogues [133].

Nevertheless, occasionally, subjects can still develop severe antibody reactions to insulin as observed for Subject 122 in [36]. The effect of insulin antibodies, as they are not involved in the degradation of insulin, can be modelled by assuming that a fraction of insulin is constantly bound to the antibodies, thus delaying the clearance of insulin from the system. Also, antibody-bound insulin does not affect the glucoregulatory system. Antibody binding of insulin is accounted for via the fraction unbound property of the PBPK/PD models developed within PK-Sim®.

V.5.1.1.4 Pathophysiology of T2DM

As described at start of Section II.2.1, the human metabolism is a highly regulated system. Numerous metabolites are involved in the control of the metabolic system and pathological conditions or exogenous influences like illness, stress or medication can severely impair the performance of this system and disturb glucose homeostasis.

In individuals with diabetes, the glucoregulatory system is severely impaired. The following two sections give a brief overview on the pathological conditions in both, type 1 and type 2 diabetes mellitus.

In general T2DM can be referred to as “permanent insulin resistance” often connected to Metabolic Syndrome, adiposity, inflammation, and stress [158, 250]. The current rise in prevalence of T2DM and the metabolic syndrome is believed to be a result of increasingly sedentary life-styles combined with ready access to energy-rich food sources in genetically susceptible individuals.

More than 90 per cent of patients with diabetes have T2DM [5]. Although the primary factors causing this disease are unknown, it is clear that insulin resistance has a primary role in its development [250]. As with T1DM, T2DM is characterized by elevated blood glucose if left untreated. However, here the cause of hyperglycaemia is more complex. In summary, subjects with type two diabetes are spiralling down a

vicious cycle of insulin resistance and beta-cell dysfunction [251], which is triggered, either by a genetic predisposition or unhealthy lifestyle, through the onset of minor insulin resistance. Insulin resistance forces the beta-cells to produce more insulin than they are in many cases capable of, thus overpowering their normal capacities. This can lead to hyperplasia of beta-cells and ultimately to an impaired function of insulin production, thus marking the onset of T2DM as exogenous insulin needs to be administered to supplement the decrease in beta-cell functionality.

The increase in insulin resistance seen in subjects with T2DM appears often to be accompanied by hypertension, obesity, and specific dyslipidaemia. Insulin resistance, along with one or more of the previously mentioned metabolic abnormalities, can often be found in individuals before the diagnosis of T2DM and is referred to as metabolic syndrome [106]. Due to the complexity of the disease including partly unknown pathophysiological changes and varying levels of endogenous insulin production, no detailed model capturing these influences has been developed for T2DM, yet.

V.5.1.2 Parameter Sets

Table 4: Global parameter set of the GIM model

Parameter	Value	Dim.	Description	Source ^a
Pharmacokinetic Parameters: Insulin				
$LogP$	0.218	[-]	Lipophilicity	[252]
MW	5808	[g/mol]	Molar Weight	[252]
GFR_{frac}	10	[-]	Renal clearance as a multiple of glomerular filtration rate	Fit
Pharmacokinetic Parameters: Glucose				
$LogP$	-2.5	[-]	Lipophilicity	[252]
MW	180	[g/mol]	Molar Weight	[252]
GFR_{frac}	0	[-]	Renal clearance as a multiple of glomerular filtration rate (Renal clearance modeled by a reabsorption function instead [32])	[32]
Pharmacokinetic Parameters: Glucagon				
$LogP$	-1.197	[-]	Lipophilicity	[252]
MW	3483	[g/mol]	Molar Weight	[252]
GFR_{frac}	10	[-]	Renal clearance as a multiple of glomerular filtration rate	Fit
Hexokinase (Concentrations Recalculated from basal rates in [32])				
K_m	0,2	[mmol/l]	Concentration of half max. rate of intracellular glucose metabolization	Fit
v_{max}	267	[1/min]	Max. rate of metabolization	Fit
Passive Organ	0.029	[μ mol/l]	Intracellular enzyme concentration	Recal [32]
Fat	0.016	[μ mol/l]	Intracellular enzyme concentration	Recal [32]
Muscle	0.0214	[μ mol/l]	Intracellular enzyme concentration	Recal [32]
Liver	0.272	[μ mol/l]	Intracellular enzyme concentration	Recal [32]
Brain	1.05	[μ mol/l]	Intracellular enzyme concentration	Recal [32]
RBC	0.082	[μ mol/l]	Intracellular enzyme concentration	Recal [32]
Threshold Functions				
V_0^{GHGP}	1.33	[-]	Rate at zero substrate concentration	Refit [32]

V_0^{IHGP}	3	[-]	Rate at zero substrate concentration	Fit
V_0^{NHGP}	0.14	[-]	Rate at zero substrate concentration	Fit
V_0^{NHGU}	2.06	[-]	Rate at zero substrate concentration	Fit
V_0^{GHGU}	0	[-]	Rate at zero substrate concentration	Fit
V_0^{IHGU}	0.7	[-]	Rate at zero substrate concentration	Fit
ΔV_{max}^{GHGP}	-1.33	[-]	Max. change in transporter rate	Refit [32]
ΔV_{max}^{IHGP}	-2.95	[-]	Max. change in transporter rate	Fit
ΔV_{max}^{NHGP}	2.69	[-]	Max. change in transporter rate	Fit
ΔV_{max}^{NHGU}	2	[-]	Max. change in transporter rate	Fit
ΔV_{max}^{GHGU}	5	[-]	Max. change in transporter rate	Fit
ΔV_{max}^{IHGU}	18	[-]	Max. change in transporter rate	Fit
K_m^{GHGP}	1.45	[-]	Concentration of half max. rate	Refit [32]
K_m^{IHGP}	0.78	[-]	Concentration of half max. rate	Fit
K_m^{NHGP}	1.52	[-]	Concentration of half max. rate	Fit
K_m^{NHGU}	0.97	[-]	Concentration of half max. rate	Fit
K_m^{GHGU}	1.41	[-]	Concentration of half max. rate	Fit
K_m^{IHGU}	4	[-]	Concentration of half max. rate	Fit
n^{GHGP}	3	[-]	Hill/cooperativity exponent	Refit [32]
n^{IHGP}	3	[-]	Hill/cooperativity exponent	Fit
n^{NHGP}	1.8	[-]	Hill/cooperativity exponent	Fit
n^{NHGU}	3.77	[-]	Hill/cooperativity exponent	Fit
n^{GHGU}	4	[-]	Hill/cooperativity exponent	Fit
n^{IHGU}	3	[-]	Hill/cooperativity exponent	Fit
$Glucose_0^{liv}$	5750	[$\mu\text{mol/l}$]	Basal cellular hepatic glucose	Refit [32]
$Glucagon_0^{liv}$	2e-5	[$\mu\text{mol/l}$]	Basal interstitial hepatic glucagon	Refit [32]
$Glucose_0^{pan}$	4500	[$\mu\text{mol/l}$]	Basal interstitial pancreatic glucose	Refit [32]
$Insulin_0^{pan}$	1,4e-4	[$\mu\text{mol/l}$]	Basal interstitial pancreatic insulin	Refit [32]
Sensitivities				
S_{RI}	1	[-]	Insulin Responsiveness	Default
S_{RG}	0.7	[-]	Glucose Responsiveness	Fit
S_{RN}	1	[-]	Glucagon Responsiveness	Default
S_I	1	[-]	Insulin Sensitivity	Default
S_G	1	[-]	Glucose Sensitivity	Default
S_N	1	[-]	Glucagon Sensitivity	Default
GLUT4				
k_{GLUT4}	0.0037	[1/mg]	Rate constant scaling factor	Fit
r_{BPGU}^{mus}	35	[mg/min]	Basal peripheral glucose uptake	[32]
K_m	8	[mmol/l]	Concentration of half max. rate	[128]
$GLUT4_0^{mus}$	3.36	[$\mu\text{mol/l}$]	Total muscular transporter concentration	Recal [32, 119]
$GLUT4_0^{fat}$	3,72	[$\mu\text{mol/l}$]	Total fat transporter concentration	Recal [32, 119]
GLUT3				
k_{cat}	1000	[1/min]	Catalytic rate constant	Fit
K_m^{pls}	3	[mmol/l]	Concentration of half max. rate of transport from plasma to intracellular	[128]
K_m^{cell}	3	[mmol/l]	Concentration of half max. rate of transport from intracellular to plasma	[128]
C_{GLUT3}	8.5	[$\mu\text{mol/l}$]	Concentration of cerebral transporter expression	Fit
GLUT2				
k_{cat}	10	[1/min]	Catalytic rate constant	Fit
K_m^{int}	17	[mmol/l]	Concentration of half max. rate of transport from interstitial to intracellular	[128]
K_m^{cell}	17	[mmol/l]	Concentration of half max. rate of transport from intracellular to	[128]

			interstitial	
C_{GLUT2}^{liv}	0.55	[$\mu\text{mol/l}$]	Concentration of hepatic transporter expression	Fit
C_{GLUT2}^{duo}	2.22	[$\mu\text{mol/l}$]	Concentration of transporter expression in the small intestine duodenum	Fit
C_{GLUT2}^{ujej}	6.15	[$\mu\text{mol/l}$]	Concentration of transporter expression in the small intestine upper jejunum	Fit
C_{GLUT2}^{uile}	1.82	[$\mu\text{mol/l}$]	Concentration of transporter expression in the small intestine upper ileum	Fit
C_{GLUT2}^{ljej}	1.79	[$\mu\text{mol/l}$]	Concentration of transporter expression in the small intestine lower jejunum	Fit
C_{GLUT2}^{lile}	0.57	[$\mu\text{mol/l}$]	Concentration of transporter expression in the small intestine lower ileum	Fit
SGLT1				
k_{cat}	40	[1/min]	Catalytic rate constant	Fit
K_m^{lum}	0,2	[mmol/l]	Concentration of half max. rate of transport from lumen to intracellular	[128]
C_{SGLT1}^{duo}	2.22	[$\mu\text{mol/l}$]	Concentration of transporter expression in the small intestine duodenum	Fit
C_{SGLT1}^{ujej}	6.15	[$\mu\text{mol/l}$]	Concentration of transporter expression in the small intestine upper jejunum	Fit
C_{SGLT1}^{uile}	1.82	[$\mu\text{mol/l}$]	Concentration of transporter expression in the small intestine upper ileum	Fit
C_{SGLT1}^{ljej}	1.79	[$\mu\text{mol/l}$]	Concentration of transporter expression in the small intestine lower jejunum	Fit
C_{GLUT2}^{lile}	0.57	[$\mu\text{mol/l}$]	Concentration of transporter expression in the small intestine lower ileum	Fit
Clearance of glucagon				
k_1	100	[l/ $\mu\text{mol}/\text{min}$]	Glucagon receptor binding affinity	Fit
k_2	0	[1/min]	Rate constant of glucagon recycling	Fit
k_3	0.01	[1/min]	Rate constant of GPCR recycling	Fit
$GPCR_{total}$	1e-5	[$\mu\text{mol/l}$]	Total concentration of hepatic GPCR	Fit
$CL_{int_{pls}}^{DPP4}$	2	[1/min]	Intrinsic plasma clearance	Fit
Secretion of glucagon				
k_{GLPNR}		[-]	GLP-1-dependent secretion constant	Fit
The incretin Effect				
k_1	1.2	[1/min]	GLP-1 clearance rate constant	Fit
k_2	15	[$\mu\text{mol/l}/\text{min}$]	GLP-1 production rate constant	Fit
GLP_0	1e-4	[$\mu\text{mol/l}$]	Basal GLP-1 concentration	Fit
K_m^{rGA}	17	[mmol/l/min]	Rate of half max. rate of glucose absorption-dependent GLP-1 production	Fit
K_{GLP}	2	[-]	GLP-1-dependent insulin secretion constant	Fit
K_m^{GLP}	0.6	[$\mu\text{mol/l}$]	Concentration of half max. rate of GLP-1-dependent insulin secretion	Fit
^a The table includes, besides the fitted values, parameter values taken from literature.				

A large share was either recalculated ("Recal.", i.e. organ glucose metabolism was distributed over the larger number of organs, but remained the same in total) or refitted ("Refit", this was only done for the threshold functions when transferred from tanh-functions to Michaelis-Menten functions) from Sorensen [32].

1. Knox C, Law V, Jewison T, Liu P, Ly S, Frolkis A, *et al.* DrugBank 3.0: a comprehensive resource for 'omics' research on drugs. *Nucleic Acids Res* 2011, **39**(Database issue): D1035-1041.
2. Sorensen JT. A Physiologic Model of Glucose Metabolism in Man and its Use to Design and Assess Improved Insulin Therapies for Diabetes. PhD thesis, MIT, 1985.
3. Zierler K. Whole-body glucose metabolism. *Am J Physiol* 1999, **276**(3 Pt 1): E409-426.
4. Sedaghat AR, Sherman A, Quon MJ. A mathematical model of metabolic insulin signaling pathways. *Am J Physiol Endocrinol Metab* 2002, **283**(5): E1084-1101.

Table 5: Patient Group Parameter Set

Parameter	Value T1	Value H	Dim.	Description	Source
Endosomal insulin receptor					
IR_{fat}^{tot}	0.1	0.04	[nmol/l]	Total conc. of fat endosomal IR	Fit
IR_{liv}^{tot}	18	6	[nmol/l]	Total conc. of liver endosomal IR	Fit
IR_{mus}^{tot}	0.4	0.15	[nmol/l]	Total conc. of muscle endosomal IR	Fit
IR_{pass}^{tot}	0.2	0.05	[nmol/l]	Total conc. of non-target-tissue endosomal IR	Fit
$IR_{p\ fat}^0$	0.01	0.004	[nmol/l]	Conc. of phosphorylated fat endosomal IR at basal insulin	Fit
$IR_{p\ liv}^0$	1.8	0.6	[nmol/l]	Conc. of phosphorylated liver endosomal IR at basal insulin	Fit
$IR_{p\ mus}^0$	0.04	0.015	[nmol/l]	Conc. of phosphorylated muscle endosomal IR at basal insulin	Fit
$IR_{p\ pass}^0$	0.02	0.005	[nmol/l]	Conc. of phosphorylated non-target-tissue endosomal IR at basal insulin	Fit
$RecFac$	50	65	[-]	Receptor recycling factor	Fit
$IntFac$	3	3	[-]	Receptor internalization factor	Fit
Target tissue insulin receptor					
IR_{fat}^{tot}	0.1	0.1	[μ mol/l]	Total conc. of fat cellular IR	Fit
IR_{liv}^{tot}	12	8	[μ mol/l]	Total conc. of liver cellular IR	Fit
IR_{mus}^{tot}	0.5	0.5	[μ mol/l]	Total conc. of muscle cellular IR	Fit
$IR_{p\ fat}^0$	0.0044	0.005	[μ mol/l]	Conc. of phosphorylated fat cellular IR at basal insulin	Fit
$IR_{p\ liv}^0$	0.19	0.15	[μ mol/l]	Conc. of phosphorylated liver cellular IR at basal insulin	Fit
$IR_{p\ mus}^0$	0.011	0.01	[μ mol/l]	Conc. of phosphorylated muscle cellular IR at basal insulin	Fit
$RecFac_{fat}$	7	10	[-]	Fat receptor recycling factor	Fit
$IntFac_{fat}$	3	3	[-]	Fat receptor internalization	Fit

				factor	
$RecFac_{liv}$	20	25	[-]	Liver receptor recycling factor	Fit
$IntFac_{liv}$	5	5	[-]	Liver receptor internalization factor	Fit
$RecFac_{mus}$	7	10	[-]	Muscle receptor recycling factor	Fit
$IntFac_{mus}$	3	3	[-]	Muscle receptor internalization factor	Fit
Glucose-dependent Glucagon Secretion					
V_0^{GPNR}	1.3	4.16	[-]	Rate at zero substrate concentration	Fit
ΔV_{max}^{GPNR}	-0.6	-3.66	[-]	Max. change in transporter rate	Fit
K_m^{GPNR}	1.07	0.65	[-]	Concentration of half max. rate	Fit
n^{GPNR}	3	4.25	[-]	Hill/cooperativity exponent	Fit

Table 6: Individual Parameter Set (T1DM)

Parameter	Unit	Value for Subject No.							
		110	115	117	122	126	128	129	132
k_{cat}^{SGLT1a}	[1/min]	40	20	40	40	40	20	40	60
S_I^b	[-]	0.4	0.65	0.65	0.9	0.45	0.75	0.4	0.65
S_N^c	[-]	1.3	1.3	0.9	1	1	1	1.1	1
Q_{fac}^d	[U/ μ mol]	3500	6000	4000	100	2000	6500	12000	5000
Q_N^e	[-]	1	5	3	6	0.3	3	7	5
k_{SCD}^f	[1/min]	1e-6	1e-5	6e-6	1.4e-5	1e-7	1.4e-5	1.3e-6	2e-5
k_{SCD}^N	[1/min]	7e-5	11e-5	6e-5	7e-5	1.5e-5	15e-5	5.5e-5	15e-5
GFR_{frac}^g	[-]	1	1	1	0.1	1	3	4	0.1
GFR_{frac}^N	[-]	15	4.5	10	10	25	1	8	5
$SITT^i$	[min]	150	350	120	120	120	350	200	120
f_u^j	[-]	1	1	1	0.02	1	0.95	1	0.25

^a Catalytic rate constant of SGLT1
^b Glucagon Sensitivity
^c Insulin Sensitivity
^d Subcutaneous insulin binding factor
^e Subcutaneous glucagon binding factor
^f Rate constant of subcutaneous insulin degradation
^g Rate constant of subcutaneous glucagon degradation
^h Fractional glomerular filtration rate of insulin
ⁱ Fractional glomerular filtration rate of glucagon
^j Fraction unbound

Table 7: Patient Properties

Subject	Gender ^a	T # ^b	Age	BW ^c	Height [cm]	BMI ^d	Av. BG ^e	HbA1c[%]	I_{min}^f	I_{max}^g	TDD ^h	BG _{min} ⁱ	BG _{max} ^j
110	M	2	49	73	1.58	29.2	7.89	6.57	25	140	58.6	3.72	14.67
		3	49	73			8.56	6.98	20	70	43.3	4.33	14.78
115	M	2	19	80.8	1.87	23	8.00	6.65	10	80	73.3	2.61	15.94
		3	20	80.4			9.78	7.74	10	80	56.9	5.50	15.89
117	F	1	28	85	1.66	30.9	7.11	6.09	10	70	57.3	3.67	14.67
		2	29	80.6			8.94	7.24	10	55	55.7	4.33	17.39
122	M	1	47	110	1.89	30.9	7.61	6.39	500	1200	95.1	2.50	16.56
		2	48	107			8.61	7.04	200	750	62.7	3.83	14.67
126	F	1	50	68.6	1.61	26.5	7.61	6.39	25	110	54	4.11	15.28

		2	51	69.8			8.11	6.73	25	100	37.4	4.56	14.11
128	M	1	30	94.8	1.77	30.1	7.61	6.40	10	55	68.9	4.11	12.72
		2	31	98.3			8.50	6.97	12	50	55.6	4.67	14.22
129	M	1	47	90.9	1.73	30.2	9.11	7.33	30	140	106.6	2.50	20.00
		2	48	90.2			11.00	8.52	35	80	76.4	5.11	18.50
132	M	1	71	79.5	1.85	23.3	7.17	6.11	50	210	66.5	1.78	14.94
		2	71	77			8.72	7.10	25	150	52.2	4.22	16.28

^a Gender (M = male; F = female)

^b Trial Number

^c Body Weight [kg]

^d Body mass index [cm/m²]

^e Average blood glucose [mmol/l]

^f Minimal measured plasma Insulin levels [mU/l]

^g Maximal measured plasma Insulin levels [mU/l]

^h Total daily dose of insulin, given [U]

ⁱ Minimal measured blood glucose levels [mmol/l]

^j Maximal measured blood glucose levels [mmol/l]

V.5.2 Control Algorithm

V.5.2.1 Challenges in Glucose Control (Detail)

V.5.2.1.1 Disturbances

V.5.2.1.1.1 Meals

Before the artificial pancreas can be applied in everyday life or even in hospitals, a number of challenges remain to be solved. One of the most critical challenges is the regulation of glucose levels after a meal. This problem could, in principle, be solved with two different approaches. The first approach could be feed-forward control: by pushing a button the patient informs the controller that a meal is occurring, thus initiating an insulin bolus. However, even if the carbohydrate (CHO) content of a meal is known beforehand, it is not assured that the controlled subject will show the same glucose response for meals with the same CHO content as the absorption of a meal also depends on the specific type of CHO [126] as well as on the amount of fat a protein contained in the meal. Meal composition may have an effect on gastric emptying time as well as on the speed CHOs are processed for absorption. As both these properties can be explicitly taken into account by the PBPK/PD model kernel, the effect of nutrition-based variability of glucose absorption is currently investigated.

The second approach could be feedback control, where the controller only reacts after a sufficiently large increase in blood glucose levels. However, due to system-inherent time-delays this strategy has proven difficult in practice [253].

V.5.2.1.1.2 Exercise

One of the main influences on whole-body glucose metabolism is the cellular energy expenditure during exercise. Physical (muscular) activity increases the whole-body energy expenditure and thereby muscular glucose consumption and hepatic glucose output. Reliable mechanistic models, based on the concepts of metabolic and regulatory networks [204] in energy metabolism that describe the effects of exercise in muscular [204] and hepatic [205] tissue, could improve overall glucose control performance [194, 195].

However, it has to be assumed that the model-based control algorithm may need to get informed by the user regarding oncoming exercise episodes. In the case of an uninformed exercise episode, the controller will not be able to use model predictions

alone to handle the oncoming disturbances in blood glucose levels. Nevertheless, even if the controller is informed about an oncoming episode of exercise, the effecting disturbances on glucose levels may vary depending on exercise duration and intensity (intra-individual property), and on fitness and gender (inter-individual property) of the controlled subject. Thus, the chosen algorithm should have robustness properties that could handle occurring episodes of exercise and their intra- and inter-individual variability. To overcome some of the uncertainties related to exercise, multi-parametric sensors measuring heart rate and the Q-T interval could be used for run-to-run control to adapt to changes in the subjects fitness. However, further evidence, e.g. from literature search, is necessary in order to clarify if measurements of heart rate and Q-T interval are sufficient for the unambiguous identification of exercise episodes or if they cannot, for example, be distinguished from adrenalin surges.

V.5.2.1.2 Inter- and Intra-Individual Variability

V.5.2.1.2.1 Diurnal Variations

One of the main challenges of optimal blood glucose control in humans is the change in the body's response to insulin, i.e. insulin sensitivity, over time (morning vs. evening, day vs. night). As insulin is the major component that controls the uptake and production of glucose in the human body, glucose control performance could be vastly improved with reliable models that describe this change in insulin sensitivity.

It is known that certain metabolic processes and hormonal activities follow a circadian pattern managed by a hormonal circadian clock within the body [254].

The binding of insulin to the insulin receptor triggers a signalling cascade that is responsible for the action of insulin. Interaction with the signalling network may severely affect the propagation of the signal triggered by insulin receptor binding. Although the detailed mechanisms of interaction are not known [223], it is generally accepted that glucocorticoids (cortisol i.e.) cause insulin resistance [223, 247]. Glucocorticoids themselves are produced by the human body and their blood concentration levels follow a circadian rhythm [255] and are also believed to have a strong influence on the circadian rhythm themselves [256]. Glucocorticoids that are administered exogenously as medication in critically ill patients could therefore cause a disturbance of the circadian profile of endogenous glucocorticoids and cause changes in insulin action.

V.5.2.1.2.2 Severe Changes

In all subjects with T2DM, some subjects with T1DM, and also the critically ill, the metabolic system is compromised in its ability to maintain homeostatic control of glucose levels. This is due to a reduced sensitivity to insulin. Insulin sensitivity is of major importance at intensive care units, where the effects of inflammation and its treatment, e.g. with anti-inflammatory steroids like cortisone, can cause severe dynamic changes in insulin sensitivity [158, 229-234]. Hyperglycaemia is prevalent in critical care [75, 235-238]. Tight control of blood glucose has been shown to improve clinical outcomes [237, 238]. More importantly, van den Berghe et al [235-238], and Chase et al [75] have shown that tight glucose control can reduce mortality in the intensive care unit (ICU) by 18-45%. Glucocorticoids are used in critical care to treat a variety of inflammatory and allergic disorders, but may inadvertently cause hyperglycaemia through reduced insulin sensitivity. Although tight glycaemic control in critical care is not a foremost objective within the scope of this work, similar severe

conditions could also arise in any subject with diabetes. These implications have to be taken into consideration when glycaemic control is performed at a clinical site.

V.5.2.2 Insulin On-board (IOB) as a Safety Constraint

As mentioned in Section III.2.1.2, time delays associated with physiological lag-times, e.g. the time it takes for subcutaneous insulin to reach the target tissue, do complicate glycaemic control. For example, a standard feedback controller like a PID controller has no information on remaining circulating insulin levels. During the meal, as glucose levels rise, the controller may calculate a high dose to prevent hyperglycaemia. If, within a short period of time, a second control input is calculated, glucose levels may still be rising and the controller would again calculate a high dose. Depending on the sampling time of the control system, this may occur several times during a meal and the body would accumulate large quantities of insulin that would then cause postprandial hypoglycaemia. Consequently, the aggressiveness of the controller would have to be reduced or the sampling times would have to be increased to accommodate for the large lag-times (to approx. one control input every 2 hours). Both strategies however would severely reduce the quality of control [257].

For that reason, recent control algorithms proposed for a closed-loop artificial pancreas make use of “insulin-on-board” (IOB) to reduce the probability of hypoglycaemic events. Also, to help subjects avoid problems associated with accumulating circulating insulin most current insulin pumps include an IOB feature. Current state-of-the-art algorithms use simple decay functions to describe the pharmacokinetics of IOB [257]. For this work, circulating insulin levels are used, as they can be simulated using the here developed PBPK/PD model, to calculate IOB and the associated constraint for the control system.

A penalty function to account for the effect of endogenous (on-board) insulin (EIOB) was defined. To calculate the constraint for the control system, the functions of the model describing the pharmacodynamic effect of insulin, acting through the amount of phosphorylated insulin receptor at the respective target tissue, are used. For this, the function for insulin mediated hepatic glucose uptake (M_{IHGU}), Figure 34 (left)) and insulin mediated peripheral translocated glucose transporter 4 ($GLUT4_{mem}$, Figure 35 (left)) are used.

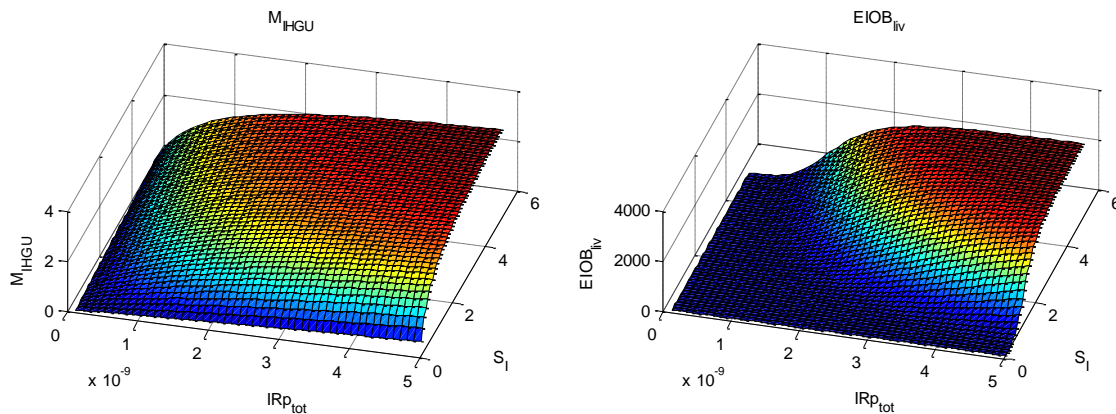


Figure 34: Surface plot of the pharmacodynamic effect of insulin at the liver (left plot; insulin-dependent hepatic glucose production, M_{IHGU}) and the surface plot of the constraint function based on the saturation of the pharmacodynamic effect of insulin at the liver (right plot; hepatic effect of insulin on board, $EIOB_{liv}$ with $W_{EIOB} = 3000$).

The EIOB functions are parameterized such that only insulin doses are penalized for which the resulting tissue concentration of insulin reaches levels at which the pharmacodynamics at the respective target tissue become over-saturated. Based on the individuals S_I and the amount of phosphorylated insulin receptor, the EIOB function for hepatic ($EIOB_{liv}$) and peripheral/muscular ($EIOB_{mus}$) insulin action is calculated:

$$EIOB_{mus/liv}(IR_{eff}^{mus/liv}) = \frac{W_{EIOB}(S_I IR_{eff}^{mus/liv})^8}{\left((K_m^{mus/liv})^8 + (S_I IR_{eff}^{mus/liv})^8\right)}$$

with relative effect of phosphorylated insulin receptors $IR_{eff} = IR_p/IR_p^0$ and sum of phosphorylated insulin receptor IR_p , sum of basal phosphorylated insulin receptor IR_p^0 , insulin sensitivity S_I , threshold value K_m , and the weight W_{EIOB} , of the constraint. When the PBPK/PD model is individualized, the pharmacodynamic functions are automatically adapted via the insulin sensitivity (parameter S_I) allowing individualization of EIOB for each subject. K_m is calculated based on the patients basal state at the beginning of the clamp phase and EIOB is solved for K_m with $EIOB(IR_{eff} = K_m) = 1$.

When the PBPK/PD model is individualized, the pharmacodynamic functions are automatically adapted via the insulin sensitivity (parameter S_I). The function of $EIOB_{liv}$ is shown in Figure 34 (right) the function of $EIOB_{mus}$ is shown in Figure 35 (right). The functions of EIOB were parameterized in such a way that the control input was only penalized for resulting concentrations of insulin at which the pharmacodynamics at the respective target tissue were nearly saturated (red area in the surface plots of M_{IHGU} , Figure 34 (left) and GLUT4, Figure 35 (left)). Thus, through the parameter S_I the constraints are also individualized for each subject.

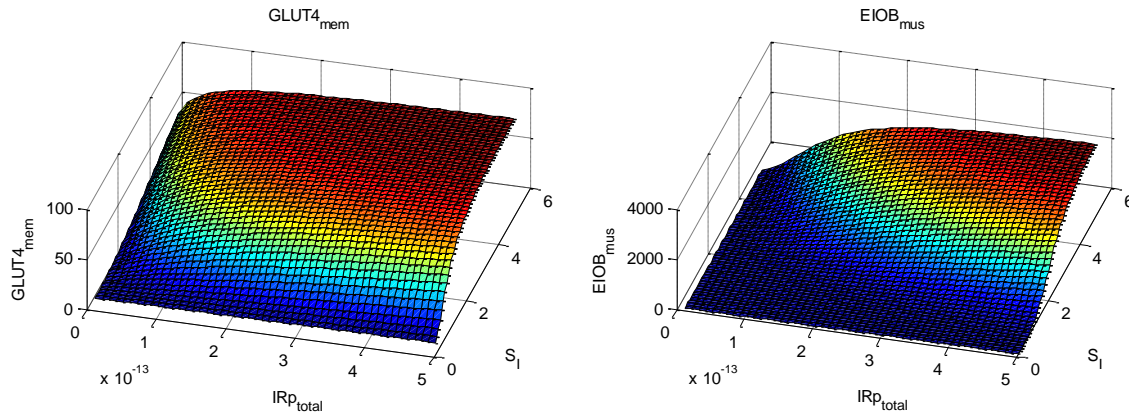


Figure 35: Surface plot of the pharmacodynamic effect of insulin at the muscle (left plot; relative (in % of total GLUT4) concentration of insulin-dependent translocated GLUT4, $GLUT4_{mem}$) and the surface plot of the constraint function based on the saturation of the translocation of GLUT4 (right plot; muscular effect of insulin on board, $EIOB_{mus}$ with $W_{EIOB} = 3000$).

The constraint for EIOB was used for both, the Fading Memory Proportional Derivative controller as well as the model predictive control algorithm. The details of the application of the EIOB within the respective control system are described in the following.

V.5.2.2.1 MPC Cost Function

Performance of the MPC algorithm strongly depends on the design of the cost function $V(x, k, u)$, or the stage cost $l(x_i)$, respectively. A general approach would be to use sum-of-squares to penalize the control error with $l(x_i) = f(DTV - x_i)$ (dynamic target value vs. predicted glucose). However, as hypoglycaemia is more critical than hyperglycemia, an asymmetrical cost function was chosen. For this, two overlapping exponential functions were chosen with the function penalizing low glucose levels (lower threshold value function, $LTHV$) defined as:

$$LTHV_i = e^{1/8(LT-x_i)}, \text{ with } LT = DTV - 40 \text{ ([mg/dl])}$$

and the function penalizing high glucose levels (upper threshold value function, $UTHV$) defined as:

$$UTHV_i = e^{1/70(x_i-UT)}, \text{ with } UT = DTV - 10 \text{ ([mg/dl])}$$

and the stage cost

$$l(x_i) = W_{TV}(LTHV_i + UTHV_i - c)$$

with the correction constant $c = 2$ to set $l(x_i = DTV) = 0$ and weight $W_{TV} = 100$.

V.5.2.2.2 Insulin on Board

The MPC cost function is penalized in case of insulin oversaturation. The EIOB value is added to the cost function giving:

$$V(x, k, u) = \sum_{i=k}^{k+N} l(x_i) + \text{EIOB}_i^{\text{mus}} + \text{EIOB}_i^{\text{liv}} + u_k.$$

The weight chosen for EIOB is $W_{\text{EIOB}} = 3000$.

V.5.2.2.3 Negative Slope

A negative slope of the blood glucose trajectory at glucose concentrations around the target value or below are undesired, as they indicate that glucose levels are still falling. Thus, an additional penalty for a negative glucose slope NGS was added to the cost function $V(x, k, u)$ if glucose levels below target value were falling, i.e. the slope was negative. The penalty was defined as:

$$NGS = W_{NGS} \sum_{i=k}^{k+N} -\tilde{e}_i \cdot \exp(-k_d(\tilde{e}_i - \tilde{e}_{i-1})), \quad \text{with } \tilde{e}_i = (x_i - DTV),$$

if $(\tilde{e}_i - \tilde{e}_{i-1}) < 0$

with a penalty weight of $W_{NGS} = 1/2000$ and the constant $k_d = 1/100$.

V.5.2.3 FMPD Constraints

V.5.2.3.1 Insulin on Board (IOB)

Control of blood glucose via the subcutaneous route introduces severe time delays between application of the controller input and effect of control. These time-delays pose a significant challenge in glucose control as they in general cause the system (w.r.t. insulin levels and their effect) to overshoot, and more importantly for glucose levels, to undershoot. If not handled properly, severe episodes of hypoglycemia could occur. Feedback-systems with time-delay are especially prone to overshoot after

severe disturbances due to the delayed effect of control. With respect to glucose control, this is the case after the consumption of a meal or after physical activity

The FMPD controller was combined with the EIOB constraint by weighing the feedback control input (dose correction) Δu_k with the sum of the weighted EIOB constraints:

$$\Delta u_k = \frac{K_p \sum_{j=0}^k e^{-W_p(k-j)} \hat{e}_j + K_i \sum_{j=0}^k \hat{e}_j + K_d \sum_{j=0}^k e^{-W_d(k-j)} (\hat{e}_j - \hat{e}_{j-1})}{1 + \text{EIOB}_{liv} + \text{EIOB}_{mus}}$$

V.5.2.3.2 Gain Scheduling

In general, a standard PD or PID controller is symmetric, i.e. both, positive and negative deviations from the target value are treated equally. However, depending on the tuning of the controller it could happen that after a meal, the integral component, or in the case of the FMPD the memorized proportional component could still cause the controller to inject insulin. It is common practice that if blood glucose levels go below the chosen target value, insulin infusion by the insulin pump is suspended to stop all insulin input until blood glucose reaches levels above the target value. However, experience with the dataset at hand revealed that if insulin levels reach very low values, which could happen during pump suspension, hepatic glucose output reacts very sensitive and large amounts of glucose are released by the liver. Thus, here, an approach is chosen that penalizes the input gain with the relative error below target value. Thus, the adjusted controller gains are calculated as:

$$\tilde{k}_{p,d} = k_{p,d} (1 + 3\bar{e}(t)), \quad \text{with } \bar{e}(t) = TV - y(t), \quad \text{if } \bar{e}(t) < 0.$$

All calculated control inputs that are negative are set to zero.

V.5.2.3.3 Target Value Attenuation

As especially the integral components of both, the target value shift and offset-control adapt only slowly to prediction errors, the controller starts with an increased Target value (150 mg/dl) at start of control, which is continuously lowered to the desired target level (110 mg/dl)

V.5.2.4 Parameter Sets

Table 8: Parameter set of the Control Algorithm

Parameter	Value	Dim.	Description	Source ^a
MPC				
UT	140	[mg/dl]	Upper glucose target range limit	GCP
LT	70	[mg/dl]	Lower glucose target range limit	GCP
W_{TV}	100	[-]	Weight for target value cost function	fit
c	2	[-]	Ordinate shift for value cost function	fit
W_{NGS}	1/2000	[-]	Weight for Negative Slope penalty	fit
k_d	1/100	[-]	Gain for Negative Slope penalty	fit
W_{EIOB}	3000	[-]	Weight of insulin-on-board constraint	fit
Offset Controller (FMPD)				
$K_p^{\Delta TV}$	0.2	[-]	Controller gain for P-controller	fit
$K_i^{\Delta TV}$	0.02	[-]	Controller gain for I-controller	fit
$W_p^{\Delta TV}$	0.02	[-]	Forgetting factor for P-controller	fit
$K_p^{\Delta u}$	4e-8	[U/(mg/dl)]	Controller gain for P-controller	fit
$K_i^{\Delta u}$	1e-9	[U/(mg/dl)]	Controller gain for I-controller	fit
$K_d^{\Delta u}$	5e-7	[U/(mg/dl)]	Controller gain for D-controller	fit
$W_p^{\Delta u}$	0.02	[-]	Forgetting factor for P-controller	fit
$W_d^{\Delta u}$	0.1	[-]	Forgetting factor for D-controller	fit
W_{EIOB}	30	[-]	Weight of insulin-on-board constraint	fit
$k_{p,d}$	3	[-]	Constant for Gain Scheduling	fit

V.5.3 Clinical Trials

V.5.3.1 Trial Criteria

V.5.3.1.1 Withdrawal Criteria

The following have been used as withdrawing criteria for participating subjects:

- Abnormal laboratory tests judged to be of clinical significance
- Intercurrent illness requiring medication
- Volunteers not wishing to continue with the study for other reasons, e.g. unavailability
- Changes in concomitant medication of clinical relevance for continuing in the study
- Strenuous exercise within 24 hours prior to the experiment
- Consummation of alcohol within 24 hours prior to the experiment
- Pregnancy or intention of becoming pregnant

V.5.3.1.2 Stopping Rules

The following have been used as stopping rules for discontinuation of the trial:

1. If more than 2 subsequent blood samples cannot be obtained
2. If blood glucose cannot be controlled with subcutaneous insulin infusion and insulin boluses according to the calculations of the algorithm

3. If the variable insulin infusion is interrupted for more than 30 minutes
4. If the experiment is stopped due to point 1 or 3, the subject may undergo the experiment on another occasion

V.5.3.2 Individual Patient Profiles

V.5.3.2.1 Trial #1

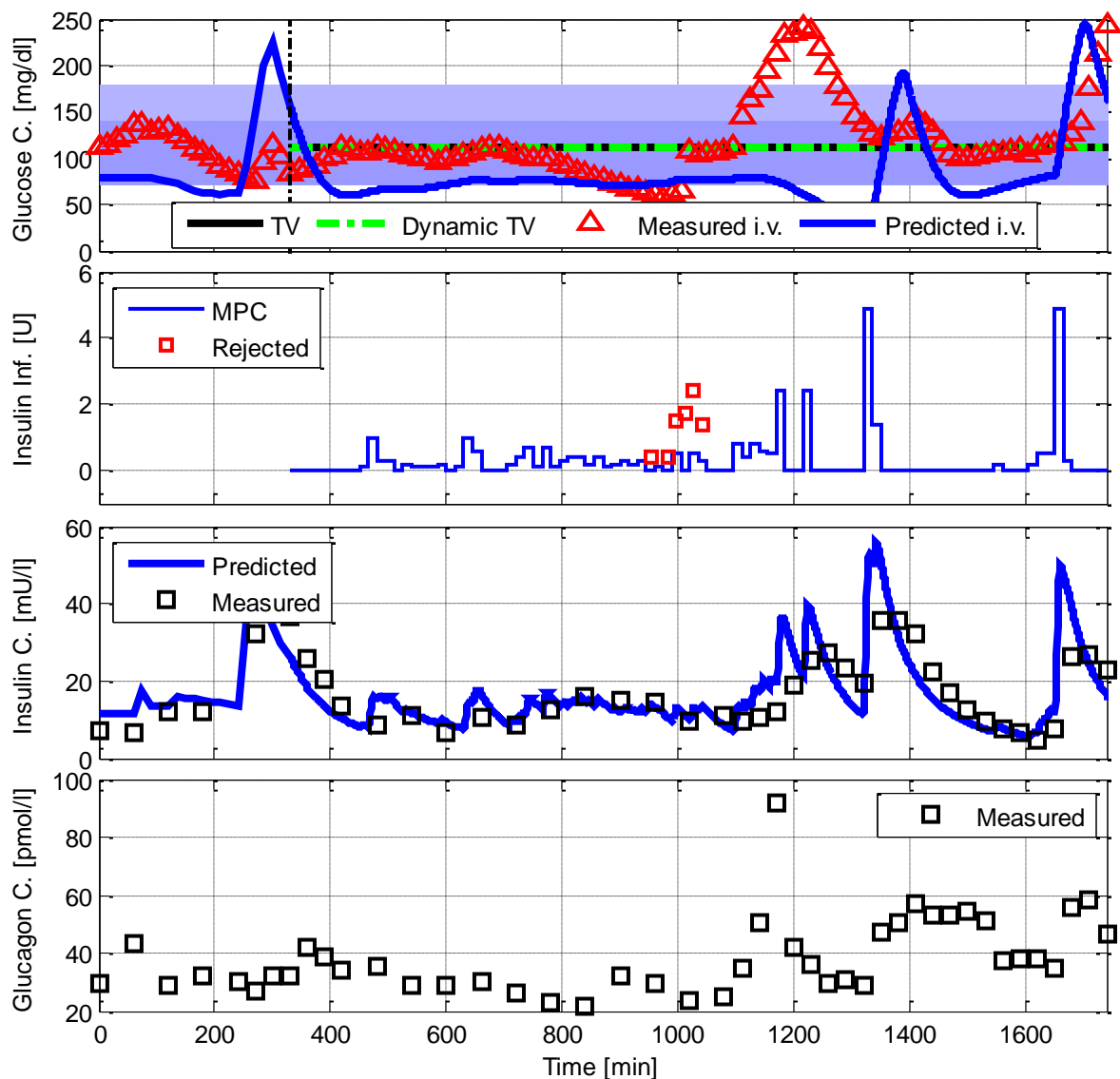


Figure 36: Glucose control in Subject 01. This was the individual with the second and last technical failure during the trial at 6:00 a.m. ($t = 960$ min) resulting in oral carbohydrate intervention (12 g CHO (orange juice) at 6:15 a.m. and 6:30 a.m.). Algorithm was reset at 7:30 a.m. ($t = 1050$ min). Subject 01 did not consider nutritional effects on meal absorption due to the issues discovered with Subject 02. Predicted meal absorption in Subject 01 is thus handled like a glucose solution (fast absorption). Also, meal information at breakfast was not transmitted to the controller and was thus treated like a disturbance. Also, the Dynamic TV shift was not recorded/stored and is thus displayed as zero.

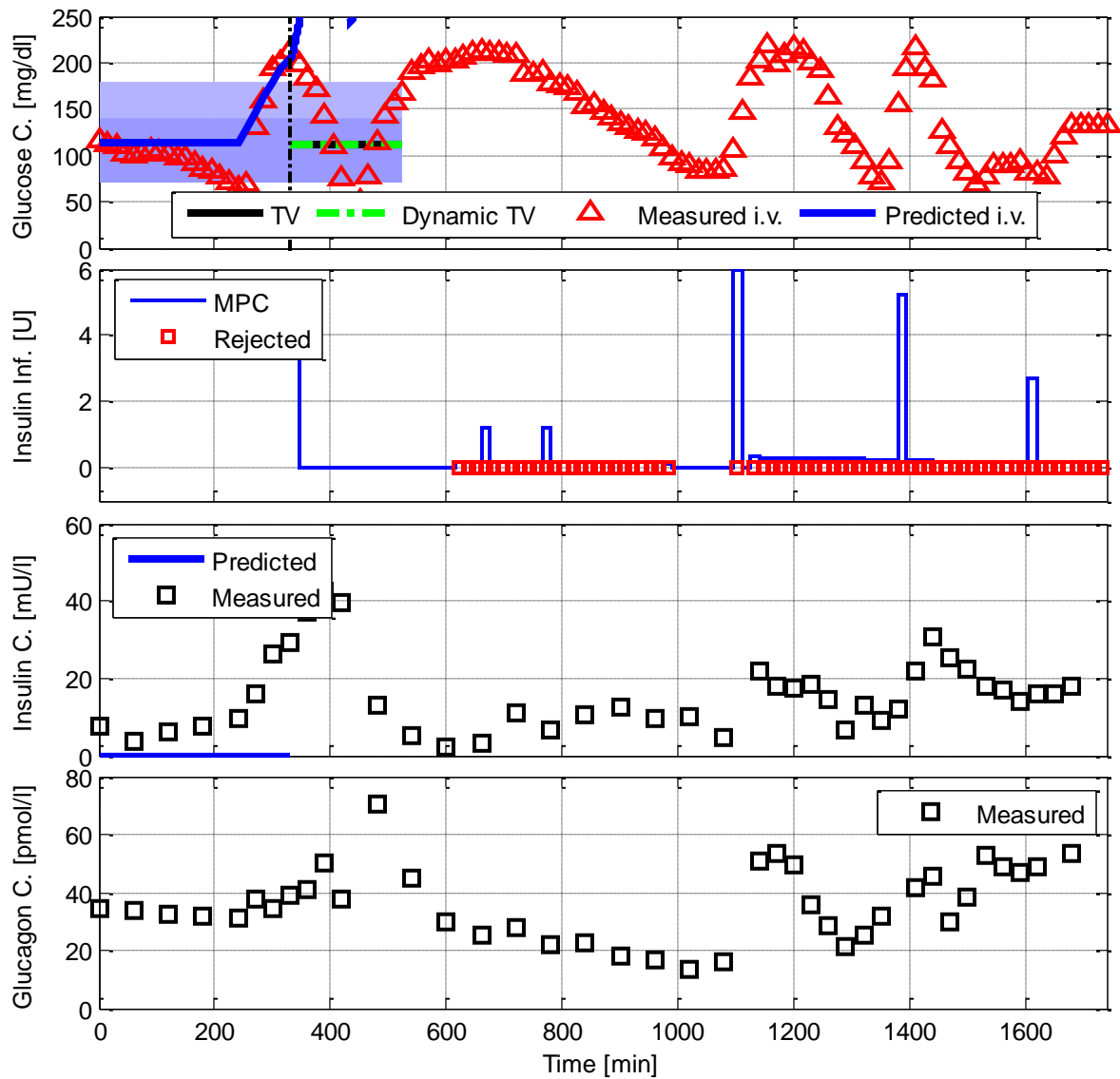


Figure 37: Glucose control in Subject 02. First technical failure at start of control (7:30 p.m. ($t = 330$ min)), due to erroneous handover of meal effect parameters to the controller, requiring oral carbohydrate intervention (36 g and 24 g CHO (orange juice) at 9:15 p.m. and 9:30 p.m.). Control was discontinued at 9:30 a.m. ($t = 450$ min). During this first experiment, predictions for insulin were not stored. This was only commenced after the first experiment. Predictions for glucagon were only stored in the second trial.

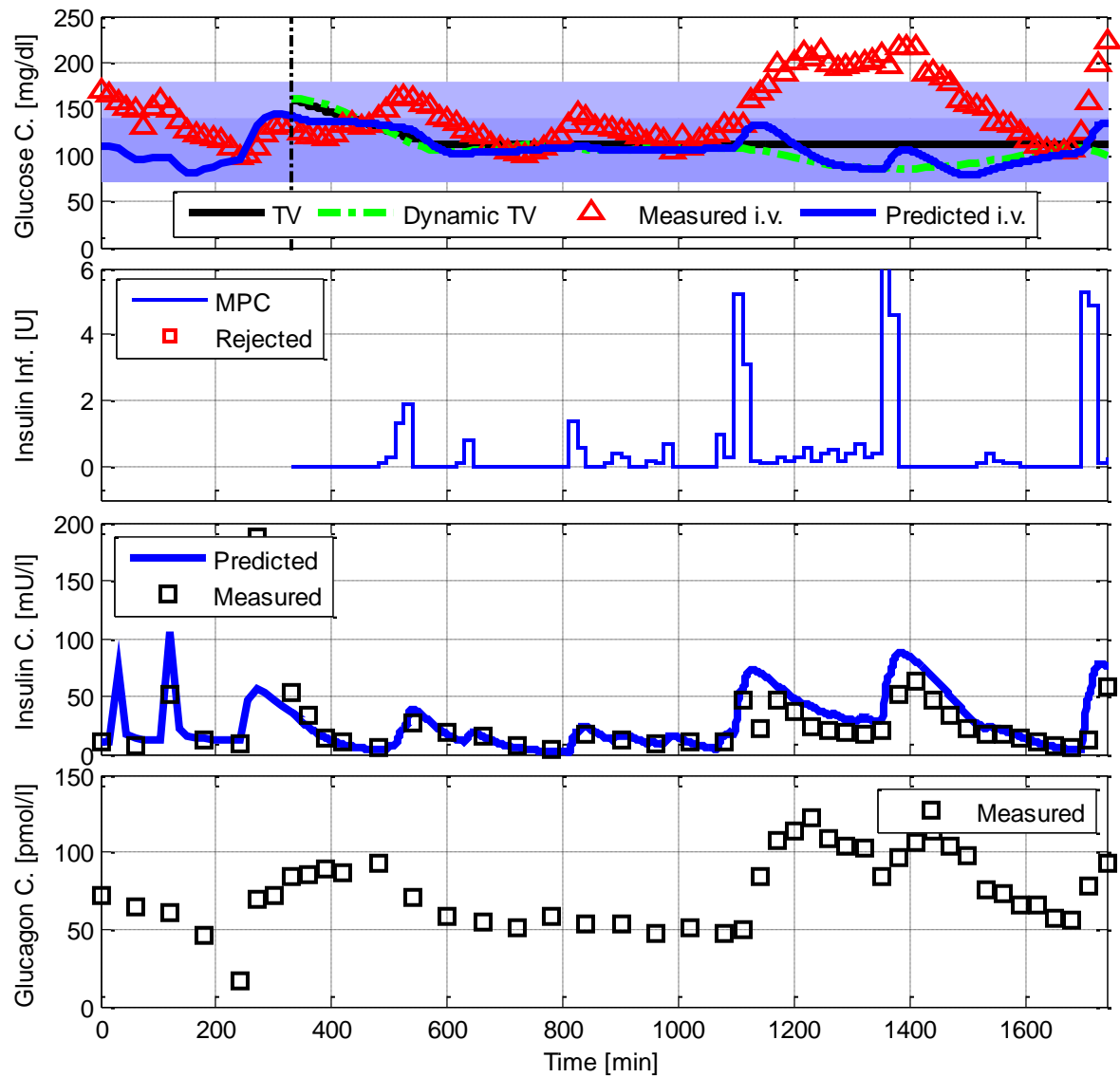


Figure 38: Glucose control in Subject 03. First dose was rejected (7:45 p.m. ($t = 345$ min)).

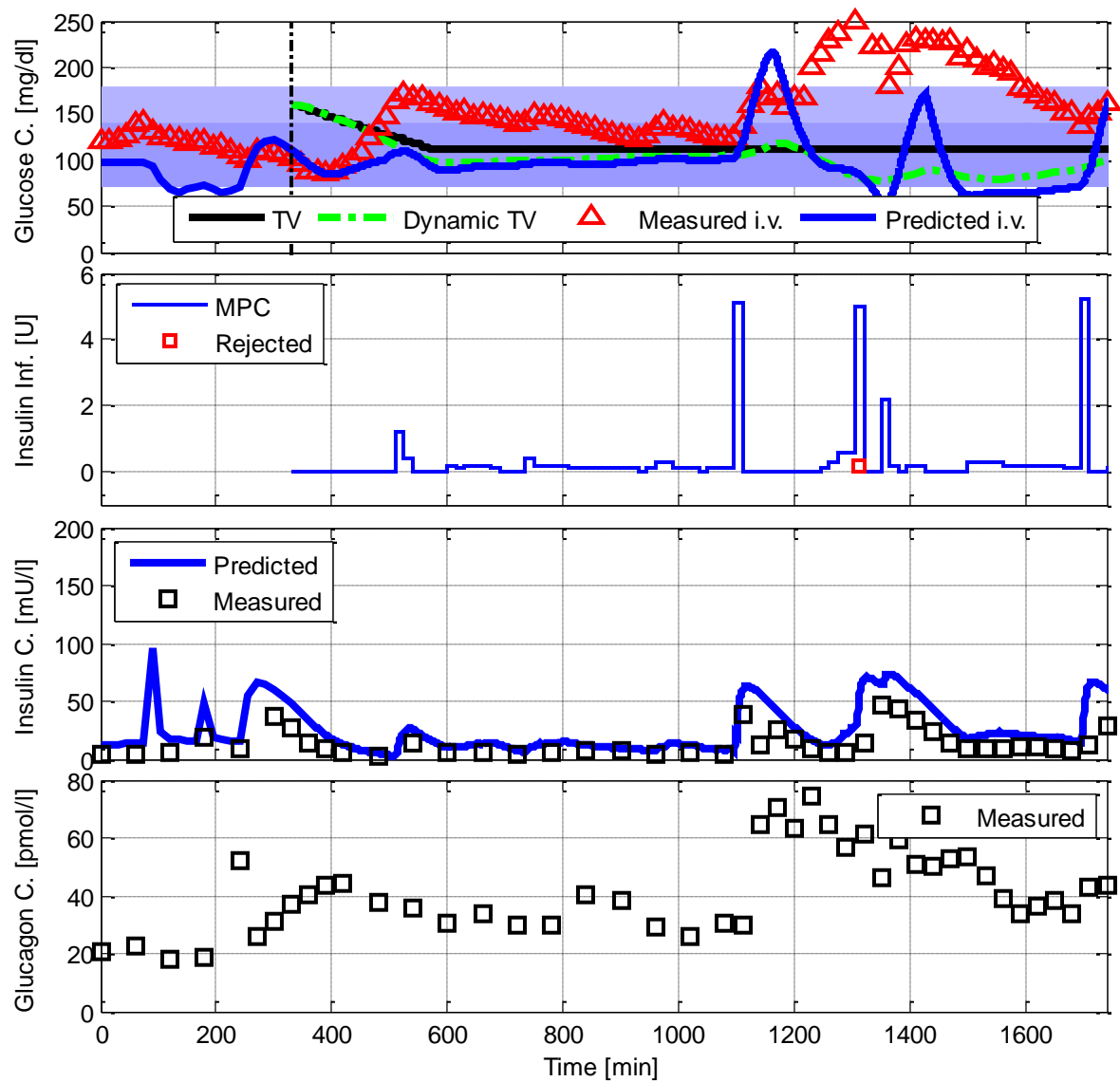


Figure 39: Glucose control in Subject 04. A single dose was rejected (7:45 p.m. ($t = 345$ min), 0.2 U rejected and 5 U applied). Divergence of predictions and measurements after breakfast could have been caused by the unexpected rise in glucagon levels after each meal.

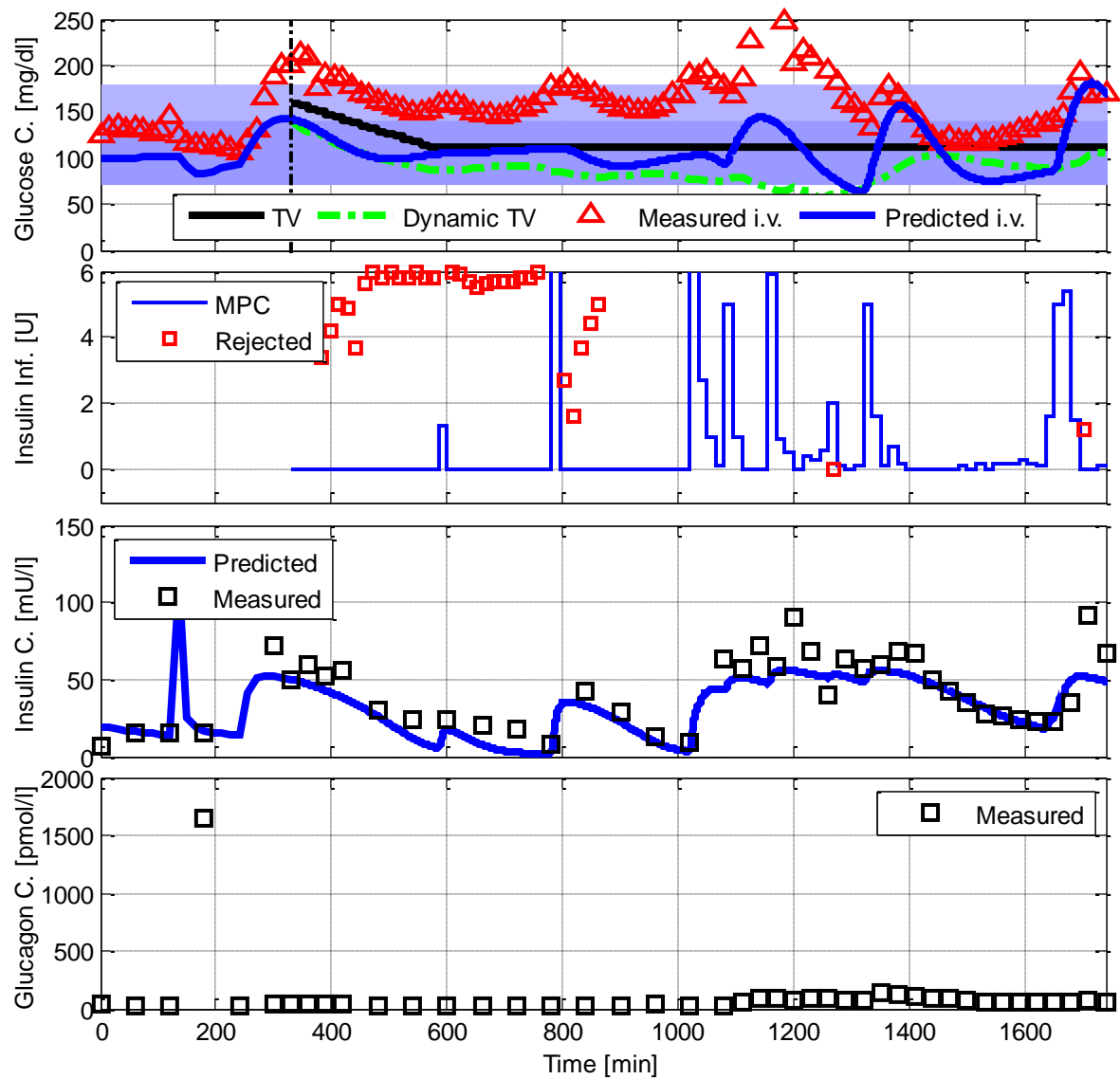


Figure 40: Glucose control in Subject 05. MPC dose recommendations were rejected from the start of control (7:30 p.m., $t = 330$ min) until 7:00 a.m. ($t = 1020$ min). Following that, dose recommendations were accepted and control results were good. Two more dose rejection at 11:00 a.m. ($t = 1260$ min, recommendation of 0 units was raised to 2 units of insulin, unnecessarily as glucose levels were already falling steeply) and 6:15 p.m. ($t = 1695$ min, 1.2 U recommended, 0 U applied, medical staff was taking no risks for overdose as this was shortly before end of trial).

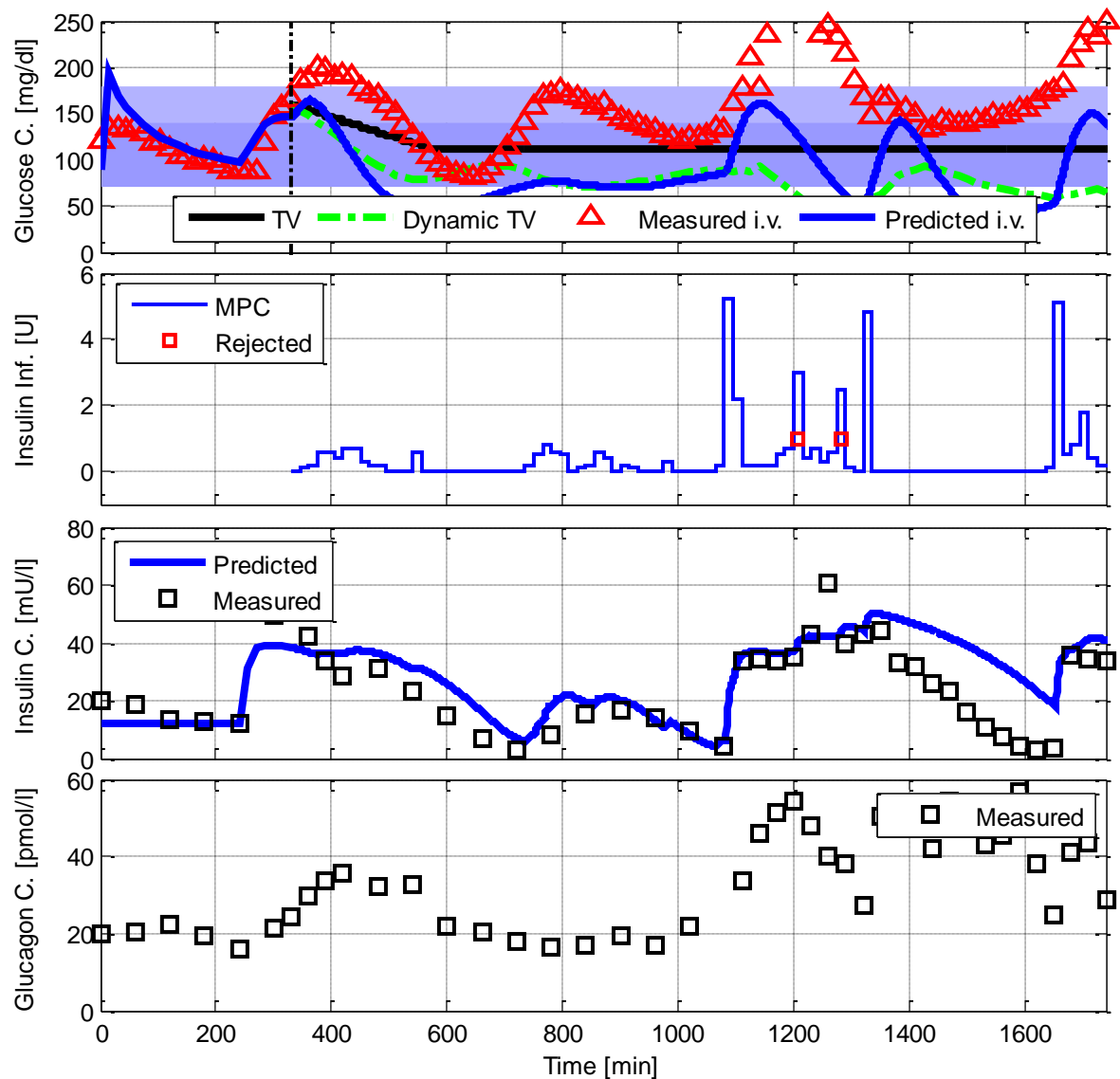


Figure 41: Glucose control in Subject 06. Subject had very unstable conditions at start of clamp and required extensive amounts of i.v. glucose. Although this was taken into consideration, it made initial parameterization challenging. Two dose recommendations at 10:00 and 11:15 a.m. ($t = 1200$ and 1275 min), both 1 U, were rejected and raised to 3 and 2.5 U. Half-life time of insulin was overestimated causing a lay-off in insulin dosing after meal doses. Patient glucose levels subsequently rose quicker than predicted, causing oscillations upon delayed counter-regulation.

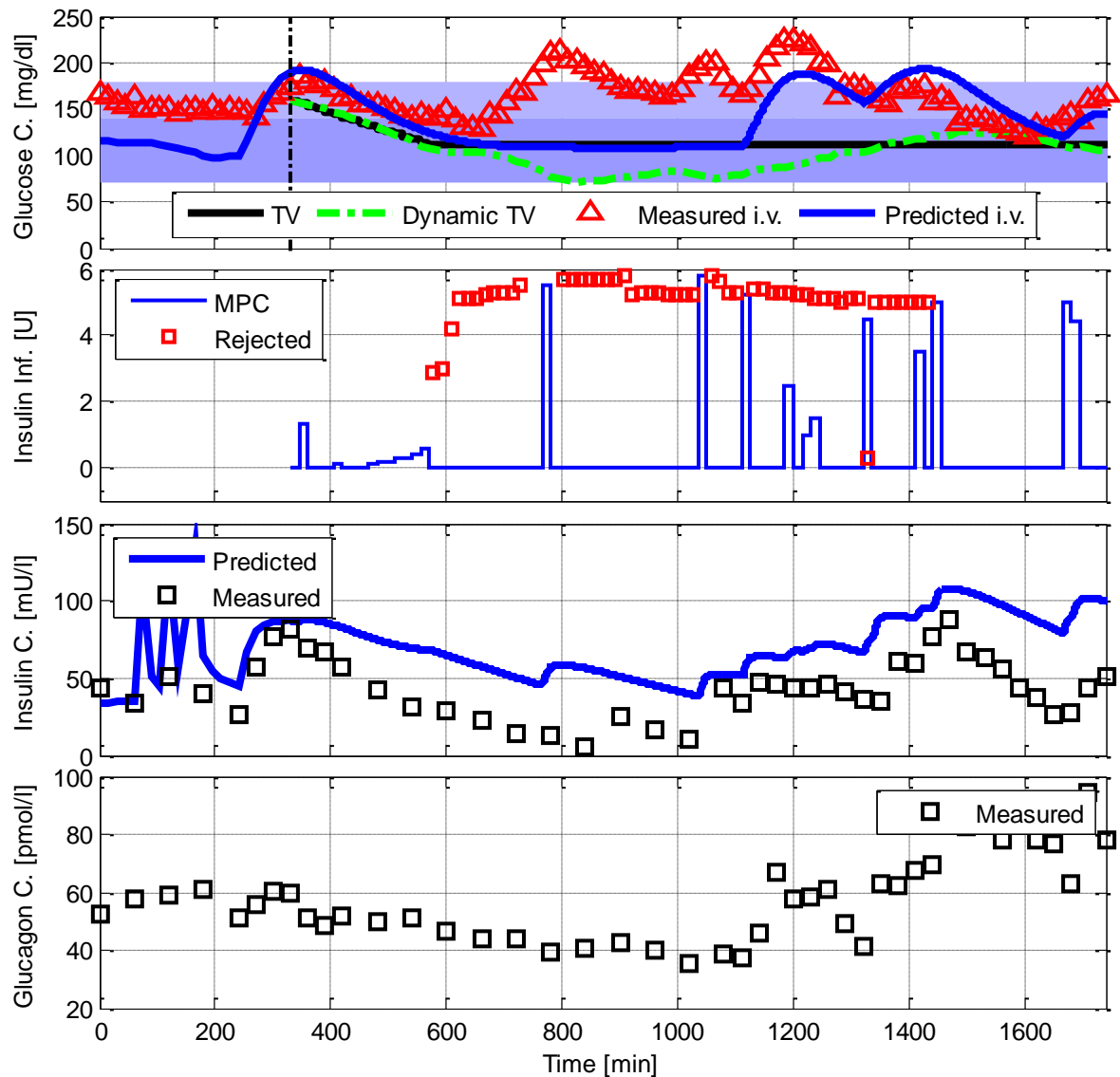


Figure 42: Glucose control in Subject 07. Half-life time of insulin was overestimated and insulin Sensitivity was underestimated (in relation to predicted vs. observed insulin levels). Patient glucose levels subsequently rose quicker than predicted, nevertheless, this was corrected by the dynamic target shift. However, the resulting increase dose recommendation was judged as too risky and subsequent recommendations were rejected. In between (7:15 a.m., $t = 1035$ min, 8:30 a.m., $t = 1110$ min) calculate doses were applied tentatively, but again rejected thereafter, even though glucose levels were too high. Only after 2:00 p.m. doses were after another tentative test, accepted and control was significantly improved.

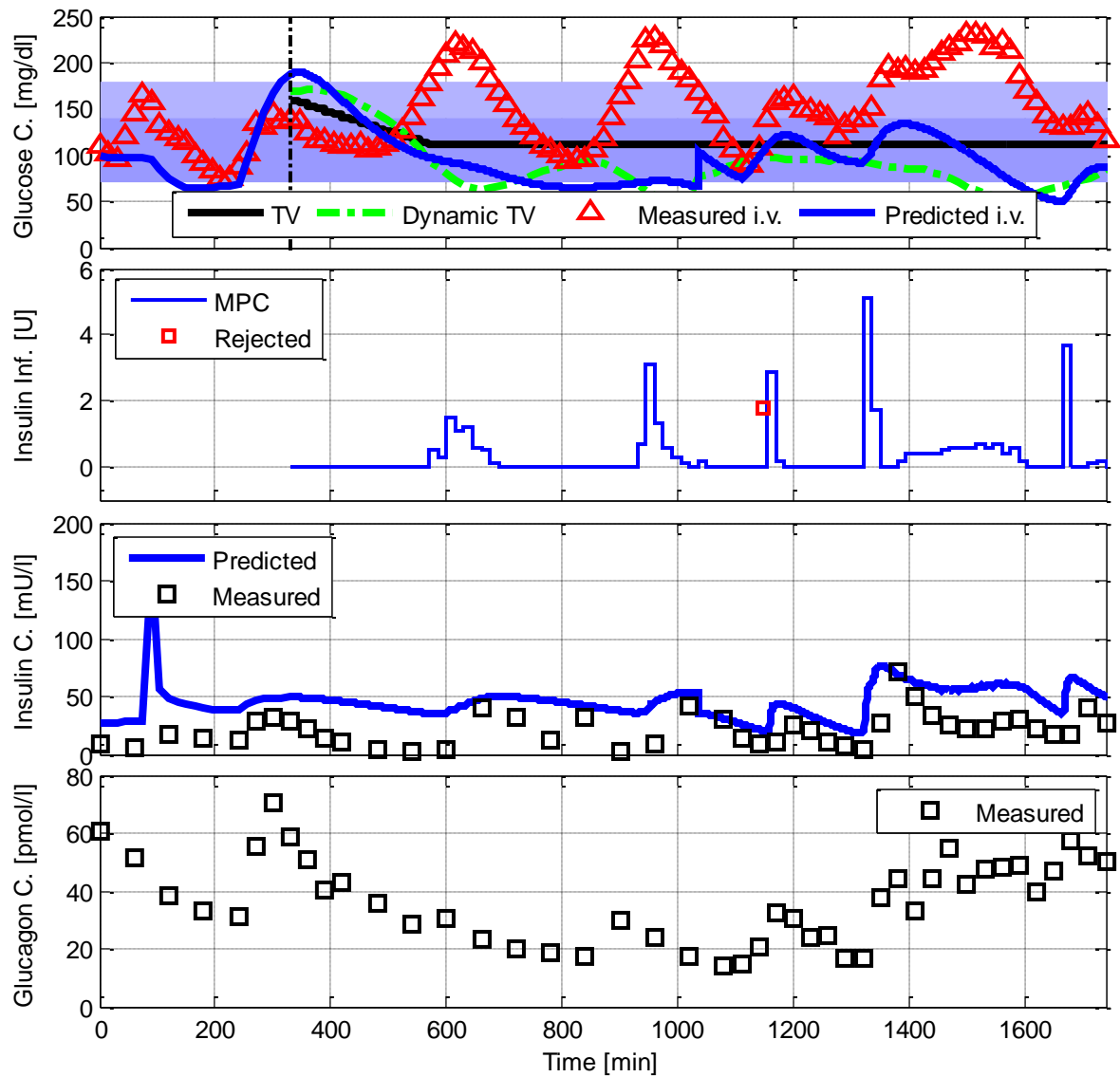


Figure 43: Glucose control in Subject 08. This was the first experiment with a successful model kernel update. Subject arrived at clinic at 12:30 a.m. with hypo and received 48 g CHO (orange juice) and omitted basal insulin before clamp. The following clamp phase was very unpredictable resulting in initial overestimation of insulin half-life time causing strong oscillations during night-time control. Model kernel was updated at 7:15 a.m. ($t = 1035$) with improved estimate of insulin half-life time and subsequent improvement of control. One dose rejection (1.8 U set to zero) after breakfast (9:00 a.m., $t = 1140$ min).

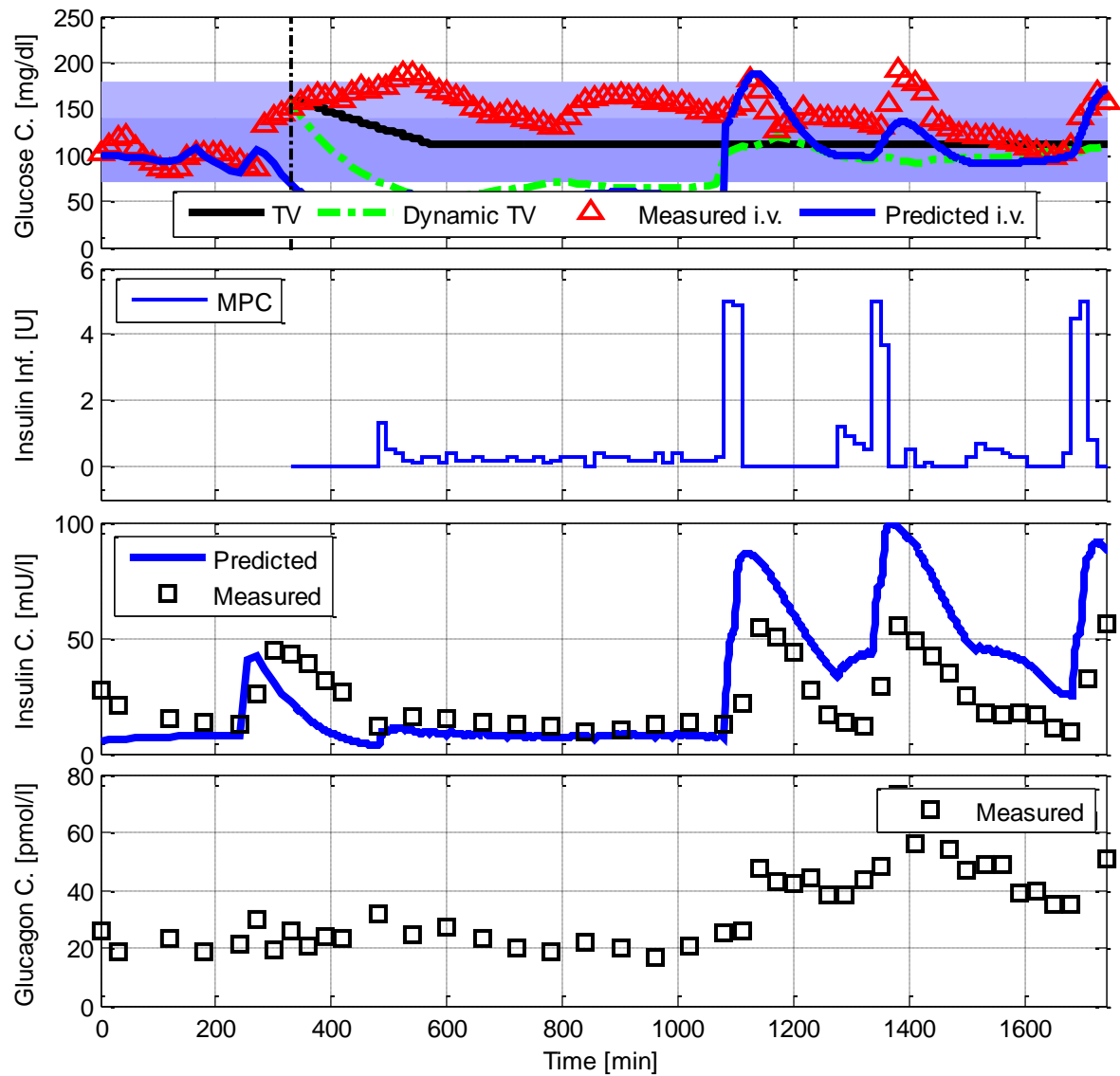


Figure 44: Glucose control in Subject 09. Second experiment with a successful model kernel update. Subject arrived at clinic at 12:30 a.m. with hypo and received 48 g CHO (orange juice) and omitted basal insulin before clamp. All dose recommendations were accepted. Even though basal insulin was suspended 90 min before the trial, initial measured insulin values were extremely high (approx. 4 times higher than predicted). This caused a severe overestimation of insulin sensitivity and a strong divergence of predicted and measured glucose. Model Kernel was updated at 8:00 a.m. ($t = 1080$) and model prediction and consequently control performance was improved significantly.

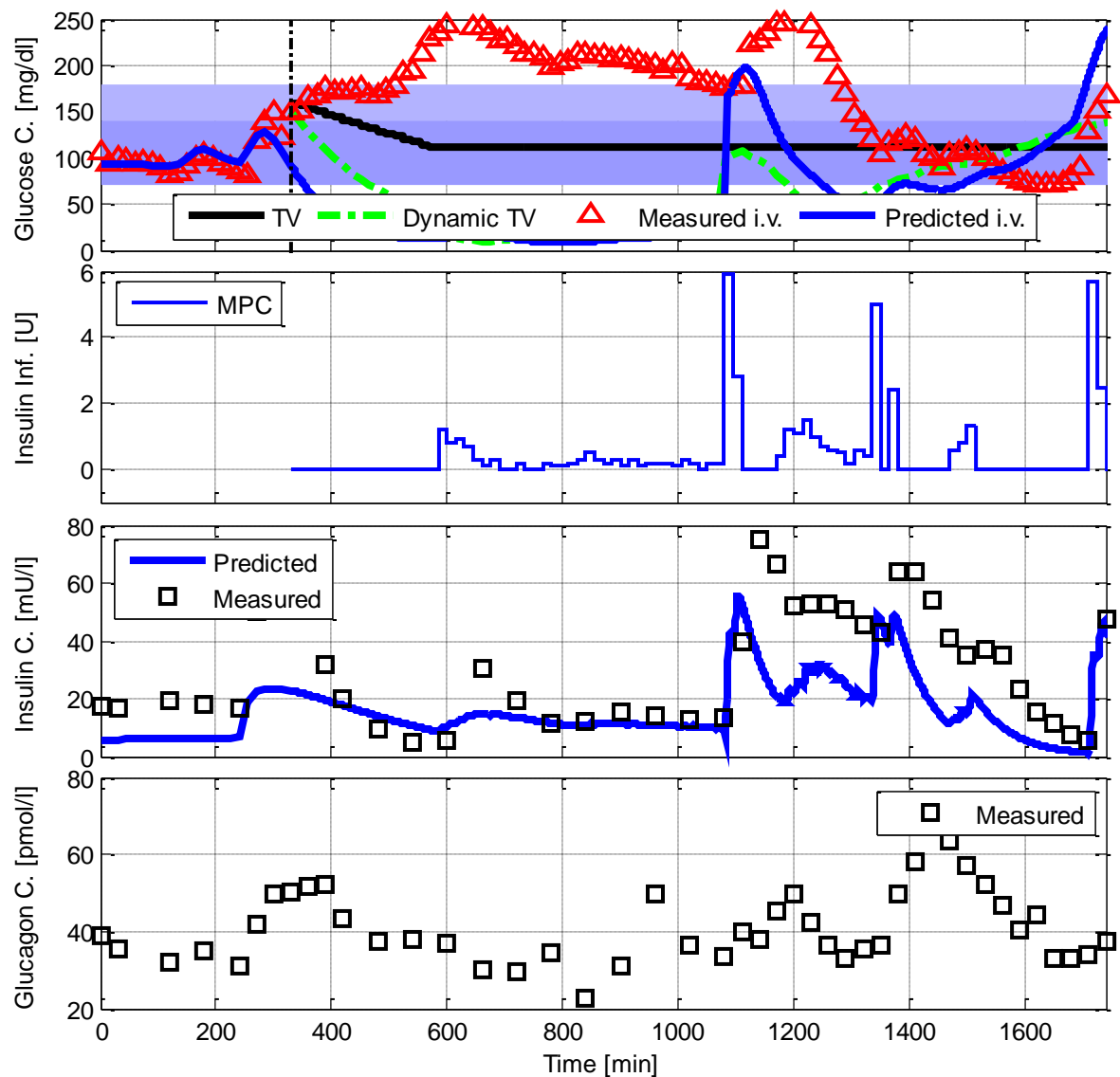


Figure 45: Glucose control in Subject 10. Third experiment with a successful model kernel update. Subject measured low glucose at 11:30 a.m. and stepwise reduced basal insulin to 50%, 30% and 0% before clamp. All dose recommendations were accepted. Even though basal insulin was significantly reduced and in the end suspended 150 min before the trial, initial measured insulin values were extremely high (approx. 4 times higher than predicted). This again caused a severe overestimation of insulin sensitivity and a strong divergence of predicted and measured glucose. Model Kernel was updated at 8:00 a.m. ($t = 1080$) and model prediction and consequently control performance was improved.

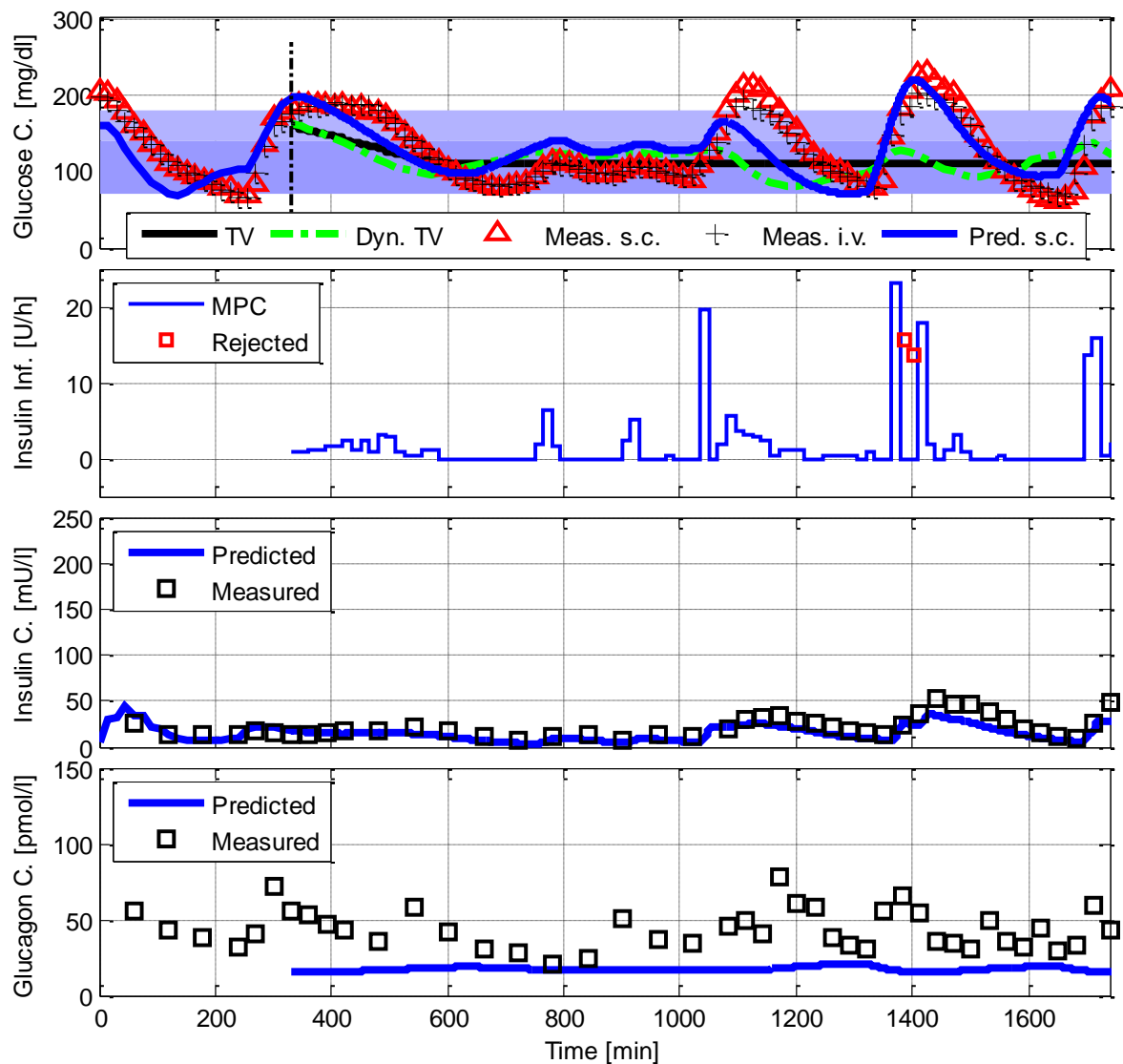
V.5.3.2.2 Trial #2

Figure 46: Glucose control in Subject 01. The subject had 2 and 3.5 BE for breakfast (+ coffee) and second dinner. Overall good model fit (glucose and insulin PK) but glucagon surges were not identified. The controller achieved very good overnight control but the subject showed slight morning insulin resistance (“dawn-effect”) and increased midday insulin sensitivity. No oral glucose interventions were required, but twice at 1 and 1:15 p.m. ($t = 1380/95$ min) insulin suggestions were declined.

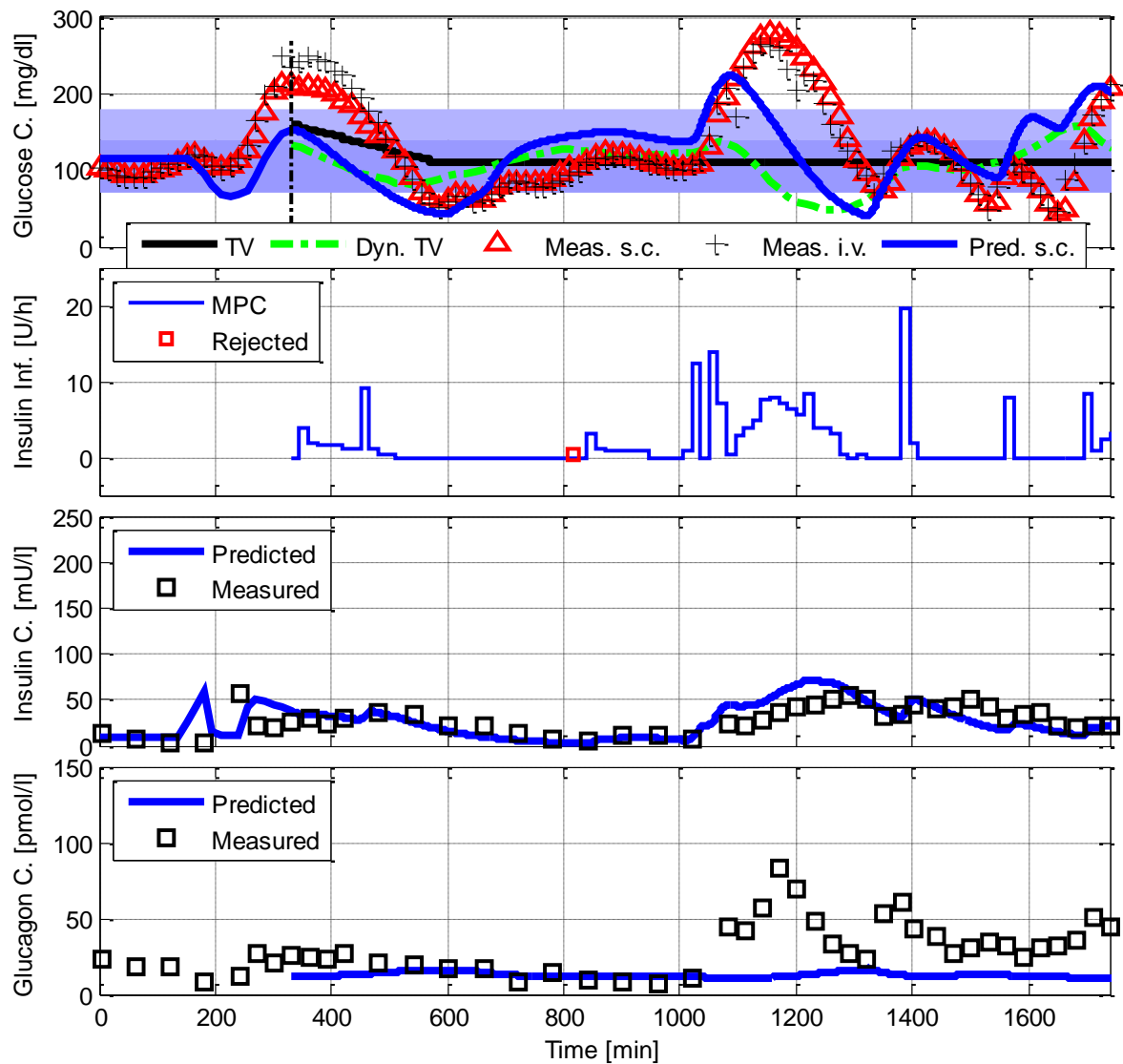


Figure 47: Glucose control in Subject 02. The subject had 5 and 4 BE for breakfast and second dinner. Model fit overestimated insulin absorption and clearance and glucagon surges were not identified. The controller achieved very good overnight control after initial oral glucose intervention at around midnight ($t = 600$ min, 2 BE). The subject showed a strong morning insulin resistance ("dawn-effect") and increased midday insulin sensitivity. Oral glucose interventions were required again after midday (3:30 p.m., $t = 1530$ min). A suggestion (0.1 IU at 3:30 a.m., $t = 910$) was once not given due to a delay.

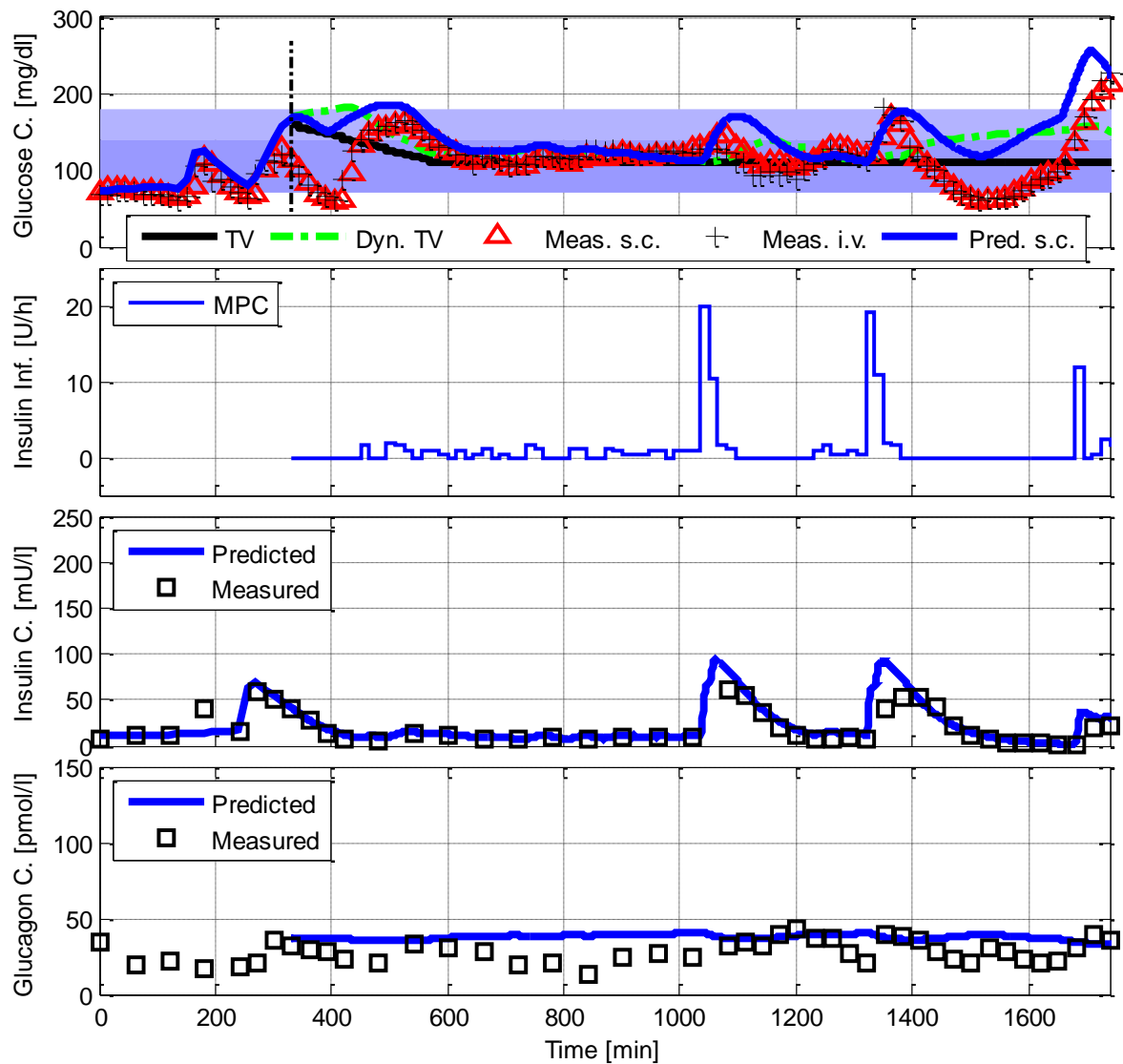


Figure 48: Glucose control in Subject 03. The subject had twice 5 BE for breakfast (no coffee) and second dinner. Except for meal absorption, model fit (insulin and glucose PK) was very good. Subject showed almost no changes in glucagon. The subject went into hypo after self-injection for the first dinner and required oral glucose intervention with zero insulin dose suggestions yet (8:30 p.m., $t = 390$ min). The controller achieved very good overnight control. The subject showed no morning insulin resistance (“dawn-effect”) but a strong increase in midday insulin sensitivity. The subjects showed altered insulin PK for the lunch insulin injections.

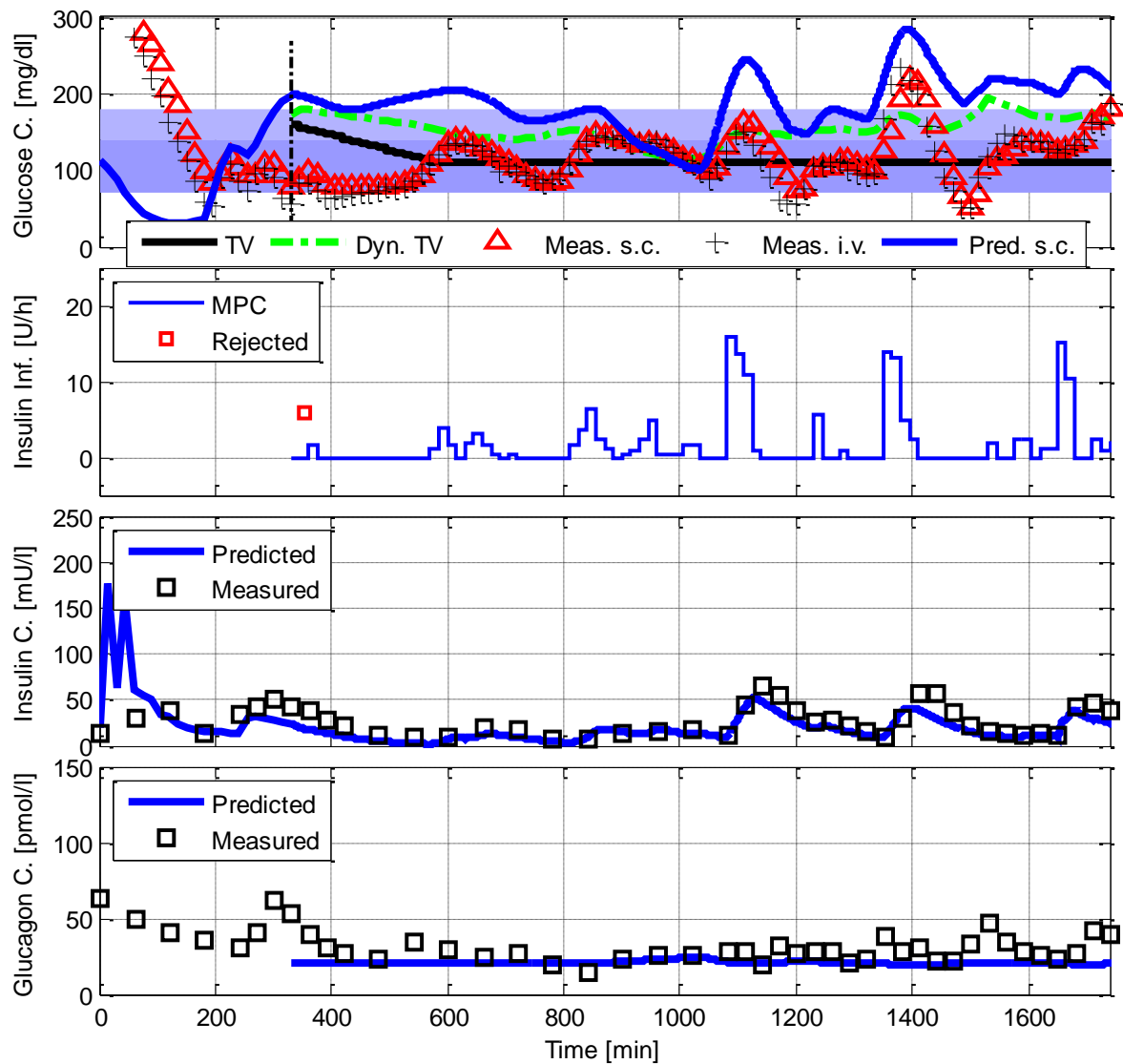


Figure 49: Glucose control in Subject 04. The subject had twice 5 BE for breakfast (no coffee) and second dinner. Initial accuracy of model fit was insufficient due to extreme glucose levels at start of clamp causing the first dose suggestion to be declined (7:30 and 7:45 p.m., $t = 330$ and 345 min, 3.6 and 1.5 IU). Insulin PK model fit was good with a slight underestimation of rate of absorption. Except for the clamp phase, subject showed almost no changes in glucagon. The subject required oral glucose intervention after breakfast and lunch (10 a.m., $t = 1200$ min, 3 BE and 3 p.m., $t = 1500$ min, also 3 BE). The controller achieved satisfactory overnight control. The subject showed no morning insulin resistance ("dawn-effect") but a slight increase in midday insulin sensitivity.

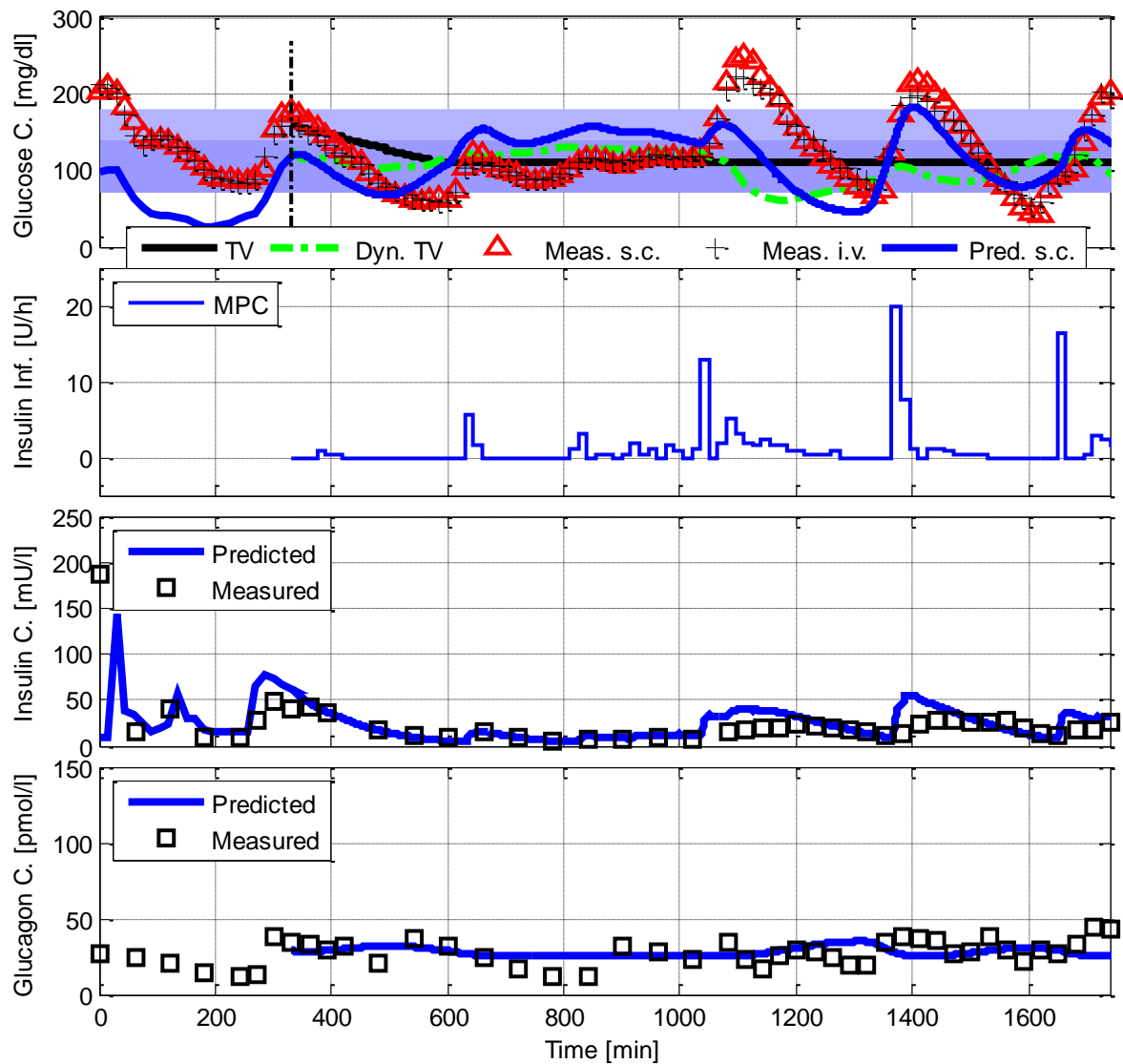


Figure 50: Glucose control in Subject 05. The subject had twice 3 BE for breakfast and second dinner. Insulin absorption and clearance were overestimated. Except for the first dinner, subject showed only marginal changes in glucagon. The subject required a single glucose intervention just before the last dinner (4:45 p.m., $t = 1605$ min, 1 BE). The controller achieved good overnight control. The subject showed both a strong morning insulin resistance ("dawn-effect") and a strong increase in midday insulin sensitivity. No dose suggestions were declined.

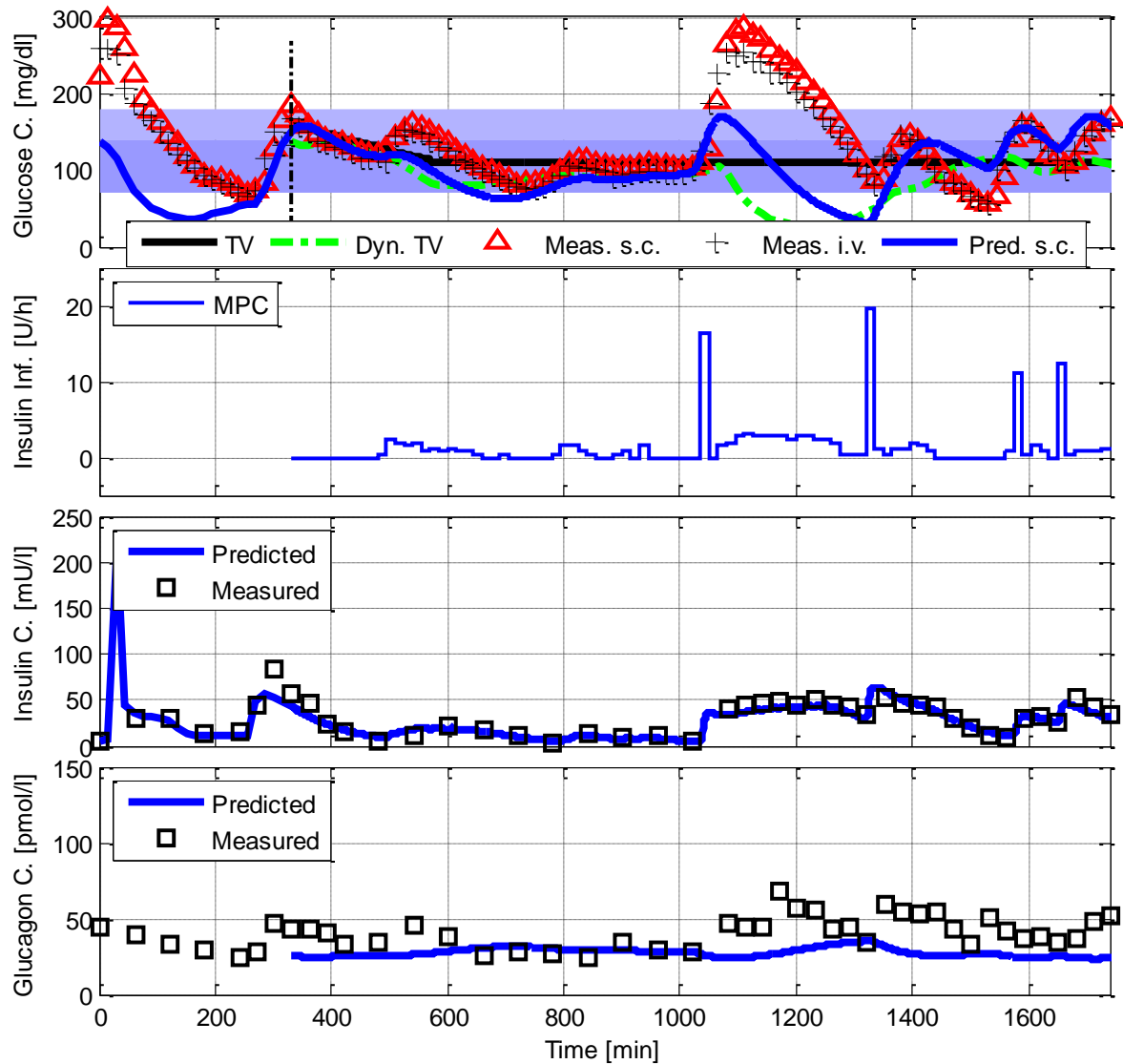


Figure 51: Glucose control in Subject 06. The subject had twice 3 BE for breakfast (+ coffee) and second dinner. Except for a strong morning insulin resistance (“dawn-effect”) and a strong increase in midday insulin sensitivity, model fit (insulin and glucose PK) was very good. Subject showed a slight increase in glucagon levels after breakfast. The subject required a single glucose intervention just before the last dinner (3:30 p.m., $t = 1530$ min, 2 BE). The controller achieved good overnight control. No dose suggestions were declined.

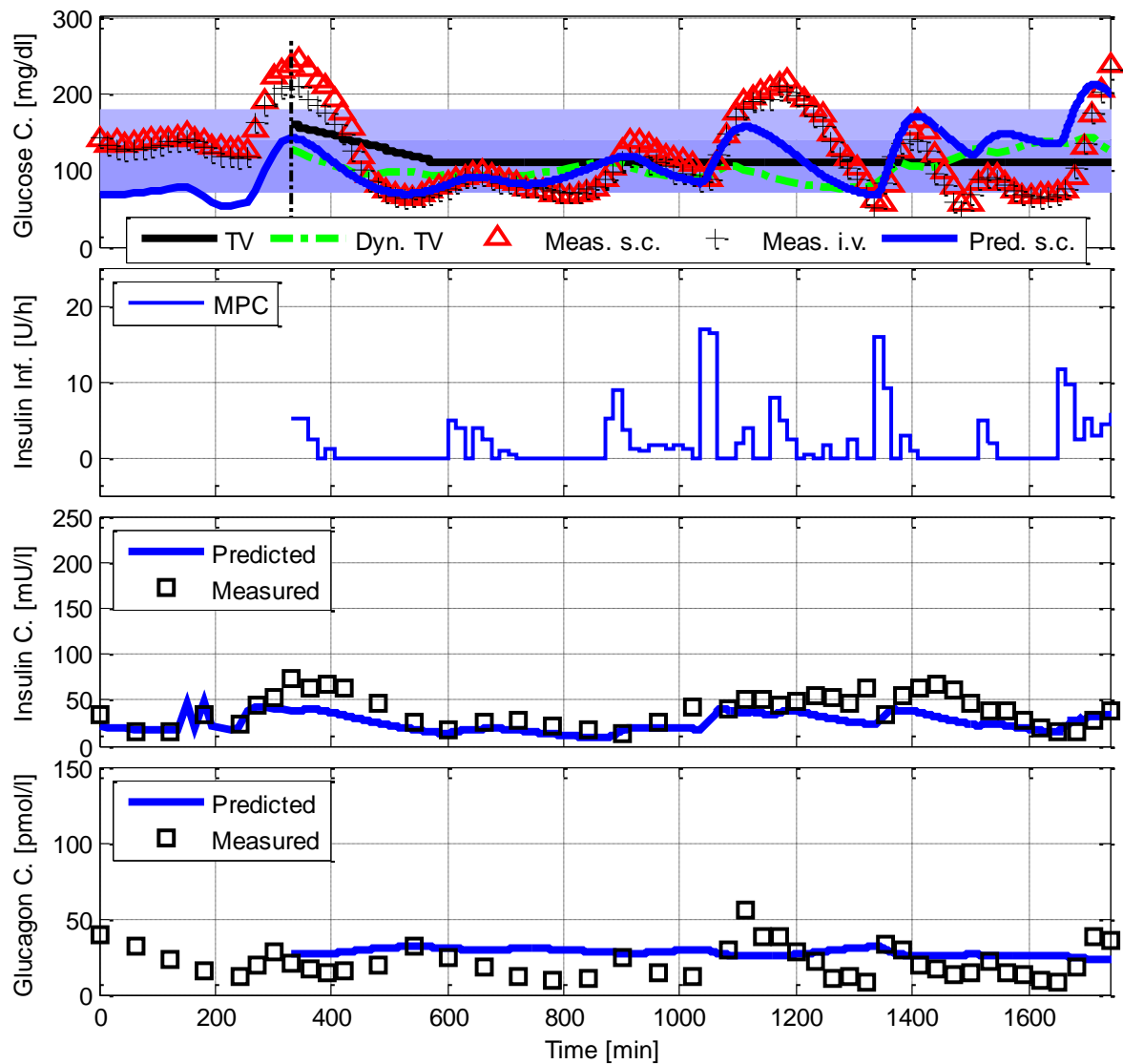


Figure 52: Glucose control in Subject 07. The subject had 5 and 4 BE for breakfast and second dinner. Subject showed strong insulin resistance at enrolment and in the morning (“dawn-effect”) and a strong increase in midday insulin sensitivity, which was not captured by the model. Insulin absorption was underestimated. Subject showed a slight increase in glucagon levels after breakfast. The subject required a single glucose intervention just before the last dinner (3:00 p.m., $t = 1500$ min, 2 BE). The controller achieved good control. No dose suggestions were declined.

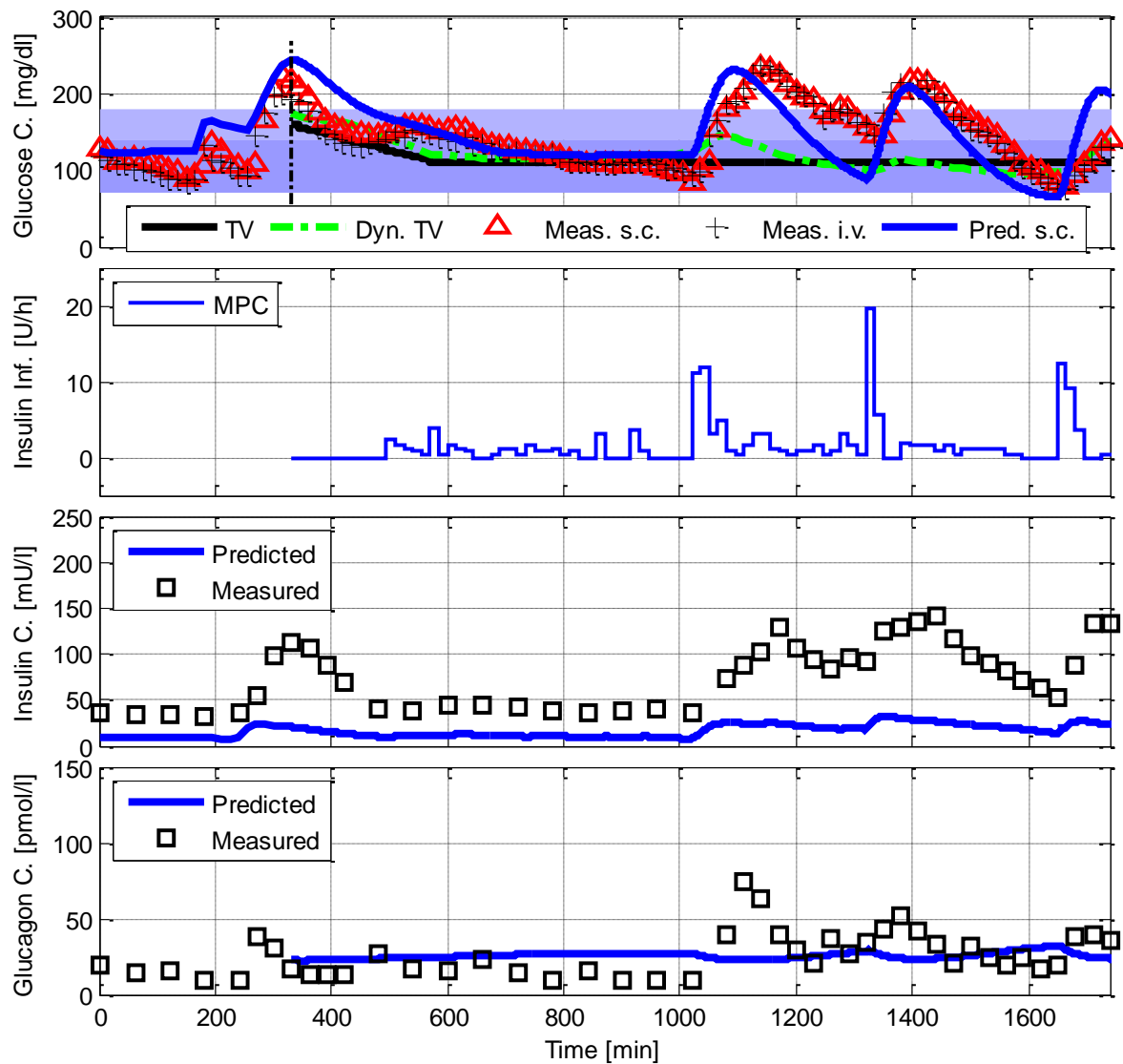


Figure 53: Glucose control in Subject 08. The subject had 5 and 6 BE for breakfast (+ coffee) and second dinner. Subject showed no insulin resistance at enrolment but in the morning (“dawn-effect”) and a marginal increase in midday insulin sensitivity, which was not captured by the model. Insulin absorption was quantitatively underestimated. Subject showed a slight increase in glucagon levels only after breakfast. The subject required no oral glucose intervention. The controller achieved very good overall control. No dose suggestions were declined.

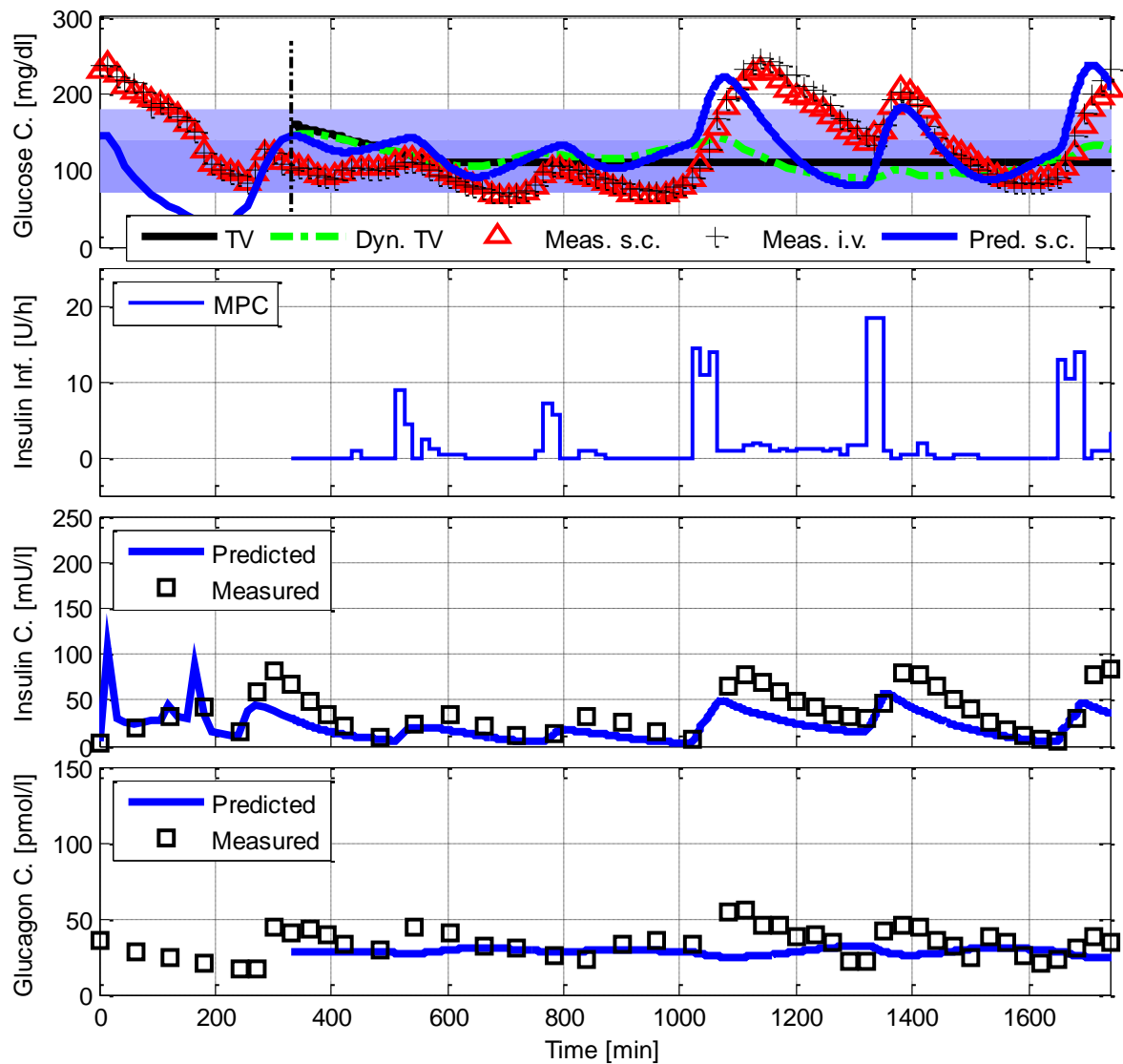


Figure 54: Glucose control in Subject 09. The subject had 5 and 6 BE for breakfast (+ coffee) and second dinner. Subject showed insulin resistance at enrolment and in the morning (“dawn-effect”) and a marginal increase in midday insulin sensitivity, which was not captured by the model. Insulin absorption was slightly underestimated. Subject showed a slight increase in glucagon levels during meals. The subject required no oral glucose intervention. The controller achieved very good overall control. No dose suggestions were declined.

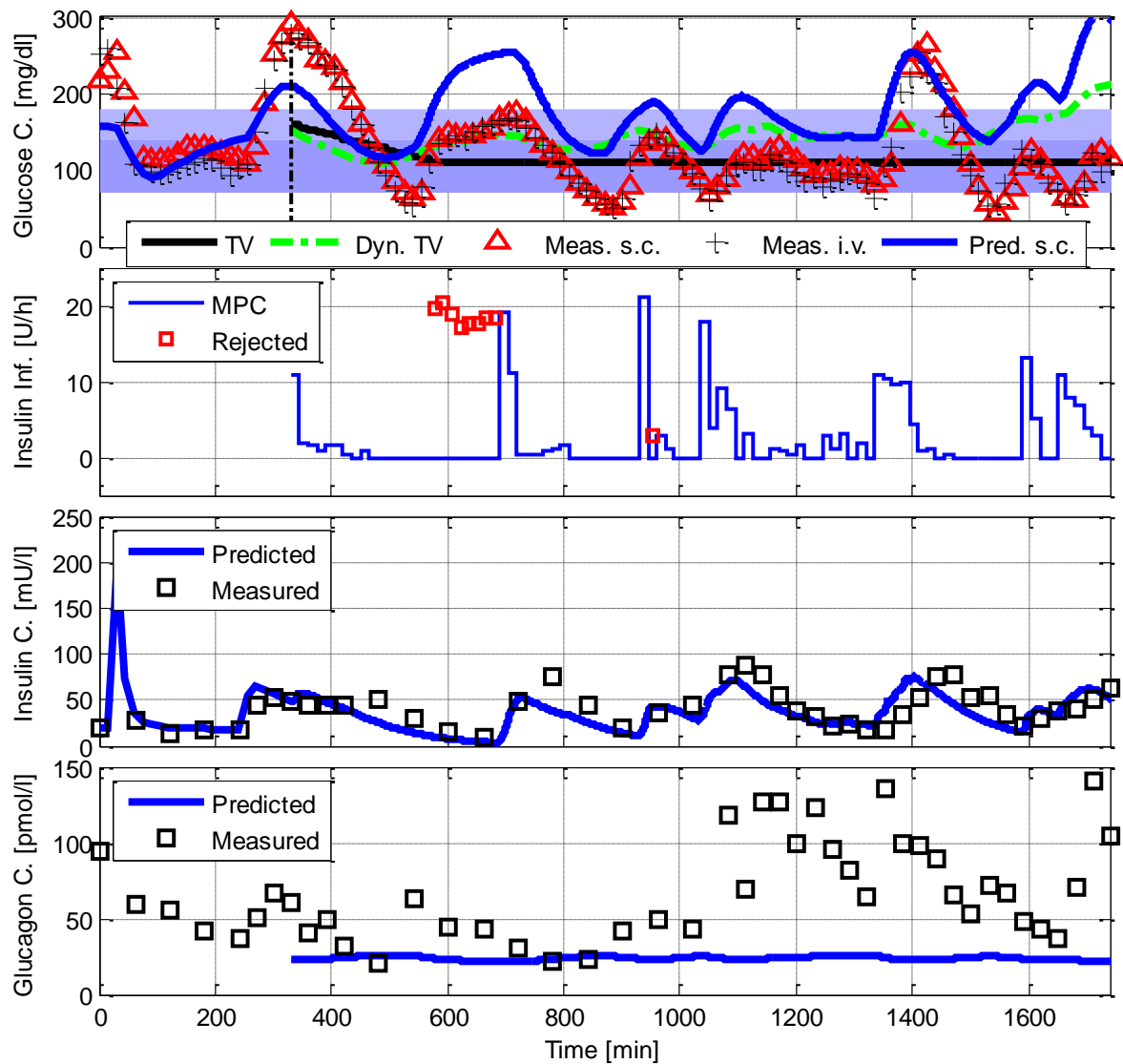


Figure 55: Glucose control in Subject 10. The subject had 5 and 6 BE for breakfast and second dinner. Subject showed insulin resistance at enrolment with a steep increase in glucose levels and concomitant high glucagon levels. Although the model fit for glucose showed a constant offset, there was no IOV in insulin sensitivity. Insulin PK was captured very well but Subject showed an enormous glucagon surges after meals. The subject required oral glucose intervention at night (10:45 p.m., $t = 575$ min, 2 BE). After the first oral intervention the controller continuously suggested insulin doses of approx. 4.5 IU between 11:30 p.m. ($t = 570$ min) and 1:15 a.m. ($t = 675$ min) (8 times) until the suggestion was accepted (4.8 IU) which led to an oral intervention of 2 BE at 4:30 a.m. ($t = 870$ min). Another does was declined at 5:45 a.m. ($t = 945$ min). Again at midday oral intervention of 3 BE 3:45 p.m. ($t = 1545$ min) was required.

V.6 References

1. Bergman RN, Ider YZ, Bowden CR, Cobelli C: **Quantitative estimation of insulin sensitivity.** *Am J Physiol* 1979, **236**:E667-677.
2. Schaller S, Willmann S, Schaupp L, Pieber TR, Schuppert A, Lippert J, Eissing T: **A generic integrated physiologically-based whole-body model of the glucose-insulin-glucagon regulatory system.** *CPT: PSP* 2013.
3. Schaller S, Willmann S, Schaupp L, Pieber TR, Schuppert A, Lippert J, Eissing T: **Robust PBPK/PD based Model Predictive Control of Blood Glucose.** *Submitted to IEEE Transactions on Biomedical Engineering* 2014.
4. Schaller S, Eissing T, Schlender J, Schaupp L, Solodenko J, Lippert J, Schuppert A, Pieber TR: **Blood glucose control in T1DM subjects- prospects for generic whole-body physiology-based PK/PD model kernels: Clinical Trial and Post-Hoc Study.** *In preparation* 2014.
5. International-Diabetes-Federation: **IDF Diabetes Atlas.** 6 edition. Brussels, Belgium: International Diabetes Federation; 2013.
6. Group' WTfDCaTEoDIaCR: **Effect of intensive therapy on the microvascular complications of type 1 diabetes mellitus.** *JAMA* 2002, **287**:2563-2569.
7. White NH, Cleary PA, Dahms W, Goldstein D, Malone J, Tamborlane WV: **Beneficial effects of intensive therapy of diabetes during adolescence: outcomes after the conclusion of the Diabetes Control and Complications Trial (DCCT).** *J Pediatr* 2001, **139**:804-812.
8. Leese GP, Wang J, Broomhall J, Kelly P, Marsden A, Morrison W, Frier BM, Morris AD: **Frequency of severe hypoglycemia requiring emergency treatment in type 1 and type 2 diabetes: a population-based study of health service resource use.** *Diabetes Care* 2003, **26**:1176-1180.
9. Kovatchev B: **Closed loop control for type 1 diabetes.** *BMJ* 2011, **342**:d1911.
10. Ban K, Hui S, Drucker DJ, Husain M: **Cardiovascular consequences of drugs used for the treatment of diabetes: potential promise of incretin-based therapies.** *J Am Soc Hypertens* 2009, **3**:245-259.
11. Charbonnel B, Cariou B: **Pharmacological management of type 2 diabetes: the potential of incretin-based therapies.** *Diabetes Obes Metab* 2011, **13**:99-117.
12. El Youssef J, Castle J, Ward WK: **A Review of Closed-Loop Algorithms for Glycemic Control in the Treatment of Type 1 Diabetes.** *Algorithms* 2009, **2**:518-532.
13. Hovorka R: **Closed-loop insulin delivery: from bench to clinical practice.** *Nat Rev Endocrinol* 2011, **7**:385-395.
14. Cobelli C, Renard E, Kovatchev B: **Artificial Pancreas: Past, Present, Future.** *Diabetes* 2011, **60**:2672-2682.
15. Dassau E, Atlas E, Phillip M: **Closing the loop.** *Int J Clin Pract Suppl* 2010, **65**:20-25.
16. Hovorka R, Kumareswaran K, Harris J, Allen JM, Elleri D, Xing D, Kollman C, Nodale M, Murphy HR, Dunger DB, et al: **Overnight closed loop insulin delivery (artificial pancreas) in adults with type 1 diabetes: crossover randomised controlled studies.** *BMJ* 2011, **342**:d1855.
17. Steil GM, Panteleon AE, Rebrin K: **Closed-loop insulin delivery-the path to physiological glucose control.** *Adv Drug Deliv Rev* 2004, **56**:125-144.
18. Gopakumaran B, Duman HM, Overholser DP, Federiuk IF, Quinn MJ, Wood MD, Ward WK: **A novel insulin delivery algorithm in rats with type 1 diabetes: the fading memory proportional-derivative method.** *Artif Organs* 2005, **29**:599-607.
19. Castle JR, Engle JM, El Youssef J, Massoud RG, Yuen KC, Kagan R, Ward WK: **Novel use of glucagon in a closed-loop system for prevention of hypoglycemia in type 1 diabetes.** *Diabetes Care* 2010, **33**:1282-1287.
20. Atlas E, Nimri R, Miller S, Grunberg EA, Phillip M: **MD-logic artificial pancreas system: a pilot study in adults with type 1 diabetes.** *Diabetes Care* 2010, **33**:1072-1076.
21. Miller S, Nimri R, Atlas E, Grunberg EA, Phillip M: **Automatic learning algorithm for the MD-logic artificial pancreas system.** *Diabetes Technol Ther* 2011, **13**:983-990.
22. Bequette BW: **A critical assessment of algorithms and challenges in the development of a closed-loop artificial pancreas.** *Diabetes Technol Ther* 2005, **7**:28-47.

23. Parker RS, Doyle FJ, 3rd, Peppas NA: **A model-based algorithm for blood glucose control in type I diabetic patients.** *IEEE Trans Biomed Eng* 1999, **46**:148-157.
24. Hovorka R, Canonico V, Chassin LJ, Haueter U, Massi-Benedetti M, Orsini Federici M, Pieber TR, Schaller HC, Schaupp L, Vering T, Wilinska ME: **Nonlinear model predictive control of glucose concentration in subjects with type 1 diabetes.** *Physiol Meas* 2004, **25**:905-920.
25. Magni L, Forgone M, Toffanin C, Dalla Man C, Kovatchev B, De Nicolao G, Cobelli C: **Run-to-Run Tuning of Model Predictive Control for Type 1 Diabetes Subjects: In Silico Trial.** *J Diabetes Sci Technol* 2009, **3**:1091-1098.
26. Russell SJ, El-Khatib FH, Nathan DM, Magyar KL, Jiang J, Damiano ER: **Blood glucose control in type 1 diabetes with a bihormonal bionic endocrine pancreas.** *Diabetes Care* 2012, **35**:2148-2155.
27. Bolie VW: **Coefficients of normal blood glucose regulation.** *J Appl Physiol* 1961, **16**:783-788.
28. Renard E: **Closed-loop insulin delivery: is the Holy Grail near?** *Lancet* 2010, **375**:702-703.
29. Dalla Man C, Rizza RA, Cobelli C: **Meal simulation model of the glucose-insulin system.** *IEEE Trans Biomed Eng* 2007, **54**:1740-1749.
30. Kovatchev BP, Breton M, Man CD, Cobelli C: **In Silico Preclinical Trials: A Proof of Concept in Closed-Loop Control of Type 1 Diabetes.** *J Diabetes Sci Technol* 2009, **3**:44-55.
31. Hovorka R, Chassin LJ, Ellmerer M, Plank J, Wilinska ME: **A simulation model of glucose regulation in the critically ill.** *Physiol Meas* 2008, **29**:959-978.
32. Sorensen JT: **A Physiologic Model of Glucose Metabolism in Man and its Use to Design and Assess Improved Insulin Therapies for Diabetes.** *PhD Thesis.* MIT, Chemical Engineering; 1985.
33. Kovatchev B, Cobelli C, Renard E, Anderson S, Breton M, Patek S, Clarke W, Bruttomesso D, Maran A, Costa S, et al: **Multinational study of subcutaneous model-predictive closed-loop control in type 1 diabetes mellitus: summary of the results.** *J Diabetes Sci Technol* 2010, **4**:1374-1381.
34. Steil GM, Rebrin K, Darwin C, Hariri F, Saad MF: **Feasibility of automating insulin delivery for the treatment of type 1 diabetes.** *Diabetes* 2006, **55**:3344-3350.
35. Clarke WL, Anderson S, Breton M, Patek S, Kashmer L, Kovatchev B: **Closed-loop artificial pancreas using subcutaneous glucose sensing and insulin delivery and a model predictive control algorithm: the Virginia experience.** *J Diabetes Sci Technol* 2009, **3**:1031-1038.
36. El-Khatib FH, Russell SJ, Nathan DM, Sutherlin RG, Damiano ER: **A bihormonal closed-loop artificial pancreas for type 1 diabetes.** *Sci Transl Med* 2010, **2**:27ra27.
37. Bakhtiani PA, Zhao LM, El Youssef J, Castle JR, Ward WK: **A review of artificial pancreas technologies with an emphasis on bi-hormonal therapy.** *Diabetes Obes Metab* 2013, **15**:1065-1070.
38. Russell SJ, El-Khatib FH, Nathan DM, Damiano ER: **Efficacy determinants of subcutaneous microdose glucagon during closed-loop control.** *J Diabetes Sci Technol* 2010, **4**:1288-1304.
39. Cryer PE: **Minireview: Glucagon in the pathogenesis of hypoglycemia and hyperglycemia in diabetes.** *Endocrinology* 2012, **153**:1039-1048.
40. Greenbaum CJ, Prigeon RL, D'Alessio DA: **Impaired beta-cell function, incretin effect, and glucagon suppression in patients with type 1 diabetes who have normal fasting glucose.** *Diabetes* 2002, **51**:951-957.
41. Atiea JA, Luzio S, Owens DR: **The dawn phenomenon and diabetes control in treated NIDDM and IDDM patients.** *Diabetes Res Clin Pract* 1992, **16**:183-190.
42. Porcellati F, Lucidi P, Bolli GB, Fanelli CG: **Thirty years of research on the dawn phenomenon: lessons to optimize blood glucose control in diabetes.** *Diabetes Care* 2013, **36**:3860-3862.
43. Srinivasan R, Kadish AH, Sridhar R: **A mathematical model for the control mechanism of free fatty acid-glucose metabolism in normal humans.** *Comput Biomed Res* 1970, **3**:146-165.
44. Bergman RN: **Minimal model: perspective from 2005.** *Horm Res* 2005, **64 Suppl 3**:8-15.

45. Regittnig W, Trajanoski Z, Leis HJ, Ellmerer M, Wutte A, Sendlhofer G, Schaupp L, Brunner GA, Wach P, Pieber TR: **Plasma and interstitial glucose dynamics after intravenous glucose injection: evaluation of the single-compartment glucose distribution assumption in the minimal models.** *Diabetes* 1999, **48**:1070-1081.
46. Markakis MG, Mitsis GD, Marmarelis VZ: **Computational study of an augmented minimal model for glycaemia control.** *Conf Proc IEEE Eng Med Biol Soc* 2008, **2008**:5445-5448.
47. Panunzi S, Palumbo P, De Gaetano A: **A discrete Single Delay Model for the Intra-Venous Glucose Tolerance Test.** *Theor Biol Med Model* 2007, **4**:35.
48. Silber HE, Jauslin PM, Frey N, Gieschke R, Simonsson US, Karlsson MO: **An integrated model for glucose and insulin regulation in healthy volunteers and type 2 diabetic patients following intravenous glucose provocations.** *J Clin Pharmacol* 2007, **47**:1159-1171.
49. Jauslin PM, Silber HE, Frey N, Gieschke R, Simonsson US, Jorga K, Karlsson MO: **An integrated glucose-insulin model to describe oral glucose tolerance test data in type 2 diabetics.** *J Clin Pharmacol* 2007, **47**:1244-1255.
50. Fabietti PG, Canonico V, Orsini-Federici M, Sarti E, Massi-Benedetti M: **Clinical validation of a new control-oriented model of insulin and glucose dynamics in subjects with type 1 diabetes.** *Diabetes Technol Ther* 2007, **9**:327-338.
51. Sturis J, Polonsky KS, Mosekilde E, Van Cauter E: **Computer model for mechanisms underlying ultradian oscillations of insulin and glucose.** *Am J Physiol* 1991, **260**:E801-809.
52. Li J, Kuang Y, Mason CC: **Modeling the glucose-insulin regulatory system and ultradian insulin secretory oscillations with two explicit time delays.** *J Theor Biol* 2006, **242**:722-735.
53. Tolic IM, Mosekilde E, Sturis J: **Modeling the insulin-glucose feedback system: the significance of pulsatile insulin secretion.** *J Theor Biol* 2000, **207**:361-375.
54. Krudys KM, Dodds MG, Nissen SM, Vicini P: **Integrated model of hepatic and peripheral glucose regulation for estimation of endogenous glucose production during the hot IVGTT.** *Am J Physiol Endocrinol Metab* 2005, **288**:E1038-1046.
55. Derouich M, Boutayeb A: **The effect of physical exercise on the dynamics of glucose and insulin.** *J Biomech* 2002, **35**:911-917.
56. Andersen KE, Hojbjerg M: **A population-based Bayesian approach to the minimal model of glucose and insulin homeostasis.** *Stat Med* 2005, **24**:2381-2400.
57. Finan D, Zisser H, Jovanovic Z, Bevier W, Seborg D: **Identification of Linear Dynamic Models for Type 1 Diabetes: A Simulation Study.** In *IFAC*. Gramado, Brazil: ADCHEM; 2006.
58. Picchini U, Ditlevsen S, De Gaetano A: **Maximum likelihood estimation of a time-inhomogeneous stochastic differential model of glucose dynamics.** *Math Med Biol* 2008, **25**:141-155.
59. Mitsis GD, Marmarelis VZ: **Nonlinear modeling of glucose metabolism: comparison of parametric vs. nonparametric methods.** *Conf Proc IEEE Eng Med Biol Soc* 2007, **2007**:5968-5971.
60. Makroglou A, Li J, Kuang Y: **Mathematical models and software tools for the glucose-insulin regulatory system and diabetes: an overview.** *Applied Numerical Mathematics* 2006, **56**:559-573.
61. Landersdorfer CB, Jusko WJ: **Pharmacokinetic/pharmacodynamic modelling in diabetes mellitus.** *Clin Pharmacokinet* 2008, **47**:417-448.
62. Boutayeb A, Chetouani A: **A critical review of mathematical models and data used in diabetology.** *Biomed Eng Online* 2006, **5**:43.
63. Wilinska ME, Hovorka R: **Simulation models for in silico testing of closed-loop glucose controllers in type 1 diabetes.** *Drug Discovery Today: Disease Models* 2008, **5**:289-298.
64. Doyle FJ, Huyett LM, Lee JB, Zisser HC, Dassau E: **Closed-Loop Artificial Pancreas Systems: Engineering the Algorithms.** *Diabetes Care* 2014, **37**:1191-1197.
65. Bergman RN, Finegood DT, Ader M: **Assessment of insulin sensitivity in vivo.** *Endocr Rev* 1985, **6**:45-86.
66. Bergman RN, Hope ID, Yang YJ, Watanabe RM, Meador MA, Youn JH, Ader M: **Assessment of insulin sensitivity in vivo: a critical review.** *Diabetes Metab Rev* 1989, **5**:411-429.

67. Bergman RN: **Orchestration of glucose homeostasis: from a small acorn to the California oak.** *Diabetes* 2007, **56**:1489-1501.
68. Dalla Man C, Yarasheski KE, Caumo A, Robertson H, Toffolo G, Polonsky KS, Cobelli C: **Insulin sensitivity by oral glucose minimal models: validation against clamp.** *Am J Physiol Endocrinol Metab* 2005, **289**:E954-959.
69. Dalla Man C, Caumo A, Basu R, Rizza R, Toffolo G, Cobelli C: **Minimal model estimation of glucose absorption and insulin sensitivity from oral test: validation with a tracer method.** *Am J Physiol Endocrinol Metab* 2004, **287**:E637-643.
70. Mari A: **Mathematical modeling in glucose metabolism and insulin secretion.** *Curr Opin Clin Nutr Metab Care* 2002, **5**:495-501.
71. Liu W, Hsin C, Tang F: **A molecular mathematical model of glucose mobilization and uptake.** *Math Biosci* 2009, **221**:121-129.
72. Chew YH, Shia YL, Lee CT, Majid FA, Chua LS, Sarmidi MR, Aziz RA: **Modeling of glucose regulation and insulin-signaling pathways.** *Mol Cell Endocrinol* 2009, **303**:13-24.
73. Liu W, Tang F: **Modeling a simplified regulatory system of blood glucose at molecular levels.** *J Theor Biol* 2008, **252**:608-620.
74. Chase JG, Shaw GM, Lotz T, LeCompte A, Wong J, Lin J, Lonergan T, Willacy M, Hann CE: **Model-based insulin and nutrition administration for tight glycaemic control in critical care.** *Curr Drug Deliv* 2007, **4**:283-296.
75. Chase JG, Shaw GM, Wong XW, Lotz T, Lin J, Hann CE: **Model-based glycaemic control in critical care--A review of the state of the possible.** *Biomedical Signal Processing and Control* 2006, **1**:3-21.
76. Hann CE, Chase JG, Lin J, Lotz T, Doran CV, Shaw GM: **Integral-based parameter identification for long-term dynamic verification of a glucose-insulin system model.** *Comput Methods Programs Biomed* 2005, **77**:259-270.
77. Lin J, Razak NN, Pretty CG, Le Compte A, Docherty P, Parente JD, Shaw GM, Hann CE, Geoffrey Chase J: **A physiological Intensive Control Insulin-Nutrition-Glucose (ICING) model validated in critically ill patients.** *Comput Methods Programs Biomed* 2011, **102**:192-205.
78. Lin J, Parente JD, Chase JG, Shaw GM, Blakemore AJ, Lecompte AJ, Pretty C, Razak NN, Lee DS, Hann CE, Wang SH: **Development of a model-based clinical sepsis biomarker for critically ill patients.** *Comput Methods Programs Biomed* 2011, **102**:149-155.
79. Blakemore A, Wang SH, Le Compte A, G MS, Wong XW, Lin J, Lotz T, C EH, Chase JG: **Model-based insulin sensitivity as a sepsis diagnostic in critical care.** *J Diabetes Sci Technol* 2008, **2**:468-477.
80. Man CD, Breton MD, Cobelli C: **Physical activity into the meal glucose-insulin model of type 1 diabetes: in silico studies.** *J Diabetes Sci Technol* 2009, **3**:56-67.
81. Hovorka R, Shojaee-Moradie F, Carroll PV, Chassin LJ, Gowrie IJ, Jackson NC, Tudor RS, Umpleby AM, Jones RH: **Partitioning glucose distribution/transport, disposal, and endogenous production during IVGTT.** *Am J Physiol Endocrinol Metab* 2002, **282**:E992-1007.
82. Hovorka R, Jayatilake H, Rogatsky E, Tomuta V, Hovorka T, Stein DT: **Calculating glucose fluxes during meal tolerance test: a new computational approach.** *Am J Physiol Endocrinol Metab* 2007, **293**:E610-619.
83. Wilinska ME, Bodenlenz M, Chassin LJ, Schaller HC, Schaupp LA, Pieber TR, Hovorka R: **Interstitial glucose kinetics in subjects with type 1 diabetes under physiologic conditions.** *Metabolism* 2004, **53**:1484-1491.
84. Hovorka R, Allen JM, Elleri D, Chassin LJ, Harris J, Xing D, Kollman C, Hovorka T, Larsen AM, Nodale M, et al: **Manual closed-loop insulin delivery in children and adolescents with type 1 diabetes: a phase 2 randomised crossover trial.** *Lancet* 2010.
85. Strougo A, Eissing T, Yassen A, Willmann S, Danhof M, Freijer J: **First dose in children: physiological insights into pharmacokinetic scaling approaches and their implications in paediatric drug development.** *J Pharmacokinet Pharmacodyn* 2012.
86. Hovorka R, Chassin LJ, Wilinska ME, Canonico V, Akwi JA, Federici MO, Massi-Benedetti M, Hutzli I, Zaugg C, Kaufmann H, et al: **Closing the loop: the adicol experience.** *Diabetes Technol Ther* 2004, **6**:307-318.
87. Schaller HC, Schaupp L, Bodenlenz M, Wilinska ME, Chassin LJ, Wach P, Vering T, Hovorka R, Pieber TR: **On-line adaptive algorithm with glucose prediction capacity for**

- subcutaneous closed loop control of glucose: evaluation under fasting conditions in patients with Type 1 diabetes.** *Diabet Med* 2006, **23**:90-93.
88. Blaha J, Kopecky P, Matias M, Hovorka R, Kunstyr J, Kotulak T, Lips M, Rubes D, Stritesky M, Lindner J, et al: **Comparison of three protocols for tight glycemic control in cardiac surgery patients.** *Diabetes Care* 2009, **32**:757-761.
 89. Pachler C, Plank J, Weinhandl H, Chassin LJ, Wilinska ME, Kulnik R, Kaufmann P, Smolle KH, Pilger E, Pieber TR, et al: **Tight glycaemic control by an automated algorithm with time-variant sampling in medical ICU patients.** *Intensive Care Med* 2008, **34**:1224-1230.
 90. Cordingley JJ, Vlasselaers D, Dormand NC, Wouters PJ, Squire SD, Chassin LJ, Wilinska ME, Morgan CJ, Hovorka R, Van den Bergh G: **Intensive insulin therapy: enhanced Model Predictive Control algorithm versus standard care.** *Intensive Care Med* 2009, **35**:123-128.
 91. Lehmann ED, Deutsch T: **A physiological model of glucose-insulin interaction in type 1 diabetes mellitus.** *J Biomed Eng* 1992, **14**:235-242.
 92. Lehmann ED, Hermanyi I, Deutsch T: **Retrospective validation of a physiological model of glucose-insulin interaction in type 1 diabetes mellitus.** *Med Eng Phys* 1994, **16**:193-202.
 93. Lehmann ED, Tarin C, Bondia J, Teufel E, Deutsch T: **Incorporating a generic model of subcutaneous insulin absorption into the AIDA v4 diabetes simulator: 2. preliminary bench testing.** *J Diabetes Sci Technol* 2007, **1**:780-793.
 94. Lehmann ED, Tarin C, Bondia J, Teufel E, Deutsch T: **Incorporating a generic model of subcutaneous insulin absorption into the AIDA v4 diabetes simulator: 1. a prospective collaborative development plan.** *J Diabetes Sci Technol* 2007, **1**:423-435.
 95. Lehmann ED, Tarin C, Bondia J, Teufel E, Deutsch T: **Incorporating a Generic Model of Subcutaneous Insulin Absorption into the AIDA v4 Diabetes Simulator 3. Early Plasma Insulin Determinations.** *J Diabetes Sci Technol* 2009, **3**:190-201.
 96. **AIDA** [<http://www.2aida.net/welcome/>]
 97. Ramprasad Y, Rangaiah GP, Lakshminarayanan S: **Robust PID Controller for Blood Glucose Regulation in Type I Diabetics.** *Industrial & Engineering Chemistry Research* 2004, **43**:8257-8268.
 98. Ruiz-Velázquez E, Femat R, Campos-Delgado DU: **Blood glucose control for type I diabetes mellitus: A robust tracking $H[\infty]$ problem.** *Control Engineering Practice* 2004, **12**:1179-1195.
 99. Campos-Delgado DU, Hernandez-Ordonez M, Femat R, Gordillo-Moscoso A: **Fuzzy-based controller for glucose regulation in type-1 diabetic patients by subcutaneous route.** *IEEE Trans Biomed Eng* 2006, **53**:2201-2210.
 100. Parker RS, III FJD, Ward JH, Peppas NA: **Robust H-infinity glucose control in diabetes using a physiological model.** *AIChE Journal* 2000, **46**:2537-2549.
 101. Hernandez-Ordonez M, Campos-Delgado DU: **An extension to the compartmental model of type 1 diabetic patients to reproduce exercise periods with glycogen depletion and replenishment.** *J Biomech* 2008, **41**:744-752.
 102. Willmann S, Lippert J, al. E: **PK-Sim®: a physiologically based pharmacokinetic 'whole-body' model.** *Biosilico* 2003, **1**:121-124.
 103. Eissing T, Kuepfer L, Becker C, Block M, Coboeken K, Gaub T, Goerlitz L, Jaeger J, Loosen R, Ludewig B, et al: **A computational systems biology software platform for multiscale modeling and simulation: integrating whole-body physiology, disease biology, and molecular reaction networks.** *Front Physiol* 2011, **2**:4.
 104. Bayer-Technology-Services: **SB Model Suite 5.1.4 - users manual.** 2012.
 105. Eissing T, Lippert J, Willmann S: **Pharmacogenomics of Codeine, Morphine, and Morphine-6-Glucuronide: Model-Based Analysis of the Influence of CYP2D6 Activity, UGT2B7 Activity, Renal Impairment, and CYP3A4 Inhibition.** *Mol Diagn Ther* 2012, **16**:43-53.
 106. Boron WF, Boulpaep EL: *Medical Physiology*. 2nd edn: Saunders; 2008.
 107. Rippe B, Haraldsson B: **Transport of macromolecules across microvascular walls: the two-pore theory.** *Physiol Rev* 1994, **74**:163-219.
 108. Thelen K, Coboeken K, Willmann S, Burghaus R, Dressman JB, Lippert J: **Evolution of a detailed physiological model to simulate the gastrointestinal transit and**

- absorption process in humans, part 1: oral solutions.** *J Pharm Sci* 2011, **100**:5324-5345.
109. Mosekilde E, Jensen KS, Binder C, Pramming S, Thorsteinsson B: **Modeling absorption kinetics of subcutaneous injected soluble insulin.** *J Pharmacokinet Biopharm* 1989, **17**:67-87.
 110. Tarin C, Teufel E, Pico J, Bondia J, Pfeleiderer HJ: **Comprehensive pharmacokinetic model of insulin Glargine and other insulin formulations.** *IEEE Trans Biomed Eng* 2005, **52**:1994-2005.
 111. Bodenlenz M, Schaupp LA, Druml T, Sommer R, Wutte A, Schaller HC, Sinner F, Wach P, Pieber TR: **Measurement of interstitial insulin in human adipose and muscle tissue under moderate hyperinsulinemia by means of direct interstitial access.** *Am J Physiol Endocrinol Metab* 2005, **289**:E296-300.
 112. Barrett EJ, Wang H, Upchurch CT, Liu Z: **Insulin regulates its own delivery to skeletal muscle by feed-forward actions on the vasculature.** *Am J Physiol Endocrinol Metab* 2011, **301**:E252-263.
 113. Dalla Man C, Rizza RA, Cobelli C: **Mixed meal simulation model of glucose-insulin system.** *Conf Proc IEEE Eng Med Biol Soc* 2006, **1**:307-310.
 114. Quon MJ, Campfield LA: **A mathematical model and computer simulation study of insulin receptor regulation.** *J Theor Biol* 1991, **150**:59-72.
 115. Koschorreck M, Gilles ED: **Mathematical modeling and analysis of insulin clearance in vivo.** *BMC Syst Biol* 2008, **2**:43.
 116. Steinert A: **Entwicklung und Analyse eines Insulinrezeptor-Modells zur Untersuchung der Entstehungsursachen von Insulinresistenz.** *MSc Thesis.* OVGU, Process Control; 2011.
 117. Huber CT, Solomon SS, Duckworth WC: **Time-course of insulin degradation in perfused isolated rat adipose cells.** *J Clin Invest* 1980, **65**:461-468.
 118. Duckworth WC, Bennett RG, Hamel FG: **Insulin degradation: progress and potential.** *Endocr Rev* 1998, **19**:608-624.
 119. Sedaghat AR, Sherman A, Quon MJ: **A mathematical model of metabolic insulin signaling pathways.** *Am J Physiol Endocrinol Metab* 2002, **283**:E1084-1101.
 120. Thelen K, Coboeken K, Willmann S, Dressman JB, Lippert J: **Evolution of a detailed physiological model to simulate the gastrointestinal transit and absorption process in humans, part II: Extension to describe performance of solid dosage forms.** *J Pharm Sci* 2012, **101**:1267-1280.
 121. Dressman JB, Thelen K, Willmann S: **An update on computational oral absorption simulation.** *Expert Opinion on Drug Metabolism & Toxicology* 2011, **7**:1345-1364.
 122. Zhao FQ, Keating AF: **Functional properties and genomics of glucose transporters.** *Curr Genomics* 2007, **8**:113-128.
 123. Silverman M: **Structure and function of hexose transporters.** *Annu Rev Biochem* 1991, **60**:757-794.
 124. Shepherd PR, Kahn BB: **Glucose transporters and insulin action--implications for insulin resistance and diabetes mellitus.** *N Engl J Med* 1999, **341**:248-257.
 125. Wright EM: **The intestinal Na⁺/glucose cotransporter.** *Annu Rev Physiol* 1993, **55**:575-589.
 126. Galgani J, Aguirre C, Diaz E: **Acute effect of meal glycemic index and glycemic load on blood glucose and insulin responses in humans.** *Nutr J* 2006, **5**:22.
 127. Liebermeister W, Klipp E: **Bringing metabolic networks to life: convenience rate law and thermodynamic constraints.** *Theor Biol Med Model* 2006, **3**:41.
 128. Zierler K: **Whole body glucose metabolism.** *Am J Physiol* 1999, **276**:E409-426.
 129. Meyer M, Schneekener S, Ludewig B, Kuepfer L, Lippert J: **Using expression data for quantification of active processes in physiologically based pharmacokinetic modeling.** *Drug Metab Dispos* 2012, **40**:892-901.
 130. Klausen B, Toubro S, Astrup A: **Age and sex effects on energy expenditure.** *Am J Clin Nutr* 1997, **65**:895-907.
 131. Wood IS, Trayhurn P: **Glucose transporters (GLUT and SGLT): expanded families of sugar transport proteins.** *Br J Nutr* 2003, **89**:3-9.
 132. Holman GD, Cushman SW: **Subcellular trafficking of GLUT4 in insulin target cells.** *Seminars in Cell & Developmental Biology* 1996, **7**:259-268.

133. Bolli GB, Di Marchi RD, Park GD, Pramming S, Koivisto VA: **Insulin analogues and their potential in the management of diabetes mellitus.** *Diabetologia* 1999, **42**:1151-1167.
134. Drachev VP, Thoreson MD, Khaliullin EN, Davisson VJ, Shalaev VM: **Surface-Enhanced Raman Difference between Human Insulin and Insulin Lispro Detected with Adaptive Nanostructures.** *The Journal of Physical Chemistry B* 2004, **108**:18046-18052.
135. Tanaka M, Itoh H: **Management of Diabetes Mellitus with Insulin Lispro.** *Clinical Medicine Insights: Therapeutics* 2011, **3**:275.
136. Wong J, Chase JG, Hann CE, Shaw GM, Lotz TF, Lin J, Le Compte AJ: **A subcutaneous insulin pharmacokinetic model for computer simulation in a diabetes decision support role: model structure and parameter identification.** *J Diabetes Sci Technol* 2008, **2**:658-671.
137. Baxter LT, Zhu H, Mackensen DG, Jain RK: **Physiologically based pharmacokinetic model for specific and nonspecific monoclonal antibodies and fragments in normal tissues and human tumor xenografts in nude mice.** *Cancer Res* 1994, **54**:1517-1528.
138. Abbott NJ, Romero IA: **Transporting therapeutics across the blood-brain barrier.** *Mol Med Today* 1996, **2**:106-113.
139. King GL, Johnson SM: **Receptor-mediated transport of insulin across endothelial cells.** *Science* 1985, **227**:1583-1586.
140. Soda R, Tavassoli M: **Insulin uptake by rat liver endothelium studied in fractionated liver cell suspensions.** *Mol Cell Biochem* 1985, **65**:117-123.
141. Graf CJ, Woodworth JR, Seger ME, Holcombe JH, Bowsher RR, Lynch R: **Pharmacokinetic and glucodynamic comparisons of recombinant and animal-source glucagon after IV, IM, and SC injection in healthy volunteers.** *J Pharm Sci* 1999, **88**:991-995.
142. Trebbien R, Klarskov L, Olesen M, Holst JJ, Carr RD, Deacon CF: **Neutral endopeptidase 24.11 is important for the degradation of both endogenous and exogenous glucagon in anesthetized pigs.** *Am J Physiol Endocrinol Metab* 2004, **287**:E431-438.
143. Hupe-Sodmann K, McGregor GP, Bridenbaugh R, Goke R, Goke B, Thole H, Zimmermann B, Voigt K: **Characterisation of the processing by human neutral endopeptidase 24.11 of GLP-1(7-36) amide and comparison of the substrate specificity of the enzyme for other glucagon-like peptides.** *Regul Pept* 1995, **58**:149-156.
144. Pospisilik JA, Hinke SA, Pederson RA, Hoffmann T, Rosche F, Schlenzig D, Glund K, Heiser U, McIntosh CH, Demuth H: **Metabolism of glucagon by dipeptidyl peptidase IV (CD26).** *Regul Pept* 2001, **96**:133-141.
145. Hinke SA, Pospisilik JA, Demuth HU, Mannhart S, Kuhn-Wache K, Hoffmann T, Nishimura E, Pederson RA, McIntosh CH: **Dipeptidyl peptidase IV (DPIV/CD26) degradation of glucagon. Characterization of glucagon degradation products and DPIV-resistant analogs.** *J Biol Chem* 2000, **275**:3827-3834.
146. Deacon CF, Kelstrup M, Trebbien R, Klarskov L, Olesen M, Holst JJ: **Differential regional metabolism of glucagon in anesthetized pigs.** *Am J Physiol Endocrinol Metab* 2003, **285**:E552-560.
147. Klipp E: *Systems biology in practice: concepts, implementation and application.* Wiley-VCH; 2005.
148. Steil GM, Clark B, Kanderian S, Rebrin K: **Modeling insulin action for development of a closed-loop artificial pancreas.** *Diabetes Technol Ther* 2005, **7**:94-108.
149. Magni L, Raimondo DM, Bossi L, Man CD, De Nicolao G, Kovatchev B, Cobelli C: **Model predictive control of type 1 diabetes: an in silico trial.** *J Diabetes Sci Technol* 2007, **1**:804-812.
150. Cherrington AD: **The role of hepatic insulin receptors in the regulation of glucose production.** *J Clin Invest* 2005, **115**:1136-1139.
151. Brown RJ, Sinaii N, Rother KI: **Too much glucagon, too little insulin: time course of pancreatic islet dysfunction in new-onset type 1 diabetes.** *Diabetes Care* 2008, **31**:1403-1404.
152. Landahl HD, Grodsky GM: **Comparison of models of insulin release.** *Bull Math Biol* 1982, **44**:399-409.
153. Boge A, Sauerwein H, Meyer HH: **IGF-I and insulin receptors in bovine skeletal muscle: comparisons of different developmental ages, two different genotypes and various individual muscles.** *Exp Clin Endocrinol Diabetes* 1995, **103**:99-104.

154. Kozka IJ, Clark AE, Reckless JP, Cushman SW, Gould GW, Holman GD: **The effects of insulin on the level and activity of the GLUT4 present in human adipose cells.** *Diabetologia* 1995, **38**:661-666.
155. Huang S, Czech MP: **The GLUT4 glucose transporter.** *Cell Metab* 2007, **5**:237-252.
156. Muller WA, Faloona GR, Aguilar-Parada E, Unger RH: **Abnormal alpha-cell function in diabetes. Response to carbohydrate and protein ingestion.** *N Engl J Med* 1970, **283**:109-115.
157. Heptulla RA, Rodriguez LM, Bomgaars L, Haymond MW: **The role of amylin and glucagon in the dampening of glycemic excursions in children with type 1 diabetes.** *Diabetes* 2005, **54**:1100-1107.
158. Kumar S, O'Rahilly S: *Insulin Resistance*. 1 edn: John Wiley & Sons; 2005.
159. Andrews RC, Walker BR: **Glucocorticoids and insulin resistance: old hormones, new targets.** *Clin Sci (Lond)* 1999, **96**:513-523.
160. Magni L, Raimondo DM, Dalla Man C, De Nicolao G, Kovatchev B, Cobelli C: **Model predictive control of glucose concentration in type I diabetic patients: An in silico trial.** *Biomedical Signal Processing and Control* 2009, **4**:338-346.
161. Di Guglielmo GM, Drake PG, Baass PC, Authier F, Posner BI, Bergeron JJ: **Insulin receptor internalization and signalling.** *Mol Cell Biochem* 1998, **182**:59-63.
162. Bottaro DP, Bonner-Weir S, King GL: **Insulin receptor recycling in vascular endothelial cells. Regulation by insulin and phorbol ester.** *J Biol Chem* 1989, **264**:5916-5923.
163. Gorden P, Arakaki R, Collier E, Carpentier JL: **Biosynthesis and regulation of the insulin receptor.** *Yale J Biol Med* 1989, **62**:521-531.
164. Guerci B, Sauvanet JP: **Subcutaneous insulin: pharmacokinetic variability and glycemic variability.** *Diabetes Metab* 2005, **31**:4S7-4S24.
165. Heinemann L: **Variability of insulin absorption and insulin action.** *Diabetes Technol Ther* 2002, **4**:673-682.
166. Cedersund G, Stralfors P: **Putting the pieces together in diabetes research: towards a hierarchical model of whole-body glucose homeostasis.** *Eur J Pharm Sci* 2009, **36**:91-104.
167. Teixeira RE, Malin S: **The next generation of artificial pancreas control algorithms.** *J Diabetes Sci Technol* 2008, **2**:105-112.
168. Hovorka R: **Continuous glucose monitoring and closed-loop systems.** *Diabet Med* 2006, **23**:1-12.
169. Cryer PE: **Hypoglycaemia: the limiting factor in the glycaemic management of Type I and Type II diabetes.** *Diabetologia* 2002, **45**:937-948.
170. Steil GM, Deiss D, Shih J, Buckingham B, Weinzimer S, Agus MS: **Intensive Care Unit Insulin Delivery Algorithms: Why So Many? How to Choose?** *J Diabetes Sci Technol* 2009, **3**:125-140.
171. Ziegler JG, Nichols NB: **Optimum Settings for Automatic Controllers.** *Journal of Dynamic Systems, Measurement, and Control* 1993, **115**:220-222.
172. Dorf RC, Bishop RH (Eds.): **Modern Control Systems**, 12 edition: Prentice Hall; 2011.
173. Franklin GF, Powell JD, Emami-Naeini A (Eds.): **Feedback control of dynamic systems**, 4 edition: Prentice Hall; 2002.
174. Umpierrez GE, Smiley D, Zisman A, Prieto LM, Palacio A, Ceron M, Puig A, Mejia R: **Randomized study of basal-bolus insulin therapy in the inpatient management of patients with type 2 diabetes (RABBIT 2 trial).** *Diabetes Care* 2007, **30**:2181-2186.
175. Chase JG, Shaw G, Le Compte A, Lonergan T, Willacy M, Wong XW, Lin J, Lotz T, Lee D, Hann C: **Implementation and evaluation of the SPRINT protocol for tight glycaemic control in critically ill patients: a clinical practice change.** *Crit Care* 2008, **12**:R49.
176. Mader JK, Neubauer KM, Schaupp L, Augustin T, Beck P, Spat S, Holl B, Treiber GM, Fruhwald FM, Pieber TR, Plank J: **Efficacy, usability and sequence of operations of a workflow-integrated algorithm for basal-bolus insulin therapy in hospitalized type 2 diabetes patients.** *Diabetes Obes Metab* 2013.
177. Steil GM, Rebrin K, Janowski R, Darwin C, Saad MF: **Modeling beta-cell insulin secretion-implications for closed-loop glucose homeostasis.** *Diabetes Technol Ther* 2003, **5**:953-964.

178. Marchetti G, Barolo M, Jovanovic L, Zisser H, Seborg DE: **A Feedforward-Feedback Glucose Control Strategy for Type 1 Diabetes Mellitus.** *J Process Control* 2008, **18**:149-162.
179. Driankov D, Hellendoorn H, Reinfrank M: *An introduction to fuzzy control.* Springer; 1996.
180. Kandel A, Langholz G: *Fuzzy control systems.* CRC Press; 1994.
181. Phillip M, Battelino T, Atlas E, Kordonouri O, Bratina N, Miller S, Biester T, Avbelj Stefanija M, Muller I, Nimri R, Danne T: **Nocturnal Glucose Control with an Artificial Pancreas at a Diabetes Camp.** *New England Journal of Medicine* 2013, **368**:824-833.
182. Ibbini MS, Masadeh MA: **A fuzzy logic based closed-loop control system for blood glucose level regulation in diabetics.** *J Med Eng Technol* 2005, **29**:64-69.
183. Dazzi D, Taddei F, Gavarini A, Uggeri E, Negro R, Pezzarossa A: **The control of blood glucose in the critical diabetic patient: a neuro-fuzzy method.** *J Diabetes Complications* 2001, **15**:80-87.
184. Doyle JC, Glover K, Khargonekar PP, Francis BA: **State-space solutions to standard H2 and H ∞ control problems.** *IEEE Transactions on Automatic Control* 1989, **34**:831-847.
185. Skogestad S, Postlethwaite I: *Multivariable feedback control: analysis and design.* Wiley; 1996.
186. Kovács L, Szalay P, Benyó B, Chase JG: **Robust Tight Glycaemic Control of ICU patients.** *Proceedings IFAC 2011, 18th World Congress.*
187. Rawlings JB, Mayne DQ: *Model Predictive Control Theory and Design.* Nob Hill Pub.; 2009.
188. Mayne DQ, Rawlings JB, Rao CV, Scokaert POM: **Constrained model predictive control: Stability and optimality.** *Automatica* 2000, **36**:789-814.
189. Elleri D, Allen JM, Nodale M, Wilinska ME, Mangat JS, Larsen AM, Acerini CL, Dunger DB, Hovorka R: **Automated overnight closed-loop glucose control in young children with type 1 diabetes.** *Diabetes Technol Ther* 2011, **13**:419-424.
190. Soru P, De Nicolao G, Toffanin C, Dalla Man C, Cobelli C, Magni L: **MPC based Artificial Pancreas: Strategies for individualization and meal compensation.** *Annual Reviews in Control* 2012, **36**:118-128.
191. Heinemann L, Benesch C, DeVries JH: **AP@home: a novel European approach to bring the artificial pancreas home.** *J Diabetes Sci Technol* 2011, **5**:1363-1372.
192. Del Favero S, Bruttomesso D, Di Palma F, Lanzola G, Visentin R, Filippi A, Scotton R, Toffanin C, Messori M, Scarpellini S, et al: **First use of model predictive control in outpatient wearable artificial pancreas.** *Diabetes Care* 2014, **37**:1212-1215.
193. Leelarathna L, Dellweg S, Mader JK, Allen JM, Benesch C, Doll W, Ellmerer M, Hartnell S, Heinemann L, Kojzar H, et al: **Day and night home closed-loop insulin delivery in adults with type 1 diabetes: three-center randomized crossover study.** *Diabetes Care* 2014, **37**:1931-1937.
194. Chassin LJ, Wilinska ME, Hovorka R: **Intense exercise in type 1 diabetes: exploring the role of continuous glucose monitoring.** *J Diabetes Sci Technol* 2007, **1**:570-573.
195. Breton MD: **Physical activity-the major unaccounted impediment to closed loop control.** *J Diabetes Sci Technol* 2008, **2**:169-174.
196. Kovatchev BP: **Diabetes technology: markers, monitoring, assessment, and control of blood glucose fluctuations in diabetes.** *Scientifica (Cairo)* 2012, **2012**:283821.
197. Hovorka R, Kremen J, Blaha J, Matias M, Anderlova K, Bosanska L, Roubicek T, Wilinska ME, Chassin LJ, Svacina S, Haluzik M: **Blood glucose control by a model predictive control algorithm with variable sampling rate versus a routine glucose management protocol in cardiac surgery patients: a randomized controlled trial.** *J Clin Endocrinol Metab* 2007, **92**:2960-2964.
198. Facchinetti A, Sparacino G, Cobelli C: **Reconstruction of glucose in plasma from interstitial fluid continuous glucose monitoring data: role of sensor calibration.** *J Diabetes Sci Technol* 2007, **1**:617-623.
199. Magni L, Raimondo DM, Man CD, Breton M, Patek S, Nicolao GD, Cobelli C, Kovatchev BP: **Evaluating the efficacy of closed-loop glucose regulation via control-variability grid analysis.** *J Diabetes Sci Technol* 2008, **2**:630-635.
200. Damiano ER, McKeon K, El-Khatib FH, Zheng H, Nathan DM, Russell SJ: **A Comparative Effectiveness Analysis of Three Continuous Glucose Monitors: The Navigator, G4 Platinum, and Enlite.** *J Diabetes Sci Technol* 2014.

201. Moisey LL, Kacker S, Bickerton AC, Robinson LE, Graham TE: **Caffeinated coffee consumption impairs blood glucose homeostasis in response to high and low glycemic index meals in healthy men.** *Am J Clin Nutr* 2008, **87**:1254-1261.
202. Chen CL, Tsai HW, Wong SS: **Modeling the physiological glucose-insulin dynamic system on diabetics.** *J Theor Biol* 2010, **265**:314-322.
203. Puig O, Tjian R: **Transcriptional feedback control of insulin receptor by dFOXO/FOXO1.** *Genes Dev* 2005, **19**:2435-2446.
204. Richter EA, Nielsen JN, Jorgensen SB, Frosig C, Birk JB, Wojtaszewski JF: **Exercise signalling to glucose transport in skeletal muscle.** *Proc Nutr Soc* 2004, **63**:211-216.
205. Chalhoub E, Xie L, Balasubramanian V, Kim J, Belovich J: **A distributed model of carbohydrate transport and metabolism in the liver during rest and high-intensity exercise.** *Ann Biomed Eng* 2007, **35**:474-491.
206. Fleisher D, Li C, Zhou Y, Pao LH, Karim A: **Drug, meal and formulation interactions influencing drug absorption after oral administration. Clinical implications.** *Clin Pharmacokinet* 1999, **36**:233-254.
207. Moore MC, Cherrington AD, Mann SL, Davis SN: **Acute fructose administration decreases the glycemic response to an oral glucose tolerance test in normal adults.** *J Clin Endocrinol Metab* 2000, **85**:4515-4519.
208. Moore MC, Coate KC, Winnick JJ, An Z, Cherrington AD: **Regulation of hepatic glucose uptake and storage in vivo.** *Adv Nutr* 2012, **3**:286-294.
209. Lentz KA: **Current methods for predicting human food effect.** *AAPS J* 2008, **10**:282-288.
210. Lentz KA, Quitko M, Morgan DG, Grace JE, Jr., Gleason C, Marathe PH: **Development and validation of a preclinical food effect model.** *J Pharm Sci* 2007, **96**:459-472.
211. Leuenberger Jockel JP, Roebrock P, Shergold OA: **Insulin Depot Formation in Subcutaneous Tissue.** *J Diabetes Sci Technol* 2013, **7**:227-237.
212. Schade DS, Duckworth WC: **In search of the subcutaneous-insulin-resistance syndrome.** *N Engl J Med* 1986, **315**:147-153.
213. Saad A, Man CD, Nandy DK, Levine JA, Bharucha AE, Rizza RA, Basu R, Carter RE, Cobelli C, Kudva YC, Basu A: **Diurnal Pattern to Insulin Secretion and Insulin Action in Healthy Individuals.** *Diabetes* 2012.
214. Hagstrom-Toft E, Bolinder J, Ungerstedt U, Arner P: **A circadian rhythm in lipid mobilization which is altered in IDDM.** *Diabetologia* 1997, **40**:1070-1078.
215. Bollen M, Keppens S, Stalmans W: **Specific features of glycogen metabolism in the liver.** *Biochem J* 1998, **336 (Pt 1)**:19-31.
216. Hetherington J, Sumner T, Seymour RM, Li L, Rey MV, Yamaji S, Saffrey P, Margoninski O, Bogle ID, Finkelstein A, Warner A: **A composite computational model of liver glucose homeostasis. I. Building the composite model.** *J R Soc Interface* 2012, **9**:689-700.
217. Patek SD, Breton MD, Chen Y, Solomon C, Kovatchev B: **Linear Quadratic Gaussian-Based Closed-Loop Control of Type 1 Diabetes.** *J Diabetes Sci Technol* 2007, **1**:834-841.
218. El-Khatib FH, Jiang J, Damiano ER: **A feasibility study of bihormonal closed-loop blood glucose control using dual subcutaneous infusion of insulin and glucagon in ambulatory diabetic swine.** *J Diabetes Sci Technol* 2009, **3**:789-803.
219. Schrezenmeir J, Tatò F, Tatò S, Laue C, Beyer J: **Differences between Basal and Postprandial Circadian Variation of Insulin Sensitivity in Healthy Subjects and Type 1 Diabetics.** In *Hormones in Lipoprotein Metabolism*. Edited by Steinmetz A, Schneider J, Kaffarnik H: Springer Berlin Heidelberg; 1993: 45-64: *Recent Developments in Lipid and Lipoprotein Research*].
220. Shapiro ET, Polonsky KS, Copinschi G, Bosson D, Tillil H, Blackman J, Lewis G, Van Cauter E: **Nocturnal elevation of glucose levels during fasting in noninsulin-dependent diabetes.** *J Clin Endocrinol Metab* 1991, **72**:444-454.
221. Radziuk J, Pye S: **Diurnal rhythm in endogenous glucose production is a major contributor to fasting hyperglycaemia in type 2 diabetes. Suprachiasmatic deficit or limit cycle behaviour?** *Diabetologia* 2006, **49**:1619-1628.
222. Pisu E, Diana A, Lombardi A, Cassader M, Pagano G: **Diurnal variations in insulin secretion and insulin sensitivity in aged subjects.** *Acta Diabetol Lat* 1980, **17**:153-160.
223. Saklatvala J: **Glucocorticoids: do we know how they work?** *Arthritis Res* 2002, **4**:146-150.

224. Bollyky J, Greenbaum CJ: **Editorial: The role of glucagon in postprandial hyperglycemia--the jury's still out.** *J Clin Endocrinol Metab* 2007, **92**:2879-2881.
225. Meier JJ, Kjems LL, Veldhuis JD, Lefebvre P, Butler PC: **Postprandial suppression of glucagon secretion depends on intact pulsatile insulin secretion: further evidence for the intra-islet insulin hypothesis.** *Diabetes* 2006, **55**:1051-1056.
226. Tomas E, Lin YS, Dagher Z, Saha A, Luo Z, Ido Y, Ruderman NB: **Hyperglycemia and insulin resistance: possible mechanisms.** *Ann N Y Acad Sci* 2002, **967**:43-51.
227. Sparacino G, Facchinetti A, Cobelli C: **"Smart" continuous glucose monitoring sensors: on-line signal processing issues.** *Sensors (Basel)* 2010, **10**:6751-6772.
228. Kopecky P, Mraz M, Blaha J, Lindner J, Svacina S, Hovorka R, Haluzik M: **The use of continuous glucose monitoring combined with computer-based eMPC algorithm for tight glucose control in cardio-surgical ICU.** *Biomed Res Int* 2013, **2013**:186439.
229. Rosen ED, Spiegelman BM: **Adipocytes as regulators of energy balance and glucose homeostasis.** *Nature* 2006, **444**:847-853.
230. Pirola L, Johnston AM, Van Obberghen E: **Modulation of insulin action.** *Diabetologia* 2004, **47**:170-184.
231. Shulman GI: **Cellular mechanisms of insulin resistance.** *J Clin Invest* 2000, **106**:171-176.
232. Bloomgarden ZT: **Insulin resistance concepts.** *Diabetes Care* 2007, **30**:1320-1326.
233. Solomon SS, Usdan LS, Palazzolo MR: **Mechanisms involved in tumor necrosis factor- α induction of insulin resistance and its reversal by thiazolidinedione(s).** *Am J Med Sci* 2001, **322**:75-78.
234. Kroder G, Bossenmaier B, Kellerer M, Capp E, Stoyanov B, Muhlhofer A, Berti L, Horikoshi H, Ullrich A, Haring H: **Tumor necrosis factor- α - and hyperglycemia-induced insulin resistance. Evidence for different mechanisms and different effects on insulin signaling.** *J Clin Invest* 1996, **97**:1471-1477.
235. Lehrke M, Broedl UC, Biller-Friedmann IM, Vogeser M, Henschel V, Nassau K, Goke B, Kilger E, Parhofer KG: **Serum concentrations of cortisol, interleukin 6, leptin and adiponectin predict stress induced insulin resistance in acute inflammatory reactions.** *Crit Care* 2008, **12**:R157.
236. Marik PE, Raghavan M: **Stress-hyperglycemia, insulin and immunomodulation in sepsis.** *Intensive Care Med* 2004, **30**:748-756.
237. Van den Berghe G, Wilmer A, Hermans G, Meersseman W, Wouters PJ, Milants I, Van Wijngaerden E, Bobbaers H, Bouillon R: **Intensive insulin therapy in the medical ICU.** *N Engl J Med* 2006, **354**:449-461.
238. van den Berghe G, Wouters P, Weekers F, Verwaest C, Bruyninckx F, Schetz M, Vlasselaers D, Ferdinande P, Lauwers P, Bouillon R: **Intensive insulin therapy in critically ill patients.** *N Engl J Med* 2001, **345**:1359-1367.
239. Samra JS, Summers LK, Frayn KN: **Sepsis and fat metabolism.** *Br J Surg* 1996, **83**:1186-1196.
240. Hauner H, Petruschke T, Russ M, Rohrig K, Eckel J: **Effects of tumour necrosis factor α (TNF α) on glucose transport and lipid metabolism of newly-differentiated human fat cells in cell culture.** *Diabetologia* 1995, **38**:764-771.
241. Lang CH, Dobrescu C, Bagby GJ: **Tumor necrosis factor impairs insulin action on peripheral glucose disposal and hepatic glucose output.** *Endocrinology* 1992, **130**:43-52.
242. Halse R, Pearson SL, McCormack JG, Yeaman SJ, Taylor R: **Effects of tumor necrosis factor- α on insulin action in cultured human muscle cells.** *Diabetes* 2001, **50**:1102-1109.
243. Li YP, Reid MB: **Effect of tumor necrosis factor- α on skeletal muscle metabolism.** *Curr Opin Rheumatol* 2001, **13**:483-487.
244. Bruce CR, Dyck DJ: **Cytokine regulation of skeletal muscle fatty acid metabolism: effect of interleukin-6 and tumor necrosis factor- α .** *Am J Physiol Endocrinol Metab* 2004, **287**:E616-621.
245. Chambrier C, Laville M, Rhzioual Berrada K, Odeon M, Bouletreau P, Beylot M: **Insulin sensitivity of glucose and fat metabolism in severe sepsis.** *Clin Sci (Lond)* 2000, **99**:321-328.

246. Macfarlane DP, Forbes S, Walker BR: **Glucocorticoids and fatty acid metabolism in humans: fuelling fat redistribution in the metabolic syndrome.** *J Endocrinol* 2008, **197**:189-204.
247. Qi D, Rodrigues B: **Glucocorticoids produce whole body insulin resistance with changes in cardiac metabolism.** *Am J Physiol Endocrinol Metab* 2007, **292**:E654-667.
248. Gentilcore D, Chaikomin R, Jones KL, Russo A, Feinle-Bisset C, Wishart JM, Rayner CK, Horowitz M: **Effects of Fat on Gastric Emptying of and the Glycemic, Insulin, and Incretin Responses to a Carbohydrate Meal in Type 2 Diabetes.** *Journal of Clinical Endocrinology & Metabolism* 2006, **91**:2062-2067.
249. Stacher G, Bergmann H, Gaupmann G, Schneider C, Kugi A, Hobart J, Binder A, Mittelbach-Steiner G: **Fat preload delays gastric emptying: reversal by cisapride.** *Br J Clin Pharmacol* 1990, **30**:839-845.
250. Savage DB, Petersen KF, Shulman GI: **Disordered lipid metabolism and the pathogenesis of insulin resistance.** *Physiol Rev* 2007, **87**:507-520.
251. Weyer C, Bogardus C, Mott DM, Pratley RE: **The natural history of insulin secretory dysfunction and insulin resistance in the pathogenesis of type 2 diabetes mellitus.** *J Clin Invest* 1999, **104**:787-794.
252. Knox C, Law V, Jewison T, Liu P, Ly S, Frolkis A, Pon A, Banco K, Mak C, Neveu V, et al: **DrugBank 3.0: a comprehensive resource for 'omics' research on drugs.** *Nucleic Acids Res* 2011, **39**:D1035-1041.
253. Dassau E, Bequette BW, Buckingham BA, Doyle FJ, 3rd: **Detection of a meal using continuous glucose monitoring: implications for an artificial beta-cell.** *Diabetes Care* 2008, **31**:295-300.
254. Leloup JC, Goldbeter A: **Toward a detailed computational model for the mammalian circadian clock.** *Proc Natl Acad Sci U S A* 2003, **100**:7051-7056.
255. Debono M, Ghobadi C, Rostami-Hodjegan A, Huatan H, Campbell MJ, Newell-Price J, Darzy K, Merke DP, Arlt W, Ross RJ: **Modified-release hydrocortisone to provide circadian cortisol profiles.** *J Clin Endocrinol Metab* 2009, **94**:1548-1554.
256. Hastings M, O'Neill JS, Maywood ES: **Circadian clocks: regulators of endocrine and metabolic rhythms.** *J Endocrinol* 2007, **195**:187-198.
257. Ellingsen C, Dassau E, Zisser H, Grosman B, Percival MW, Jovanovic L, Doyle FJ, 3rd: **Safety constraints in an artificial pancreatic beta cell: an implementation of model predictive control with insulin on board.** *J Diabetes Sci Technol* 2009, **3**:536-544.

V.7 Lebenslauf (CV)

Persönliche Angaben:

Name:	Stephan
Nachname:	Schaller
Geburtsdatum:	22.03.1984
Geburtsort:	Stuttgart, Deutschland
Nationalität:	Deutsch

Werdegang:

2003:	Abitur
2003/4:	Grundwehrdienst
ab 2004 bis 2009:	Studium der Technischen Kybernetik an der Universität Stuttgart; Abschluss: Diplom-Ingenieur
2009/10:	Forschungsingenieur bei Insilico Biotechnology AG
2010-2013:	Promotionsstudium am Aachen Institute for Advanced Study
	in Computational Engineering Science (siehe Schriftstück)
ab 2013:	Wissenschaftler (Systems Pharmacology) bei Bayer Technology Services GmbH (Leverkusen)

Curriculum vitae:

2003:	Abitur (High School)
2003/4:	Military Service
2004-2009:	Studied Engineering Cybernetics at the University of Stuttgart; Degree: Dipl.-Ing. (Diploma in Engineering)
2009/10:	Research Engineer at Insilico Biotechnology AG
2010-2013:	Doctorate in Engineering at the Aachen Institute for Advanced Study in Computational Engineering Science (see Thesis)
since 2013:	Scientist (Systems Pharmacology) at Bayer Technology Services GmbH (Leverkusen)